EXPLORING BRAIN CONNECTIVITY USING A FUNCTIONAL-STRUCTURAL IMAGING FUSION PIPELINE

by

Sondos Ayyash

Ph.D., McMaster University, 2021

A THESIS SUBMITTED IN FULFILLMENT OF

THE REQUIREMENTS FOR THE DEGREE OF

Doctorate of Philosophy

in

THE SCHOOL OF BIOMEDICAL ENGINEERING

(Program Name: Biomedical Engineering)

McMaster University

(Hamilton, Ontario)

October 2021

The following individuals certify that they have read, and recommend to the Faculty of Graduate and Postdoctoral Studies for acceptance, the dissertation entitled:

Exploring Brain Connectivity using a Functional-Structural Imaging Fusion Pipeline

submitted by Sondos Ayyash in fulfillment of the requirements for

the degree of PhD

in Biomedical Engineering

Examining Committee:

Geoffrey Hall
Supervisor

Nicholas Bock
Supervisory Committee Member

Michael Noseworthy
Supervisory Committee Member

Signe Bray, University of Calgary
External Examiner

Ram Mishra
Chair

Additional Supervisory Committee Members:

Supervisory Committee Member

Supervisory Committee Member

Abstract

In this thesis we were interested in combining functional connectivity (from functional Magnetic Resonance Imaging) and structural connectivity (from Diffusion Tensor Imaging) with a data fusion approach. While data fusion approaches provide an abundance of information they are underutilized due to their complexity. To solve this problem, we integrated the ease of a neuroimaging toolbox, known as the Functional And Tractographic Analysis Toolbox (FATCAT) with a data fusion approach known as the anatomically weighted functional connectivity (awFC) approach - to produce a practical and more efficient pipeline. We studied the connectivity within resting-state networks of different populations using this novel pipeline. We performed separate analyses with traditional structural and functional connectivity for comparison with the awFC findings - across all three projects. In the first study we evaluated the awFC of participants with major depressive disorder compared to controls. We observed significant connectivity differences in the default mode network (DMN) and the ventral attention network (VAN). In the second study we studied the awFC of MDD remitters compared to non-remitters at baseline and week-8 (post antidepressant), and evaluated awFC in remitters longitudinally from baseline to to week-8. We found significant group differences in the DMN, VAN, and frontoparietal network (FPN) for remitters and non-remitters at week-8. We also found significant awFC longitudinally from baseline to week-8 in the dorsal attention network (DAN) and FPN. We also tested the associations between connectivity strength and cognition. In the third study we studied the awFC in children exposed to pre- and postnatal adversity compared to controls. We observed significant differences in the DMN, FPN, VAN, DAN, and limbic network (LIM). We also assessed the association between connectivity strength in middle

childhood and motor and behavioral scores at age 3. Therefore, the FATCAT-awFC pipeline, we designed was capable of identifying group differences in RSN in a practical and more efficient manner.

List of Publications

i) Exploring brain connectivity changes in major depressive disorder using functional-structural data fusion: A CAN-BIND-1 study

Sondos Ayyash, Andrew D. Davis, Gésine L. Alders, Glenda MacQueen, Stephen C. Strother, Stefanie Hassel, Mojdeh Zamyadi, Stephen R. Arnott, Jacqueline K. Harris, Raymond W. Lam, Roumen Milev, Daniel J. Müller, Sidney H. Kennedy, Susan Rotzinger, Benicio N. Frey, Luciano Minuzzi, Geoffrey B. Hall, CAN-BIND Investigator Team, Human Brain Mapping, 2021 September.

Preface

This thesis includes previously published research, research that is under review or in preparation for submission for publication in peer-reviewed scientific journals. Chapter 2 consists of a manuscript that is published in Human Brain Mapping. The primary author of this publication is the same as the author of this thesis. Chapter 3 contains a manuscript that has been submitted to - Elsevier Neuroscience. The paper presented in chapter 4 is in preparation for submission to Elsevier Neuroscience.

Table of Contents

Abstract iii

List of Publications v

Preface vi

List of Symbols x

List of Abbreviations xi

Acknowledgements xiv

Chapter 1: Introduction 16

1.1 Resting-State Functional Magnetic Resonance Imaging (fMRI) 16

1.2 Diffusion Tensor Imaging 17

1.3 Brain connectivity analysis using brain imaging 19

1.4 Methodology development 21

1.5 Imaging Background 22

1.6 FATCAT-awFC Pipeline design, novelty and limitations 26

1.7 Changes made to the Conventional awFC technique proposed by Bowman et al (2012) in our novel FATCAT-awFC pipeline 30

1.8 Applications of our FATCAT-awFC Pipeline to Different Populations 40

1.9 Thesis Goals and Objectives 43

1.10 Specific Hypothesis/Aims 44

1.11 Contributions 46

Chapter 2: Exploring Brain Connectivity Changes in Major Depressive Disorder Using Functional-Structural Data Fusion: A CAN-BIND-1 Study 68

2.1 Abstract 69

2.2 Introduction 70

2.3 Materials and Methods 76

2.4 Results 90

2.5 Discussion 97

2.6 References 106

Chapter 3: Assessing Remission In Major Depressive Disorder Using a Functional-Structural Data Fusion Pipeline: A CAN-BIND-1 Study 120

3.1 Abstract 120

3.2 Introduction 123

3.3 Materials and Methods 127

3.4 Results 137

3.5 Discussion 150

3.6 References 162

Chapter 4: Anatomically Weighted Functional Connectivity Analysis Using a Data-Fusion Pipeline Reveals Aberrant Connectivity In Children Exposed To Maternal Adversity: Impact On Middle Childhood. A MAVAN Study. 176

4.1 Abstract 176

4.2 Introduction 177

4.3 Methods 182

4.4 Results 192

4.5 Discussion 198

4.6 References 220

Chapter 5: General Discussion 250

5.1 Designing a faster and simpler pipeline for the combined structural and functional connectivity analysis of brain networks 250

5.2 Functional ROIs and Tractography 251

5.3 Limitations to the Method 253

5.4 Neural circuitry abnormalities underlying MDD 256

5.5 Neural circuitry abnormalities underlying REM and NREM in MDD 257

5.6 Neural circuitry abnormalities within middle childhood caused by pre- and/or postnatal adversity 258

5.7 Connectivity across studies 259

5.8 Future work 260

5.9 General Conclusion 263

5.10 References 264

Appendices 270

List of Symbols

g_{ij}: Distance between each region pair

S_{ij}: Un-biased number of tracts

α_1: Effect to adjust Distance Bias

π: Probabilities of structural connectivity

i: starting ROI

j: target ROI

m: third ROI connection

List of Abbreviations

MRI: Magnetic Resonance Imaging

fMRI: Functional Magnetic Resonance Imaging

rsfMRI: Resting State fMRI

DTI: Diffusion Tensor Imaging

RD: Radial Diffusivity

AD: Axial Diffusivity

ICA: Independent Component Analysis

gICA: Group Independent Component Analysis

RSN: Resting-State Networks

DMN: Default Mode Network

FPN: FrontoParietal Network

LIM: Limbic Network

VAN: Ventral Attention Network

DAN: Dorsal Attention Network

MDD: Major Depressive Disorder

HC: healthy comparison participants

NREM: Non-Remitters

REM: Remitters

CON: Controls (No pre/postnatal adversity)

ADV: Pre/Postnatal Adversity

awFC: Anatomically-Weighted Functional Connectivity

SC: Structural Connectivity

FC: Functional Connectivity

FATCAT: Functional and Tractographic Connectivity Analysis Toolbox

FATCAT-awFC: Novel Pipeline that combines FATCAT and awFC

GAT: Graph Analysis Toolbox

BRAINCAT: Brain Connectivity Analysis Toolbox

MIBCA: Multimodal Imaging Brain Connectivity Analysis

BCT: Brain Connectivity Toolbox

FA: Fractional Anisotropy

CAN-BIND: Canadian Biomarker Integration Network in Depression

MINI: Mini International Neuropsychiatric Interview

MADRS: Montgomery-Åsberg Depression Rating Scale

TR: Repetition Time

TE: Echo Time

FOV: Field of View

EPI: Echo-Planar Imaging

PCA: Principle component analysis

OPPNI: Optimized Preprocessing Pipeline

MNI: Montreal Neurological Institute

rsFC: Resting State Functional Connectivity

FD_{jenk}: Jenkinsons Framewise Displacement

SNR: Signal to Noise Ratio

BET: Brain Extraction Tool

FDR: False Discovery Rate

ROI: Region Of Interest

SD: Standard Deviation

SE: Standard Error

MD: Mean Diffusivity

L1, L2, L3: Eigenvalues

V1, V2, V3: Eigenvectors

e_1: primary eigenvector

MELODIC: Multivariate Exploratory Linear Decomposition into Independent Components

PCR: Principal Component Regression

PCA: Principal Component Analysis

PCs: Principal Components

SSRI: Selective Serotonin Reuptake Inhibitors

DSM-IV-TR: The Diagnostic and Statistical Manual-IV

BSID-II: The Bayley Scale of Infant Development

OB: Orientation Behaviour

PDI: Psychomotor Development Index

MAVAN: Maternal Adversity, Vulnerability and Neurodevelopment

BET: Brain Extraction Toolbox

Acknowledgements

I would first like to start by giving a heartfelt thank you to my PhD advisor, Dr.Geoffrey Hall. My sincerest appreciation goes to him, as he has guided me throughout my graduate education. His help has been the source of my success as he has always provided me with the right tools, and resources to allow me to overcome any obstacles throughout my research. He has been a source of support and encouragement throughout my journey. I am grateful to have had the opportunity to work under his supervision throughout my time in graduate school.

I would also like to express my thanks to Andrew Davis, who was a great mentor. Thank you for the many informative discussions we have had, for all the knowledge you have passed on to me, and for all the help you have offered me.

A special thanks to my CAN-BIND family for giving me insight and guidance, and pushing me to think and grow beyond my comfort, to allow me to think critically about research, and to my committee members Dr. Michael Noseworthy and Dr. Nicholas Bock for their valuable input as members of my advisory committee, and for their kind and encouraging feedback. To Dr. Ram Mishra, who has been a supportive Chair, and who I've had the pleasure of TA'ing for his courses, thank you for being an incredible mentor.

More than anything, nobody has been more important to me in the pursuit of my PhD than the members of my family. Especially my parents, Haifa Toum and Mohammad Ayyash, they have been the greatest sources of support along my journey and throughout my life. Thank you for your sacrifices over the years, which has made this opportunity possible. Their unwavering love and guidance are always with me in everything I do. They have been my number one supporters,

they have firmly believed in me, and motivated me – their determination, ambition and perseverance have truly inspired me. They are my ultimate role models.

To my sister, Rana, thank you for all the laughs, for the coffee runs, the fun times, and the deep conversations and most importantly for believing in me. And to my little sister Jenna, thank you for bringing so much joy and laughter into my life, and for always being there for me; my adventure buddy and best friend. To my brother Ahmed, thank you for being a source of support, you have been with me along my educational journey from the very beginning from undergrad to graduate school. Your ability to relate to me and encourage me has been so helpful. And to my brother Mustafa, your encouragement and words of advice have been helpful. To Yasin, thank you for being the sweetest little nephew whose light-hearted spirit was always so uplifting.

Thank you to my family for their constant support, encouragement, prayers and for the unconditional love. I truly could not have asked for a more supportive family.

Last but not least, a special thank you to my cats Leo and Penny for being the cutest fur babies throughout the writing process.

Chapter 1: Introduction

1.1 Resting-State Functional Magnetic Resonance Imaging (fMRI)

Resting-state fMRI is a functional neuroimaging technique which allows researchers to record participants' brain activity while they lie down in an MRI scanner without performing any cognitive, language or motor tasks ('at rest'). Resting-state fMRI measures spontaneous low-frequency fluctuations of blood oxygen level dependant (BOLD) signal (0.01 Hz – 0.1Hz) to study the functional architecture of the brain (Lee et al., 2013). RS-fMRI was first demonstrated in (Biswal et al., 1995). -RS-fMRI identifies the underlying brain architecture, which makes it particularly suitable for studying the connectivity between brain regions. Brain regions that show similarity in their temporal BOLD signal at rest are referred to as a resting-state networks (Bijsterbosch et al., 2017).

At the macroscopic level, the resting-state fMRI is measured from BOLD signal. However, BOLD contrast is an indirect way to measure the neuronal activity (Shmuel & Leopold, 2008). Microscopically a local field potential (representing action potentials of many neurons), of synaptic activity is measured at the recording site (Logothetis, 2008). These brain regions are considered to be 'active regions' while at rest. However, neurons don't have internal reserves of energy. Therefore, they rely on a process known as hemodynamic response which involves the supply of cerebral blood flow and an increase in oxygen supply (more than required) from adjacent capillaries for the delivery of glucose (Handwerker & Bandettini, 2011; Sirotin & Das, 2009). This change of the relative levels of oxyhemoglobin and deoxyhemoglobin is detectable by MRI due to the nature of their differing magnetic susceptibilities. Echo planar imaging (EPI) is sensitive to the BOLD signal indicating neuronal activity and has a fast imaging speed capable of capturing MR images within 20-100 ms (Poustchi-Amin et al., 2001), making it suitable for

fMRI studies (Bandettini et al., 1992; Kwong et al., 1992). This fast acquisition time, allows it to capture rapidly changing physiological processes (Poustchi-Amin et al., 2001). Oxygenated hemoglobin is diamagnetic, whereas de-oxygenated hemoglobin is paramagnetic (Stippich, 2015). This alters the magnetic field within and around the blood vessels in the capillary bed and venules (Stippich, 2015). When the amount of oxygenated hemoglobin in the blood is more than the deoxygenated hemoglobin, which results in a homogenous local magnetic field. This homogenous local magnetic field results in a slower dephasing of the excited protons, which in turn leads to a stronger MRI signal in the activated state (Kwong et al., 1992; Stippich, 2015).

1.2 Diffusion Tensor Imaging

Diffusion imaging utilizes the variability of 'Brownian Motion' of the water molecules in brain tissue. Brownian motion describes the random movement of water that is dependent on temperature and the kinetic energy of the molecules. There are only a few locations in humans which free diffusion occurs such as the cerebrospinal fluid. Random diffusion is often referred to as 'isotropic diffusion'. However, water molecules in brain tissue are not truly random because there is structure to tissue. Axons, cell membranes and vascular structures, may restrict or hinder the diffusion of water molecules (Mannelli et al., 2015.; Parker, 2004; Patterson et al., 2008). Directionality dependent diffusion is also called 'anisotropic' diffusion. Water diffusion in the brain is referred to as 'apparent diffusion'.

Diffusion-weighted imaging (DWI) is an MRI technique that allows the measurement of random Brownian motion of water molecules within a voxel of brain tissue. Diffusion weighted imaging

is commonly acquired using a spin-echo echo planar sequence (SE-EPI) with diffusion sensitizing gradients. The movement of water molecules along the diffusion gradient results in a reduced DWI signal intensity (Patterson et al., 2008; Qayyum, 2009). B-value represents the strength of diffusion sensitizing gradients. Four sets of images are produced from DWI, one b = 0 s/mm^2 map (a T2- weighted image with no sensitizing gradients- to detect presence of water molecules), a b value at approximately 1000 in the x, y, and z directions (these can be combined later arithmetically), whereby T2 signal is attenuated according to how fast water molecules diffuse in a specific direction. These structural images allow researchers to study the underlying integrity and direction of white matter tracts (Beaulieu et al., 1999). Two sets of images b = 1000 s/mm^2 and b = 0 s/mm^2 are used in post-processing to calculate an image that reflects diffusion, known as the Apparent Diffusion Coefficient (ADC) (mm^2 /s) also known as the ADC map. The diffusion tensor, also referred to as the 'apparent diffusion tensor', is applied to the ADC map to represent/model the values of the ADC in function of gradient direction, in each voxel (Hecke et al., 2016; Özarslan & Mareci, 2003). From the tensor, a number of parameters may be obtained (calculated) including eigenvalues and eigenvectors. Tractography is then applied to reconstruct white matter pathways from the principal eigenvector of the tract (Hecke et al., 2016). An assumption is made in diffusion tractography that the principal direction is parallel to the direction of the fibers in each voxel (Papanicolaou, 2017). Structural connectivity measures the white matter fiber bundle count that form pathways between brain regions of the brain networks (Frau-Pascual et al., 2018).

1.3 Brain connectivity analysis using brain imaging

With the advancements of magnetic resonance imaging, scientists are able to evaluate connectivity non-invasively, with functional magnetic resonance imaging (fMRI) and diffusion tensor imaging (DTI). FMRI and DTI are two commonly used imaging modalities in brain imaging (Glover, 2011; Nucifora et al., 2007). There is merit in combining fMRI and DTI data to evaluate the connectivity that is established between brain regions (Bihan et al., 2001; Skudlarski et al., 2008). Both fMRI and DTI have historically been capable of detecting subtle abnormalities in connectivity linking brain regions (Chu, Lenglet, et al., 2018; Liu et al., 2020). Other studies have also shown that dually analyzing structural and functional connectivity in neuropsychiatric disorders has demonstrated to be useful, as both play a key role in detecting abnormalities (F. Wu et al., 2020). Functional connections (temporal correlations) are mediated through white matter fibers (structural connections); therefore the combination of functional and structural connectivity may give researchers some insight that better represents the connectivity within RSNs.

While fMRI and DTI are both powerful MRI techniques, they each have particular weaknesses. DTI is able to compute the number of fiber tracts running between different pairs of ROIs using tractography. However, tractography is prone to error, with false positives, due to limitations of spatial resolution, noise and indirect connectivity (Jbabdi & Johansen-Berg, 2011). These DTI limitations can be reduced with the technological advances that resting-state fMRI has to offer. Resting-state fMRI can readily and robustly identify distant brain regions that are functionally connected (via low frequency temporal correlations) (Smith et al., 2013). For instance,

distributed brain regions are difficult to accurately detect and interpret using DTI alone, the greater the distance in tractography the more prone to error in detecting the right pathway and the fewer the tracts that terminate at the target brain region (Zalesky, 2008; Zalesky & Fornito, 2009). However, the identification of physically distant temporally synchronous regions can be achieved with rsfMRI. On the other hand, while rsfMRI is able to robustly detect connectivity between distant brain regions, resting-state fMRI doesn't provide information on the structural basis for which the FC networks exist. While tractography has its limitations (i.e. susceptible to missing long range tracts, complex fiber orientation), it provides valuable information on the white matter connectivity strength. It is presumed that white matter tracts serve as the basis for the functional interactions, thus shaping the rsFC correlations between brain regions (Ghosh et al., 2008; Honey et al., 2007). While it is presumed that functional connectivity is constrained by structural connectivity (Park et al., 2017), the exact relationship may be complicated. There are studies that reported a negative fMRI-DTI relationship (Putnam et al., 2008), some have found a positive relationship between fMRI-DTI (Forstmann et al., 2008; Kim & Whalen, 2009), and others have found both negative and positive fMRI-DTI relationships within the same study (Baird et al., 2005). Instead of analyzing each connectivity measure separately and correlating them with one another, quantitatively combining structural and functional data, may perhaps better distinguish patients versus controls (Calhoun & Sui, 2016). The concatenation of these measures may provide a more complete view of the neural networks of brain connectivity and enrich our understanding of brain networks (Greicius et al., 2009).. The complementary nature of each modality makes it easier to combine both metrics to produce a unique measure that combines both FC and SC. Instead of assuming structural connectivity from functional

connectivity, studies are beginning to combine metrics to assess structural/functional relationship in a single connectivity measure.

1.4 Methodology development

There's increasing demand for combining functional (from fMRI) and structural (from DTI) data, specifically in an "advanced and deeply fused structure-function" approach (Zhu et al., 2014). An enhanced fusion approach can provide a more complete understanding of underlying structural-functional connectivity (Zhu et al., 2014). However, neuroimaging data fusion is not applied in literature very often due to the complex nature of combining these two datasets. Therefore the use of a toolbox to assist in the joint analysis of these data types would benefit the neuroimaging community. The unique contribution of this research was to integrate the two models, FATCAT and awFC, in a flexible and comprehensive framework to acquire the best properties of each. We integrate the two models in a user-friendly approach, by taking the output of FATCAT, the functional connectivity (Pearson r) and structural connectivity (number of tracts), as inputs for the awFC model (combines functional and structural connectivity). We predicted that the FATCAT-awFC model would identify MDD and development -related changes in connectivity in keeping with those previously documented in the RS-fMRI and DTI literature.

1.5 Imaging Background

Recent development in brain connectivity studies, have examined the relationship between structural and functional connectivity and found some level of correspondence between connectivity metrics (Hagmann et al., 2008; Honey et al., 2009; Koch et al., 2002). There is a growing body of research that combines the structural and functional connectivity in a joint analysis using different methods. According to Calhoun and Adali, data fusion is defined as the process that applies multiple image types simultaneously to utilize the cross-information (Calhoun & Adalı, 2009). Data fusion can be categorized into two types: symmetric and asymmetric. Asymmetric data fusion is using one imaging modality to constrain a dataset derived from another imaging modality in order to analyze it (Huster et al., 2012), whereas symmetric data fusion simultaneously analyzes datasets originating from different sources (Valdes-Sosa et al., 2009). The most popular form of data fusion approach for the neuroimaging field, among asymmetrical and symmetrical data fusion, is symmetric data fusion (Tulay et al., 2019). Among the symmetrical data fusion approaches, datasets can be combined in one of two ways: early integration or late integration (Turk, 2014). Early data integration involves the immediate fusion of data after low-level processing, whereas late data integration involves the data fusion of two different datasets after full unimodal processing is completed (Turk, 2014). The advantage to performing a late integration, is that software development is simpler (Turk, 2014). Given the advantages of multimodal data fusion, the problem of combining multiple datasets from multiple modalities is key to future work.

New metrics have been derived such as anatomically-weighted functional connectivity (Bowman et al., 2012) or track-weighted functional connectivity (Calamante et al., 2013) to combine structural and functional information. Bowman et al (2012) applied a structural connectivity measure in the functional connectivity maps, producing an improved functional connectivity map. This was demonstrated in a simulation study that found awFC to produce comparable, and at times superior accuracy compared to the standard approach. Calamante et al (2013), on the other hand, suggested that propagating the functional connectivity information along white matter pathway connecting functionally correlated brain regions, produces a unique quantitative white matter connections image that contains functional information. Some studies combine structural-functional information to enhance estimation of functional connectivity by incorporating structural connectivity (Bowman et al., 2012; Xue et al., 2015), while other research aims to enhance estimation of structural connectivity by incorporating functional connectivity (Calamante et al., 2013). The benefit of combining structural and functional data with a multimodal fusion approach, is its capacity to reveal hidden patterns that may only be discovered within a combined structural-functional dataset (Calhoun & Sui, 2016). As demonstrated in Calhoun and Sui, 2016, there is an increasing interest in multimodal data fusion - 2-way multimodal fusion included. Despite the countless benefits associated with multimodal neuroimaging (Tulay et al., 2019), data fusion still remains underutilized in research studies and not yet a universally accepted approach to studying brain networks (Calhoun & Sui, 2016). A possible explanation for this may be due to the complex nature of fusing multimodal data.

Recent advances in data fusion for neuroimaging that rely on joint blind source separation have become particularly popular (Chen et al., 2016). Joint blind source separation allows the

combination of data from different imaging modalities by assessing statistical dependencies among datasets (Adali et al., 2014). To date, there are many biomedical research studies that have utilized JBSS methods (Anderson et al., 2012; Correa et al., 2010; X.-L. Li et al., 2011; Y.-O. Li et al., 2009). New brain imaging techniques that use a blind source separation approach have provided researchers with new opportunities to assess the brain, from different perspectives. A blind source separation technique to combine fMRI and DTI was proposed by Sui et al (2011), which is a two-step method that relies on higher order statistics to combine a multi-set canonical correlation analysis (mCCA) with a joint independent component analysis (jICA), known as 'mCCA+jICA' (Sui et al., 2011). This framework performs a correlation analysis using mCCA to compare multiple datasets, and identifies the associated components; jICA is then applied on the horizontally concatenated components to extract joint independent components (Sui et al., 2011). The joint independent component analysis, allowed the fMRI (contrast map derived from GLM) and DTI (fractional anisotropy) scans to be combined within a single analysis. The extracted components represent areas where associations between both modalities exist. While there is benefit to using this approach, it is mathematically dense and a complex approach.

A number of studies have utilized a Bayesian model for the joint analysis of functional and structural data (Bielza & Larrañaga, 2014). For instance, Xue et al (2015) and Kang et al (2017) applied a Bayesian method, which used the probabilistic tractography (from DTI) as priors, to construct and analyze functional connectivity (from rs-fMRI). However, Bayesian statistical methods, such as the hierarchical Bayesian approach used in joint FC-SC analysis (Kang et al., 2017; Xue et al., 2015), are computationally expensive (S. Wu et al., 2016). The high

computational cost that comes with Bayesian models may discourage users from utilizing it (Kitanidis, 2005).

Another approach that aims to combine functional and structural data is known as the activated fibers method. The activated fibers method measures dynamic functional connectivity via the functional synchronization of two end voxels that are structurally connected (white matter tract connecting two brain regions). A GLM is then applied to the dynamic functional connectivity time series of fibers, which generates activation maps of fibers (Lv et al., 2011). This method is said to produce network-level responses compared to conventional voxel based activation, which reflects local voxel-level response to stimuli (Lv et al., 2011). The activated fibers method is said to detect more activated brain regions compared to the raw fMRI BOLD signal. Other studies employing this method have also demonstrated this relationship (Lim et al., 2011; Lindenberger et al., 2009).

Alternatively, a multilayer network framework (Kivelä et al., 2014) has been proposed for the joint structural-functional connectivity analysis of human neuroimaging. Mathematical advances have allowed for a multilayer motif analysis to study multiplex (multilayer) networks. Motifs are subgraphs of networks, usually made up of three to four nodes (Milo, 2002). These multiplex (multilayer) networks can be represented with two layers: one layer constituting structural connectivity, and the other functional connectivity. This allows one to analyze the interaction between the layers. Battison et al. (2017), reported that the joint structural-functional multiplex network differed from monoplex networks. Studies that have utilized this technique include Battiston et al (2017) and De Domenico (2017) (Battiston et al., 2017; De Domenico, 2017).

While it seems to be an appealing approach, multilayer network framework has many parameters, whereby each node is highly interconnected with other nodes in a dense web (Hammoud & Kramer, 2020). Higher dimensions (multilayers) can result in redundancy (De Domenico et al., 2014) and inefficiency. While convergence (back propagation) has been proposed in multilayer studies, it is extremely slow and time-consuming process (Elliott, 2001; Haykin, 2000; Zhang & Lei, 2011). The mapping of the neural network is dependent on the correct training of the system, training method and the sample size which must be large to achieve accuracy (Zhang & Lei, 2011).

To date, new data fusion approaches have emerged due to the interest of jointly analyzing functional and structural data, which may provide different but complementary aspects of brain connectivity. Joint analysis models can have clinical relevance across many neuropsychiatric disorders and also among healthy individuals to understand normal/typical brain patterns and connections. The added value of DTI-tractography information to functional connectivity and vice versa, has been demonstrated to be useful. It allows researchers to discover potentially new and unique information about the data (Staempfli et al., 2008; Vassal et al., 2016) and capitalize on the strengths of each modality (Sui et al., 2013).

1.6 FATCAT-awFC Pipeline design, novelty and limitations

1.6.1 Popular Neuroimaging Software Packages

In its early days, fMRI analysis software packages were programmed in-lab and not widely distributed (Poldrack et al., 2011). This made consistency between packages difficult to compare. As fMRI became more popular, the software packages became distributed as analysis suites to perform different aspects of fMRI analysis. Today, the most commonly used fMRI analysis packages are: Analysis of Functional NeuroImages (AFNI), FMRIB Software Library (FSL), and Statistical and Parametric Mapping (SPM). SPM was one of the earliest, most popular and openly distributed software for fMRI analysis (Poldrack et al., 2011). It is built in MATLAB, and is considered 'readable' in that one can understand the code from reading it (Poldrack et al., 2011). It is useful for processing data, reading and writing data files and has several extensions that are open source and freely downloadable (Poldrack et al., 2011). However, SPM's visualization tools are limited (Poldrack et al., 2011). Another platform, FSL, is popular because it offers cutting-edge techniques such as: 1) novel modeling, estimation and inference techniques (i.e. FEAT) 2) performs robust ICA analysis 3) utilizes sophisticated tools for DTI analysis 4) has powerful visualization tool: FSLeyes, that allows the easy and simple overlay of a number of atlases and functional/structural images (Poldrack et al., 2011). Lastly, AFNI was developed in the early days of fMRI and is popular among researchers for fMRI analysis. One of the main advantages of AFNI is its flexibility and its ability to be highly customizable (Poldrack et al., 2011). A disadvantage to the implementation of AFNI is the steep learning curve and the need to understand each command in a processing pipeline.

1.6.2 Software and Programming Utilized in the Development of our FATCAT-awFC Pipeline

In this thesis, a FATCAT-awFC pipeline was designed. This included a number of neuroimaging software, and programming languages to perform these tasks. While my pipeline design allows the traditional data fusion approach to be simpler and more intuitive, it requires the user to have proficient knowledge of programming and mathematical understanding. In order to run any of these commands, the researcher must be able to enter commands and navigate files using terminal. It must be understood that this is not a simple point-and-click GUI application. This thesis work reflects a proficient experience of Python, R programming and command line knowledge. The Mac terminal command line was used to run the AFNI commands in batch processing. Beyond FATCAT, Python was used to perform mathematical operations. This thesis also reflects a proficient understanding of matrices, and mathematical concepts.

A limitation of this pipeline was that ROIs suitable for the DTI data are not automatically generated from the command 3dROIMaker. An added benefit would be to transform ROIs into diffusion-weighted space. Another limitation of this approach was the lack of optimal ROI selection in the 3dROIMaker step; which was a more arbitrary selection process. Another limitation to this pipeline was the 3dTrackID step. This command acted as a bottleneck to our study, as it slowed processing speed. It took a long time to process the tractography for each individual subject. In order to work around this limitation, we used SHARCNET, which allowed us to perform 3dTrackID at a much faster rate and more reasonable time frame. SHARCNET is a consortium of 16 universities, colleges and research institutes, which utilizes parallel clusters for high performance tasks.

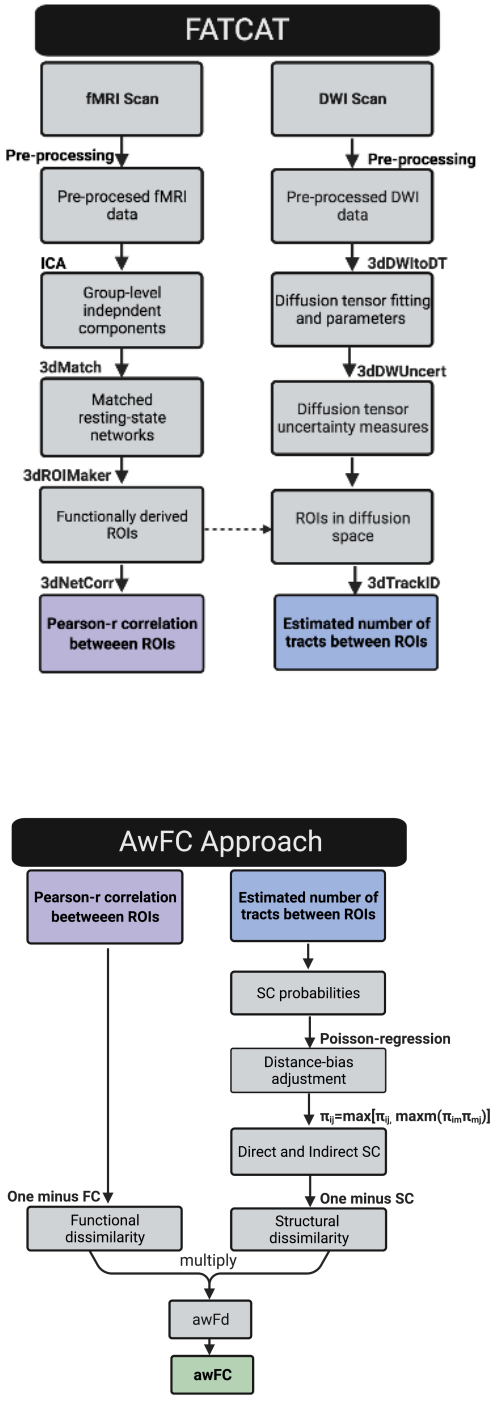

Fig.1| FATCAT-awFC pipeline. (a) FATCAT pipeline. The Functional and Tractographic Connectivity Analysis Toolbox (FATCAT) pipeline. Functional connectivity (from fMRI)

.

and tract count (from DTI) were output from FATCAT. (b) awFC pipeline demonstrating that the output of Functional and Tractographic Connectivity Analysis Toolbox (FATACT) was used as input for the awFC pipeline.

Note: fMRI = functional magnetic resonance imaging, DWI = diffusion weighted imaging, ICA = independent component analysis, ROIs = regions of interest, SC = structural connectivity, FC = functional connectivity, awFd = anatomically weighted functional dissimilarity, awFC = anatomically weighted functional connectivity.

Aside from the fMRI/DTI software packages applied and the programming languages involved in our pipeline, there is novelty to our pipeline. There are differences in the conventional awFC technique and the FATCAT suggested pipeline that produced a novel FATCAT-awFC pipeline. To get a deeper understanding of the design of the FATCAT-awFC pipeline shown above, we provide a more detailed explanation of the differences and added value of our approach has compared to the conventional awFC technique and FATCAT pipeline.

1.7 Changes made to the Conventional awFC technique proposed by Bowman et al (2012) in our novel FATCAT-awFC pipeline

1.7.1 Different approaches for Network Analysis

To understand the changes made in our pipeline, one must first understand different types of network analysis that exist, in order to fully understand the reasoning for making this change. Thus, we will discuss seed-based correlation, ICA and clustering.

Conventionally, functional connectivity studies are analyzed using seed-based analysis (Khosla et al., 2018). The time series of the seed is correlated with the time series from each and every voxel from the brain (Khosla et al., 2018). Although this is a powerful technique, seed-based correlation requires the selection of a seed region a-priori and the outcome is dependent on the way in which seeds are defined (hypothesis driven) (Khosla et al., 2018). It can only extract one functional system at a time, which may result in missing some interesting correlations that are not associated with the chosen seed region (Khosla et al., 2018). Another popular approach for analyzing functional connectivity is through data-driven techniques such as ICA and clustering (Khosla et al., 2018). These methods allows the study of the whole brain RSNs (Khosla et al., 2018). Clustering can be divided into two main types: flat (i.e. k-means) or hierarchical.

Hierarchical clustering iteratively merges the least dissimilar clusters according to a predefined distance metric, until the entire data is labeled as one large cluster whereby a threshold distance is set to obtain clusters (Khosla et al., 2018). While hierarchical clustering has been demonstrated to be a powerful technique, it has inherent disadvantages (Bansal et al., 2012; Khosla et al., 2018). Errors in clustering at an early stage in the hierarchical clustering process cannot be changed or modified later in the process (Khosla et al., 2018). Furthermore, hierarchical clustering is sensitive to noise and outliers (Khosla et al., 2018). Hierarchical clustering is computationally taxing and time consuming. Given N voxels to be clustered,

hierarchical clustering requires N^2 CPU memory space for storing the dissimilarity matrices and requires a long timeframe of N^3 CPU time (Embrechts et al., 2013). Therefore hierarchical clustering does not perform well with large datasets (Khosla et al., 2018). For this reason, hierarchical clustering approaches often use a small cohort, i.e., the awFC approach proposed by Bowman et al, used a small cohort of 6 healthy females for rsfMRI and DTI data (Bowman et al., 2012). To account for the computationally demanding nature of hierarchical clustering, oftentimes dimension reduction strategies are applied as well, i.e. using an anatomical template (results in parcellation bias) or limiting number of slices (poor spatial resolution) (Khosla et al., 2018).

1.7.2 Conventional awFC technique proposed by Bowman et al (2012)

1.7.3 Network Selection

Hierarchical clustering requires a lengthy and complicated process to obtain resting-state networks. The Bowman method uses hierarchical clustering approach to group clusters into networks. A data reduction approach is applied in the Bowman et al (2012) approach by using an anatomical atlas (AAL) and analyzing 20 fMRI slices (Bowman et al., 2012). Within each AAL region, the time domain signals are transformed to the frequency domain using fast Fourier transform. Then the singular value decomposition (SVD) is applied to each region to identify the most dominant frequency pattern (Bowman et al., 2012). The voxel that has frequency patterns that most resembles the regional summary is identified, and the 150 most proximal voxels (that fall within the AAL region) are taken to be part of that cluster (Bowman et al., 2012). Once the

clusters are identified, a check is done to confirm that the primary singular vector correctly characterize the cluster. Therefore, the primary singular vector output from the SVD is compared to the mean signal of the sub-region (Bowman et al., 2012). If the primary singular vector is not representative of the data the second singular vector is used, and the steps are repeated (Bowman et al., 2012). Once the clusters that fall within the AAL regions are identified, based on the dominant voxel, hierarchical clustering can be applied. A hierarchical cluster is generated in order to group the least dissimilar clusters together until the whole data is one large cluster. A threshold can now be set to group clusters into different networks, this threshold is chosen arbitrarily, and can be differently grouped across subjects (Khosla et al., 2018). This hierarchical clustering process is repeated for each subject separately, it is done on an individual basis. As hierarchical clustering is performed for each subject separately, grouping of clusters into networks may not be consistent across all subjects (Bowman et al., 2012). To achieve consistent networks of clusters across subjects, for performing a group analysis, networks are compared across subjects to inspect the grouping of clusters (Bowman et al., 2012). If the clusters are consistent across networks for each subject, they are included in the group network being analyzed (Bowman et al., 2012). The hierarchical clustering process for large groups is a tedious one, with several complex calculations and manual steps involved to adjust the data. These considerations detract from use of hierarchical clustering and the make ICA an appealing alternative.

ICA relies on simple linear algebra calculations and identifies maximally statistically independent sources from observed data. Multi-subject studies, most widely use Group Independent Component Analysis (GICA) for the decomposition of fMRI data and extracting

brain networks. When group ICA is performed for multi-subject analysis a PCA approach is applied to perform group and subject level reductions in the data (Erhardt et al., 2011). GICA assesses the entire brain to determine temporally correlated regions, and is not limited to assessing only ROIs selected a-priori (Faro et al., 2011). ICA has several advantages, including being naturally robust to noise and having the ability to capture noise sources as separate components (removal of structured noise) (Faro et al., 2011). Unlike hierarchical clustering, the ICA approach is optimized and feasible for both the number of operations performed and the computer memory required (Varoquaux et al., 2010). The ICA approach is fast and feasible on average hardware (Varoquaux et al., 2010). The components extracted by ICA for neuroimaging studies are distinct, and consistent with known RSN's previously reported in literature (Varoquaux et al., 2010). The common spatial maps generated by GICA makes it easier for researchers to draw inferences about group data.

The FATCAT approach adopts an ICA approach for identifying networks and filtering out noise. Group ICA, is the most popular method for analyzing large datasets, and concatenated along the temporal dimension (Joel et al., 2011). This approach adopts consistent spatial maps across subjects but does not enforce restrictions on the temporal map for each subject (Joel et al., 2011). In thesis chapters 2 and 3, both HC and MDD groups were concurrently input into the ICA step, to decompose the 4D fMRI time series into independent component maps. This approach reduces the likelihood of bias that would result from the selection of HC solely, and results in a consistent number of ROIs between both groups; making them comparable (Bijsterbosch et al., 2017). A benefit to including both groups as input for GICA is that it will return spatial components (and structured noise) that are well representative of the entire dataset (Bijsterbosch

et al., 2017). As such, it will be highly sensitive to detecting differences between groups since it accurately represents the dataset (Bijsterbosch et al., 2017). However, a disadvantage to this approach is that the group ICA may split components in a way that is discordant with the ??? described in the literature (Bijsterbosch et al., 2017). Therefore, it is important to include a template matching process to ease the identification of best matching IC's to standard networks. Typically, a pre-specified number of 20 components are defined. It has been shown in pervious studies that selecting the number of components to be 20-30 results in 8-10 functionally relevant networks (Joel et al., 2011). However, it does not identify which components are signal and which are noise. An advantage of GICA is its ability to isolate noise sources from signal sources of interest (Khosla et al., 2018). A drawback of ICA is its inability to distinguish source signals and nuisance signals (Joel et al., 2011). Identifying and choosing significant components, requires manual intervention and is subjective and time consuming (De Blasi et al., 2018; Khosla et al., 2018). However, with our FATCAT-awFC '3dMatch' command, we are capable of identifying the source signals from noise quickly and efficiently, by matching them to a standard RSN template (Yeo et al., 2011). According to Grecius et al (2007), a spatial template matching procedure is often performed after ICA to select the "best fit", and discards the remaining components (due to noise, other networks not of interest, etc.) (Greicius et al., 2007). To match with the ICA components, a standard template was used known as the Yeo network (Yeo et al., 2011) to extract 5 known resting-state networks. This matching approach does not modify the networks; instead it simply calculates and identifies the component that best matches the standard template (Greicius et al., 2007). This makes for a fast and easy identification of RSN's that are comparable to standard RSN's (since RSN's are robust and reproducible). Any structured noise will not match the standard template and therefore will not be included in the

study (Greicius et al., 2007). The selected templates that match the standard network will be consistent with the literature definition of that RSN, and therefore will be easily compared to past studies (Greicius et al., 2007). Using a standard template alone without GICA is possible but may not accurately represent our dataset, therefore it is best to use GICA with template matching to make the most of our data-driven results (Bijsterbosch et al., 2017). The network-based approach is important because these are known networks that are capable of detecting neuropsychiatric disorders. For instance, the default mode network (DMN) has been reported to have a high degree of heritability, and is a commonly used to distinguish MDD from HC (alterations in connectivity) (Allen et al., 2011). Next, 3dROIMaker is used to parcellate the FC maps by thresholding and spatial clustering. Thresholding can also suppress clusters that were formed by chance. This is performed using software to make this process easier. Group ICA uses a common spatial template that allows direct comparisons of networks across subjects, which eliminates the challenges found in cluster analysis(Du et al., 2016).

By design, the FATCAT-awFC approach uses a set of software tools to perform a fast and efficient pipeline for extracting data-driven RSN's. It eliminates the process of having to perform several complicated steps that place large demands on computer memory and CPU space, that are associated with the hierarchical clustering approach (awFC approach alone).

1.7.4 Changes made to the Conventional awFC technique proposed by Bowman et al (2012) in our novel FATCAT-awFC pipeline

1.7.5 Node selection: aROI versus fROI

Another difference to our combined FATCAT-awFC approach is that unlike the awFC approach, the FATCAT-awFC uses functionally defined ROIs to identify network nodes. The awFC approach, on the other hand, used structurally defined regions from the AAL atlas to identify anatomical nodes. There are two schools of thought when it comes to identifying nodes in functional connectivity, either based on anatomical or functional ROIs (Nord et al., 2017). Indeed, it can be argued that functional ROI's are more ideal when studying functional connectivity. Since the awFC approach is a modified and enhanced version of the traditional functional connectivity analysis (by weighting structural connectivity) it would only make sense to identify regions based on functional landmarks instead of anatomical landmarks.

Unlike anatomical brain atlases, which are used to define ROIs a-priori in the awFC presented by Bowman et. al, data-driven approaches such as ICA, do not reflect a pre-defined parcellation of brain structures(Thirion et al., 2014). Data-driven functional ROIs are regarded as better at representing the brain parcellation for functional brain activation patterns(Thirion et al., 2014).

The Bowman et al method relies on anatomically defined ROIs. The problem with the anatomical ROIs is that voxels from functional data are forcibly clustered into separate anatomically defined ROIs , which impose spatial constraints on the functional activity (DonGiovanni & Vaina, 2016). Anatomical ROIs are derived from high spatial resolutions, which may not apply to functional data.-Therefore, ROIs should be functionally homogeneous, so that all voxels in a cluster have similar time course, which is not guaranteed in anatomical ROIs. Data-driven functional ROIs are regarded as better at representing the brain parcellation

for functional brain activation patterns (Thirion et al., 2014). According to Saxe et al, functional ROIs identify "stable, coherent and interesting regional response profiles"(Saxe et al., 2006). Functional ROIs have an advantage in multi-subject studies because they have been found to be consistent across subjects and studies.(Saxe et al., 2006). Functional ROIs are more biologically grounded, i.e. most cortical regions have functional correspondence in both hemispheres(Bijsterbosch et al., 2017). A disadvantage of the awFC method proposed by Bowman et. al was that they used an AAL atlas to define ROIs. However, it is important to note that there is a key tradeoff when choosing anatomical ROIs versus functional ROIs. Functional ROIs suffer from a lack of spatial contiguity, whereas anatomical ROIs suffer from a lack of functional homogeneity(Craddock et al., 2012).

In our FATCAT-awFC approach, the derived functional regions are named to identify the region. While many research studies that use functional ROIs opt out of naming these ROIs, it can be of value to name functional regions, in order to draw inferences about these regions (Saxe et al., 2006). Functional ROIs are useful for specifying brain locations across subjects, for testing hypotheses concerning the function of specific brain regions.

1.7.6 Changes made to the Conventional awFC technique proposed by Bowman et al (2012) in our novel FATCAT-awFC pipeline

1.7.7 Hard parcellation versus soft parcellation

In addition, brain parcellations can be divided into hard and soft (Bijsterbosch et al., 2017). Non-overlapping ROIs are known as hard parcellations, whereas a soft parcellation is one in which a

voxel can belong to two or more ROIs (Bijsterbosch et al., 2017). Soft parcellations more accurately represent the underlying biology (Bijsterbosch et al., 2017). This is due to the fact that single brain region may play a role in more than one function (Bijsterbosch et al., 2017). For instance, in the visual network, there is a group of voxels associated with distance of a fixation to a point but also associated with sensitivity to orientation of visual stimuli. Therefore, to account for this complexity, a soft parcellation is often best. FATCAT (ICA) offers a soft parcellation, whereas hierarchical clustering provides a hard parcellation (using the AAL atlas). As such, the FATCAT-awFC approach more accurately represents the data as compared with awFC alone.

1.7.8 Additions to the Conventional FATCAT pipeline proposed by Taylor and Saad (2013) in our novel FATCAT-awFC pipeline

FATCAT is a suite of software tools aimed at facilitating the combination of functional and structural data in a network. However, the FATCAT method combines functional and structural data using an integrative approach. While data integration works to enhance one imaging modality with another by constraining certain features (i.e. functionally defined regions to extract structural connections between them), it has its limitations (Sui et al., 2014). Data integration, does not maximally exploit the complimentary information obtained by each modality and does not allow for the direct interaction between both data types (Calhoun & Sui, 2016; Guo et al., 2018) [see Introduction for more information]. To capitalize on the wealth of information we collect from one neuroimaging study, we aim to fuse the data through a data fusion approach. The neuroimaging data fusion approach is reported to contain maximal information. The

FATCAT pipeline was also modified to include the awFC for this reason. The FATCAT pipeline was also greatly enhanced by combining the functional and structural connectivity output by FATCAT into a single metric, the awFC. In addition, distance bias and indirect connectivity were included which both greatly improve structural connectivity measurements [See figure 1b]. Therefore by combining a toolbox (for the easy integration of functional and structural data) with awFC (a technically and computationally taxing method for fusing functional and structural connectivity), we arrive at a re-designed, easy-to-use toolbox of data fusion connectivity for large-scale networks. Our research highlighted the wealth of information that can be collected and evaluated from a single neuroimaging study and the combined awFC measure from both functional and structural connectivity can be associated with MDD changes within subjects (Hayasaka & Laurienti, 2010).

1.8 Applications of our FATCAT-awFC Pipeline to Different Populations

Once the FATCAT-awFC pipeline was established, it was ready to be applied on the datasets of different populations.

1.8.1 MDD, REM, and NREM

Depression affects as many as one in five people in their lifetime and often runs a recurrent lifetime course (Rycroft-Malone et al., 2017). According to World Health Organization (WHO), depression is the leading cause of disability worldwide, and affects 300 million people globally (WHO | Depression, 2021). MDD has been well-documented to impact neural networks (Liu et

al., 2020). The most prevalent symptoms of MDD are anhedonia, irritability and depressed mood (*Diagnostic And Statistical Manual Of Mental Disorders*, 2015). In addition, many cognitive deficits occur as a result of MDD (Gotlib & Joormann, 2010; McIntyre et al., 2013; Roca et al., 2015).

Antidepressants have been shown to reduce depressive symptoms substantially within weeks or months (Trivedi et al., 2006). In some cases improvement in mood can be experienced as soon as one week following treatment (Ballenger, 2008; Smagula et al., 2015). However, MDD antidepressants may be ineffective for more than one-third of the population of depressed patients (Trivedi et al., 2006). An example of this was that a STAR*D study assessed the effect citalopram antidepressant had on MDD participants, and found that only 28% of participants reached remission (with the Hamilton Depression Rating Scale) (Trivedi et al., 2006).

1.8.2 Development & Adversity

By age 6 the brain is almost developed to adult size (Giedd & Rapoport, 2010). The brain in middle childhood continues to undergo development, with intensive synaptogenesis (including synaptic pruning) in gray matter, and white matter (axonal) maturation. The majority of white matter myelination occurs during the first two years of life (Yu et al., 2020). Middle childhood is characterized with slow white matter maturation (Yu et al., 2020). This includes changes in axonal packing, myelination, and synaptic density, which plays an important role in white matter maturation in children up to 8 years of age (Yu et al., 2020). However, myelination nevertheless continues to undergo changes throughout the first two to three decades of life (Yakovlev &

Lecours, 1967). The development changes of white matter is highly influenced by the environment and may be altered by learning or through activities (Fields, 2008; Zatorre et al., 2012). A hierarchical maturation occurs in the developing brain from primary sensorimotor systems to higher order functional systems. For instance the commissural tract splenium are among the first tracts to develop (part of the primary sensorimotor system) (Yu et al., 2020). Likewise, synaptogenesis happens most intensely in the first two years of life, afterwards it slows (Gattaz et al., 2004). However, synaptogenesis and synaptic pruning occur at different stages in different brain regions. For instance, the synapse elimination in the human brain may continue in the prefrontal cortex until the age of 12, whereas maximum synaptogenesis occurs at 15 months in the middle frontal gyrus. Functionally, the DMN at the ages 7-9 years old are sparsely functionally connected and becomes increasingly interconnected over development (Fair et al., 2008). This would be observed as an increased functional connectivity and the strengthening of networks.

Pre- and/or postnatal adversity has been known to impact the developing fetus and predispose children to developing psychopathological, neurobiological and behavioral issues (Monk et al., 2012). One area of particular interest is the influence of pre- or postnatal adversity on neurodevelopment (Thomason et al., 2021). Research in this area suggests that early adversity, typically leading to chronic stress, activates the stress response system (Shonkoff et al., 2012). The stress response system can hyper-activate the hypothalamic-pituitary-adrenal (HPA) axis (Boullier & Blair, 2018). The HPA axis triggers a Glucocorticoid response, in order to prepare for fight or flight. This chronic activation of the HPA axis is neurotoxic and may result in long-term effects negative effects and impact the immune system, endocrine system, and cause

dysregulated neural pathways (Boullier & Blair, 2018). Prenatal stress exposure may affect the offspring long term, causing cognitive deficits, psychiatric and behavioral issues (Lupien et al., 2009). Aside from this, maternal-fetal HPA axis hyper-activationdue to prenatal stress, prenatal depression, prenatal anxiety is capable of impacting children's long-term development and growth (Kinsella & Monk, 2009). Maternal anxiety and stress may also impact the offspring neurodevelopmental trajectories, which are reflected as atypical functional connectivity (De Asis-Cruz et al., 2020). However, regardless of the stress experienced some children form a coping mechanism, whereby they form a resilience to the adversity (Luthar & Cicchetti, 2000). These may appear in the form of higher tolerance to negative experiences, acceptance of change, tenacity, secure relationships and goal orientation (Connor & Davidson, 2003). This may also be reflected in brain connectivity and brain maturation.

1.9 Thesis Goals and Objectives

1.9.1 Objective

The global objective of this thesis was to propose a novel pipeline for combining fMRI and DTI data in a more intuitive manner, by integrating a toolbox with a sophisticated data fusion approach to allow us to detect atypical brain connectivity within RSNs. We propose using this intuitive multimodal analysis pipeline on brain imaging data of neuropsychiatric disorders such as MDD to utilize the complementary information embedded in different imaging modalities. This thesis develops a novel pipeline that combines a neuroimaging toolbox with a mathematically dense approach (for the data fusion of fMRI and DTI), to make the merging of neuroimaging data a simpler and more intuitive approach to apply on future work.

We hypothesized that we will be able to detect brain connectivity (either increases/decreases) within RSNs among different groups. In this thesis, we developed a FATCAT-awFC pipeline that utilizes two multivariate approaches (FATCAT and awFC) which shows promising application for the use in the neuroimaging community. Combining fMRI and DTI is typically a complicated and time-consuming task. Therefore, an engineering approach may help facilitate this process dramatically, by designing a user-friendly pipeline. A simpler and more straightforward approach to combining fMRI and DTI would encourage other researchers to combine these metrics. The FATCAT-awFC pipeline produced in this work, will reduce processing time, as it will be more intuitive for users to combine and analyze structural and functional connectivity.

1.9.2 Goal

A primary goal was to be able to successfully detect awFC group differences in different populations using the FATCAT-awFC pipeline. A secondary goal was to compute traditional structural and functional connectivity to compare the awFC measures to traditional structural and functional connectivity measures. A tertiary goal of this thesis was to test the hypothesis that cognitive and psychomotor deficits may be associated with atypical brain connectivity.

1.10 Specific Hypothesis/Aims

1. **Determine brain regions that are impacted due to MDD across multiple resting state networks using our designed FATCAT-awFC approach.** The aim of this thesis was to

develop a fast, practical and intuitive approach for combining functional and structural connectivity for the analysis of neuropsychiatric disorders in adults and to assess atypical brain development, within resting-state networks. Thus, we hypothesized that MDD patients will display reduced connectivity changes compared to healthy control participants.

2. **Investigate connectivity between brain regions in MDD non-remitters and MDD remitters and the cognitive dysfunction that is identified in MDD, using our novel FATCAT-awFC approach.** The hypothesis is that brain connectivity for i) MDD REM and NREM at baseline ii) MDD REM and NREM at week-8 iii) REM at baseline and REM at week-8, are distinguishable from one another with reduced connectivity for the REM compared to NREM.
3. **The FATCAT-awFC was used to investigate the brain connectivity of children during middle childhood with pre and/or postnatal adversity, and studied the associations between brain connectivity, orientation behavior and motor control at age three.** The hypothesis for this project is that the offspring (middle childhood aged) exposed to pre and/or postnatal adversity will have increased awFC between regions in RSNs compared to children without pre and/or postnatal adversity, which will be detectable with our novel FATCAT-awFC pipeline.

1.11 Contributions

This study applies our newly developed multimodal fusion pipeline – FATCAT-awFC - to different populations, to assess typical and atypical brain connectivity differences for different populations. The main contributions are as follows:

- In the first study:
    - We have proposed a new two-part pipeline that consists of a toolbox and a sophisticated data fusion approach, to combine structural and functional data. This allowed us to assess MDD and HC subjects.
    - The complementary nature of structural (obtained from DTI) and functional (obtained from fMRI), may provide users with a weighted measure that utilizes information from both modalities for a unique perspective
    - Since DTI data is routinely collected along with fMRI data, we propose that our FATCAT-awFC approach is able to be applied to other work in the future without the need to modify the data collection process for specific requirements
    - Our FATCAT-awFC method was able to identify distinguishable differences in RSN brain connectivity between MDD and HCs.
    - With this study we demonstrate that structural and functional connectivity may sometimes both be contributing to the awFC measure that compares two groups, and at times functional connectivity may be the one detecting the group differences whereas structural connectivity does not detect these differences.

- Therefore the fusion of these two metrics appears to be complimentary and may provide us a value that is better representative of the connectivity underlying neuropsychiatric disorders

- In the second study:
  - We applied our previously developed (from the first publication) FATCAT-awFC pipeline to MDD REM and NREM groups to assess whether there were distinguishable connectivity differences for participants unable to reach remission compared to participants that reached remission, at baseline and week-8. We also assessed whether there were detectable changes in connectivity for remitters at baseline within this study, compared to their brain connectivity 8-weeks post-treatment.
  - With this study we demonstrate that we are capable of identifying connectivity differences among groups.
  - The traditional structural and functional connectivity revealed that the awFC is, at times, supported by differences in functional connectivity alone, and other times supported by differences in both structural and functional connectivity.
  - With this study we were able to demonstrate the ease in which we were able to combine data into a single awFC metric using the FATCAT-awFC pipeline. We were able to assess 3 different comparisons between groups, all within a reasonable timeframe and with regular memory space using a MAC OS X operating system. Typically, data with higher dimension (due to the combination of fMRI and DTI) often have excessive memory requirements, and processing

speed for batch processing. However, our pipeline is user-friendly and may be used on a standard computer with no specific requirements.

- Extending our work, we also assessed the association between the awFC metric derived from our FATCAT-awFC pipeline and cognitive variables from the CNS-Vital Signs, using regression analysis
- It was revealed to us that cognitive flexibility was associated with awFC in non-remitters

- In the third study:
  - We propose that the combination of a toolbox with a complex mathematical approach to combine two metrics with ease, allows users to produce a fused metric, which may be better representative of the brain connectivity and may provide more information than performing one modality alone
  - We applied the novel FATCAT-awFC pipeline (introduced in the first project) which combines structural and functional data in a user-friendly and straightforward pipeline, and assessed a child population
  - The established FATCAT-awFC pipeline was applied to a child population (children with pre and/or postnatal adversity vs children without pre and/or postnatal adversity) to assess the different awFC between the groups
  - We demonstrate that the complementary information output from our FATCAT-awFC pipeline was able to detect differences between groups
  - What's more interesting is that with our FATCAT-awFC pipeline we were able to capture the combined effect of structural and functional connectivity on the brain

within RSNs rather than separating them out and analyzing how each may impact the overall connectivity

- With this study, we also demonstrate that brain connectivity measures (produced from our FATCAT-awFC pipeline) are associated with the Bayley scale outcome (i.e. psychomotor development and orientation behavior) in children within the middle childhood age group

References

Adali, T., Anderson, M., & Fu, G.-S. (2014). Diversity in Independent Component and Vector Analyses: Identifiability, algorithms, and applications in medical imaging. *IEEE Signal Processing Magazine*, *31*(3), 18–33. https://doi.org/10.1109/MSP.2014.2300511

Allen, E. A., Erhardt, E. B., Damaraju, E., Gruner, W., Segall, J. M., Silva, R. F., Havlicek, M., Rachakonda, S., Fries, J., Kalyanam, R., Michael, A. M., Caprihan, A., Turner, J. A., Eichele, T., Adelsheim, S., Bryan, A. D., Bustillo, J., Clark, V. P., Feldstein Ewing, S. W., … Calhoun, V. D. (2011). A baseline for the multivariate comparison of resting-state networks. *Frontiers in Systems Neuroscience*, *5*, 2. https://doi.org/10.3389/fnsys.2011.00002

Anderson, M., Adali, T., & Li, X.-L. (2012). Joint Blind Source Separation With Multivariate Gaussian Model: Algorithms and Performance Analysis. *IEEE Transactions on Signal Processing*, *60*(4), 1672–1683. https://doi.org/10.1109/TSP.2011.2181836

Baird, A. A., Colvin, M. K., Vanhorn, J. D., Inati, S., & Gazzaniga, M. S. (2005). Functional connectivity: Integrating behavioral, diffusion tensor imaging, and functional magnetic

resonance imaging data sets. *Journal of Cognitive Neuroscience*, *17*(4), 687–693. https://doi.org/10.1162/0898929053467569

Ballenger, J. C. (2008). Early Onset of Selective Serotonin Reuptake Inhibitor Antidepressant Action: Systematic Review and Meta-analysis. *Yearbook of Psychiatry and Applied Mental Health*, *2008*, 195–197. https://doi.org/10.1016/S0084-3970(08)70774-6

Bandettini, P. A., Wong, E. C., Hinks, R. S., Tikofsky, R. S., & Hyde, J. S. (1992). Time course EPI of human brain function during task activation. *Magnetic Resonance in Medicine*, *25*(2), 390–397. https://doi.org/10.1002/mrm.1910250220

Bansal, R., Staib, L., Laine, A., Hao, X., Xu, D., Liu, J., Weissman, M., & Peterson, B. (2012). Anatomical Brain Images Alone Can Accurately Diagnose Chronic Neuropsychiatric Illnesses. *PloS One*, *7*, e50698. https://doi.org/10.1371/journal.pone.0050698

Battiston, F., Nicosia, V., Chavez, M., & Latora, V. (2017). Multilayer motif analysis of brain networks. *Chaos: An Interdisciplinary Journal of Nonlinear Science*, *27*(4), 047404. https://doi.org/10.1063/1.4979282

Beaulieu, C., D'Arceuil, H., Hedehus, M., de Crespigny, A., Kastrup, A., & Moseley, M. E. (1999). Diffusion-weighted magnetic resonance imaging: Theory and potential applications to child neurology. *Seminars in Pediatric Neurology*, *6*(2), 87–100. https://doi.org/10.1016/s1071-9091(99)80035-7

Bielza, C., & Larrañaga, P. (2014). Bayesian networks in neuroscience: A survey. *Frontiers in Computational Neuroscience*, *0*. https://doi.org/10.3389/fncom.2014.00131

Bihan, D. L., Mangin, J.-F., Poupon, C., Clark, C. A., Pappata, S., Molko, N., & Chabriat, H. (2001). Diffusion tensor imaging: Concepts and applications. *Journal of Magnetic Resonance Imaging*, *13*(4), 534–546. https://doi.org/10.1002/jmri.1076

Bijsterbosch, J., Smith, S. M., & Beckmann, C. F. (2017). *Introduction to Resting State fMRI Functional Connectivity*. Oxford University Press.

Biswal, B., Zerrin Yetkin, F., Haughton, V. M., & Hyde, J. S. (1995). Functional connectivity in the motor cortex of resting human brain using echo-planar mri. *Magnetic Resonance in Medicine*, *34*(4), 537–541. https://doi.org/10.1002/mrm.1910340409

Boullier, M., & Blair, M. (2018). Adverse childhood experiences. *Paediatrics and Child Health*, *28*(3), 132–137. https://doi.org/10.1016/j.paed.2017.12.008

Bowman, F. D., Zhang, L., Derado, G., & Chen, S. (2012). Determining Functional Connectivity using fMRI Data with Diffusion-Based Anatomical Weighting. *NeuroImage*, *62*(3), 1769–1779. https://doi.org/10.1016/j.neuroimage.2012.05.032

Calamante, F., Masterton, R. A. J., Tournier, J.-D., Smith, R. E., Willats, L., Raffelt, D., & Connelly, A. (2013). Track-weighted functional connectivity (TW-FC): A tool for characterizing the structural–functional connections in the brain. *NeuroImage*, *70*, 199–210. https://doi.org/10.1016/j.neuroimage.2012.12.054

Calhoun, V. D., & Adalı, T. (2009). Feature-Based Fusion of Medical Imaging Data. *IEEE Transactions on Information Technology in Biomedicine : A Publication of the IEEE Engineering in Medicine and Biology Society*, *13*(5), 711–720. https://doi.org/10.1109/TITB.2008.923773

Calhoun, V. D., & Sui, J. (2016). Multimodal fusion of brain imaging data: A key to finding the missing link(s) in complex mental illness. *Biological Psychiatry : Cognitive Neuroscience and Neuroimaging*, *1*(3), 230–244. https://doi.org/10.1016/j.bpsc.2015.12.005

Chen, X., Wang, Z. J., & McKeown, M. (2016). Joint Blind Source Separation for Neurophysiological Data Analysis: Multiset and multimodal methods. *IEEE Signal Processing Magazine*, *33*(3), 86–107. https://doi.org/10.1109/MSP.2016.2521870

Chu, S.-H., Lenglet, C., Schreiner, M. W., Klimes-Dougan, B., Cullen, K. R., & Parhi, K. K. (2018). Altered Structural Connection Between Hippocampus and Insula in Adolescent Major Depressive Disorder using DTI. *2018 52nd Asilomar Conference on Signals, Systems, and Computers*, 1182–1186. https://doi.org/10.1109/ACSSC.2018.8645183

Connor, K. M., & Davidson, J. R. T. (2003). Development of a new resilience scale: The Connor-Davidson Resilience Scale (CD-RISC). *Depression and Anxiety*, *18*(2), 76–82. https://doi.org/10.1002/da.10113

Correa, N. M., Adali, T., Li, Y.-O., & Calhoun, V. D. (2010). Canonical Correlation Analysis for Data Fusion and Group Inferences: Examining applications of medical imaging data. *IEEE Signal Processing Magazine*, *27*(4), 39–50. https://doi.org/10.1109/MSP.2010.936725

Craddock, R. C., James, G. A., Holtzheimer, P. E., Hu, X. P., & Mayberg, H. S. (2012). A whole brain fMRI atlas generated via spatially constrained spectral clustering. *Human Brain Mapping*, *33*(8), 1914–1928. https://doi.org/10.1002/hbm.21333

De Asis-Cruz, J., Krishnamurthy, D., Zhao, L., Kapse, K., Vezina, G., Andescavage, N., Quistorff, J., Lopez, C., & Limperopoulos, C. (2020). Association of Prenatal Maternal Anxiety With Fetal Regional Brain Connectivity. *JAMA Network Open*, *3*(12), e2022349–e2022349. https://doi.org/10.1001/jamanetworkopen.2020.22349

De Blasi, B., Galazzo, I. B., Pasetto, L., Storti, S. F., Koepp, M., Barnes, A., & Menegaz, G. (2018). Pipeline Comparison for the Pre-Processing of Resting-State Data in Epilepsy.

2018 26th European Signal Processing Conference (EUSIPCO), 1137–1141. https://doi.org/10.23919/EUSIPCO.2018.8553119

De Domenico, M. (2017). Multilayer modeling and analysis of human brain networks. *GigaScience*, *6*(5). https://doi.org/10.1093/gigascience/gix004

De Domenico, M., Nicosia, V., Arenas, A., & Latora, V. (2014). *Layer aggregation and reducibility of multilayer interconnected networks*. https://doi.org/10.1038/ncomms7864

Diagnostic And Statistical Manual Of Mental Disorders (5th ed.). (2015). American Psychological Association.

DonGiovanni, D., & Vaina, L. M. (2016). Select and Cluster: A Method for Finding Functional Networks of Clustered Voxels in fMRI. *Computational Intelligence and Neuroscience*, *2016*, 1–19. https://doi.org/10.1155/2016/4705162

Du, Y., Allen, E. A., He, H., Sui, J., Wu, L., & Calhoun, V. D. (2016). Artifact removal in the context of group ICA: A comparison of single-subject and group approaches. *Human Brain Mapping*, *37*(3), 1005–1025. https://doi.org/10.1002/hbm.23086

Elliott, S. J. (2001). 8—Active Control of Nonlinear Systems. In S. J. Elliott (Ed.), *Signal Processing for Active Control* (pp. 367–409). Academic Press. https://doi.org/10.1016/B978-012237085-4/50010-7

Embrechts, M. J., Gatti, C. J., Linton, J., & Roysam, B. (2013). Hierarchical Clustering for Large Data Sets. In P. Georgieva, L. Mihaylova, & L. C. Jain (Eds.), *Advances in Intelligent Signal Processing and Data Mining* (Vol. 410, pp. 197–233). Springer Berlin Heidelberg. https://doi.org/10.1007/978-3-642-28696-4_8

Erhardt, E. B., Rachakonda, S., Bedrick, E., Allen, E., Adali, T., & Calhoun, V. D. (2011). Comparison of multi-subject ICA methods for analysis of fMRI data. *Human Brain Mapping*, *32*(12), 2075–2095. https://doi.org/10.1002/hbm.21170

Fair, D. A., Cohen, A. L., Dosenbach, N. U. F., Church, J. A., Miezin, F. M., Barch, D. M., Raichle, M. E., Petersen, S. E., & Schlaggar, B. L. (2008). The maturing architecture of the brain's default network. *Proceedings of the National Academy of Sciences of the United States of America*, *105*(10), 4028–4032. https://doi.org/10.1073/pnas.0800376105

Faro, S. H., Mohamed, F. B., Law, M., & Ulmer, J. T. (2011). *Functional Neuroradiology: Principles and Clinical Applications*. Springer.

Fields, R. D. (2008). White matter in learning, cognition and psychiatric disorders. *Trends in Neurosciences*, *31*(7), 361–370. https://doi.org/10.1016/j.tins.2008.04.001

Forstmann, B. U., Jahfari, S., Scholte, H. S., Wolfensteller, U., van den Wildenberg, W. P. M., & Ridderinkhof, K. R. (2008). Function and Structure of the Right Inferior Frontal Cortex Predict Individual Differences in Response Inhibition: A Model-Based Approach. *Journal of Neuroscience*, *28*(39), 9790–9796. https://doi.org/10.1523/JNEUROSCI.1465-08.2008

Frau-Pascual, A., Fogarty, M., Fischl, B., Yendiki, A., Aganj, I., & Initiative, for the A. D. N. (2018). Quantification of Structural Brain Connectivity via a Conductance Model. *BioRxiv*, 415489. https://doi.org/10.1101/415489

Gattaz, W., Abrahão, A., & Foccacia, R. (2004). Childhood meningitis, brain maturation and the risk of psychosis. *European Archives of Psychiatry and Clinical Neuroscience*, *254*, 23–26. https://doi.org/10.1007/s00406-004-0431-3

Ghosh, A., Rho, Y., McIntosh, A. R., Kötter, R., & Jirsa, V. K. (2008). Noise during Rest Enables the Exploration of the Brain's Dynamic Repertoire. *PLoS Computational Biology*, *4*(10), e1000196. https://doi.org/10.1371/journal.pcbi.1000196

Giedd, J. N., & Rapoport, J. L. (2010). Structural MRI of Pediatric Brain Development: What Have We Learned and Where Are We Going? *Neuron*, *67*(5), 728–734. https://doi.org/10.1016/j.neuron.2010.08.040

Glover, G. H. (2011). Overview of Functional Magnetic Resonance Imaging. *Neurosurgery Clinics of North America*, *22*(2), 133–139. https://doi.org/10.1016/j.nec.2010.11.001

Gotlib, I. H., & Joormann, J. (2010). Cognition and Depression: Current Status and Future Directions. *Annual Review of Clinical Psychology*, *6*, 285–312. https://doi.org/10.1146/annurev.clinpsy.121208.131305

Greicius, M. D., Flores, B. H., Menon, V., Glover, G. H., Solvason, H. B., Kenna, H., Reiss, A. L., & Schatzberg, A. F. (2007). Resting-State Functional Connectivity in Major Depression: Abnormally Increased Contributions from Subgenual Cingulate Cortex and Thalamus. *Biological Psychiatry*, *62*(5), 429–437. https://doi.org/10.1016/j.biopsych.2006.09.020

Greicius, M. D., Supekar, K., Menon, V., & Dougherty, R. F. (2009). Resting-State Functional Connectivity Reflects Structural Connectivity in the Default Mode Network. *Cerebral Cortex*, *19*(1), 72–78. https://doi.org/10.1093/cercor/bhn059

Guo, S., Huang, C.-C., Zhao, W., Yang, A. C., Lin, C.-P., Nichols, T., & Tsai, S.-J. (2018). Combining multi-modality data for searching biomarkers in schizophrenia. *PLOS ONE*, *13*(2), e0191202. https://doi.org/10.1371/journal.pone.0191202

Hagmann, P., Cammoun, L., Gigandet, X., Meuli, R., Honey, C. J., Wedeen, V. J., & Sporns, O. (2008). Mapping the Structural Core of Human Cerebral Cortex. *PLOS Biology*, *6*(7), e159. https://doi.org/10.1371/journal.pbio.0060159

Hammoud, Z., & Kramer, F. (2020). Multilayer networks: Aspects, implementations, and application in biomedicine. *Big Data Analytics*, *5*(1), 2. https://doi.org/10.1186/s41044-020-00046-0

Handwerker, D. A., & Bandettini, P. A. (2011). Hemodynamic signals not predicted? Not so: a comment on Sirotin and Das (2009). *NeuroImage*, *55*(4), 1409–1412. https://doi.org/10.1016/j.neuroimage.2010.04.037

Hayasaka, S., & Laurienti, P. J. (2010). Comparison of Characteristics between Region- and Voxel-Based Network Analyses in Resting-State fMRI Data. *NeuroImage*, *50*(2), 499–508. https://doi.org/10.1016/j.neuroimage.2009.12.051

Haykin, S. (2000). CHAPTER 4 - Neural Networks: A Guided Tour. In N. K. Sinha & M. M. Gupta (Eds.), *Soft Computing and Intelligent Systems* (pp. 71–80). Academic Press. https://doi.org/10.1016/B978-012646490-0/50007-X

Hecke, W. V., Emsell, L., & Sunaert, S. (Eds.). (2016). *Diffusion Tensor Imaging: A Practical Handbook*. Springer-Verlag. https://www.springer.com/gp/book/9781493931170

Honey, C. J., Kötter, R., Breakspear, M., & Sporns, O. (2007). Network structure of cerebral cortex shapes functional connectivity on multiple time scales. *Proceedings of the National Academy of Sciences*, *104*(24), 10240–10245.

Honey, C. J., Sporns, O., Cammoun, L., Gigandet, X., Thiran, J. P., Meuli, R., & Hagmann, P. (2009). Predicting human resting-state functional connectivity from structural

connectivity. *Proceedings of the National Academy of Sciences of the United States of America*, *106*(6), 2035–2040. https://doi.org/10.1073/pnas.0811168106

Huster, R. J., Debener, S., Eichele, T., & Herrmann, C. S. (2012). Methods for Simultaneous EEG-fMRI: An Introductory Review. *Journal of Neuroscience*, *32*(18), 6053–6060. https://doi.org/10.1523/JNEUROSCI.0447-12.2012

Jbabdi, S., & Johansen-Berg, H. (2011). Tractography: Where do we go from here? *Brain Connectivity*, *1*(3), 169–183. https://doi.org/10.1089/brain.2011.0033

Joel, S. E., Caffo, B. S., van Zijl, P. C. M., & Pekar, J. J. (2011). On the relationship between seed-based and ICA-based measures of functional connectivity. *Magnetic Resonance in Medicine*, *66*(3), 644–657. https://doi.org/10.1002/mrm.22818

Kang, H., Ombao, H., Fonnesbeck, C., Ding, Z., & Morgan, V. L. (2017). A Bayesian Double Fusion Model for Resting-State Brain Connectivity Using Joint Functional and Structural Data. *Brain Connectivity*, *7*(4), 219–227. https://doi.org/10.1089/brain.2016.0447

Khosla, M., Jamison, K., Ngo, G. H., Kuceyeski, A., & Sabuncu, M. R. (2018). Machine learning in resting-state fMRI analysis. *ArXiv:1812.11477 [Cs, q-Bio, Stat]*. http://arxiv.org/abs/1812.11477

Kim, M. J., & Whalen, P. J. (2009). The Structural Integrity of an Amygdala-Prefrontal Pathway Predicts Trait Anxiety. *Journal of Neuroscience*, *29*(37), 11614–11618. https://doi.org/10.1523/JNEUROSCI.2335-09.2009

Kinsella, M. T., & Monk, C. (2009). Impact of Maternal Stress, Depression and Anxiety on Fetal Neurobehavioral Development. *Clinical Obstetrics & Gynecology*, *52*(3), 425–440. https://doi.org/10.1097/GRF.0b013e3181b52df1

Kitanidis, P. (2005). New Vistas in Geostatistical and Bayesian Methods in Interpolation and Inverse Problems. *AGU Fall Meeting Abstracts*.

Kivelä, M., Arenas, A., Barthelemy, M., Gleeson, J. P., Moreno, Y., & Porter, M. A. (2014). Multilayer networks. *Journal of Complex Networks*, *2*(3), 203–271. https://doi.org/10.1093/comnet/cnu016

Koch, M. A., Norris, D. G., & Hund-Georgiadis, M. (2002). An investigation of functional and anatomical connectivity using magnetic resonance imaging. *NeuroImage*, *16*(1), 241–250. https://doi.org/10.1006/nimg.2001.1052

Kwong, K. K., Belliveau, J. W., Chesler, D. A., Goldberg, I. E., Weisskoff, R. M., Poncelet, B. P., Kennedy, D. N., Hoppel, B. E., Cohen, M. S., & Turner, R. (1992). Dynamic magnetic resonance imaging of human brain activity during primary sensory stimulation. *Proceedings of the National Academy of Sciences of the United States of America*, *89*(12), 5675–5679. https://doi.org/10.1073/pnas.89.12.5675

Lee, M. H., Smyser, C. D., & Shimony, J. S. (2013). Resting-state fMRI: A review of methods and clinical applications. *AJNR. American Journal of Neuroradiology*, *34*(10), 1866–1872. https://doi.org/10.3174/ajnr.A3263

Li, X.-L., Adalı, T., & Anderson, M. (2011). Joint blind source separation by generalized joint diagonalization of cumulant matrices. *Signal Processing*, *91*(10), 2314–2322. https://doi.org/10.1016/j.sigpro.2011.04.016

Li, Y.-O., Adali, Tü., Wang, W., & Calhoun, V. D. (2009). Joint Blind Source Separation by Multiset Canonical Correlation Analysis. *IEEE Transactions on Signal Processing*, *57*(10), 3918–3929. https://doi.org/10.1109/TSP.2009.2021636

Lim, C., Li, X., Li, K., Guo, L., & Liu, T. (2011). Brain state change detection via fiber-centered functional connectivity analysis. *2011 IEEE International Symposium on Biomedical Imaging: From Nano to Macro*, 2155–2160. https://doi.org/10.1109/ISBI.2011.5872839

Lindenberger, U., Li, S.-C., Gruber, W., & Müller, V. (2009). Brains swinging in concert: Cortical phase synchronization while playing guitar. *BMC Neuroscience*, *10*(1), 22. https://doi.org/10.1186/1471-2202-10-22

Liu, Y., Chen, Y., Liang, X., Li, D., Zheng, Y., Zhang, H., Cui, Y., Chen, J., Liu, J., & Qiu, S. (2020). Altered Resting-State Functional Connectivity of Multiple Networks and Disrupted Correlation With Executive Function in Major Depressive Disorder. *Frontiers in Neurology*, *11*. https://doi.org/10.3389/fneur.2020.00272

Logothetis, N. K. (2008). What we can do and what we cannot do with fMRI. *Nature*, *453*(7197), 869–878. https://doi.org/10.1038/nature06976

Lupien, S. J., McEwen, B. S., Gunnar, M. R., & Heim, C. (2009). Effects of stress throughout the lifespan on the brain, behaviour and cognition. *Nature Reviews Neuroscience*, *10*(6), 434–445. https://doi.org/10.1038/nrn2639

Luthar, S. S., & Cicchetti, D. (2000). The construct of resilience: Implications for interventions and social policies. *Development and Psychopathology*, *12*(4), 857–885. https://doi.org/10.1017/S0954579400004156

Lv, J., Guo, L., Li, K., Hu, X., Zhu, D., Han, J., & Liu, T. (2011). Activated fibers: Fiber-centered activation detection in task-based FMRI. *Information Processing in Medical Imaging: Proceedings of the ... Conference*, *22*, 574–587. https://doi.org/10.1007/978-3-642-22092-0_47

Mannelli, L., Nougaret, S., Vargas, H. A., & Do, R. K. G. (2015). Advances in Diffusion-Weighted Imaging. *Radiologic Clinics*, *53*(3), 569–581. https://doi.org/10.1016/j.rcl.2015.01.002

McIntyre, R. S., Cha, D. S., Soczynska, J. K., Woldeyohannes, H. O., Gallaugher, L. A., Kudlow, P., Alsuwaidan, M., & Baskaran, A. (2013). COGNITIVE DEFICITS AND FUNCTIONAL OUTCOMES IN MAJOR DEPRESSIVE DISORDER: DETERMINANTS, SUBSTRATES, AND TREATMENT INTERVENTIONS: Review: Cognitive Deficits and Functional Outcomes in MDD. *Depression and Anxiety*, *30*(6), 515–527. https://doi.org/10.1002/da.22063

Milo, R. (2002). Network Motifs: Simple Building Blocks of Complex Networks. *Science*, *298*(5594), 824–827. https://doi.org/10.1126/science.298.5594.824

Monk, C., Spicer, J., & Champagne, F. A. (2012). Linking prenatal maternal adversity to developmental outcomes in infants: The role of epigenetic pathways. *Development and Psychopathology*, *24*(4), 1361–1376. https://doi.org/10.1017/S0954579412000764

Nord, C. L., Gray, A., Charpentier, C. J., Robinson, O. J., & Roiser, J. P. (2017). Unreliability of putative fMRI biomarkers during emotional face processing. *NeuroImage*, *156*, 119–127. https://doi.org/10.1016/j.neuroimage.2017.05.024

Nucifora, P. G. P., Phd, R. V., Lee, S., & Melhem, E. R. (2007). *Diffusion-Tensor MR imaging and tractography: Exploring brain microstructure and connectivity*.

Özarslan, E., & Mareci, T. H. (2003). Generalized diffusion tensor imaging and analytical relationships between diffusion tensor imaging and high angular resolution diffusion imaging. *Magnetic Resonance in Medicine*, *50*(5), 955–965. https://doi.org/10.1002/mrm.10596

.

Papanicolaou, A. C. (2017). *The Oxford Handbook of Functional Brain Imaging in Neuropsychology and Cognitive Neurosciences*. Oxford University Press.

Park, B., Eo, J., & Park, H.-J. (2017). Structural Brain Connectivity Constrains within-a-Day Variability of Direct Functional Connectivity. *Frontiers in Human Neuroscience*, *11*. https://doi.org/10.3389/fnhum.2017.00408

Parker, G. J. M. (2004). Analysis of MR diffusion weighted images. *The British Journal of Radiology*, *77*(suppl_2), S176–S185. https://doi.org/10.1259/bjr/81090732

Patterson, D. M., Padhani, A. R., & Collins, D. J. (2008). Technology Insight: Water diffusion MRI—a potential new biomarker of response to cancer therapy. *Nature Clinical Practice Oncology*, *5*(4), 220–233. https://doi.org/10.1038/ncponc1073

Poldrack, R. A., Mumford, J. A., & Nichols, T. E. (2011). *Handbook of Functional MRI Data Analysis*. Cambridge University Press. https://www.cambridge.org/core/books/handbook-of-functional-mri-data-analysis/8EDF966C65811FCCC306F7C916228529

Poustchi-Amin, M., Mirowitz, S. A., Brown, J. J., McKinstry, R. C., & Li, T. (2001). Principles and Applications of Echo-planar Imaging: A Review for the General Radiologist. *RadioGraphics*, *21*(3), 767–779. https://doi.org/10.1148/radiographics.21.3.g01ma23767

Putnam, M. C., Wig, G. S., Grafton, S. T., Kelley, W. M., & Gazzaniga, M. S. (2008). Structural organization of the corpus callosum predicts the extent and impact of cortical activity in the nondominant hemisphere. *The Journal of Neuroscience: The Official Journal of the Society for Neuroscience*, *28*(11), 2912–2918. https://doi.org/10.1523/JNEUROSCI.2295-07.2008

Qayyum, A. (2009). Diffusion-weighted Imaging in the Abdomen and Pelvis: Concepts and Applications. *RadioGraphics*, *29*(6), 1797–1810. https://doi.org/10.1148/rg.296095521

Roca, M., Vives, M., López-Navarro, E., García-Campayo, J., & Gili, M. (2015). Cognitive impairments and depression: A critical review. *Actas Espanolas De Psiquiatria*, *43*(5), 187–193.

Rycroft-Malone, J., Gradinger, F., Griffiths, H. O., Crane, R., Gibson, A., Mercer, S., Anderson, R., & Kuyken, W. (2017). *Accessibility and implementation in the UK NHS services of an effective depression relapse prevention programme: Learning from mindfulness-based cognitive therapy through a mixed-methods study*. NIHR Journals Library. http://www.ncbi.nlm.nih.gov/books/NBK425272/

Saxe, R., Brett, M., & Kanwisher, N. (2006). Divide and conquer: A defense of functional localizers. *NeuroImage*, *30*(4), 1088–1096. https://doi.org/10.1016/j.neuroimage.2005.12.062

Shmuel, A., & Leopold, D. A. (2008). Neuronal correlates of spontaneous fluctuations in fMRI signals in monkey visual cortex: Implications for functional connectivity at rest. *Human Brain Mapping*, *29*(7), 751–761. https://doi.org/10.1002/hbm.20580

Shonkoff, J. P., Garner, A. S., The Committee on Psychosocial Aspects of Child and Family Health, C. on E. C., Siegel, B. S., Dobbins, M. I., Earls, M. F., Garner, A. S., McGuinn, L., Pascoe, J., & Wood, D. L. (2012). The Lifelong Effects of Early Childhood Adversity and Toxic Stress. *Pediatrics*, *129*(1), e232–e246. https://doi.org/10.1542/peds.2011-2663

Sirotin, Y. B., & Das, A. (2009). Anticipatory haemodynamic signals in sensory cortex not predicted by local neuronal activity. *Nature*, *457*(7228), 475–479. https://doi.org/10.1038/nature07664

Skudlarski, P., Jagannathan, K., Calhoun, V. D., Hampson, M., Skudlarska, B. A., & Pearlson, G. (2008). Measuring Brain Connectivity: Diffusion Tensor Imaging Validates Resting

State Temporal Correlations. *NeuroImage*, *43*(3), 554–561. https://doi.org/10.1016/j.neuroimage.2008.07.063

Smagula, S. F., Butters, M. A., Anderson, S. J., Lenze, E. J., Dew, M. A., Mulsant, B. H., Lotrich, F. E., Aizenstein, H., & Reynolds, C. F., III. (2015). Antidepressant Response Trajectories and Associated Clinical Prognostic Factors Among Older Adults. *JAMA Psychiatry*, *72*(10), 1021–1028. https://doi.org/10.1001/jamapsychiatry.2015.1324

Smith, S. M., Vidaurre, D., Beckmann, C. F., Glasser, M. F., Jenkinson, M., Miller, K. L., Nichols, T. E., Robinson, E. C., Salimi-Khorshidi, G., Woolrich, M. W., Barch, D. M., Uğurbil, K., & Essen, D. C. V. (2013). Functional connectomics from resting-state fMRI. *Trends in Cognitive Sciences*, *17*(12), 666–682. https://doi.org/10.1016/j.tics.2013.09.016

Staempfli, P., Reischauer, C., Jaermann, T., Valavanis, A., Kollias, S., & Boesiger, P. (2008). Combining fMRI and DTI: A framework for exploring the limits of fMRI-guided DTI fiber tracking and for verifying DTI-based fiber tractography results. *NeuroImage*, *39*(1), 119–126. https://doi.org/10.1016/j.neuroimage.2007.08.025

Stippich, C. (2015). *Clinical Functional MRI: Presurgical Functional Neuroimaging*. Springer.

Sui, J., He, H., Yu, Q., Chen, J., Rogers, J., Pearlson, G. D., Mayer, A., Bustillo, J., Canive, J., & Calhoun, V. D. (2013). Combination of Resting State fMRI, DTI, and sMRI Data to Discriminate Schizophrenia by N-way MCCA + jICA. *Frontiers in Human Neuroscience*, *7*. https://doi.org/10.3389/fnhum.2013.00235

Sui, J., Huster, R., Yu, Q., Segall, J. M., & Calhoun, V. D. (2014). Function-Structure Associations of the Brain: Evidence from Multimodal Connectivity and Covariance Studies. *NeuroImage*, *102 Pt 1*, 11–23. https://doi.org/10.1016/j.neuroimage.2013.09.044

Sui, J., Pearlson, G., Caprihan, A., Adali, T., Kiehl, K. A., Liu, J., Yamamoto, J., & Calhoun, V. D. (2011). Discriminating schizophrenia and bipolar disorder by fusing fMRI and DTI in a multimodal CCA+ joint ICA model. *NeuroImage*, *57*(3), 839–855. https://doi.org/10.1016/j.neuroimage.2011.05.055

Thirion, B., Varoquaux, G., Dohmatob, E., & Poline, J.-B. (2014). Which fMRI clustering gives good brain parcellations? *Frontiers in Neuroscience*, *8*. https://doi.org/10.3389/fnins.2014.00167

Thomason, M. E., Hect, J. L., Waller, R., & Curtin, P. (2021). Interactive relations between maternal prenatal stress, fetal brain connectivity, and gestational age at delivery. *Neuropsychopharmacology*, *46*(10), 1839–1847. https://doi.org/10.1038/s41386-021-01066-7

Trivedi, M. H., Rush, A. J., Wisniewski, S. R., Nierenberg, A. A., Warden, D., Ritz, L., Norquist, G., Howland, R. H., Lebowitz, B., McGrath, P. J., Shores-Wilson, K., Biggs, M. M., Balasubramani, G. K., Fava, M., & STAR*D Study Team. (2006). Evaluation of Outcomes With Citalopram for Depression Using Measurement-Based Care in STAR*D: Implications for Clinical Practice. *American Journal of Psychiatry*, *163*(1), 28–40. https://doi.org/10.1176/appi.ajp.163.1.28

Tulay, E. E., Metin, B., Tarhan, N., & Arıkan, M. K. (2019). Multimodal Neuroimaging: Basic Concepts and Classification of Neuropsychiatric Diseases. *Clinical EEG and Neuroscience*, *50*(1), 20–33. https://doi.org/10.1177/1550059418782093

Turk, M. (2014). Multimodal interaction: A review. *Pattern Recognition Letters*, *36*, 189–195. https://doi.org/10.1016/j.patrec.2013.07.003

.

Valdes-Sosa, P. A., Sanchez-Bornot, J. M., Sotero, R. C., Iturria-Medina, Y., Aleman-Gomez, Y., Bosch-Bayard, J., Carbonell, F., & Ozaki, T. (2009). Model driven EEG/fMRI fusion of brain oscillations. *Human Brain Mapping*, *30*(9), 2701–2721. https://doi.org/10.1002/hbm.20704

Varoquaux, G., Sadaghiani, S., Pinel, P., Kleinschmidt, A., Poline, J. B., & Thirion, B. (2010). A group model for stable multi-subject ICA on fMRI datasets. *NeuroImage*, *51*(1), 288–299. https://doi.org/10.1016/j.neuroimage.2010.02.010

Vassal, F., Schneider, F., Boutet, C., Jean, B., Sontheimer, A., & Lemaire, J.-J. (2016). Combined DTI Tractography and Functional MRI Study of the Language Connectome in Healthy Volunteers: Extensive Mapping of White Matter Fascicles and Cortical Activations. *PLOS ONE*, *11*(3), e0152614. https://doi.org/10.1371/journal.pone.0152614

Vouche, M., Kulik, L., Atassi, R., Memon, K., Hickey, R., Ganger, D., Miller, F. H., Yaghmai, V., Abecassis, M., Baker, T., Mulcahy, M., Nayar, R., Lewandowski, R. J., & Salem, R. (2013). Radiological-Pathological Analysis of WHO, RECIST, EASL, mRECIST and DWI: Imaging Analysis from a Prospective Randomized Trial of Y90 +/− Sorafenib. *Hepatology (Baltimore, Md.)*, *58*(5), 1655–1666. https://doi.org/10.1002/hep.26487

WHO | Depression. (2021). WHO. http://www.who.int/mediacentre/factsheets/fs369/en/

Wu, F., Tu, Z., Sun, J., Geng, H., Zhou, Y., Jiang, X., Li, H., & Kong, L. (2020). Abnormal Functional and Structural Connectivity of Amygdala-Prefrontal Circuit in First-Episode Adolescent Depression: A Combined fMRI and DTI Study. *Frontiers in Psychiatry*, *10*. https://doi.org/10.3389/fpsyt.2019.00983

Wu, S., Angelikopoulos, P., Papadimitriou, C., Moser, R., & Koumoutsakos, P. (2016). A hierarchical Bayesian framework for force field selection in molecular dynamics

simulations. *Philosophical Transactions of the Royal Society A: Mathematical, Physical and Engineering Sciences*, *374*(2060), 20150032. https://doi.org/10.1098/rsta.2015.0032

Xue, W., Bowman, F. D., Pileggi, A. V., & Mayer, A. R. (2015). A multimodal approach for determining brain networks by jointly modeling functional and structural connectivity. *Frontiers in Computational Neuroscience*, *9*. https://doi.org/10.3389/fncom.2015.00022

Yakovlev, P., & Lecours, A. (1967). The myelogenetic cycles of regional maturation of the brain. *Undefined*. https://www.semanticscholar.org/paper/The-myelogenetic-cycles-of-regional-maturation-of-Yakovlev-Lecours/ae1b5cb44581d479695c9263f37aa04ea570c322

Yeo, B. T. T., Krienen, F. M., Sepulcre, J., Sabuncu, M. R., Lashkari, D., Hollinshead, M., Roffman, J. L., Smoller, J. W., Zöllei, L., Polimeni, J. R., Fischl, B., Liu, H., & Buckner, R. L. (2011). The organization of the human cerebral cortex estimated by intrinsic functional connectivity. *Journal of Neurophysiology*, *106*(3), 1125–1165. https://doi.org/10.1152/jn.00338.2011

Yu, Q., Peng, Y., Kang, H., Peng, Q., Ouyang, M., Slinger, M., Hu, D., Shou, H., Fang, F., & Huang, H. (2020). Differential White Matter Maturation from Birth to 8 Years of Age. *Cerebral Cortex*, *30*(4), 2674–2690. https://doi.org/10.1093/cercor/bhz268

Zalesky, A. (2008). DT-MRI Fiber Tracking: A Shortest Paths Approach. *IEEE Transactions on Medical Imaging*, *27*(10), 1458–1471. https://doi.org/10.1109/TMI.2008.923644

Zalesky, A., & Fornito, A. (2009). A DTI-Derived Measure of Cortico-Cortical Connectivity. *IEEE Transactions on Medical Imaging*, *28*(7), 1023–1036. https://doi.org/10.1109/TMI.2008.2012113

Zatorre, R. J., Fields, R. D., & Johansen-Berg, H. (2012). Plasticity in gray and white: Neuroimaging changes in brain structure during learning. *Nature Neuroscience*, *15*(4), 528–536. https://doi.org/10.1038/nn.3045

Zhang, D., & Lei, J. (2011). Kinematic analysis of a novel 3-DOF actuation redundant parallel manipulator using artificial intelligence approach. *Robotics and Computer-Integrated Manufacturing*, *27*(1), 157–163. https://doi.org/10.1016/j.rcim.2010.07.003

Zhu, D., Zhang, T., Jiang, X., Hu, X., Chen, H., Yang, N., Lv, J., Han, J., Guo, L., & Liu, T. (2014). Fusing DTI and FMRI Data: A Survey of Methods and Applications. *NeuroImage*, *102 Pt 1*, 184–191. https://doi.org/10.1016/j.neuroimage.2013.09.071

Chapter 2: Exploring Brain Connectivity Changes in Major Depressive Disorder Using Functional-Structural Data Fusion: A CAN-BIND-1 Study

Published in Human Brain Mapping on September 2021

Sondos Ayyash[1], Andrew D. Davis[2,6], Gésine L. Alders[3], Glenda MacQueen[4,5] , Stephen C. Strother[6-8] , Stefanie Hassel[4,5], Mojdeh Zamyadi[6], Stephen R. Arnott[6], Jacqueline K. Harris[12], Raymond W. Lam[13], Roumen Milev[14], Daniel J. Müller[10,15], Sidney H. Kennedy[7,9-11,16], Susan Rotzinger [10, 11,16], Benicio N. Frey[2,3,17], Luciano Minuzzi[2,3,17], Geoffrey B. Hall[2,3,18,] on behalf of the CAN-BIND Investigator Team.*

[1] School of Biomedical Engineering, McMaster University, Hamilton, ON, Canada

[2] Department of Psychiatry and Behavioural Neurosciences, McMaster University, Hamilton, ON, Canada

[3] Neuroscience Graduate Program, McMaster University, Hamilton, ON, Canada

[4] Mathison Centre for Mental Health Research and Education, Cumming School of Medicine, University of Calgary, Calgary, AB, Canada

[5] Department of Psychiatry, Cumming School of Medicine, University of Calgary, Calgary, AB, Canada

[6] Rotman Research Institute, Baycrest, Toronto, ON, Canada

[7] Institute of Medical Science, University of Toronto, Toronto, ON, Canada

[8] Department of Medical Biophysics, University of Toronto, ON, Canada

[9] Centre for Mental Health, University Health Network, Toronto, ON, Canada

[10] Department of Psychiatry, University of Toronto, Toronto, ON, Canada

[11] Krembil Research Institute, University Health Network, Toronto, ON, Canada

[12] Department of Computer Science, University of Alberta, Edmonton, AB, Canada

[13] Department of Psychiatry, University of British Columbia, Vancouver, BC, Canada

[14] Departments of Psychiatry and Psychology, Queen's University, Providence Care Hospital, Kingston, ON, Canada

[15] Campbell Family Mental Health Research Institute, Centre for Addiction and Mental Health, Toronto, ON, Canada

[16] Centre for Depression and Suicide Studies, and Li Ka Shing Knowledge Institute, St. Michael's Hospital, Toronto, ON, Canada

[17] Mood Disorders Treatment and Research Centre and Women's Health Concerns Clinic, St. Joseph's Healthcare, Hamilton, ON, Canada

[18] Department of Psychology Neuroscience & Behaviour, McMaster University, Hamilton, ON, Canada *

2.1 Abstract

There is a growing interest in examining the wealth of data generated by fusing functional and structural imaging information sources. These approaches may have clinical utility in identifying disruptions in the brain networks that underlie Major Depressive Disorder (MDD). We

combined an existing software toolbox with a mathematically dense statistical method to produce a novel processing pipeline for the fast and easy implementation of data fusion analysis. The novel *FATCAT-awFC* pipeline was then utilized to identify connectivity (conventional functional, conventional structural and anatomically weighted functional connectivities) changes in MDD patients compared to healthy comparison participants (HC). Data was acquired from the Canadian Biomarker Integration Network for Depression (CAN-BIND-1) study. Large-scale resting-state networks were assessed. We found statistically significant awFC group differences in the default mode network and the ventral attention network, with a small effect size ($d<0.4$). Functional and structural connectivity seemed to overlap in significance between one region-pair within the default mode network. By combining structural and functional data, anatomically weighted functional connectivity served to heighten or reduce the magnitude of connectivity differences in various regions distinguishing MDD from HC. This can help us more fully understand the interconnected nature between structural and functional connectivity as it relates to depression.

Key Words: Neuroimaging; major depressive disorder; Structural connectivity; Functional connectivity; data fusion; Resting brain networks; Toolbox

2.2 Introduction

Increasing interest in brain connectivity patterns in illness and in health has given rise to the development of multimodal imaging analysis approaches, utilized to combine functional magnetic resonance imaging (fMRI) data with diffusion tensor imaging (DTI) data (Reddi, 2017; Zhu et al., 2014). Multimodal imaging analysis methods aim to capture the complex interactions

between structural and functional connectivity in brain networks and provide new insights into brain connectivity. Complex and heterogeneous disorders such as major depressive disorder (MDD) can benefit from multimodal imaging analysis, which offers a better understanding of the joint structural and functional changes in human brain connectivity patterns (Zhu et al., 2014).

MDD is associated with both structural and functional abnormalities between brain regions within a number of resting-state networks (Coloigner et al., 2019; Kaiser, Andrews-Hanna, Wager, & Pizzagalli, 2015). Functional connectivity analyses use resting state fMRI (rsfMRI) to identify synchronous inter-regional temporal correlations in blood oxygen level dependent signals (Biswal, Van Kylen, & Hyde, 1997). Common approaches to identify these functionally connected brain networks utilize independent component analysis (ICA) or Pearson-*r* correlations to isolate and index the connectivity between regions in anatomically segregated brain networks (Yoo et al., 2018). Group ICA has been widely used for multi-participant studies to identify a set of commonly replicable, temporally synchronized resting-state networks (RSNs) (Beckmann, DeLuca, Devlin, & Smith, 2005; Damoiseaux et al., 2006; Esposito et al., 2005). Typically, these networks include the visual, somatomotor, default mode (DMN), frontoparietal (FPN), dorsal attention (DAN), ventral attention (VAN), and limbic networks (LIM) (Yeo et al., 2011). From diffusion tensor imaging (DTI), a wide range of metrics, including fractional anisotropy, mean diffusivity, tract density, tract volume and number of tracts, can be used to represent structural connectivity in MDD (Klooster et al., 2020). However, edge weight (which includes a combination of number of tracts, tract length and region of interest (ROI) size) may be a more suitable metric for the measurement of structural connectivity in relation to functional connectivity (Huang & Ding, 2016). While previous studies have reported significant alterations in structural connectivity in MDD, these findings have shown considerable variability, and

depending on the network and/or tracts examined, have pointed to increases (de Kwaasteniet et al., 2013), decreases (Davis et al., 2019; Wu et al., 2020), or both increases and decreases (Wu et al., 2011) in connectivity. Supplementing the structural connectivity data with functional indices may provide some clarity regarding the brain changes that are having the greatest impact in depression.

Importantly, the above studies do point to a concordance between the functional brain regions that are dysregulated in MDD and their associated internodal structural connectivity (Greicius, Supekar, Menon, & Dougherty, 2009). However, the indices of functional connectivity do not map directly, one to one, with the white matter connectivity alterations identified by DTI (Greicius et al., 2009). Indeed, it has been suggested that neither functional nor structural imaging modalities are reliable enough alone to reflect the highly interconnected nature of the brain (Kambeitz et al., 2017; Park & Friston, 2013). Functional connectivity may arise from indirect white-matter pathways (*N*th-order structural connections) or undetectable white matter connections (from DTI imaging techniques) (Koch, Norris, & Hund-Georgiadis, 2002). Moreover, with DTI, branching or crossing fibers can make it difficult to resolve long-range interhemispheric connections and therefore imposes limits on the mapping of structural connectivity (Behrens, Berg, Jbabdi, Rushworth, & Woolrich, 2007; Peled, Friman, Jolesz, & Westin, 2006; Wiegell, Larsson, & Wedeen, 2000). As a consequence, recently there has been considerable interest in the application of multimodal approaches that jointly examine the structural and functional integrity of parallel distributed neural circuits implicated in psychopathology (Reddi, 2017).

Some researchers have argued that multimodal fusion techniques may provide a better representation for whole brain connectivity and a better diagnostic classification between groups

(Pineda-Pardo et al., 2014). Instead of inferring structural connectivity from functional connectivity, and vice versa, their interconnected structural-functional relationship is quantitatively measured.

There are a number of different approaches to combining structural and functional datasets including: (1) joint analysis (data integration) which extracts common features from separate data sources to perform statistical analysis such as correlations (Honey et al., 2009; van den Heuvel et al., 2013); (2) asymmetric data fusion which uses one dataset to constrain and analyze another (i.e., deriving structural connectivity from functional data) (Taylor & Saad, 2013); (3) symmetric data fusion (data fusion based on higher order statistics) which performs separate analyses for functional and structural data but combines them statistically (Bowman, Zhang, Derado, & Chen, 2012; Zhu et al., 2014) and (4) machine learning algorithms which utilize computational models that are automated to improve through iterative optimization (Dyrba et al., 2012; Rosa et al., 2015). Calhoun and Sui (2016) argued that among all multimodal approaches, asymmetric and symmetric data fusion, respectively, provide the most information (Calhoun & Sui, 2016). Data fusion uses statistical methods to combine the effects of different metrics (retrieved from separate complementary modalities) in a single measure. It is a more realistic representation of the real biology of brain networks, instead of studying brain networks from one angle alone (from a single modality).

To date only two studies have been published that combine functional and structural neuroimaging data in a symmetric data fusion approach for the study of MDD, both of which used a joint-ICA fusion approach. Choi and associates conducted a preliminary study with a small sample size of four MDD participants and nine healthy comparison participants (HC) employed a joint ICA approach for combining functional and structural connectivity (Choi et

al., 2008). These researchers reported changes in fractional anisotropy (FA) white matter values and changes in the strength of functional connectivity in MDD patients compared with HC (Choi et al., 2008). Furthermore, there were detectable differences in both the functional and structural connectivity in the "subgenual anterior cingulate cortex (sACC) and perigenual ACC, anterior midcingulate cortex, caudate, thalamus, medial frontal cortex, amygdala, hippocampus, insula, and lateral temporal lobe" (Choi et al., 2008). Ramezani et al. (2015), also reported a joint analysis approach with a small sample size of 25 participants (11 MDD, 14 HC). Their results indicated no detectable differences between MDD and healthy control participants when examining either fMRI or DTI in isolation, but when employing the joint-ICA fusion approach, detectable differences in hippocampal volume loss were identified (Ramezani et al., 2015). This illustrates the added value of utilizing a combined fMRI and DTI approach for the study of MDD connectivity in a symmetric data fusion approach. Another joint-model, which has not yet been applied to MDD data in the literature, is the "a*natomically-weighted functional connectivity*" (awFC) (Bowman et al., 2012). This approach combines structural and functional connectivity in a mathematically dense approach.

Software packages for the analysis of functional and structural connectivity can substantially speed up processing time and reduce the likelihood of human error (Man et al., 2015). Presently available toolboxes designed to combine functional and structural data include: Graph Analysis Toolbox (GAT) (Hosseini, Hoeft, & Kesler, 2012), Brain Connectivity Analysis Toolbox (BrainCAT) (Marques, Soares, Alves, & Sousa, 2013), Multimodal Imaging Brain Connectivity Analysis (MIBCA) (Ribeiro, Lacerda, & Ferreira, 2015) and Brain Connectivity Toolbox (BCT) (Rubinov & Sporns, 2010). Another toolbox is the "*Functional and Tractographic Analysis Toolbox*" (FATCAT) (Taylor & Saad, 2013) which extracts functional connectivity (Pearson

correlation) and corresponding tractography metrics (i.e., FA, tract count) between functionally-derived ROI-pairs. However, it does not combine these two modalities in a fusion approach. A processing toolbox consists of a set of software tools and a recommended (or definitive) pipeline. Some of these toolboxes are overly simplified (fully automated with no control over parameters), while others are highly specialized (i.e., only used for task-based or only rsfMRI), computationally demanding (i.e., nonlinear fitting of DTI) or have complex workflows (Cusack et al., 2015).

Here, for the first time, we combine a connectivity toolbox (FATCAT) (Taylor & Saad, 2013) and a data fusion method (awFC) (Bowman et al., 2012), into a novel single pipeline known as "*FATCAT-awFC*." This yields a single powerful hybrid pipeline that combines functional and structural connectivity information into a single index, known as anatomically weighted functional connectivity (awFC). While FATCAT uses functionally derived ROIs to extract DTI parameters, awFC fuses both datasets together in a complex approach. The *FATCAT-awFC* pipeline preserves the complexity of the relationship between structural and functional connectivity and provides maximal information, while allowing for simple implementation. To the best of our knowledge, this article is the first to design, explore, and compare a unique multimodal fusion approach with unimodal approaches in a large sample of patients with MDD. Using the *FATCAT-awFC* pipeline, we expect to find differences between MDD patients and HC in commonly identified RSNs, including the DMN, FPN, DAN, VAN, and LIM (Yeo et al., 2011). We hypothesized that performing a joint functional-structural connectivity analysis using the *FATCAT-awFC* approach may allow us to better discriminate connectivity changes between MDD and HC groups compared to analyzing these changes using a single modality.

2.3 Materials and Methods

This study was executed as part of the Canadian Biomarker Integration Network in Depression (CAN-BIND-1) (Kennedy et al., 2019; Lam et al., 2016; MacQueen et al., 2019).

2.3.1 Participants

The CAN-BIND-1 study enlisted a total of 267 participants (164 MDD and 103 Healthy Comparison participants), which were available. Of these, 17 participants were excluded due to high levels of motion in rsfMRI data (Jenkinson, Bannister, Brady, & Smith, 2002), 4 participants were excluded following a visual inspection of fMRI data for artifacts paired with a Jaccard similarity index, and 7 participants were excluded due to missing DTI data. This left a total of 239 participants, 143 MDD and 96 HC (excluded participants = 21 MDD: 7 HC). Data was collected in unmedicated MDD patients prior to the initiation of the selective serotonin reuptake inhibitor (SSRI) escitalopram. Participants were recruited from six sites across Canada: Calgary (Hotchkiss Brain Institute), Hamilton (St. Joseph's Healthcare Hamilton), and Kingston (Providence Care Mental Health Services) (Kennedy et al., 2019; Lam et al., 2016; MacQueen et al., 2019), Toronto (2 sites: University Health Network, and Centre for Addiction and Mental Health), Vancouver (Djavad Mowafaghian Centre for Brain Health). Research ethics approval for the study was obtained from the local ethics boards at each site. Study group demographic information can be found in Table 1. The demographic data was analyzed using *gtsummary* packages (Sjoberg, 2021) in R software (R Core Team, 2018). The Bonferroni method was applied to correct for of multiple comparisons where appropriate.

Table 1 | Demographic and clinical characteristics of the study group

Characteristic	Healthy control participants, $N = 96$[a]	Patients with MDD, $N = 143$[a]	Group comparison *p*-value [b]
Sex			.9
Female *n* (%)	62 (64.6%)	94 (65.7%)	
Male *n* (%)	34 (35.4%)	49 (34.3%)	
Age, years mean (SD)	32 (10)	33 (12)	.8
Education, years, mean (SD)	18.5 (2)	16.9 (2)	<.001[d]
MADRS mean (SD)	1 (2)	29 (6)	<.001[d]
Age of onset of MDD, years, mean (SD)	NA	19 (8)	
Number of MDE's mean (SD)	NA	4 (3)	
Duration of current MDE *n* (%)			
≤1 year	NA	77 (53.8%)	
1–2 years	NA	14 (9.8%)	
>2 years	NA	42 (29.4%)	
Unknown/unreported	NA	10 (7.0%)	
Antidepressants *n* (%)			
Drug naïve	0	73 (51.0%)	
Past history of antidepressants	0	70 (49.0%)	
Comorbidities[c] *n* (%)			

Social anxiety disorder	0	31 (21.7%)
Generalized anxiety disorder	0	32 (22.4%)
Panic disorder	0	23 (16.1%)
Agoraphobia	0	14 (9.8%)
Posttraumatic stress disorder	0	10 (7.0%)
Bulimia nervosa	0	3 (2.1%)
Alcohol abuse (past 12 months)	0	2 (1.4%)
Non-alcohol substance abuse (past 12 months)	0	2 (1.4%)

- Abbreviations: MDE, major depressive episode; MADRS, Montgomery Åsberg Depression Rating Scale; NA, not applicable; *n*, the number of participants.
- [a] *n* (%); mean (SD).
- [b] Pearson's Chi-squared test; Wilcoxon rank sum test; Fisher's exact test.
- [c] The Mini-International Neuropsychiatric Interview was used to diagnose the DSM-IV-TR disorders (Diagnostic and Statistical Manual).
- [d] Significant after Bonferroni correction.

2.3.2 Inclusion and exclusion criteria

Inclusion criteria for HC included: 18–60 years of age with no history of psychiatric disorder or unstable medical diagnosis, and able to understand instructions in English. The inclusion criteria for MDD were: 18–60 years of age, currently experiencing a major depressive episode with a duration of three or more months as defined in the Diagnostic and Statistical Manual IV-TR (American Psychiatric Association, 2000) and as identified by the Mini International

Neuropsychiatric Interview (MINI; Sheehan et al., 1998), with a Montgomery-Åsberg Depression Rating Scale (MADRS) (Montgomery & Åsberg, 1979) score equal to or greater than 24 and sufficient fluency in English to complete study procedures. In addition, MDD participants were required to have been free of psychotropic medications for at least 5 half-lives prior to baseline testing, and able to comprehend instructions in English.

The exclusion criteria for MDD patients excluded patients with any axis I (aside from MDD) diagnosis which would be considered a primary disorder that could interfere with the study, or bipolar I/II disorder. Additional exclusion criteria included high suicide risk or heightened risk of hypomanic switch, and previous failure to respond to more than four pharmacological interventions. Participants were also excluded if they previously failed to respond to aripiprazole or escitalopram treatments, and/or received psychological treatment within the past 3 months from baseline and planned to continue psychological treatment.

Exclusion criteria common to both groups (HC and MDD) involved individuals with: a history of substance abuse within the past six months, neurological disorders, head trauma, pregnant or breastfeeding, and/or have any other contraindications to MRI. Every participant in the study provided informed written consent and was compensated for their participation. MDD patient comorbidities are listed in Table 1.

2.3.3 Data acquisition

Cognitive Testing: A computerized cognitive test battery, the CNS-Vital Signs (CNS-VS) was used to assess participants' level of cognitive functioning (Gualtieri & Johnson, 2006). Five cognitive subscales of the CNS-VS were administered: memory, cognitive flexibility, complex attention, processing speed and neurocognitive index (a summary score that consists of the mean

of five cognitive variables: complex attention, memory, psychomotor speed, reaction time, and cognitive flexibility) (Iverson et al., 2009).

Images were acquired using receiver head coils on six 3T MR scanners: (One Signa HDxt from GE Healthcare, USA; Three Discovery MR750 from GE Healthcare, USA; One Intera from Phillips, Netherlands; One Trio Tim from Siemens, Germany) [see (MacQueen et al., 2019) for more details].

Functional images were acquired using a whole-brain T2*-sensitive blood oxygen level dependent (BOLD) echo planar imaging series with the following parameters: repetition time (TR)/echo time (TE)/flip angle = 2000 ms/30 ms/75°, voxel size = $4 \times 4 \times 4$ mm^3, field of view (FOV) = 256 mm for all sites, matrix size = 64×64 and, slices = 34–40 for full brain coverage. During rsfMRI acquisition, participants were required to lie still, and keep their gaze on a fixation cross for a scanning time of 10 minutes, with 300 volumes recorded in total.

Anatomical reference scans were acquired across sites following a similar acquisition protocol, although Siemens scanners reported different repetition times from their MPRAGE sequence. The parameters were visually optimized to produce similar image contrast levels across sites. The 3D T1-weighted scans were acquired using a whole-brain magnetization-prepared gradient echo sequence with the following parameters: TR/TE/flip angle: 6.4–7.5 ms/2.7–3.5 ms/8–15° (Exception: Siemens Scanners TR = 1760, 1840 ms), inversion time: 450–950 ms, voxel size: $1 \times 1 \times 1$ mm^3, matrix dimensions 240×240 and 256×256, slice thickness: 1 mm, number of slices: 155–192. A vitamin E pill was taped on the right side of the participants' heads as a fiducial marker. Acquisition time for anatomical data ranged from 3:30 to 9:53 minutes [see (Lam et al., 2016) and (MacQueen et al., 2019) for more details].

The DTI acquisition used single-shot spin-echo echo-planar imaging (EPI) with the following parameters: TR/TE/flip angle: 8000–9000 ms/94 ms/90°, voxel size: 2.5 × 2.5 × 2.5 mm^3, FOV = 240 × 240 mm, matrix dimensions 96 × 96, 155–192 slices at 2.5 mm thickness, axial slices = 52–58. A single *b*-value (*b* = 1000 s/mm^2) was applied to 30–31 noncollinear gradient directions. Image space reconstruction was completed with an acceleration factor of 2 at individual sites including: GE ASSET, Philips SENSE, or the GRAPPA k-space method. Acquisition time for DTI data was approximately 5 min [see (Lam et al., 2016) and (MacQueen et al., 2019) for more details].

2.3.4 Data preprocessing

To begin, dicom images were converted to nifti using *MRIcron* (Rorden & Brett, 2000). An optimized preprocessing pipeline, *OPPNI* (Churchill, Raamana, Spring, & Strother, 2017; Churchill, Spring, Afshin-Pour, Dong, & Strother, 2015), was used to perform the following resting-state preprocessing steps. Principle component analysis (*PCA*) was used to identify the centroid of the data and measure the Euclidean distance of each volume to the centroid of all volumes. The volume with the least amount of head displacement was chosen based on the smallest Euclidean distance to the centroid. This was considered the reference volume from which the mean distance for all other volumes was calculated. Data was motion corrected using AFNI's *3dVolreg* (Cox, 1996), by matching each volume displacement to the reference volume. Basic Censoring (*CENSOR*—from the *OPPNI* pipeline) was applied, to remove outlier volumes and replace them with interpolated values from neighboring volumes (Churchill & Strother, 2013). Slice timing offsets were corrected (*TIMECOR*—from the *OPPNI* pipeline) for the interleaved acquisition by using AFNI's *3dTshift* (Cox, 1996) using Fourier interpolation. This was followed by AFNIs *3dBlurtoFWHM* (Cox, 1996), which was used to spatially smooth

fMRI images with a 6 mm full width at half maximum smoothing kernel along three directions (*x*,*y*,*z*). A binary mask was created for each functional run using AFNIs *3dAutomask* in which non-brain voxels were excluded and only voxels corresponding to brain areas remained. Afterwards, a neuronal tissue mask (to exclude non-neuronal tissues such as ventricles and sinuses) was obtained using the *PHYCAA+* (first part) algorithm (Churchill & Strother, 2013). In the next few steps, nuisance regressors were calculated using linear regression. A general linear model using second order Legendre polynomial was applied to the functional data to regress low frequency fluctuations, in the range of 0.01–0.1 Hz. Next, the motion parameters (derived from *3dvolreg*) were used as motion parameter estimates for *PCA*, and were regressed from the data. PCA was performed on the six motion parameter estimates (pitch, yaw, rol l, *x, y, z*), whereby the PC with the largest variance (accounting for 85% variance) was taken to be the first PC (of the six PCs) and regressed out. PCA was able to correct for the maximum variance caused by head motion while simultaneously reducing multicollinearity and preserving power. A global signal removal step was performed that regressed out the first PC (highly correlated with global signal effects) of the fMRI data (Carbonell, Bellec, & Shmuel, 2011). Physiological (i.e., cardiac and/or respiratory) noise was corrected using the *PHYLUS*, *PHYCAA+* (second part) algorithm. A low-pass filter was then applied (*LOWPASS*) to remove BOLD frequencies above 0.10 Hz. FSL's *FLIRT* tool was then applied: first, functional data was aligned to the structural image in native space, second, functional data was transformed to register the structural image to the Montreal Neurological Institute (MNI) template (4 mm resolution). The first 5 functional volumes were discarded to avoid relaxation effects at scan start. The remaining 295 consecutive volumes were used for data analysis.

Motion artifacts (i.e., physiological motion causing ghosting), inhomogeneity (signal intensity changes and image distortions), digital imaging artifacts (i.e., phase wrap-around artifacts) and hardware related artifacts (radio frequency inferences and spike noise) are confounding factors that affect connectivity (Maknojia, Churchill, Schweizer, & Graham, 2019; McRobbie, Moore, Graves, & Prince, 2017). However, head motion is the most problematic confounding factor that can significantly impact resting state functional connectivity (rsFC), as each voxel relies on the spatial correspondence over a time course. Sub-millimeter motion may distort functional connectivity estimates (Maknojia et al., 2019). Motion-related artifacts are also strongly correlated with framewise displacement (FD) measures (Dosenbach et al., 2017). Censoring the data was achieved based on the Jenkinson mean framewise displacement criteria (FD_{jenk}). Volumes were marked as motion contaminated if $FD_{jenk} > 0.20$ mm. If 125 volumes of data (~5 min or more) were retained, participants were not excluded, otherwise the participant was removed from the sample for not having enough data for the stable estimation of rsFC (Lanka & Deshpande, 2019). Thus, seventeen participants were removed due to gross motion. The Jenkinson volume-based FD formula was calculated as follows (Jenkinson, 1999; Jenkinson et al., 2002):

$$FD_{vol}(t) = \sqrt{\frac{1}{5}R^2 Trace(A^T A) + (b + Ac)^T (b + Ac)}$$

where R is the radius of the head (R = 80 mm), c represents the coordinates for the center of the volume, and A and b are defined as:

$$\begin{bmatrix} A & b \\ 0 & 0 \end{bmatrix} = T_t T_{t-1}^{-1} - I$$

In addition, the correspondence between the functional data transformed to MNI space and the MNI 152 template was calculated using the Jaccard similarity index to evaluate the accuracy of registration.

When acquiring DTI data, rapid switching of applied diffusion gradients can introduce eddy currents, which warp the DTI image in the phase encoding direction (Hecke, Emsell, & Sunaert, 2016). Each participants diffusion-weighted volumes was aligned to the $b = 0$ images using an affine transformation (*eddy_correct*) (Hecke et al., 2016; Jenkinson, Beckmann, Behrens, Woolrich, & Smith, 2012) to minimize distortion by eddy currents, reduce head motion effects, and improve the signal to noise ratio (SNR). The diffusion tensor model was fit with the weighted least-squares technique to minimize the influence of outlier volumes. In addition, the brain tissues types (gray matter, white matter and cerebrospinal fluid) were extracted using the FSL (Jenkinson et al., 2012) Brain Extraction Tool (*BET*) to improve co-registration. Afterwards, the diffusion data was registered to the standard space FA atlas ($1 \times 1 \times 1$ mm resolution; average of 58 FA images) FMRIB58 (Webster, 2012).

2.3.5 Modifications in the awFC approach

Building on the awFC approach proposed by Bowman et al. (2012), our current study utilized independent component analysis (ICA) and FATCAT to extract networks of regions of interest, rather than performing cluster analysis as outlined in Bowman et al. (2012). The singular value decomposition (SVD) clustering process implemented by Bowman et al. (2012) is computationally expensive for a matrix of size $n \times m$ and becomes increasingly more complex between each region pair as the number of ROIs increases (Vasudevan & Ramakrishna, 2019).

ICA, on the other hand, reveals distinct spatial maps, across healthy and clinical study populations (Juneja, Rana, & Agrawal, 2016; Vergun et al., 2016). ICA is a powerful methodology, and is straightforward to apply with FATCAT's recommended pipeline involving FSL's MELODIC (Griffanti, 2019; Nascimento et al., 2017).

2.3.6 Generated resting-state networks (RSNs)

In our study, we used an ICA (data-driven) approach to identify RSNs, which were then thresholded to generate ROIs. It has been suggested that data-driven approaches are more accurate and more sensitive at detecting the greatest effects between groups (Ma, Wang, Chen, & Xiong, 2007; van de Ven, Formisano, Prvulovic, Roeder, & Linden, 2004). Group ICA (gICA) was used to derive standard RSNs from 239 participants (143 MDD, 96 HC). The rsfMRI data of MDD and HC groups was concatenated in time for each session across participants into a single 4D dataset and decomposed into 20 independent component (IC) maps using the *MELODIC* gICA in FSL (Smith et al., 2004). Twenty ICs is the typical dimensionality in rsfMRI studies (Taylor & Saad, 2013). Matching is performed based on spatial correlation; to match ICs to the Yeo 7-network template (Yeo et al., 2011). This was performed using FATCAT's *3dMatch* tool (Taylor & Saad, 2013), along with visual inspection. Binarized maps were created for the selected ICs that best matched the standard functional RSNs template. *3dMatch* identified and extracted a total of five ICs that matched the five of the standard functional networks, which included the DMN, FPN, LIM, VAN, and DAN. However, through visual inspection, we were able to identify that gICA split the LIM into two distinct components. Consequently, to better match the LIM, we combined the ROIs of both of these components into one network by applying the *fslmaths* function. These combined ROIs were

then defined as the LIM (see Figure 1). The remaining 14 ICA components were not included in the study because they contained non-gray matter regions, motion artifacts, edge alignment artifacts and other networks that were not of interest.

2.3.7 ROI selection

The binarized spatial maps (derived from ICs) that were identified as RSNs, were stacked in a 4D image file. The 4D stacked image file was then separated out so that each network had its own 4D file (using *fslsplit*). This step was necessary to set an appropriate threshold for each individual network. Functional connectivity should not be set to the same unified threshold across all networks since this would inaccurately define network ROIs, as each network may vary significantly in noise level (Wang, Adeli, Wang, Shi, & Suk, 2016). Therefore, a different threshold was applied for each component: DMN ($Z > 6$), FPN ($Z > 9$), DAN ($Z > 5.5$), VAN ($Z > 11$), LIM ($Z > 6$), with a minimum ROI size restriction of 30 voxels (see Table 2). The levels of thresholding were selected to qualitatively and visually capture the networks observed in Yeo et al. (2011) and in line with commonly identified RSNs in the literature (Sala-Llonch, Bartrés-Faz, & Junqué, 2015). The FATCAT tool 3dNetCorr (Taylor & Saad, 2013) was used to generate a functional connectivity matrix using Pearson's correlation for each participant's five RSNs.

Table 2 | *Z*-threshold values for 3dROIMaker and number of ROIs per network

Network	Threshold, *Z*	Number of ROIs
DMN	6	5
FPN	9	7
VAN	11	5
DAN	5.5	4
LIM	6	3

- Abbreviations: DAN, dorsal attention network; DMN, default mode network; FPN, front parietal network; LIM, limbic network; ROIs, region of interest; VAN, ventral attention network.

2.3.8 DTI image processing

Raw DTI dicom images from the scanner were converted into a single 4-D nifti file using *dcm2nii*. Tensors were estimated from diffusion data using AFNI's *3dDWItoDT* (Taylor & Saad, 2013) using nonlinear fits and a scheme file containing both the b-value and b-vectors. The following indices were estimated from the diffusion tensor: Eigenvalues (L1, L2, L3), eigenvectors (V1, V2, V3), FA, mean diffusivity (MD), axial diffusivity (AD) and radial diffusivity (average of two radial eigenvalues; RD), all of which were done in the participant's native space. All parameter estimates have some noise and errors included in their values. Thus, an advantage of probabilistic tractography is its ability to incorporate confidence intervals and uncertainty parameters into the calculation. Uncertainty of the diffusion tensor parameter was calculated using Monte-Carlo simulation with nonparametric resampling (i.e., bootstrap and direct variants). The variance of the FA and the primary eigenvector (e_1) was estimated with FATCATs *3dDWUncert* (Taylor & Saad, 2013) using 300 jackknife-resampling iterations. Together, the DTI parameters and uncertainty measures with target ROIs were used to perform probabilistic tractography.

The *3dROIMaker* step (outlined above) (Taylor & Saad, 2013), also returned inflated ROIs for use with the DTI data. The inflated ROIs were necessary to allow regions to maintain contact with the mean FA tract skeleton (defined as FA > 0.2) (Nugent et al., 2019). The ROIs were transformed to each individuals' DTI space, from MNI standard space, using nonlinear transformations (Bowman et al., 2012; Yeatman, Dougherty, Myall, Wandell, & Feldman, 2012). *3dTrackID* (Taylor & Saad, 2013) was applied to perform probabilistic tracking between each region pair with the following settings: tract length > 20 mm; turning angle < 60°; Nseed = 5 tract seeds per voxel; Nmc = 1000 Monte Carlo iterations; and a fractional threshold (ftr) = 0.05 (to calculate the number of tracts per voxel, included in the final white matter (WM) ROI: ftr × Nseed × Nmc = 250 tracts/voxel). An FA threshold of 0.2 was set to reduce partial volume effects after warping (Yeatman et al., 2012). The *3dTrackID*(Taylor & Saad, 2013) step returned DTI metrics including: white matter volume (physical volume and number of voxels), counts of tracts, FA, MD, L1, RD and AD. Number of tracts and tract length are used later along the *FATCAT-awFC* pipeline.

2.3.9 Generating structural connectivity matrix

A Poisson-regression based adjustment was applied (to reduce the likelihood of false positives due to distance bias): $\log(\mu(S_{ij}|g_{ij}) = \alpha_0 + \alpha_1 g_{ij}$, where g_{ij} is the distance between each region

pair, S_{ij} is the unbiased number of tracts (Bowman et al., 2012). We estimated and adjusted for the bias that exists between the number of tracts and physical distance with the effect α_1 to more accurately represent structural connectivity strength. To account for indirect structural connectivity, we relied on the awFC approach to calculate all possible second-order connections (indirect connections) with the following equation: $\pi_{ij} = \max[\pi_{ij}, \max_m(\pi_{im}\pi_{mj})]$, where π is the probabilities of structural connectivity, i is the starting ROI, j is target ROI, and m is the third connection. This equation calculated the structural connectivity probabilities of direct connections and indirect connections, taking the higher connectivity value to be the neural pathway. For instance, if the connectivity is such that the structural connectivity is higher for indirect connections versus direct connections, we took the indirect connection to be the pathway used to connect the functional regions (see Supplemental for more information).

2.3.10 Functional and structural connectivity combined into one unit (awFC)

Once structural connection probabilities, distance bias, direct/indirect structural pathways were calculated and factored into structural connectivity using the awFC approach, the structural connectivity was ready to be integrated into the functional connectivity (Figure 2). In this study, a multiplicative combination technique was used to derive the fused model, whereby the dissimilarity between region pairs (for connectivity) were multiplied together to generate the fused dissimilarity matrix (Liu, Li, Xu, & Natarajan, 2018). We first computed functional dissimilarity (1 − functional connectivity) and the structural dissimilarity (1 − structural connectivity) between each region pair. To transform the fused dissimilarity metric back to a correlational value (awFC), we performed a simple subtraction: 1-|awFd|. The dissimilarity metric (which emphasized correlations and differences) was transformed back to a connectivity metric; the awFC (Bowman et al., 2012) (see Supplemental for more information).

2.3.11 Correction for multiple comparisons

To test the hypothesis that the awFC underlying the RSNs varies between groups, we performed a Mann–Whitney test between each region pair within each RSN and within-group contrasts between MDD and HC groups. Unless otherwise noted, all reported p-values for the statistical tests of functional connectivity, structural connectivity, and awFC were corrected for multiple comparisons using the false discovery rate (FDR) criterion proposed by Benjamini and Hochberg (Waite & Campbell, 2006). The significance level was set to p(FDR corrected) < .05. Effect sizes were generated using Cohen's d in the statistics package R (R Core Team, 2018).

2.3.12 Statistical analysis

To evaluate the association between awFC within RSNs and cognitive changes in the MDD group compared to HC, a post-hoc test was performed on regions with significant associations. First, multicollinearity was assessed using Pearson correlation pair plots, among the cognitive variables (neurocognitive index, memory domain, complex attention, cognitive flexibility, processing speed). Pearson correlation pairwise comparisons were produced using the function *ggpairs* from the *GGally* package (Schloerke et al., 2018) in R. Since multicollinearity exists among variables (see Figure S1a), PCA can be applied to reduce information redundancy and preserve important information (Kassambara, 2017; Refaat, 2010). PCA was performed with the R package (R Core Team, 2018) using the *princomp* function, in which a set of orthogonal PCs were produced corresponding to a linear combination of the original variables (Hair, Black, Babin, & Anderson, 2009). PCs were retained based on two criteria: if they had an eigenvalues >1.0 (Kaiser, 1960) and visually from the “first elbow” of the scree plot. A scree plot was created using the *fviz_eig* function from the *factoextra* package (Kassambara, 2017) in R. The PCs that met this criterion were taken to be independent variables in a PC regression model with awFC as

the dependent variable. PC regression was performed using *lme* function in R's *nlme* package (R Core Team, 2018). PC regression (PCR) was used to evaluate any potential PC effects. If the PC showed a significant effect, it was evaluated further to interpret the results in terms of the original cognitive variables. This was done in order to interpret the data in a more meaningful manner. Only factor loadings greater than 0.40 were considered. Multiple regression analysis was performed to investigate whether cognitive variables interacted with the connectivity pattern within RSNs. They were conducted using the *lme* function in R's *lme*package R (R Core Team, 2018), whereby the awFC was taken as the dependent variable and each loadings > 0.40 as the independent variable. The regression was evaluated using the participant within site as a random effect. Age and sex were added as covariates in each statistical model. All the index scores were standard scores, which were mean centered. Multiple comparisons were corrected for using FDR.

2.4 Results

2.4.1 Regions of interest

See Table 2 for ROI thresholds selected and resultant number of ROIs. Table 3 presents information on ROIs MNI coordinates of peak voxel and size of ROIs per network.

Table 3 | Regions of interest (ROIs) defined within the five resting state networks

		MNI coordinates			Volume (# of voxels)
ROI #	**Anatomical location**	***x***	***y***	***z***	

Default mode network					
1	Cerebellum/lateral occipital cortex	34	−86	−40	726
2	Posterior cingulate cortex (PCC)	−2	−54	24	559
3	Medial prefrontal lobe	−6	42	12	1200
4	Middle temporal gyrus	−58	−22	−20	168
5	Left inferior parietal lobe	−50	−70	28	278
Frontoparietal network					
6	Middle and inferior temporal gyrus	62	−42	−16	182
7	Right parietal lobe and lateral occipital cortex	50	−58	44	703
8	Right frontal lobe	−42	46	−4	43
9	Left frontal lobe	46	22	36	1200
10	Left parietal lobe	−50	−54	44	145
11	Cerebellum	−46	−70	−36	394
12	Frontal pole	46	14	20	127
Limbic network					
13	Left cerebral cortex and temporal lobe	−30	−6	−36	400
14	Right cerebral cortex/right temporal lobe	30	−10	−36	400
15	Frontal pole, frontal medial pole	30	42	−12	850
Ventral attention network					
16	Left temporal lobe	−38	−18	−8	1169
17	Cingulate gyrus	14	−34	40	962
18	Left DLPFC (frontal lobe)	−30	34	24	215

19	Right DLPFC (frontal lobe)	46	42	0	241
20	Right temporal lobe	46	−10	−16	1293
Dorsal attention network					
21	Right superior parietal lobule	50	−30	40	1339
22	Right lateral occipital cortex, inferior temporal gyrus	54	−62	−12	100
23	Left lateral occipital cortex, inferior temporal gyrus	−50	−66	−8	112
24	Left superior parietal lobule	−50	−30	36	1454

- *Note*: All ROIs were derived from FATCAT's "*3dROIMaker*" command. MNI coordinates and volume of each individual ROI were identified. The functionally defined ROIs covered a number of anatomical structures that were reported.
- Abbreviations: ROI, region of interest; RSNs, resting state networks.

2.4.2 Functional connectivity group differences

Compared to HC, the MDD group showed less functional connectivity in the DMN between the posterior cingulate cortex (ROI 1) and cerebellum/occipital regions (ROI 2), ($W = 8406.5$, $p_{adj} = .0332$). In addition, reduced functional connectivity in MDD compared to HC within the VAN was found between the left temporal lobe (ROI 16) and the right dorsolateral prefrontal cortex (DLPFC) (ROI 19) ($W = 8365$, $p_{adj} = .0211$). We did not find significant functional connectivity differences between MDD and HC groups within the LIM, FPN, or the DAN (see Table 4).

Table 4 | A Wilcoxon test was used to identify significant connectivity (structural, functional and anatomically weighted functional connectivity) differences between MDD and HC participants between regions of interest (ROIs).

Start ROI	End ROI	SC *p*-value (FDR corrected)	FC *p*-value (FDR corrected)	AwFC *p*-value (FDR corrected)
Default mode network				
1	2	.009**	.033*	.032*
1	5	.71	.19	.20
1	3	.71	.24	.24
2	4	.43	.23	.23
3	5	.73	.20	.20
5	2	.013*	.30	.30
Frontoparietal network				
6	7	<.001***	.82	.58
8	9	.040*	.47	.47
Limbic network				
13	14	<.001***	.76	.76
Ventral attention network				
16	17	<.001***	.72	.71
17	18	<.001***	.87	.87
18	16	<.001***	.17	.16
19	17	<.001***	.73	.73
19	16	.64	.021*	.042*
20	19	<.001***	.072	.036*
Dorsal attention network				

21	22	<.001**	.98	.90
23	24	<.001***	.76	.75
24	21	<.001***	.87	.86

- Abbreviations: HC, healthy comparison; MDD, major depressive disorder; SC, structural connectivity; FC, functional connectivity; awFC, anatomically weighted functional connectivity.
- * *p*-value (FDR corrected) < .05.
- ** *p*-value (FDR corrected) < .01.
- *** *p*-value (FDR corrected) < .001.

2.4.3 Structural connectivity group differences

Between-group comparisons of structural connectivity between HC and MDD patients, are presented in Table 4. There were significant differences in all 5 RSNs for MDD compared with HC groups (see Table 4). These were characterized by lower connectivity values for MDD compared to HC for all networks. See Table **4**, for a comparative summary of SC, FC, and awFC.

2.4.4 Anatomically weighted functional connectivity group differences

Exploratory analysis of the five RSNs awFC connectivity revealed reduced correlation differences between ROI pairs for MDD groups compared with HC in three regions: one in the DMN and two region pairs in the VAN (see Table **5**). Figure **3a,b** illustrates the group ROIs that demonstrated significant connectivity differences between MDD and HC groups. Lower awFC connectivity was found in the DMN between the PCC (ROI 1) and cerebellum/occipital regions (ROI 2), ($W = 7917$, $p_{adj} = .0322$) for the MDD group compared with the HC (see Table 5). In addition, MDD patients demonstrated lower awFC in the VAN, between the left temporal lobe (ROI 16) and the right DLPFC (ROI 19) ($W = 8274$, $p_{adj} = .0421$) compared with HC (see

Table **5**). Reduced connectivity in MDD compared with HC within the VAN was observed between the right temporal lobe (ROI 20) and the right DLPFC (ROI 19) ($W = 8366$, $p_{adj} = .0361$). No other significant differences were found within the remaining RSNs. A summary of the significant regions and *p*-values is presented in Table **5**, and a summary of the mean and standard deviations of connectivity values are presented in Table **5**. In addition, Figure **4** displays boxplots of awFC values between ROI-pairs within RSNs.

Table 5 | A Wilcoxon test was performed whereby significant anatomically weighted functional connectivity differences between MDD and HC groups, and their associated structural and functional connectivity (significance set to FDR-corrected $p < .05$) are reported. Mean, standard error and effect size are also reported for each group.

						MDD		HC	
Start ROI	**End ROI**	**SC p_{adj}**	**FC p_{adj}**	**awFC p_{adj}**	**Effect size**	**Mean**	**SE**	**Mean**	**SE**
Default mode network									
1	**2**	.00905**	0.0331*	0.0320*	0.34	−0.011	0.017	0.061	0.022
Ventral attention network									
16	**19**	0.64	0.021*	0.0421*	0.32	0.36	0.024	0.46	0.027
19	**20**	<.001***	0.0722	0.0361*	0.36	0.22	0.023	0.33	0.028

- Abbreviations: ROI, region of interest; SC, structural connectivity; FC, functional connectivity; awFC, anatomically weighted functional connectivity; padj, FDR corrected *p*-values; MDD, major depressive disorder, HC, healthy comparison; SE, standard error.
- * *p*-value (FDR corrected) <.05.
- ** *p*-value (FDR corrected) <.01.

.

- *** *p*-value (FDR corrected) <.001.

2.4.5 Post hoc analysis

Performing PCA on the cognitive variables resulted in five PCs (each PC is a linear combination of the original variables). Applying the Kaiser-Guttman rule (Guttman, **1954**; Kaiser, **1961**), of extracting only PCs with an eigenvalue >1, revealed the first PC had an eigenvalue >1 ($\lambda = 3.2$). In addition, from the scree plot (Figure **S1**b), we selected one PC at the marked "elbow," whereby 62.5% of the variance in the data was explained. Therefore, based on these two criteria, only the first PC was retained. PCR was then performed on the first PC, in which a significant effect was detected. This warranted further analysis to determine the cognitive variable associated with the awFC. Variables (loadings > 0.4) were investigated further. The neurocognitive index (NCI) (loading = 0.40), cognitive flexibility (loading = 0.45), processing speed (loading = 0.49), and complex attention (loading = 0.52) met this criterion. Therefore, multiple linear regressions were performed on each variable individually. Therefore, multiple mixed-effects linear regressions were performed, separately on each variable.

Applying PCR to the DMN (uncorrected $p = .0475$) showed significant associations between the first PC and the awFC. Multiple linear regressions revealed that awFC between the PCC and the cerebellum/occipital lobe was significantly associated with changes in MADRS (uncorrected $p = .02$) and complex attention (uncorrected $p = .047$). Second, a PCR for the VAN revealed significant associations between the first PC and awFC (uncorrected $p = .02$). Therefore, multiple linear regressions were performed for variables with loadings > 0.4. The VAN, between the right temporal lobe and the right DLPFC revealed, awFC was significantly

associated with complex attention (uncorrected $p = .028$). However, none of the cognitive associations survived correction for multiple comparisons.

2.5 Discussion

We developed a novel pipeline for combining functional connectivity (derived from fMRI) and structural connectivity (derived from DTI) and used it to study awFC connectivity changes in MDD patients. We analyzed a total of 24 ROIs (from five resting-state functional networks), three of which revealed statistically significant differences in awFC between MDD and HC groups using the *FATCAT-awFC* approach. For each region pair we also conducted standard functional and structural connectivity analyses to compare against our novel combined functional-structural analysis approach (*FATCAT-awFC*).

As predicted, the multivariate connectivity analysis was capable of revealing group differences not identified by the univariate analysis within RSNs. We found reduced awFC connectivity within the DMN between the PCC and cerebellum/lateral occipital cortex in the MDD group compared with the HC group. Aberrant connectivity between this ROI-pair was also found in both the traditional structural and traditional functional connectivity approaches, which supported the changes we found in the awFC measure output by the *FATCAT-awFC* pipeline. In MDD, similar findings in resting state functional connectivity (rsFC) have been reported by Liu et al. (2012) who found that rsFC between the PCC (associated with self-referential processing) and cerebellum was reduced in MDD groups compared to HC. Negative self-referential processing, is a common feature of MDD and has been associated with MDD severity (Lou, Lei, Mei, Leppänen, & Li, 2019). We also observed decreased awFC between the right DLPFC and the right temporal lobe (encompassing the right temporo-parietal junction). In this case, when we

examined the functional and structural data independently, we did not find differences in functional connectivity, but there were detectable changes in structural connectivity. Past literature (Hwang et al., 2015; Penner et al., 2018) has identified that reduced functional connectivity between the right temporo-parietal junction and right DLPFC in MDD, is associated with depression severity. Lower connectivity between these regions was associated with more severe depression symptomology (Hwang et al., 2015). We also observed reduced awFC between the right DLPFC and the left temporal lobe (includes the left temporo-parietal junction). It is interesting to note that we observed significant differences in functional connectivity between this region pair, but structural connectivity had no detectable changes with MDD compared to HC. With our *FATCAT-awFC* approach, it appears that significant group differences in the underlying SC do not drive the awFC connectivity differences as much as FC differences do. Our finding were supported by (Hwang et al., 2015; Penner et al., 2018), who also detected decreased functional connectivity between the right DLPFC and the left temporal lobe in MDD patients. According to (Samson, Apperly, Chiavarino, & Humphreys, 2004) the reduced connectivity between the frontal lobe and the left temporo-parietal junction may be associated with difficulty assessing thoughts that another person possesses. Inaccurately interpreting mental states, often results in reduced social interactions and may contribute to further social isolation in MDD (Weightman, Air, & Baune, 2014). Connectivity changes (between these three region pairs) in MDD reported in our study are well documented in MDD literature, confirming that our method is effective at detecting some of the neural changes associated with MDD.

In contrast to our predictions, we did not observe group differences in awFC network connections of the LIM. These findings may be a result of our use of relatively large ROIs,

which encompassed a number of brain regions with varying functions. In our analyses, the LIM that was extracted by *3dMatch* consisted of three large ROIs, where the first two were homotopic ROIs, whereby each ROI included the parahippocampal gyrus, temporal fusiform gyrus, inferior temporal gyrus; the third ROI crossed the midline and consisted of the bilateral amygdala, nucleus accumbens, caudate, paracingulate gyrus, frontal medial gyrus, and putamen. Consequently, it may be that because these ROIs were so large, they lacked the specificity necessary to identify localized group differences. In addition, in contrast to expected patterns, we did not observe group differences in awFC network connections in either the FPN, or DAN.

In our study, we conducted a post hoc test that consisted of a PCA and PCR, to study the association between connectivity and cognitive data. We found a trend in the association between complex attention and the awFC within the DMN (PCC to cerebellum/occipital regions). We also found a trend level association between complex attention and the awFC between the right temporal lobe to the right DLPFC. The standard functional Yeo template, classifies the anterior temporo-parietal junction as a component of the VAN (Yeo et al., 2011). The VAN is involved in regulating emotional salient events (Korgaonkar, Goldstein-Piekarski, Fornito, & Williams, 2020) and as such. our observation of reduced awFC between this ROI-pair may point to connectivty changes that underlie the mood dysregulation associated with MDD (American Psychiatric Association, 2013).

Our *FATCAT-awFC* approach identified region pairs that were observable in one modality but not the other. The *FATCAT-awFC* model identified group differences in connectivity, some of which were only captured using SC, and others identified through FC. Using SC alone resulted in many region pairs having detectable differences in MDD compared to HC. However, this may be a result of false positive findings in SC (Bowman et al., 2012), whereas FC identified just two

regions with group differences after correction for multiple comparisons. Furthermore, our *FATCAT-awFC* approach revealed a connectivity change in MDD that was undetected using the conventional FC approach alone. Finally, for most comparisons the *FATCAT-awFC* approach resulted in *p*-values that were lower than those in a single modality, suggesting that *FATCAT-awFC* was sensitive to connectivity changes distinguishing groups.

2.5.1 Contributions of the FATCAT-awFC

The FATCAT-awFC pipeline was designed to be a more practical solution for combining FC and SC together. With our *FATCAT-awFC* pipeline, we hope that researchers will benefit from a faster and more intuitive approach to combining SC and FC, as opposed to using a computationally intense method (*awFC method*) or a toolbox that does not provide maximal information (*FATCAT*) alone. The combination of FATCAT with awFC provides for a unique hybrid pipeline that combines the advantages of an intuitive, rapid and efficient toolbox with a computationally intense data-fusion approach that provides an abundance of information. By combining FC and SC data we are able to better represent whole brain connectivity as opposed to studying it utilizing data from one modality alone. The *awFC* metric is able to measure the combined effect of SC and FC and may provide us with a more accurate connectivity value as it relates to different neuropsychiatric disorders.

There were two main limitations in this study. The first is that one set of group ROIs (derived from gICA) were generated from the CAN-BIND participants. This was done to have a consistent number of ROIs across participants; however applying the same group networks across all participant-level networks implies spatial similarity among all participants (Sohn et al., 2015). However, gICA does not account for inter-participant variability in functional

boundaries, and does not construct participant-specific spatial maps of networks. The second limitation was the ambiguity of selecting a cut-off threshold for ROI creation. There is no standard for selecting ROIs, although many studies have selected a threshold of $Z > 2.3$ (Sohn et al., 2015). ROI selection is a threshold-dependent process and can have very different effects on the outcomes and conclusions of a study (Sohn et al., 2015). Our ROIs were fairly large and encompassed a number of functionally different regions. Tong and associates (Tong et al., 2016) found that larger ROIs are often accompanied by greater variance within connectivity data, in comparison to smaller ROIs, resulting in a smaller effect size. Consequently, the larger ROI used in this study may have reduced our capacity to detect group differences.

Hebbian theory is summarized as: "neurons that fire together, wire together" (Keysers & Perrett, 2004), which suggests that regions that are functionally connected (temporally synchronous) are in principal structurally connected through fiber tracts. The complimentary nature of FC and SC suggests their combination would provide a more complete picture of connectivity as a whole. Due to the complex nature of data fusion in neuroimaging, many researchers have not utilized this approach. By integrating a toolbox (FATCAT) with a computationally intense technique for combining SC and FC (awFC), we were able to implement a relatively straightforward approach to the combination of functional and structural data. We also showed that *FATCAT-awFC* was capable of identifying ROI-pairs, which would have been missed when only applying unimodal analyses. Hence, the joint approach of *FATCAT-awFC* allows for a more detailed understanding of the interconnected nature between structural and functional connectivity and how it relates to depression.

2.5.2 Figures

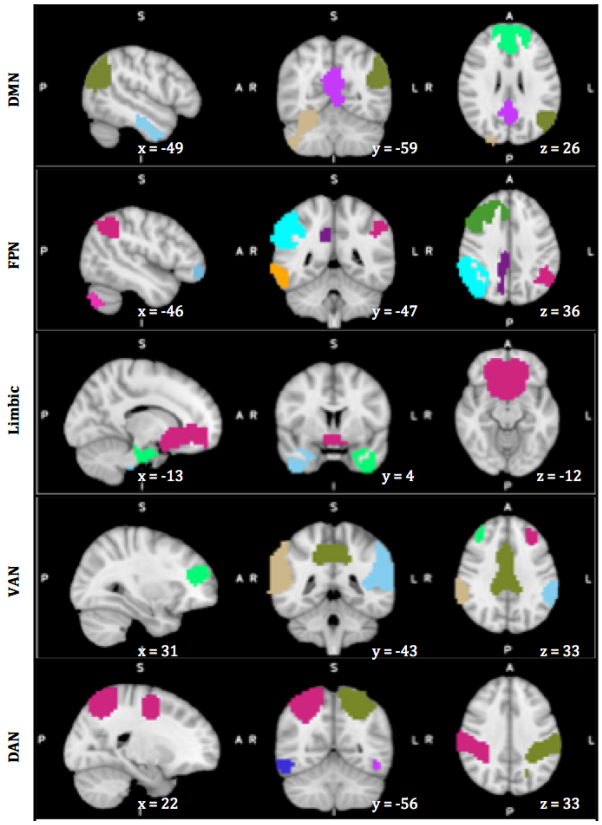

Figure 1 | The resting state networks and corresponding regions of interest (ROIs) derived through group independent component analyses of RS fMRI data. CANBIND-1 resting-state fMRI data was used to extract ROIs. Five resting-state networks were identified and extracted from the components (DMN, default mode network; DAN, dorsal attention network; FPN, fronto-parietal network; Limbic, limbic network; VAN, ventral attention network). *Z*-score maps were thresholded and binarized using FATCATs *3dROIMaker* to generate network masks

(DMN, $Z = 5.5$; FPN, $Z = 9$; Limbic, $Z = 6$; DAN, $Z = 5.5$; VAN, $Z = 11$). The colored regions depicted represent different ROIs within each network

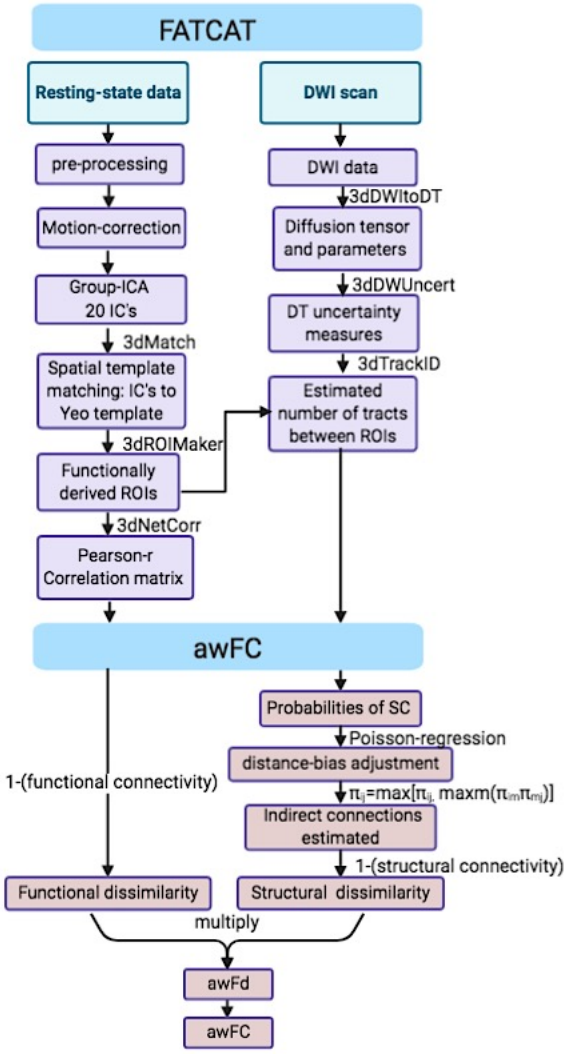

Figure 2 | The FATCAT-awFC analysis pipeline. awFC, anatomically weighted functional connectivity; FATCAT, functional and tractographic connectivity analysis toolbox

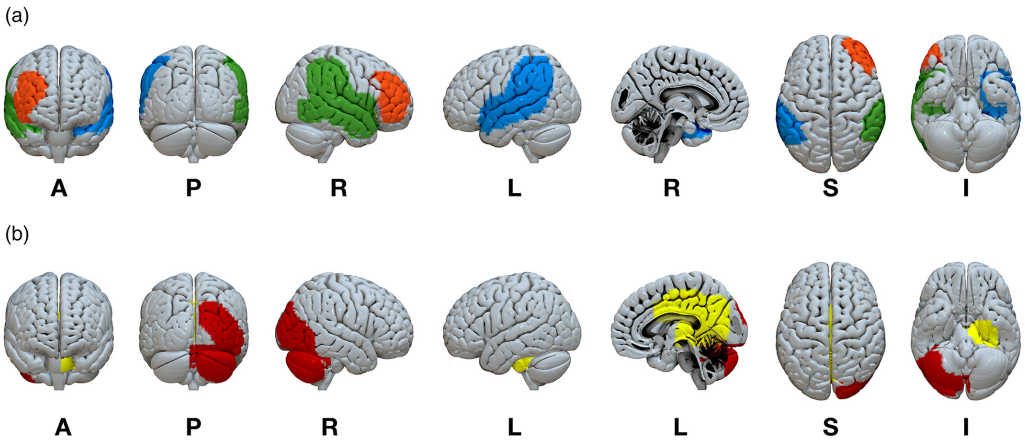

Figure 3 | ROIs within RSNs with significant brain connectivity group differences (a) VAN, orange = right DLPFC, blue = left temporal lobe, green = right temporal lobe. (b) DMN, red ROI = cerebellum/lateral occipital cortex, yellow ROI = posterior cingulate cortex (PCC). ROIs, regions of interest; RSNs, resting state networks; A, anterior; P, posterior; R, right; L, left; S, superior; I, inferior

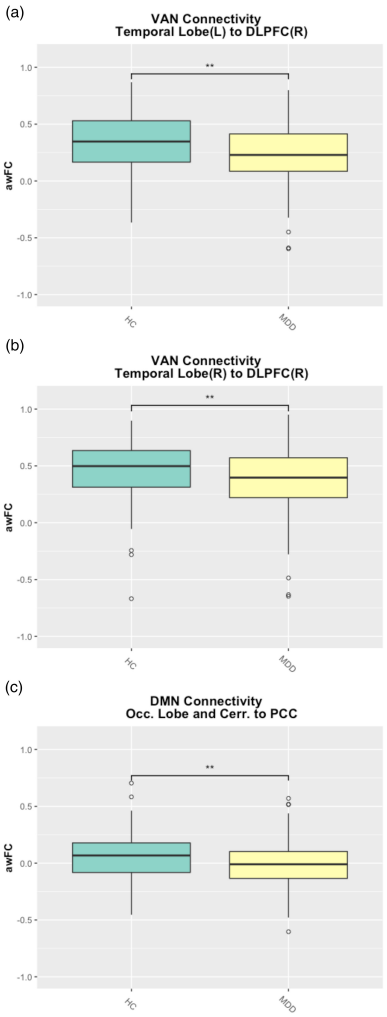

Figure 4 | Boxplots demonstrated lower anatomically weighted functional connectivity between ROI-pairs for the major depressive disorder (MDD) and healthy comparison (HC) participants. Boxplots also quantified the strength of connectivity for MDD and HC groups (a) AwFC between the left temporal lobe and the right DLPFC within the VAN (b) AwFC between the right temporal lobe and the right DLPFC within the VAN (c) AwFC between the occiptial lobe/cerebellum and the PCC within the DMN. AwFC, anatomically weighted functional connectivity; DLPFC, dorsolateral prefrontal cortex; VAN, ventral attention network; DMN, default mode network; Occ., occipital; Cerr., cerebellum; PCC, posterior cingulate cortex. Asterisks identify significant between-group differences following FDR correction ($p < .05$)

2.6 References

Beckmann, C. F., DeLuca, M., Devlin, J. T., & Smith, S. M. (2005). Investigations into resting-state connectivity using independent component analysis. *Philosophical Transactions of the Royal Society of London. Series B, Biological Sciences*, *360*(1457), 1001–1013. https://doi.org/10.1098/rstb.2005.1634

Behrens, T. E. J., Berg, H. J., Jbabdi, S., Rushworth, M. F. S., & Woolrich, M. W. (2007). Probabilistic diffusion tractography with multiple fibre orientations: What can we gain? *NeuroImage*, *34*(1), 144–155. https://doi.org/10.1016/j.neuroimage.2006.09.018

Biswal, B. B., Van Kylen, J., & Hyde, J. S. (1997). Simultaneous assessment of flow and BOLD signals in resting-state functional connectivity maps. *NMR in Biomedicine*, *10*(4–5), 165–170.

Bowman, F. D., Zhang, L., Derado, G., & Chen, S. (2012). Determining Functional Connectivity using fMRI Data with Diffusion-Based Anatomical Weighting. *NeuroImage*, *62*(3), 1769–1779. https://doi.org/10.1016/j.neuroimage.2012.05.032

Calhoun, V. D., & Sui, J. (2016). Multimodal fusion of brain imaging data: A key to finding the missing link(s) in complex mental illness. *Biological Psychiatry : Cognitive Neuroscience and Neuroimaging*, *1*(3), 230–244. https://doi.org/10.1016/j.bpsc.2015.12.005

Carbonell, F., Bellec, P., & Shmuel, A. (2011). Global and system-specific resting-state fMRI fluctuations are uncorrelated: Principal component analysis reveals anti-correlated networks. *Brain Connectivity*, *1*(6), 496–510. https://doi.org/10.1089/brain.2011.0065

Choi, K. S., Craddock, R., Holtzheimer, P. E., Yang, Z., Hu, X., & Mayberg, H. S. (2008). *A Combined Functional-Structural Connectivity Analysis of Major Depression Using Joint Independent Components Analysis*.

Churchill, N. W., Raamana, P., Spring, R., & Strother, S. C. (2017). Optimizing fMRI preprocessing pipelines for block-design tasks as a function of age. *NeuroImage*, *154*, 240–254. https://doi.org/10.1016/j.neuroimage.2017.02.028

Churchill, N. W., Spring, R., Afshin-Pour, B., Dong, F., & Strother, S. C. (2015). An Automated, Adaptive Framework for Optimizing Preprocessing Pipelines in Task-Based Functional MRI. *PLOS ONE*, *10*(7), e0131520. https://doi.org/10.1371/journal.pone.0131520

Churchill, N. W., & Strother, S. C. (2013). PHYCAA+: An optimized, adaptive procedure for measuring and controlling physiological noise in BOLD fMRI. *NeuroImage*, *82*, 306–325. https://doi.org/10.1016/j.neuroimage.2013.05.102

Coloigner, J., Batail, J.-M., Commowick, O., Corouge, I., Robert, G., Barillot, C., & Drapier, D. (2019). White matter abnormalities in depression: A categorical and phenotypic diffusion MRI study. *NeuroImage : Clinical*, *22*. https://doi.org/10.1016/j.nicl.2019.101710

Cox, R. W. (1996). AFNI: Software for analysis and visualization of functional magnetic resonance neuroimages. *Computers and Biomedical Research, an International Journal*, *29*(3), 162–173. https://doi.org/10.1006/cbmr.1996.0014

Cusack, R., Vicente-Grabovetsky, A., Mitchell, D. J., Wild, C. J., Auer, T., Linke, A. C., & Peelle, J. E. (2015). Automatic analysis (aa): Efficient neuroimaging workflows and parallel processing using Matlab and XML. *Frontiers in Neuroinformatics*, *8*. https://doi.org/10.3389/fninf.2014.00090

Damoiseaux, J. S., Rombouts, S. a. R. B., Barkhof, F., Scheltens, P., Stam, C. J., Smith, S. M., & Beckmann, C. F. (2006). Consistent resting-state networks across healthy subjects. *Proceedings of the National Academy of Sciences*, *103*(37), 13848–13853. https://doi.org/10.1073/pnas.0601417103

Davis, A. D., Hassel, S., Arnott, S. R., Harris, J., Lam, R. W., Milev, R., Rotzinger, S., Zamyadi, M., Frey, B. N., Minuzzi, L., Strother, S. C., MacQueen, G. M., Kennedy, S., & Hall, G. B. (2019). White Matter Indices of Medication Response in Major Depression: A Diffusion Tensor Imaging Study. *Biological Psychiatry: Cognitive Neuroscience and Neuroimaging*, *4*(10), 913–924. https://doi.org/10.1016/j.bpsc.2019.05.016

de Kwaasteniet, B., Ruhe, E., Caan, M., Rive, M., Olabarriaga, S., Groefsema, M., Heesink, L., van Wingen, G., & Denys, D. (2013). Relation between structural and functional connectivity in major depressive disorder. *Biological Psychiatry*, *74*(1), 40–47. https://doi.org/10.1016/j.biopsych.2012.12.024

Dosenbach, N. U. F., Koller, J. M., Earl, E. A., Miranda-Dominguez, O., Klein, R. L., Van, A. N., Snyder, A. Z., Nagel, B. J., Nigg, J. T., Nguyen, A. L., Wesevich, V., Greene, D. J., & Fair, D. A. (2017). Real-time motion analytics during brain MRI improve data quality and reduce costs. *NeuroImage*, *161*, 80–93. https://doi.org/10.1016/j.neuroimage.2017.08.025

Dyrba, M., Ewers, M., Wegrzyn, M., Kilimann, I., Plant, C., Oswald, A., Meindl, T., Pievani, M., Bokde, A. L. W., Fellgiebel, A., Filippi, M., Hampel, H., Klöppel, S., Hauenstein, K., Kirste, T., & Teipel, S. J. (2012). Combining DTI and MRI for the Automated Detection of Alzheimer's Disease Using a Large European Multicenter Dataset. In P.-T. Yap, T.

Liu, D. Shen, C.-F. Westin, & L. Shen (Eds.), *Multimodal Brain Image Analysis* (pp. 18–28). Springer. https://doi.org/10.1007/978-3-642-33530-3_2

Esposito, F., Scarabino, T., Hyvarinen, A., Himberg, J., Formisano, E., Comani, S., Tedeschi, G., Goebel, R., Seifritz, E., & Di Salle, F. (2005). Independent component analysis of fMRI group studies by self-organizing clustering. *NeuroImage*, *25*(1), 193–205. https://doi.org/10.1016/j.neuroimage.2004.10.042

Geerligs, L., Cam-CAN, & Henson, R. N. (2016). Functional connectivity and structural covariance between regions of interest can be measured more accurately using multivariate distance correlation. *NeuroImage*, *135*, 16–31. https://doi.org/10.1016/j.neuroimage.2016.04.047

Greicius, M. D., Supekar, K., Menon, V., & Dougherty, R. F. (2009). Resting-State Functional Connectivity Reflects Structural Connectivity in the Default Mode Network. *Cerebral Cortex*, *19*(1), 72–78. https://doi.org/10.1093/cercor/bhn059

Griffanti, L. (2019, July 9). *MELODIC - FslWiki*. https://fsl.fmrib.ox.ac.uk/fsl/fslwiki/MELODIC

Guttman, L. (1954). Some necessary conditions for common-factor analysis | SpringerLink. *Psychometrika*, *19*, 149–161.

Hair, J., Black, W., Babin, B., & Anderson, R. (2009). *Multivariate Data Analysis* (7th ed.). Pearson. https://www.pearson.ch/HigherEducation/Pearson/EAN/9780138132637/Multivariate-Data-Analysis

Hecke, W. V., Emsell, L., & Sunaert, S. (Eds.). (2016). *Diffusion Tensor Imaging: A Practical Handbook*. Springer-Verlag. https://www.springer.com/gp/book/9781493931170

Honey, C. J., Sporns, O., Cammoun, L., Gigandet, X., Thiran, J. P., Meuli, R., & Hagmann, P. (2009). Predicting human resting-state functional connectivity from structural connectivity. *Proceedings of the National Academy of Sciences of the United States of America*, *106*(6), 2035–2040. https://doi.org/10.1073/pnas.0811168106

Hosseini, S. M. H., Hoeft, F., & Kesler, S. R. (2012). GAT: A Graph-Theoretical Analysis Toolbox for Analyzing Between-Group Differences in Large-Scale Structural and Functional Brain Networks. *PLOS ONE*, *7*(7), e40709. https://doi.org/10.1371/journal.pone.0040709

Huang, H., & Ding, M. (2016). Linking Functional Connectivity and Structural Connectivity Quantitatively: A Comparison of Methods. *Brain Connectivity*, *6*(2), 99–108. https://doi.org/10.1089/brain.2015.0382

Hwang, J. W., Egorova, N., Yang, X. Q., Zhang, W. Y., Chen, J., Yang, X. Y., Hu, L. J., Sun, S., Tu, Y., & Kong, J. (2015). Subthreshold depression is associated with impaired resting-state functional connectivity of the cognitive control network. *Translational Psychiatry*, *5*(11), e683. https://doi.org/10.1038/tp.2015.174

Jenkinson, M., Beckmann, C. F., Behrens, T. E. J., Woolrich, M. W., & Smith, S. M. (2012). FSL. *NeuroImage*, *62*(2), 782–790. https://doi.org/10.1016/j.neuroimage.2011.09.015

Juneja, A., Rana, B., & Agrawal, R. K. (2016). A combination of singular value decomposition and multivariate feature selection method for diagnosis of schizophrenia using fMRI. *Biomedical Signal Processing and Control*, *27*, 122–133. https://doi.org/10.1016/j.bspc.2016.02.009

Kaiser, H. (1961). A note on Guttman's lower bound for the number of common factors. *British Journal of Statistical Psychology*. https://bpspsychub.onlinelibrary.wiley.com/doi/abs/10.1111/j.2044-8317.1961.tb00061.x

Kaiser, H. F. (1960). The Application of Electronic Computers to Factor Analysis. *Educational and Psychological Measurement*, *20*(1), 141–151. https://doi.org/10.1177/001316446002000116

Kaiser, R. H., Andrews-Hanna, J. R., Wager, T. D., & Pizzagalli, D. A. (2015). Large-scale network dysfunction in Major Depressive Disorder: Meta-analysis of resting-state functional connectivity. *JAMA Psychiatry*, *72*(6), 603–611. https://doi.org/10.1001/jamapsychiatry.2015.0071

Kambeitz, J., Cabral, C., Sacchet, M. D., Gotlib, I. H., Zahn, R., Serpa, M. H., Walter, M., Falkai, P., & Koutsouleris, N. (2017). Detecting Neuroimaging Biomarkers for Depression: A Meta-analysis of Multivariate Pattern Recognition Studies. *Biological Psychiatry*, *82*(5), 330–338. https://doi.org/10.1016/j.biopsych.2016.10.028

Kassambara, A. (2017). *Practical Guide To Principal Component Methods in R: PCA, M(CA), FAMD, MFA, HCPC, factoextra*. STHDA.

Kennedy, S., Lam, R., Rotzinger, S., Milev, R., Blier, P., Downar, J., Evans, K., Farzan, F., Foster, J., Frey, B., Giacobbe, P., Hall, G., Harkness, K., Hassel, S., Ismail, Z., Leri, F., McInerney, S., MacQueen, G. M., Minuzzi, L., … CAN-BIND Investigator Team. (2019). Symptomatic and Functional Outcomes and Early Prediction of Response to Escitalopram Monotherapy and Sequential Adjunctive Aripiprazole Therapy in Patients With Major Depressive Disorder: A CAN-BIND-1 Report. *The Journal of Clinical Psychiatry*, *80*(2). https://doi.org/10.4088/JCP.18m12202

Keysers, C., & Perrett, D. I. (2004). Demystifying social cognition: A Hebbian perspective. *Trends in Cognitive Sciences*, *8*, 501–507. https://doi.org/10.1016/j.tics.2004.09.005

Klooster, D. C. W., Vos, I. N., Caeyenberghs, K., Leemans, A., David, S., Besseling, R. M. H., Aldenkamp, A. P., & Baeken, C. (2020). Indirect frontocingulate structural connectivity predicts clinical response to accelerated rTMS in major depressive disorder. *Journal of Psychiatry and Neuroscience*, 243–252. https://doi.org/10.1503/jpn.190088

Koch, M. A., Norris, D. G., & Hund-Georgiadis, M. (2002). An investigation of functional and anatomical connectivity using magnetic resonance imaging. *NeuroImage*, *16*(1), 241–250. https://doi.org/10.1006/nimg.2001.1052

Korgaonkar, M. S., Goldstein-Piekarski, A. N., Fornito, A., & Williams, L. M. (2020). Intrinsic connectomes are a predictive biomarker of remission in major depressive disorder. *Molecular Psychiatry*, *25*(7), 1537–1549. https://doi.org/10.1038/s41380-019-0574-2

Kriegeskorte, N., Mur, M., & Bandettini, P. (2008). Representational Similarity Analysis – Connecting the Branches of Systems Neuroscience. *Frontiers in Systems Neuroscience*, *2*. https://doi.org/10.3389/neuro.06.004.2008

Lam, R., Milev, R., Rotzinger, S., Andreazza, A., Blier, P., Brenner, C., Daskalakis, Z., Dharsee, M., Downar, J., Evans, K., Farzan, F., Foster, J., Frey, B., Geraci, J., Giacobbe, P., Feilotter, H., Hall, G., Harkness, K., Hassel, S., … Kennedy, S. (2016). Discovering biomarkers for antidepressant response: Protocol from the Canadian biomarker integration network in depression (CAN-BIND) and clinical characteristics of the first patient cohort. *BMC Psychiatry*, *16*. https://doi.org/10.1186/s12888-016-0785-x

Lanka, P., & Deshpande, G. (2019). Combining Prospective Acquisition CorrEction (PACE) with retrospective correction to reduce motion artifacts in resting state fMRI data. *Brain and Behavior*, *9*(8), e01341. https://doi.org/10.1002/brb3.1341

Liu, K., Li, Y., Xu, N., & Natarajan, P. (2018). Learn to Combine Modalities in Multimodal Deep Learning. *ArXiv:1805.11730 [Cs, Stat]*. http://arxiv.org/abs/1805.11730

Liu, L., Zeng, L.-L., Li, Y., Ma, Q., Li, B., Shen, H., & Hu, D. (2012). Altered Cerebellar Functional Connectivity with Intrinsic Connectivity Networks in Adults with Major Depressive Disorder. *PLOS ONE*, *7*(6), e39516. https://doi.org/10.1371/journal.pone.0039516

Lou, Y., Lei, Y., Mei, Y., Leppänen, P. H. T., & Li, H. (2019). Review of Abnormal Self-Knowledge in Major Depressive Disorder. *Frontiers in Psychiatry*, *10*. https://doi.org/10.3389/fpsyt.2019.00130

Ma, L., Wang, B., Chen, X., & Xiong, J. (2007). Detecting functional connectivity in the resting brain: A comparison between ICA and CCA. *Magnetic Resonance Imaging*, *25*(1), 47–56. https://doi.org/10.1016/j.mri.2006.09.032

MacQueen, G. M., Hassel, S., Arnott, S. R., Addington, J., Bowie, C. R., Bray, S. L., Davis, A. D., Downar, J., Foster, J. A., Frey, B. N., Goldstein, B. I., Hall, G. B., Harkness, K. L., Harris, J., Lam, R. W., Lebel, C., Milev, R., Müller, D. J., Parikh, S. V., … Kennedy, S. (2019). The Canadian Biomarker Integration Network in Depression (CAN-BIND): Magnetic resonance imaging protocols. *Journal of Psychiatry & Neuroscience : JPN*, *44*(4), 223–236. https://doi.org/10.1503/jpn.180036

Maknojia, S., Churchill, N. W., Schweizer, T. A., & Graham, S. J. (2019). Resting State fMRI: Going Through the Motions. *Frontiers in Neuroscience*, *13*. https://doi.org/10.3389/fnins.2019.00825

Man, M. Y., Ong, M. S., Mohamad, M. S., Deris, S., Sulong, G., Yunus, J., & Che Harun, F. K. (2015). A Review on the Bioinformatics Tools for Neuroimaging. *The Malaysian Journal of Medical Sciences : MJMS*, *22*(Spec Issue), 9–19.

Marques, P. C. G., Soares, J. M., Alves, V., & Sousa, N. (2013). BrainCAT - a tool for automated and combined functional Magnetic Resonance Imaging and Diffusion Tensor Imaging brain connectivity analysis. *Frontiers in Human Neuroscience*, *7*. https://doi.org/10.3389/fnhum.2013.00794

McRobbie, D. W., Moore, E. A., Graves, M. J., & Prince, M. R. (2017). *MRI from Picture to Proton*. Cambridge University Press.

Montgomery, S. A., & Asberg, M. (1979). A new depression scale designed to be sensitive to change. *The British Journal of Psychiatry: The Journal of Mental Science*, *134*, 382–389. https://doi.org/10.1192/bjp.134.4.382

Nascimento, M., Silva, F. F., Sáfadi, T., Nascimento, A. C. C., Ferreira, T. E. M., Barroso, L. M. A., Azevedo, C. F., Guimarães, S. E. F., & Serão, N. V. L. (2017). Independent Component Analysis (ICA) based-clustering of temporal RNA-seq data. *PloS One*. https://doi.org/10.1371/journal.pone.0181195

Nugent, A. C., Farmer, C., Evans, J. W., Snider, S. L., Banerjee, D., & Zarate, C. A. (2019). Multimodal imaging reveals a complex pattern of dysfunction in corticolimbic pathways in major depressive disorder. *Human Brain Mapping*, *40*(13), 3940–3950. https://doi.org/10.1002/hbm.24679

Park, H.-J., & Friston, K. (2013). Structural and Functional Brain Networks: From Connections to Cognition. *Science*, *342*(6158), 1238411. https://doi.org/10.1126/science.1238411

Peled, S., Friman, O., Jolesz, F., & Westin, C.-F. (2006). Geometrically constrained two-tensor model for crossing tracts in DWI. *Magnetic Resonance Imaging*, *24*(9), 1263–1270. https://doi.org/10.1016/j.mri.2006.07.009

Penner, J., Osuch, E. A., Schaefer, B., Théberge, J., Neufeld, R. W. J., Menon, R. S., Rajakumar, N., & Williamson, P. C. (2018). Temporoparietal Junction Functional Connectivity in Early Schizophrenia and Major Depressive Disorder. *Chronic Stress*, *2*, 2470547018815232. https://doi.org/10.1177/2470547018815232

Pineda-Pardo, J. A., Bruña, R., Woolrich, M., Marcos, A., Nobre, A. C., Maestú, F., & Vidaurre, D. (2014). Guiding functional connectivity estimation by structural connectivity in MEG: An application to discrimination of conditions of mild cognitive impairment. *NeuroImage*, *101*, 765–777. https://doi.org/10.1016/j.neuroimage.2014.08.002

R Core Team. (2018). *R: A Language and Environment for Statistical Computing*. https://www.r-project.org/

Reddi, S. J. (2015). *Understanding the relationship between Functional and Structural Connectivity of Brain Networks*. 23.

Refaat, M. (2010). *Data Preparation for Data Mining Using SAS*. Elsevier.

Ribeiro, A. S., Lacerda, L. M., & Ferreira, H. A. (2015). Multimodal Imaging Brain Connectivity Analysis (MIBCA) toolbox. *PeerJ*, *3*. https://doi.org/10.7717/peerj.1078

Rorden, C., & Brett, M. (2000). Stereotaxic display of brain lesions. *Behavioural Neurology*, *12*(4), 191–200. https://doi.org/10.1155/2000/421719

Rosa, M. J., Portugal, L., Hahn, T., Fallgatter, A. J., Garrido, M. I., Shawe-Taylor, J., & Mourao-Miranda, J. (2015). Sparse network-based models for patient classification using fMRI. *NeuroImage*, *105*, 493–506. https://doi.org/10.1016/j.neuroimage.2014.11.021

Rubinov, M., & Sporns, O. (2010). Complex network measures of brain connectivity: Uses and interpretations. *NeuroImage*, *52*(3), 1059–1069. https://doi.org/10.1016/j.neuroimage.2009.10.003

Sala-Llonch, R., Bartrés-Faz, D., & Junqué, C. (2015). Reorganization of brain networks in aging: A review of functional connectivity studies. *Frontiers in Psychology*, *6*. https://doi.org/10.3389/fpsyg.2015.00663

Samson, D., Apperly, I. A., Chiavarino, C., & Humphreys, G. W. (2004). Left temporoparietal junction is necessary for representing someone else's belief. *Nature Neuroscience*, *7*(5), 499–500. https://doi.org/10.1038/nn1223

Schloerke, B., Cook, D., Larmarange, J., Briatte, F., Marbach, M., Thoen, E., Elberg, A., Toomet, O., Crowley, J., Hofmann, H., & Wickham, H. (2018). *GGally: Extension to "ggplot2."* https:// CrAn.r-project.org/package=GGally

Smith, S. M., Jenkinson, M., Woolrich, M. W., Beckmann, C. F., Behrens, T. E. J., Johansen-Berg, H., Bannister, P. R., De Luca, M., Drobnjak, I., Flitney, D. E., Niazy, R. K., Saunders, J., Vickers, J., Zhang, Y., De Stefano, N., Brady, J. M., & Matthews, P. M. (2004). Advances in functional and structural MR image analysis and implementation as FSL. *NeuroImage*, *23 Suppl 1*, S208-219. https://doi.org/10.1016/j.neuroimage.2004.07.051

Sohn, W. S., Yoo, K., Lee, Y.-B., Seo, S. W., Na, D. L., & Jeong, Y. (2015). Influence of ROI selection on resting state functional connectivity: An individualized approach for resting

state fMRI analysis. *Frontiers in Neuroscience*, *9*. https://doi.org/10.3389/fnins.2015.00280

Taylor, P. A., & Saad, Z. S. (2013). FATCAT: (An Efficient) Functional And Tractographic Connectivity Analysis Toolbox. *Brain Connectivity*, *3*(5), 523–535. https://doi.org/10.1089/brain.2013.0154

Tong, Y., Chen, Q., Nichols, T. E., Rasetti, R., Callicott, J. H., Berman, K. F., Weinberger, D. R., & Mattay, V. S. (2016). Seeking Optimal Region-Of-Interest (ROI) Single-Value Summary Measures for fMRI Studies in Imaging Genetics. *PLOS ONE*, *11*(3), e0151391. https://doi.org/10.1371/journal.pone.0151391

van den Heuvel, M. P., Sporns, O., Collin, G., Scheewe, T., Mandl, R. C. W., Cahn, W., Goñi, J., Hulshoff Pol, H. E., & Kahn, R. S. (2013). Abnormal Rich Club Organization and Functional Brain Dynamics in Schizophrenia. *JAMA Psychiatry*, *70*(8), 783. https://doi.org/10.1001/jamapsychiatry.2013.1328

Vasudevan, V., & Ramakrishna, M. (2019). A Hierarchical Singular Value Decomposition Algorithm for Low Rank Matrices. *ArXiv:1710.02812 [Cs]*. http://arxiv.org/abs/1710.02812

Ven, V. G. van de, Formisano, E., Prvulovic, D., Roeder, C. H., & Linden, D. E. J. (2004). Functional connectivity as revealed by spatial independent component analysis of fMRI measurements during rest. *Human Brain Mapping*, *22*(3), 165–178. https://doi.org/10.1002/hbm.20022

Vergun, S., Gaggl, W., Nair, V. A., Suhonen, J. I., Birn, R. M., Ahmed, A. S., Meyerand, M. E., Reuss, J., DeYoe, E. A., & Prabhakaran, V. (2016). Classification and Extraction of

Resting State Networks Using Healthy and Epilepsy fMRI Data. *Frontiers in Neuroscience*, *10*. https://doi.org/10.3389/fnins.2016.00440

Waite, T. A., & Campbell, L. G. (2006). Controlling the false discovery rate and increasing statistical power in ecological studies. *Ecoscience*, *13*(4), 439–442. https://doi.org/10.2980/1195-6860(2006)13[439:CTFDRA]2.0.CO;2

Wang, L., Adeli, E., Wang, Q., Shi, Y., & Suk, H.-I. (2016). *Machine Learning in Medical Imaging: 7th International Workshop, MLMI 2016, Held in Conjunction with MICCAI 2016, Athens, Greece, October 17, 2016, Proceedings*. Springer.

Webster, M. (2012, August 13). *FMRIB58_FA - FslWiki*. https://fsl.fmrib.ox.ac.uk/fsl/fslwiki/FMRIB58_FA

Weightman, M. J., Air, T. M., & Baune, B. T. (2014). A Review of the Role of Social Cognition in Major Depressive Disorder. *Frontiers in Psychiatry*, *5*. https://doi.org/10.3389/fpsyt.2014.00179

Wiegell, M. R., Larsson, H. B., & Wedeen, V. J. (2000). Fiber crossing in human brain depicted with diffusion tensor MR imaging. *Radiology*, *217*(3), 897–903. https://doi.org/10.1148/radiology.217.3.r00nv43897

Wu, F., Tu, Z., Sun, J., Geng, H., Zhou, Y., Jiang, X., Li, H., & Kong, L. (2020). Abnormal Functional and Structural Connectivity of Amygdala-Prefrontal Circuit in First-Episode Adolescent Depression: A Combined fMRI and DTI Study. *Frontiers in Psychiatry*, *10*. https://doi.org/10.3389/fpsyt.2019.00983

Wu, M., Andreescu, C., Butters, M. A., Tamburo, R., Reynolds, C. F., & Aizenstein, H. (2011). Default-mode network connectivity and white matter burden in late-life depression.

Psychiatry Research: Neuroimaging, *194*(1), 39–46. https://doi.org/10.1016/j.pscychresns.2011.04.003

Yeatman, J. D., Dougherty, R. F., Myall, N. J., Wandell, B. A., & Feldman, H. M. (2012). Tract Profiles of White Matter Properties: Automating Fiber-Tract Quantification. *PLoS ONE*, *7*(11), e49790. https://doi.org/10.1371/journal.pone.0049790

Yeo, B. T. T., Krienen, F. M., Sepulcre, J., Sabuncu, M. R., Lashkari, D., Hollinshead, M., Roffman, J. L., Smoller, J. W., Zöllei, L., Polimeni, J. R., Fischl, B., Liu, H., & Buckner, R. L. (2011). The organization of the human cerebral cortex estimated by intrinsic functional connectivity. *Journal of Neurophysiology*, *106*(3), 1125–1165. https://doi.org/10.1152/jn.00338.2011

Yoo, K., Rosenberg, M. D., Hsu, W.-T., Zhang, S., Li, C.-S. R., Scheinost, D., Constable, R. T., & Chun, M. M. (2018). Connectome-based predictive modeling of attention: Comparing different functional connectivity features and prediction methods across datasets. *NeuroImage*, *167*, 11–22. https://doi.org/10.1016/j.neuroimage.2017.11.010

Zhang, D., Snyder, A. Z., Shimony, J. S., Fox, M. D., & Raichle, M. E. (2010). Noninvasive Functional and Structural Connectivity Mapping of the Human Thalamocortical System. *Cerebral Cortex*, *20*(5), 1187–1194. https://doi.org/10.1093/cercor/bhp182

Zhu, D., Zhang, T., Jiang, X., Hu, X., Chen, H., Yang, N., Lv, J., Han, J., Guo, L., & Liu, T. (2014). Fusing DTI and FMRI Data: A Survey of Methods and Applications. *NeuroImage*, *102 Pt 1*, 184–191. https://doi.org/10.1016/j.neuroimage.2013.09.071

Chapter 3: Assessing Remission In Major Depressive Disorder Using a Functional-Structural Data Fusion Pipeline: A CAN-BIND-1 Study

Submitted to: Elsevier Neuroscience, October 2021

Sondos Ayyash[1,2], Andrew D Davis[3,4], Gésine L Alders[5], Glenda MacQueen[6,7], Stephen C Strother[4,8,9], Stefanie Hassel[6,7], Mojdeh Zamyadi[4], Stephen R Arnott[4], Jacqueline K Harris[10], Raymond W Lam[11], Roumen Milev[12], Daniel J Müller[13,14], Sidney H Kennedy[8,14,15,16,17], Susan Rotzinger[14,16,17], Benicio N Frey[3,5,18], Luciano Minuzzi[3,5,18], Geoffrey B Hall[1,2,3,5], CAN-BIND Investigator Team

[1] School of Biomedical Engineering, McMaster University, Hamilton, Ontario, Canada.
[2] Department of Psychology Neuroscience & Behaviour, McMaster University, Hamilton, Ontario, Canada.
[3] Department of Psychiatry and Behavioural Neurosciences, McMaster University, Hamilton, Ontario, Canada.
[4] Rotman Research Institute, Baycrest, Toronto, Ontario, Canada.
[5] Neuroscience Graduate Program, McMaster University, Hamilton, Ontario, Canada.
[6] Hotchkiss Brain Institute and Mathison Centre for Mental Health Research and Education, Cumming School of Medicine, University of Calgary, Calgary, Alberta, Canada.
[7] Department of Psychiatry, Cumming School of Medicine, University of Calgary, Calgary, Alberta, Canada.
[8] Institute of Medical Science, University of Toronto, Toronto, Ontario, Canada.
[9] Department of Medical Biophysics, University of Toronto, Ontario, Canada.
[10] Department of Computer Science, University of Alberta, Edmonton, Alberta, Canada.
[11] Department of Psychiatry, University of British Columbia, Vancouver, British Columbia, Canada.
[12] Departments of Psychiatry and Psychology, Queen's University, Providence Care Hospital, Kingston, Ontario, Canada.
[13] Campbell Family Mental Health Research Institute, Centre for Addiction and Mental Health, Toronto, Ontario, Canada.
[14] Department of Psychiatry, University of Toronto, Toronto, Ontario, Canada.
[15] Centre for Mental Health, University Health Network, Toronto, Ontario, Canada.
[16] Krembil Research Institute, University Health Network, Toronto, Ontario, Canada.
[17] Centre for Depression and Suicide Studies, and Li Ka Shing Knowledge Institute, St. Michael's Hospital, Toronto, Ontario, Canada.
[18] Mood Disorders Treatment and Research Centre and Women's Health Concerns Clinic, St. Joseph's Healthcare, Hamilton, Ontario, Canada.

3.1 Abstract

Neural network-level changes underlying symptom remission in major depressive disorder (MDD) are often studied from a single perspective. Multimodal approaches to assess neuropsychiatric disorders are evolving, as they offer richer information about brain networks. A *FATCAT-awFC* pipeline was developed to integrate a computationally intense data fusion method with a toolbox, to produce a faster and more intuitive pipeline for combining functional connectivity (FC) and structural connectivity (SC). The combined measure is known as anatomically weighted functional connectivity (*awFC*). Ninety-three participants from the Canadian Biomarker Integration Network for Depression study (CAN-BIND-1) were included. These individuals with MDD treated with 8 weeks of escitalopram and adjunctive aripiprazole for another 8 weeks, and between-group connectivity (SC, FC, *awFC*) comparisons were performed for remitters (REM) (defined as Montgomery-Asberg Depression Rating Scale score ≤10 at week-8 sustained through to week-16) versus non-remitters (NREM) (defined as MADRS score >10 at week-8 sustained through to week-16) at baseline and 8 weeks. Additionally, a longitudinal study analysis was preformed to compare connectivity changes in REM from baseline to week-8. The association between cognitive performance and awFC were also assessed. REM were distinguished from NREM by lower *awFC* within the default mode, frontoparietal, and ventral attention networks. Compared to REM at baseline, REM at week-8 revealed increased *awFC* within the dorsal attention network and decreased awFC within the frontoparietal network. A medium effect size was observed for most results. *AwFC* in the frontoparietal network was associated with cognitive flexibility for the NREM group at week-8. In conclusion the practicality of the FATCAT-awFC pipeline, allowed us to better evaluate awFC differences between groups.

Key Words: neuroimaging; major depressive disorder; structural connectivity; functional connectivity; data fusion; resting brain networks; toolbox

3.2 Introduction

Major depressive disorder (MDD) is one of the most common mental health disorders affecting approximately 163 million people worldwide, accounting for high levels of morbidity, mortality and psychosocial functional impairment (James et al., 2018). Antidepressants are one of a number of treatment options used in the management of MDD (Gautam et al., 2017; Kennedy et al., 2016). Selective serotonin reuptake inhibitors (SSRIs) are often the first choice of antidepressant treatment for MDD (Cipriani et al., 2016; Middleton et al., 2005). One of the most commonly prescribed SSRIs for the treatment of MDD is escitalopram (Kaplan & Zhang, 2012).

Clinical remission has become the gold standard and primary goal of MDD treatment (Ballenger, 1999; Khoo et al., 2015; McIntyre et al., 2006; Stahl, 1999). The Diagnostic and Statistical Manual-IV (DSM-IV-TR) (*Diagnostic and Statistical Manual of Mental Disorders*, 2000) defines remission in MDD as the 'absence or near absence of the signs and symptoms' of depression. Other important characteristics of MDD remission after treatment include: the feeling of a return to normal self, improved mental health, and improved functioning (Zimmerman et al., 2006). As such it is of interest to study the effect behavioural changes have on brain connectivity in MDD remission. It is in the MDD remitters that we expect to see changes in connectivity after treatment, because it has been extensively documented that MDD remitters show improved behavioural performance (Zimmerman et al., 2006). However, although symptom remission has become the primary goal of MDD treatment, remission rates vary from 30 to 50 percent in research-based, 6-14-week trials, involving symptomatic participants with MDD (Thase et al., 2005, 2010; Trivedi et al., 2006). In addition, participants

with MDD who fail to attain remission status from one round of antidepressant treatment, have a much lower remission rate with each subsequent treatment attempt (Rush et al., 2006). Non-remission in MDD is often associated with higher healthcare resource utilization and costs (Byford et al., 2011; Dennehy et al., 2015; Kubitz et al., 2013; Mauskopf et al., 2009).

Previous neuroimaging studies in MDD have used structural connectivity (SC) and functional connectivity (FC) to identify neural biomarkers for the prediction of treatment outcomes, including remission (Korgaonkar et al., 2014, 2020). Building on this work, examining the brain connectivity changes between baseline and follow-up in patients with remitted MDD (REM) and patients with non-remitted MDD (NREM) may provide us with a better understanding of the underlyingnetwork-level differences that distinguish these two groups. Alongside clinical remission, cognitive remission is a goal in the treatment of MDD (McIntyre et al., 2013). Cognitive dysfunction is one of the most common symptoms of MDD (Fava et al., 2006; Lee et al., 2012). Cognitive dysfunction impacts multiple cognitive domains such as memory, difficulty in decision making, and loss of cognitive flexibility (Jaeger et al., 2006; McCall & Dunn, 2003; Naismith et al., 2007). While general symptom remission may be achieved with pharmacotherapy, cognitive dysfunction may persist (Conradi et al., 2011; Hasselbalch et al., 2011; Snyder, 2013). Many of the same brain regions that play a role in these cognitive dysfunctions are implicated in MDD (Albert et al., 2019). Therefore, because of this overlap we want to try and understand the association between those cognitive domains and remission. Reports of cognitive deficits in REM have been inconsistent, with some reports of cognitive improvements (Abo Aoun et al., 2019a; Gudayol-Ferré et al., 2015) and other studies reporting persistent cognitive deficits (Bhalla et al., 2006; Conradi et al., 2011; Reppermund et al., 2009).

Combining SC and FC data can capture unique and complimentary aspects of the underlying Resting State Networks (RSN) in REM and NREM. This study focuses on connectivity within five RSNs affected in MDD: the default mode network (DMN), dorsal attention network (DAN), ventral attention network (VAN), frontoparietal network (FPN), and limbic network (LIM). These five networks were drawn from the 7-network model suggested by Buckner et al. (2011). The visual and auditory networks were excluded, similar to a meta-analysis of FC conducted by Kaiser et al. (2015), which specifically investigated RSNs implicated in MDD.

Both structural and functional network-level connectivity changes within RSNs have shown connectivity changes associated with remission status (REM or NREM after treatment), both at baseline and after a course (e.g. 8 weeks) of antidepressant treatment. Karim et al (2017) assessed resting-state FC at different intervals starting at baseline and ending at week-12. They found that REM showed decreased connectivity in the DMN from baseline to week-12, whereas there was increased connectivity in the executive control network, part of the DAN. These findings were attributed to a reduction in rumination and anxiety and greater cognitive control (Karim et al., 2017). These patterns appear to fit within the framework that MDD is characterized by functional under-activity particularly in the executive control network (i.e. pre- and post-central gyrus), and with response to antidepressant treatment there is a shift toward normalized function that is reflected in either strengthening or weakening of brain connections within the executive control network or the DMN (Karim et al., 2017). Studies have also assessed whether FC and SC after antidepressant treatment can distinguish remission status (REM vs NREM). A study by Xiao et al. (2019), found that rapid remission (within 1-5 days)

was associated with lower FC between several brain regions after five days (i.e. between subgenual cingulate cortex and DMN nodes) (Xiao et al., 2019). Additionally, Pillai et al. (2019) performed an SC analysis using fractional anisotropy (FA) after 8 weeks of antidepressant treatment and reported lower SC between the raphe nucleus and amygdala for REM compared to NREM. Hence, treatment of MDD is associated with either increases or decreases of brain connectivity, reflecting normalization – also known as reversal – of the connectivity patterns observed with MDD prior to medication therapy (Wang, Xia, et al., 2014). Combining SC and FC may then provide a more comprehensive understanding of brain changes and their association with clinical variables in REM and NREM (Zheng et al., 2018).

For this project, we examined neuroimaging and clinical data from the Canadian Biomarker Integration Network for Depression study (CAN-BIND-1) comprised of patients with MDD treated with escitalopram alone and with escitalopram and adjunctive aripiprazole (Kennedy et al., 2019; Lam et al., 2016). The goal was to evaluate whether network-level differences can be detected (1) between REM and NREM groups at baseline, (2) between REM and NREM groups at week-8, and (3) within the REM group between baseline and week-8. We applied a *FATCAT-awFC* pipeline, developed in our previous work (Ayyash et al., 2021), that involves the combination of the *Functional and Tractographic Connectivity Analysis Toolbox* (*FATCAT*) (Taylor & Saad, 2013) with a computationally intense method, known as the *Anatomically-Weighted Functional Connectivity* (*awFC*) *method* (Bowman et al., 2012). To the best of our knowledge, this is the first study to perform a data fusion analysis using functional and structural connectivity, to assess the REM and NREM population and study traditional FC and SC within RSNs. We also performed separate and comparative brain connectivity analyses between FC,

SC, and *awFC*. Finally, we explored the association of brain connectivity changes with cognition in RSNs within the REM and NREM groups at baseline and week-8. We hypothesized that NREM will produce lower connectivity strength between brain regions compared to REM, at baseline and week-8. This hypothesis was raised given consideration of the study by Korgaonkar et al. (2020), who demonstrated that at pre-treatment (baseline) NREM displayed a lower connectivity compared to REM, which was amplified post-treatment (week-8). We also hypothesized that the REM group will have reduced connectivity from baseline to week-8. Finally, we hypothesized that connectivity strength will be associated with cognitive performance in the REM and NREM groups at week-8.

3.3 Materials and Methods

3.3.1 Participants

The Canadian Biomarker Integration Network for Depression (CAN-BIND-1) study included participants from six Canadian academic health science institutions (Kennedy et al., 2019; Lam et al., 2016; MacQueen et al., 2019). At each institution, the research protocol was reviewed and approved by the respective research ethics board.

3.3.2 Inclusion and Exclusion Criteria

The included 211 participants from six Canadian academic health science institutions (Kennedy et al., 2019; Lam et al., 2016; MacQueen et al., 2019). The inclusion criteria for these participants included: 18-60 years of age; diagnosis of MDD by DSM-IV-TR criteria and

confirmed with the Mini International Neuropsychiatric Interview (Sheehan et al., 1998); and a Montgomery-Åsberg Depression Rating Scale (MADRS) (Montgomery & Asberg, 1979) score ≥ 24. If previously taking antidepressants, a medication washout of at least five half-lives was required. The exclusion criteria included: diagnoses of psychosis, bipolar I/II disorder, substance use disorder (in the past 6 months), prior brain injury, and prior neurological diseases; four failed trials of pharmacological intervention; history of non-response or intolerance to escitalopram, pregnant or breastfeeding, high suicidality risk; and any magnetic resonance imaging contraindications (MacQueen et al., 2019). Written, informed consent was obtained from all participants before participation in the study, and participants received compensation for their time and effort.

3.3.3 Treatment

Following baseline testing, MDD patients began treatment with the SSRI escitalopram, at a dose of 10mg/d, which was then increased (up to 20 mg/d) at week-2 or week-4 if a 20% or 50% MADRS reduction from baseline was not observed, respectively (Lam et al., 2016). All participants took escitalopram in the first phase of the study (duration of 8 weeks). In phase 2, responders (defined as MADRS reduction from baseline to Week 8 ≥50%) continued to take escitalopram alone, while non-responders were given adjunctive aripiprazole (0.5-2 mg/d) for another 8 weeks. Data were collected at baseline before medication treatment and at week-8 after 8 weeks of escitalopram treatment.

3.3.4 Cognitive testing

The CNS-Vital Signs (CNS-VS) computerized cognitive test battery was used to assess participants' level of cognitive functioning (Gualtieri & Johnson, 2006). Of the administered tests, five cognitive subscales of the CNS-VS test were examined: memory, cognitive flexibility, complex attention, processing speed and neurocognitive index (a summary score that encompasses the mean of five cognitive variables: complex attention, memory, psychomotor speed, reaction time, and cognitive flexibility) (Iverson et al., 2009).

3.3.5 fMRI Data Acquisition and Processing

The rsfMRI scanning was performed on 3.0 T scanners (Three Discovery MR750 from GE Healthcare, USA; One Intera from Phillips, Netherlands; One Signa HDxt from GE Healthcare, USA; One Trio Tim from Siemens, Germany), in which brain MRI images were acquired. For rsFMRI acquisition the participants lay still in the MRI scanner with eyes open, looking at a fixation cross for a total of 10 minutes. Functional images were acquired with an echo planar imaging (EPI) sequence with the following parameters: repetition time (TR)/echo time (TE) = 2000/30ms, 36-40 axial slices, 64 × 64 matrix, 75° flip angle, 256 mm field of view (FOV) (exception: Queens site FOV =1536mm), 4 mm section thickness, with no slice gap, and 300 volumes with one run per session.

3.3.6 T1-Weighted Image Acquisition

Anatomical reference scans were obtained with the following parameters: TR/TE/flip angle: 6.4–7.5 ms/2.7–3.5 ms/8–15° (exception: Siemens Scanners TR = 1760, 1840 ms), inversion time: 450–950 ms, voxel size: $1 \times 1 \times 1$ mm^3, matrix dimensions 240×240 and 256×256, slice thickness: 1 mm, number of slices: 155–192. Time of acquisition for anatomical scans varied from 3:30 to 9:53 minutes. For more information, see (Lam et al., 2016; MacQueen et al., 2019).

3.3.7 fMRI Preprocessing

The software package, Optimization of Preprocessing Pipelines for NeuroImaging-fMRI (OPPNI) was employed for image preprocessing (Churchill et al., 2015; Strother, 2006). For fMRI images, the first five images were discarded to control for destabilization of the magnetic field at scan start. To correct for participant movement during the scan a principal component analysis (PCA) was used to calculate the Euclidean distance of each volume from the median coordinates. The volume with the smallest Euclidean distance from the mean was selected to be the reference volume, and was then utilized in the motion correction step, AFNI's *3dvolreg* function. To mitigate the effects of participant motion, rigid-body realignment was performed, whereby subsequent time-series volumes were transformed to match the reference volume. In the censoring step, slices that were identified as outliers were replaced by interpolated values from neighboring time points via cubic splines. Fourier interpolation was used to correct for timing offsets between interleaved axial slices using AFNI's *3dTshift* (*TIMECOR*) a slice-timing correction function. FMRI images were then smoothed using the *3dBlurToFWHM* command in AFNI at full width half maximum = 6 mm in the x y z directions. Participant-specific non-neuronal tissue masks were generated via the *PHYCAA+* algorithm and a second-order Legendre

polynomial was used for temporal detrending. The six motion parameters obtained from the motion correction step were regressed out using PCA. Principle components explained 85% of the variance of the motion parameters. In addition, nuisance regressors (such as cerebrospinal fluid, white matter, and global signal) were used as temporal covariates and regressed out. Finally, a low-pass filter was applied to the functional data to remove physiological noise with a frequency cut-off of 0.1 Hz.

3.3.8 Resting-State Functional Connectivity Analysis

The *FATCAT-awFC* pipeline has two inputs; one is from the functional data (rsfMRI) and the second is from the structural data (DTI). First, the functional data is fed into the *FATCAT* pipeline. Resting-state functional data was evaluated using group independent component analysis (gICA) using temporal concatenation with FSL's Multivariate Exploratory Linear Decomposition into Independent Components (*MELODIC*) version 6.0 (Griffanti, 2019). REM and NREM participants were combined in the analysis (at which time points?). The group ICA chooses the main overlapping brain regions from the concatenated individual data; the dimensionality was selected to be 20 components. Each gICA component was quantitatively compared to the Yeo 7-network map to identify RSNs (Yeo et al., 2011). Using *FATCAT's 3dMatch* tool (Taylor & Saad, 2013), dice coefficients were calculated, whereby the highest dice coefficient was used to extract the independent component (IC) that most resembled the Yeo et al (2011) template (Yeo et al., 2011). This was further validated by visual inspection. *FATCAT's 3dROIMaker* (Taylor & Saad, 2013) step was applied to threshold the spatial maps (DMN, Z= 3.4; FPN, Z= 5.4; DAN, Z = 0.85; VAN, Z= 3; LIM, Z= 1.3). Network parcellation thresholds

were selected for the spatial maps with a visual similarity to networks observed in the Yeo network and are similar to the standard networks in the literature (Kaiser et al., 2015b; Yeo et al., 2011). These networks ranged in complexity from 3-5 nodes. The group-derived regions of interest (ROIs) were then projected on to each participant's functional data. *FATCAT's 3dNetCorr* (Taylor & Saad, 2013) tool was used to calculate correlations between the mean time-series of each region pair within each network for each participant. A set of inflated ROIs (which were inflated by two voxels) was also produced from the *3dROIMaker* command, for use in the diffusion side of the pipeline.

3.3.9 DTI Data Acquisition and Processing

Diffusion weighted imaging was conducted using a single-shot spin-echo EPI sequence. Diffusion gradients at b = 1000 s/mm^2, were applied sequentially along 31 non-collinear directions in most sites (exceptions, Queens: 30, University of British Columbia: 30). An additional scan without diffusion sensitizing at B=0 s/mm^2 was also collected. The DTI acquisition protocol included one-signal averages of a whole brain sequence: TR = 8000 ms (exception: University of British Columbia: 9000), TE = 94 ms, FOV: 240 × 240 mm, matrix: 96 × 96 with 52-58 slices, voxel size: 2.5 mm^3, acceleration factor R =2, with an acquisition duration of approximately 5 minutes for one dataset. Image space reconstruction (i.e. GE ASSET, Phillips SENSE) was used for most sites, except for 3 sites that used the GRAPPA k-space method.

3.3.10 DTI Preprocessing

Each volume was co-registered using an affine transformation (FSL *eddy_correct* tool) to the first B_0 volume to correct for motion and eddy current distortions(?). B-values were rotated accordingly. Data were then skull stripped, and a diffusion tensor reconstruction was calculated using a weighted least squares fit and FA maps were created. All the participant's FA data were then aligned onto a standard 2-mm FMRIB58 FA template (Webster, 2012) using the non-linear registration tool *FNIRT*. FSL's tract-based spatial statistics was used to project each participant's FA maps onto the skeletonized mean-FA template (to avoid partial volume effects).

3.3.11 DTI Analysis

As previously mentioned, the *FATCAT-awFC* pipeline has two data inputs: the functional RS data and the structural diffusion data. The diffusion data was processed using the FATCAT pipeline (Taylor & Saad, 2013) as shown in Ayyash et al. (2021). Bayesian estimation of diffusion parameters were determined using FSL's Bayesian Estimation of Diffusion Parameters Obtained using Sampling Techniques (*BEDPOSTX*). Uncertainty estimates for DTI parameters (FA and first eigenvector) were determined for each participant, using FATCAT's *3dDWUncert* (Taylor & Saad, 2013) with 300 iterations (Jackknife resampling). DTI parameters and uncertainty measures were used to perform probabilistic tractography. Inflated ROIs (produced from *3dROIMaker*) were transformed from the Montreal Neurological Institute (MNI) space (Ashburner & Ridgway, 2013) of the resting state data to the diffusion-weighted space, for tractography analysis. Next, *3dTrackID* (Taylor & Saad, 2013) was applied to produce an intensity map of probabilistic connections with the following settings for all datasets: FA > 0.15;

turning angle < 50°, N_{seed} = 5 tract seeds per voxel; N_{mc} = 1000 Monte Carlo iterations and a fractional threshold of f_{tr} = 0.05 (so that f_{tr} x N_{seed} x N_{MC} = 250 tracts/voxel). *3dTrackID* (Taylor & Saad, 2013) also generated the number of streamlines (fiber count) and anatomical distances between region pairs. The number of streamlines was then used to calculate the strength of connectivity between each pair of ROIs as a part of the *awFC* technique (refer to [Ayyash et al. (2021)]). To reduce the tractography distance bias, a Poisson regression-based adjustment was performed: $\log(\mu(S_{ij}|g_{ij}) = \alpha_0 + \alpha_1 g_{ij}$, where $g_{ij}$is the distance between each region pair, $S_{ij}$is the unbiased number of streamlines, α_1 is the bias adjustment factor. The number of streamlines between region pairs was corrected accordingly. FC between brain regions can be supported by either direct or indirect SC (Honey et al., 2009; Teipel et al., 2010). To incorporate indirect connections into the SC measure, the following was applied: $\pi_{ij}=\max[\pi_{ij}, \max_m(\pi_{im}\pi_{mj})]$, where π are the probabilities of SC, i is the starting ROI, j is the target ROI, and m is the third connection.

3.3.12 awFC Analysis

Once the FC and SC values between ROIs in each network were estimated, FC data and weighted SC data were fused together using the *awFC* technique [Refer to (Ayyash et al., 2021) for the pipeline design]. The functional and structural dissimilarity matrices were computed and constructed for each ROI pair within each network for each participant. Dissimilarity was calculated for each ROI pair by one minus connectivity similarity (functional dissimilarity, one minus FC; structural dissimilarity, one minus SC). Data fusion was calculated using the formula: $d_{ij} = w_{ij} \cdot f_{ij}$, where d_{ij} is a combined dissimilarity measure, w_{ij} is structural dissimilarity and f_{ij}

is functional dissimilarity. Next, we used the d_{ij} to calculate the *awFC* metric: $awFC = 1 - |d_{ij}|$. In the current study we examined *awFC* between ROI pairs for (1) REM and NREM at baseline, (2) REM and NREM at week-8, (3) REM at baseline and REM at week-8, within each ROI pair for every RSN using a Mann-Whitney U test. Effect sizes were calculated using Cohen's *d* (Cohen, 1998).

3.3.13 Group Analyses Using R

Mann-Whitney U tests were performed in each of the 3 paired comparisons (REM versus NREM at baseline; REM versus NREM at week-8; REM at baseline versus week-8). The significance threshold for comparisons was set at $p < 0.05$. To account for multiple comparisons, p-values were adjusted by controlling for the False Discovery Rate (FDR) using the Benjamini-Hochberg procedure. In this paper, we only report the results that survive the FDR correction for multiple testing ($p_{adj} < 0.05$).

3.3.14 Associations of Cognitive Variables to awFC Using Principal Component Analysis and Principal Component Regression

RSNs *awFC* may be related to cognitive and behavioural changes in MDD at remission. We explored the relationship between *awFC* and cognitive variables in each region pair at the level of $p < 0.05$. Associations were explored only for regions with significant *awFC* differences between REM and NREM groups.

Five cognitive variables of the CNS-VS test were examined: memory, cognitive flexibility, complex attention, processing speed and neurocognitive index. Multicollinearity among these variables was assessed with Pearson correlation using the *ggpairs* function from the *GGally* package in R (Schloerke et al., 2018), which confirmed that significant correlations existed between the five cognitive variables [See Supplementary Fig.1]. Variables that are correlated are considered redundant, thus a PCA can be applied to reduce the redundancy (Kassambara, 2017; Refaat, 2010). The Principal components produced from the PCA are orthogonal and uncorrelated to one another (Hair et al., 2009). PCA was performed with the R package (R Core Team, 2018) using the *princomp* function. A PCA was applied on the five cognitive variables and visually displayed using the *fviz_pca_var* function, from the "factoextra package" (Kassambara, 2017). It was considered sufficient to retain one component from PCA to interpret the data, if they met the following criteria: (1) Principal components (PCs) having an eigenvalue greater than one (Jackson, 1993) (2) PCs corresponding to a minimum of 60% explained variance from the data] (3) Visually, components before the first 'elbow' of the Scree plot were retained. [Refer to Supplementary Fig.1]. The output of PCA (PCs) was used as an input (independent variables) for Principal Component Regression (PCR). A linear mixed effects regression was performed, whereby the PCs, MADRS, age and sex were taken to be the explanatory variables and *awFC* was taken to be the outcome variable. A two-level factor (REM and NREM) interaction effect was included in the mixed effects model. To account for possible site bias in the data, participants nested within site were included as a random effect. Principal component regression (PCR) was applied using the *lme* function from the *nlme* package in R (R Core Team, 2018). For each region pair within a network, PCs with significant associations with the *awFC* were post-hoc tested. Interpretation of the PCs can be made by examining the

component loadings (Hair et al., 2009). The component loadings are computed correlations between the original variables and the PCs (Hair et al., 2009). A variable was considered significantly loaded on a PC with a cut-off absolute threshold correlation of 0.3 (Hair et al., 2009). The most important variables (high loadings on PCs) were identified to perform multiple linear regression models to further explore the association between the original variables (with the highest loadings on each PC), and the outcome variable (*awFC*).

Post-hoc analyses were carried out only for significant ROI-pairs within RSNs. Three separate analyses were conducted using multiple linear regression analysis. The significant regions pairs were assessed for the following groups: (1) REM and NREM at baseline, (2) REM and NREM at week-8, (3) REM at baseline and REM at week-8. For the first analysis, the association between cognitive variables at week-8 and *awFC* at week-8 were assessed using PCA/PCR. The second analysis explored the association between the change in cognitive variables (from baseline to week-8) and change in *awFC* (from baseline to week-8) using PCA/PCR. The third analysis evaluated the association between the change in cognitive variables (from baseline to week-8) and *awFC*, at baseline. Changes in *awFC* were calculated by subtracting the post-treatment (week-8 *awFC*) from the pre-treatment (baseline *awFC*) connectivity values, change in MADRS was calculated by subtracting the baseline MADRS from the week-8 MADRS as previously described (Persson et al., 2020).

3.4 Results

3.4.1 Participants in the analysis

MADRS scores were used to assess depression severity and to define remission status. We defined REM as participants that had a MADRS score ≤10 at week-8, that was maintained at week-16 of treatment (Hawley et al., 2002; Mendlewicz, 2008), whereas participants with a MADRS score >10 at week-8 and maintained a >10 score at week-16 (after 8 weeks of adjunctive treatment with aripiprazole) were labeled as NREM. This study focused exclusively on imaging data from the REM and NREM participants at baseline and week-8.

From the 211 participants in the CAN-BIND-1 study, 147 met these REM and NREM criteria. Additional participants were removed from this sample because of excessive motion in the scanner (n = 21) and missing resting state functional magnetic resonance imaging (rsfMRI) or diffusion tensor imaging (DTI) data at baseline (n = 16) and at week-8 (n = 18). This resulted in the exclusion of 23 REM and 31 NREM, leaving 93 participants (66 NREM and 27 REM) retained for this analysis.

3.4.2 Demographics

Table 1 summarizes the demographic characteristics and provides medical history of antidepressants for the participants in each group belonging to: REM and NREM.

Table 1. Demographic Characteristics

Characteristic	**Non-Remitters**,	**Remitters**,	**p-**

	N = 66[1]	N = 27[1]	**value**[2]
Sex			0.711
Female	44 (66.7%)	17 (63.0%)	
Male	22 (33.3%)	10 (37.0%)	
Age in years Mean (SD)	33 (12)	34 (11)	0.402
MADRS Mean (SD)	21 (8)	5 (3)	**<0.001***
Education, years Mean (SD)	17 (2)	17 (4)	0.724
Age of Onset of MDD, years Mean (SD)	19 (7)	19 (9)	0.731
Duration of Current MDE, Months			0.801
≤ 12 months	35 (53.0%)	14 (51.9%)	
1-2 years	8 (12.1%)	2 (7.4%)	
> 2 years	19 (28.8%)	9 (33.3%)	
Other	4 (6.1%)	2 (7.4%)	
Number of MDE's Mean (SD)	4 (3)	5 (3)	
Antidepressants			
Drug Naive	33 (50.0%)	11 (40.7%)	
Past History of Antidepressants	33 (50.0%)	16 (59.3%)	
Comorbidities			
Agoraphobia	6 (9.1%)	4 (14.8%)	
Social Anxiety Disorder	14 (21.2%)	6 (22.2%)	

.

Bulimia Nervosa	1 (1.5%)	1 (3.7%)
Generalized Anxiety Disorder	15 (22.7%)	4 (14.8%)
Obsessive-Compulsive Disorder	2 (3.0%)	1 (3.7%)
Panic Disorder	9 (13.6%)	6 (22.2%)
Posttraumatic Disorder time frame	7 (10.6%)	2 (7.4%)
Alcohol Abuse (past 12 months)	1 (1.5%)	0 (0.0%)
Non-alcohol substance abuse (past 12 months)	1 (1.5%)	0 (0.0%)

[1] n (%); Mean (SD)

[2] Pearson's Chi-squared test; Wilcoxon rank sum test; Fisher's exact test

[*] Bonferroni correction for multiple testing

Note: N= Number of participants, SD = Standard Deviation, MDD = Major Depressive Disorder, MDE = Major Depressive Episode, MADRS = Montgomery-Asberg Depression Rating Scale.

3.4.3 ROIs Defined Within RSNs

The results shown are for group-wise parcellation obtained from the REM and NREM groups. Table 2 lists the volume, anatomical names and locations of each group of ROI within each RSN.

3.4.4 Anatomically Weighted Functional Connectivity Group Comparisons

The Wilcoxon-test showed a significant difference in *awFC* between groups. Fig. 1 illustrates the ROI pairs with significant connectivity differences between groups at $p_{adj} < 0.05$ (FDR corrected). Our results revealed group differences predominantly in the comparison between REM and NREM at week-8 in all networks except the LIM. There was also a connectivity difference identified for REM at baseline compared to week-8 within the DAN. However, no group differences in connectivity were detected when comparing the REM to the NREM at baseline. These results are summarized in Table 3. In addition, as a reference, separate analyses were performed for SC and FC between each ROI pair within each RSN. Table 4 illustrates group-level comparison of FC and SC for each *awFC* comparison.

Group Comparisons at Week 8: Comparing connectivity within RSNs for REM and NREM at week-8, revealed connectivity differences in the DMN, FPN, VAN, and DAN. Table 5 contains a summary of the mean and standard error of network nodal connections with significantly different *awFC* for each group. Results showed that the *awFC* was significantly lower in the REM as compared to NREM at week-8 in the DMN: between nodes linking the a) middle prefrontal cortex and the left middle temporal gyrus [See Fig. 2a] b) the left angular gyrus and the left middle temporal gyrus [see Fig. 2b] c) between the left angular gyrus to middle prefrontal cortex [see Fig. 2c]. There were also significantly lower *awFC* values within the FPN between regions of the left cerebellum and the right orbitofrontal gyrus for the REM compared with NREM at week-8 [Fig. 2d]. In addition, lower connectivity values were found in the VAN for the REM compared to NREM at week-8 between the right insular cortex and the left middle

frontal gyrus [Fig. 2e] and between anterior cingulate gyrus and the left middle frontal gyrus [Fig. 2f].

Group Comparisons Examining Change from baseline to Week 8: Within group comparisons examining the connectivity changes associated with a positive medication response identified significantly greater *awFC* connectivity in the DAN between the pre-central and post-central gyrus and weaker connectivity in the FPN between the left cerebellum and right orbitofrontal gyrus. See figure 3g and 3h.

3.4.5 Cognitive Variables Associated with awFC

3.4.6 Principal Component Analysis

PCA was performed on five cognitive variables (processing speed, memory, cognitive flexibility, neurocognitive index and complex attention), which revealed one significant PC with an eigenvalue>1 (eigenvalue = 3.34) and accounted for 63.8% of the total variance in the data [See Supplementary Fig.1]. Processing speed was the highest contributor to the first PC, followed by memory, cognitive flexibility, neurocognitive index and complex attention (a total of five PCs). Significant associations were found with the outcome variable *awFC* and the cognitive variables from the first PC in the FPN between the right medial frontal gyrus and the left cerebellum.

3.4.7 Principal Component Regression

PCR was then performed. The PCR included *awFC* as the outcome variable and the first PC, MADRS, age and sex as independent variables. In addition, random effects (participants nested within site) were included. To further investigate which cognitive variable was driving the effect for the PCs, separate analyses were conducted for each group comparison, correlating *awFC* in different groups (at baseline, week-8 and from baseline to week-8) with cognitive variables and MADRS.

3.4.8 Baseline awFC Association with Cognitive Variables

After performing a PCA [see **Principal Component Analysis** section**],** a PCR was performed to examine associations between the first PC (among five PCs) and the *awFC* at baseline. We did not observe a significant association between the first PC and awFC.

3.4.9 Association of Week-8 Cognitive Variables with Week-8 awFC

After performing a PCA [see **Principal Component Analysis** section**],** a PCR was performed to examine associations between the first PC (among five PCs) and the *awFC* at week 8. We found a significant association between the first PC and *awFC* (p_{adj} = 0.01) between the left cerebellum to the right orbitofrontal gyrus, which prompted further analysis to investigate which cognitive variable contributed to this significance. Multiple linear regressions were performed examining each cognitive variable and *awFC*. The post-hoc regression revealed that brain connectivity between the left cerebellum to the right orbitofrontal gyrus was associated with cognitive flexibility (p_{adj} = 0.0011), and neurocognitive index (p_{adj} = 0.021) for the week-8 NR.

3.4.10 Changes (from baseline to week-8) in awFC in Association with Changes (from baseline to week-8) in Cognitive Variables

After performing a PCA [see **Principal Component Analysis** section**],** a PCR was conducted to assess the association between the first PC (among five PCs) and the changes in awFC from baseline to week-8 (calculated by subtracting week-8 *awFC* from baseline *awFC*). However, there were no significant associations between the first PC and changes in awFC.

Table 2 | Summarized characteristics of all the brain regions within each resting-state network. The volume (number of voxels), centroid location in MNI coordinates and anatomical names of each regions of interest (ROIs) are listed. ROIs were defined using FATCATs *3dROIMaker* command.

ROI no.	Anatomical location	Peak MNI coordinates			Volume (# of voxels)
		x	y	z	
DEFAULT MODE NETWORK					
1	Left middle temporal gyrus	-62	-22	-16	55
2	Middle prefrontal cortex	-2	54	8	55
3	Posterior cingulate cortex/Precuneus	-2	-54	28	55
4	Left angular gyrus	-50	-62	28	55

FRONTOPARIETAL NETWORK					
5	Left cerebellum	-34	-70	-40	45
6	Right orbitofrontal gyrus	42	54	-8	10
7	Right middle frontal gyrus	34	14	56	45
8	Right angular gyrus (lateral occipital cortex)	50	-54	44	45
9	Paracingulate gyrus	6	34	36	10
LIMBIC NETWORK					
10	Right parahippocampal gyrus, amygdala, hippocampus, temporal fusiform cortex	30	-6	-40	37
11	Lingual gyrus	-6	-94	-4	37
12	Paracingulate gyrus	2	10	52	37
VENTRAL ATTENTION NETWORK					
13	Left insular cortex (frontal operculum cortex)	-38	10	0	80
14	Right insular cortex (frontal operculum cortex)	42	14	-8	80
15	Anterior cingulate gyrus, paracingulate gyrus	-6	22	32	80
16	Left middle frontal gyrus	-30	46	20	80
DORSAL ATTENTION NETWORK					
17	Right and left postcentral gyrus	-42	-34	44	100

.

18	Left parahippocampal gyrus (anterior and posterior), lingual gyrus, temporal fusiform gyrus	-26	-26	-20	40
19	Right insular cortex	42	-2	8	36
20	Right precentral gyrus	58	10	24	100
21	Superior frontal pole, paracingulate gyrus	6	54	12	65

Table 3 | Anatomically weighted functional connectivity (*awFC*) was compared between groups using a Wilcox-test. Displayed are the significant differences of *awFC* measures between brain regions for: remitters vs non-remitters at baseline, remitters vs non-remitters at week8, and remitters at baseline vs remitters at week8

		COMPARISON		
Start ROI	**End ROI**	**REM vs NREM (baseline)**	**REM vs NREM (week-8)**	**REM (baseline) vs REM (week8)**
DEFAULT MODE NETWORK				
L-MTG	MPFC	1.00	0.0050*	0.037*
L-MTG	L-AG	1.00	0.0051*	0.108
MPFC	L-AG	1.00	0.014*	0.093
FRONTOPARIETAL NETWORK				
L-CER	R-OFG	0.921	0.008*	0.005*

VENTRAL ATTENTION NETWORK				
R-INS	L-MFG	0.802	0.021*	1.00
ACC/PCG	L-MFG	0.901	0.027*	1.00
DORSAL ATTENTION NETWORK				
R+L Post CG	R-Pre CG	0.457	1.00	0.005*

**p-value* (FDR corrected) < 0.05, REM = remitters, NREM = non-remitters, ROI = region of interest, L-MTG = left middle temporal gyrus, MPFC = middle prefrontal cortex, L-AG = left angular gyrus, L-CER = left cerebellum, R-OFG = right orbitofrontal gyrus, R-INS = right insular cortex, ACC/PCG = anterior cingulate cortex, L-MFG = left middle frontal gyrus, R+L Post CG = right and left postcentral gyrus, right Pre CG = right precentral gyrus

Table 4 | Structural connectivity, functional connectivity and anatomically weighted functional connectivity were compared between groups using a Wilcoxon-test. Regions where anatomically weighted functional connectivity was significant for: remitters at week-8 compared to NREM at week-8 and REM at baseline compared to remitters at week-8 - and their corresponding structural and functional connectivity significance.is shown

Start ROI	**End ROI**	**SC p-value (FDR corrected)**	**FC p-value (FDR corrected)**	***awFC* p-value (FDR corrected)**
Remitters at week-8 compared to non-remitters at week-8				
DEFAULT MODE NETWORK				
L-MTG	MPFC	1.00	0.0051*	0.0050*
L-MTG	L-AG	0.00815*	0.005*	0.0051*

MPFC	L-AG	0.960	0.015*	0.014*
FRONTOPARIETAL NETWORK				
L-CER	R-OFG	0.980	0.0095*	0.008*
VENTRAL ATTENTION NETWORK				
R-INS	L-MFG	0.370	0.023*	0.021*
ACC	L-MFG	0.310	0.030*	0.027*
Remitters at baseline compared to remitters at week-8				
DORSAL ATTENTION NETWORK				
R+L Post CG	R-Pre CG	1.00	0.009	0.005*
DEFAULT MODE NETWORK				
L-MTG	MPFC	1.00	0.037	0.037
FRONTOPARIETAL NETWORK				
L-CER	R-OFG	0.05*	0.009*	0.005*

**p-value* (FDR corrected) < 0.05. ROI = region of interest, SC = structural connectivity, FC = functional connectivity, *awFC* = anatomically weighted functional connectivity, FDR = false discovery rate, L-MTG = left middle temporal gyrus, MPFC = middle prefrontal cortex, L-AG = left angular gyrus, L-CER = left cerebellum, R-OFG = right orbitofrontal gyrus, R-INS = right insular cortex, ACC/PCG = anterior cingulate cortex, L-MFG = left middle frontal gyrus, R+L Post CG = right and left postcentral gyrus, right Pre CG = right precentral gyrus

Table 5 | Anatomically weighted functional connectivity (*awFC*) was compared between groups using a Wilcoxon-test. ROI-pair connectivity metrics: mean, standard error and effect size for remitters at week-8 compared to non-remitters at week-8 and remitters at baseline compared to

remitters at week-8 are displayed. Only the ROI-pairs with significant connectivity differences between groups are listed. The effect sizes were determined using Cohen's d and reported.

Start ROI	End ROI	REM at Week-8 (Mean ± SE)	NREM at Week-8 (Mean ± SE)	Effect size (Cohen's *d*)
Remitters at week-8 compared to non-remitters at week-8				
DEFAULT MODE NETWORK				
L-MTG	MPFC	0.35 ± 0.064	0.53 ± 0.034	0.60 (medium)
L-MTG	L-AG	0.45 ± 0.049	0.60 ± 0.031	0.56 (medium)
MPFC	L-AG	0.44 ± 0.053	0.60 ± 0.029	0.61 (medium)
FRONTOPARIETAL NETWORK				
L-CER	R-OFG	0.056 ± 0.045	0.22 ± 0.036	0.59 (medium)
VENTRAL ATTENTION NETWORK				
R-INS	L-MFG	0.21 ± 0.061	0.40 ± 0.031	0.69 (medium)
ACC	L-MFG	0.39 ± 0.054	0.54 ± 0.022	0.71 (medium)
Remitters at baseline compared to remitters at week-8				

Start ROI	End ROI	REM at Baseline (Mean ± SE)	REM at Week-8 (Mean ± SE)	Effect size (Cohen's d)
DORSAL ATTENTION NETWORK				
R+L Post CG	R-Pre CG	0.26 ± 0.034	0.39 ± 0.047	0.63 (medium)
DEFAULT MODE NETWORK				
L-MTG	MPFC	0.527 ± 0.038	0.358 ± 0.062	0.13 (negligible)
FRONTOPARIETAL NETWORK				
L-CER	R-OFG	0.22 ± 0.038	0.046 ± 0.044	0.923 (large)

REM = remitters, NREM = non-remitters, ROI = region of interest, SE = standard error, L-MTG = left middle temporal gyrus, MPFC = middle prefrontal cortex, L-AG = left angular gyrus, L-CER = left cerebellum, R-OFG = right orbitofrontal gyrus, R-INS = right insular cortex, ACC/PCG = anterior cingulate cortex, L-MFG = left middle frontal gyrus, R+L Post CG = right and left postcentral gyrus, right Pre CG = right precentral gyrus

3.5 Discussion

To our knowledge, this is the first study to combine fMRI and DTI in a fused manner to assess REM and NREM in MDD, while simultaneously comparing these results to traditional FC and SC. The current study investigated *awFC* in MDD in five RSNs (the DMN, FPN, DAN, VAN, and LIM), with the aim of identifying differences between a) baseline and week-8 for the REM group, b) REM and NREM at baseline prior to the initiation of medication therapy, and c) REM and NREM following 8 weeks of treatment with SSRI escitalopram. Using the *FATCAT-awFC* pipeline (Ayyash et al., 2021), we identified differences in connectivity strength in four of five RSNs examined. Within group differences for REM were observed between the baseline period and week-8, and revealed REM at week-8 to have increased *awFC* across time within the DAN between the right and left post central gyrus to right precentral gyrus. In the comparison at baseline between REM and NREM no significant group differences were identified among five RSNs. This finding is similar to reports in the literature using rsfMRI analysis, where there were no signs of group differences at baseline between REM and NREM (Wang et al., 2014). However, we did find group differences, particularly reductions in *awFC* at 8 weeks for the REM compared to NREM across different RSNs including the: DMN, FPN and VAN. This will be discussed in greater detail below. Our findings are consistent with observations that in MDD, response to medication is accompanied not only by increased connectivity within the executive control network (i.e. pre and post central gyrus) brain regions longitudinally (from baseline to week 8) (Karim et al., 2017), but also, by reductions in connectivity (following treatment) for REM (compared to NREM) between several brain regions (Xiao et al., 2019) as part of a normalisation of aberrant neural activities (Aizenstein et al., 2014; Xiao et al., 2019). Our findings suggest that utilizing our *FATCAT-awFC* pipeline, we can detect and distinguish connectivity differences associated with medication response and nonresponse.

3.5.1 Remitters at Baseline compared to Week-8: Within Group Differences in RSN Connectivity

3.5.1.1 Dorsal Attention Network

We demonstrated stronger *awFC* in the DAN between the right precentral gyrus and both the right and left post-central gyri (components of the executive control network) for REM at week-8 relative to REM at baseline. Similarly, a study by Karim et al. (2017) found that MDD participants who took antidepressants (venlafaxine in the first phase, followed by aripiprazole in second phase) showed increased FC between the executive control network and the right precentral gyrus in week-12 REM relative to REM at baseline (Karim et al., 2017). This study supports our findings that REM at week-8 have stronger connectivity compared to REM at baseline, within the DAN.

3.5.1.2 Frontoparietal Network

Significantly less connectivity was found in the REM at week-8 compared to the REM at baseline within the FPN, between regions in the right orbitofrontal gyrus and the left cerebellum. Interestingly, the REM at week-8 also seemed to have decreased connectivity compared to NREM at week-8 [See 'Remitters at Week-8 compared to Non-Remitters at Week-8: Group Differences in RSNs' for more discussion**]**. This finding suggests that the decreased connectivity

that was observed in REM at week-8 compared to REM at baseline, and for REM at week-8 compared to NREM at week-8, demonstrates the normalization of connectivity after treatment.

3.5.2 Remitters at Week-8 compared to Non-Remitters at Week-8: Group Differences in RSNs

3.5.2.1 Default Mode Network

In order to examine the brain connectivity changes that occur as a result of the favourable response to medication, we examined REM from baseline to week-8. We observed significantly lower *awFC* within the DMN for REM as compared to NREM at week-8 in three ROI-pairs within the DMN, including the a) middle prefrontal cortex (PFC) to the left middle temporal gyrus, b) left middle temporal gyrus to the left angular gyrus, and c) left angular gyrus to medial prefrontal cortex. These findings are similar to other studies suggesting that antidepressant treatment in MDD results in reduced connectivity between DMN brain regions. For instance, a study by Xiao et al (2019) found MDD participants who reached a rapid remission (5 days), displayed reductions in FC between nearly all DMN ROIs compared to unmediated MDD participants. A possible explanation for the reductions in connectivity strength for MDD remitters may be the normalization of hyperconnectivity in the DMN that has been considered an indication of remission (Xiao et al., 2019). Supporting this notion is a study by Karim et al (2017), which found that week-12 MDD remitters were characterized by decreased FC in the DMN between the right inferior frontal gyrus and the supramarginal gyrus (Karim et al., 2017).

Taken together, our findings suggest that the response to SSRIs in MDD may be associated with FC and SC reductions within DMN brain regions.

3.5.2.2 Frontoparietal Network

Significantly less connectivity was found in the REM at week-8 compared to the NREM at week-8 within the FPN, between regions in the right orbitofrontal gyrus and the left cerebellum. These findings are consistent with those of Lisiecka et al. (2011), who performed a task-based fMRI study to assess the FC changes during antidepressant treatment and their association with treatment outcome. They found increased FC between the orbitofrontal cortex and the cerebellum in patients who did not reach remission with antidepressant treatment (Lisiecka et al., 2011). They concluded that increased connectivity between the orbitofrontal gyrus and the cerebellum was reflective of a more persistent depression, rather than a more severe form of depression (Lisiecka et al., 2011). Interestingly, we found higher *awFC* in the NREM at week-8 compared to the REM at week-8. These results demonstrate that lower *awFC* within the FPN is reflective of remission status.

3.5.2.3 Ventral Attention Network

In this study, we observed weaker connectivity in REM compared with NREM at week-8 between two region pairs (a) between the insula and the middle frontal gyrus, and (b) between the anterior cingulate cortex and the middle frontal gyrus. In a similar study to ours, Karim et al. (2017) carried out rsfMRI and examined medication response in MDD. They found that REM

participants had weaker functional connectivity between the inferior frontal gyrus and the middle frontal gyrus compared to the NREM participants (Karim et al., 2017). Furthermore, in an implicit emotion processing task based fMRI study done by Godlewska et al. (2016), MDD participants were identified as REM or NREM based on their response following 6 weeks of escitalopram treatment. Participants' neural response to emotional faces was examined early in the course of treatment, after the initial 7 days of medication therapy (Godlewska et al., 2016). Responders to escitalopram, compared to non-responders, showed greater reductions in the neural activation of the insula and the dorsal anterior cingulate during the processing of negative fearful faces (Godlewska et al., 2016). Similar to the DMN, we found the VAN to also have reduced connectivity in the REM compared to NREM. Additionally, our findings are consistent with functional imaging findings identifying that response to escitalopram treatment is associated with the overall pattern of reduced connectivity in the VAN (Li et al., 2021).

3.5.3 Contribution of Traditional FC and Traditional SC in the Analysis of awFC

The traditional SC and traditional FC were performed to allow the visual comparison of significant group differences. Their combination at times allowed for a more significant connectivity measure, while at other times it performed only as well as the traditional FC alone. This is the basic principle behind the original *awFC* technique. While the *awFC* measure appears to predominantly be driven by FC, there are times that connectivity differences were supported by SC as well. At times, the significance level for group differences was amplified (i.e. DAN), even in the absence of significant SC group differences. This may perhaps be due to

the adjusted SC distance bias, and consideration of indirect structural connections between brain regions.

3.5.4 Associations Between Cognitive Variables and awFC

The significant association between cognitive variables collected at week-8, and *awFC* at week-8 (within the FPN between the right orbitofrontal gyrus and left cerebellum) was reported for the NREM. An increase in *awFC* was found to reflect an increase in cognitive flexibility, between the left cerebellum and the right orbitofrontal gyrus. This ROI-pair was found to be associated with cognitive flexibility as measured by the CNS-VS at week-8 in this study.

Previous studies have found that the orbitofrontal cortex (Boulougouris et al., 2007) and the cerebellum (De Bartolo et al., 2009) mediate cognitive flexibility. Previous studies have shown that cerebellar (De Bartolo et al., 2009) and orbitofrontal lesions (Robbins et al., 2012) impact cognitive flexibility. The cerebellum may play a role in monitoring incoming sensory information (i.e. from the orbitofrontal gyrus) and navigate appropriate behavior (i.e. motor movements) based on environmental conditions (Bower, 2002; Ito, 2002; Schmahmann, 2004; Thach, 2007).

3.5.5 Study Limitations

A limitation we encountered in our previous work (Ayyash et al., 2021) concerned the observation that each ROI encompassed several anatomical regions, and this may have impacted the overall connectivity values. We addressed this limitation in the present study through the use

of ROIs that were smaller in size. However, in a combined FC-SC study such as the current study, smaller ROIs can result in a greater effect size for the FC component. Furthermore, the use of smaller ROIs necessitated the inflation of ROI boundaries to detect white matter tracts running between ROIs. This may have produced a less accurate identification of SC parameters. Future work will need to find the best trade-off between the optimal ROI size and the optimal amount of ROI inflation to reach white matter tracts.

Another limitation is that, while combining SC-FC may result in improved detection of aberrant connectivity, it lacks specificity. In other words, it is more difficult to interpret what could be driving the connectivity changes among groups. Although in this study we performed a separate traditional connectivity analyses to reveal which connectivity analysis (SC or FC) was driving the significance, we would not be able to deduce that from the *awFC* metric.

3.5.6 Future Directions

In this paper we examined changes in *awFC* in individuals with MDD identified as REM or NREM following a course of SSRI medication escitalopram. Future studies could investigate treatment-resistant depression and the effects of different classes of medication on brain connectivity changes. In addition, it would be of interest to investigate the use of diffusion spectrum imaging (DSI) in our pipeline instead of DTI, as it is capable of delineating tracts in complex and multidirectional areas (i.e. crossing fibers, small fibers) more accurately. This will be beneficial for our pipeline, as the *FATCAT-awFC* approach uses tract count to quantify SC, and DSI is capable of assessing tract count with greater sensitivity (Bassett et al., 2011).

3.5.7 Conclusion

The consistency of our results with existing literature, demonstrates the efficacy of *FATCAT-awFC* as a novel approach that works as a fast and easy tool to explore the combined effect of FC and SC. We used the *FATCAT-awFC* analysis approach to investigate the connectivity changes within five RSNs (DMN, FPN, DAN, VAN, LIM) for patients with MDD who matched criteria for REM or NREM after 8 weeks of treatment with the SSRI escitalopram. The results demonstrated that treatment outcome was reflected in *awFC* differences between REM and NREM within four of the five RSNs. Further, the observed increased connectivity from baseline to week-8 in the DAN, and decreased connectivity from baseline to week-8 in the FPN, were an indication of the normalisation of aberrant connectivity caused by MDD. Finally, cognitive flexibility was found to be associated with *awFC* for one region pair in the FPN. This demonstrated the impact that alterations of the orbitofrontal gyrus and cerebellum connectivity have on cognitive flexibility for non-remitted MDD participants. Our findings corroborate the notion that the *FATCAT-awFC* pipeline (Ayyash et al., 2021) is able to distinguish REM from NREM at week-8.

Acknowledgements

CAN-BIND is an Integrated Discovery Program carried out in partnership with, and financial support from, the Ontario Brain Institute, an independent non-profit corporation, funded partially by the Ontario government. The opinions, results and conclusions are those of the authors and no

endorsement by the Ontario Brain Institute is intended or should be inferred. All study medications were independently purchased at wholesale market values.

We would like to thank Keith Ho for his help with organizing the clinical data, and all the patients, controls, and health care workers involved in this project for the generous contribution of their time and their participation in this work

3.5.8 Figures

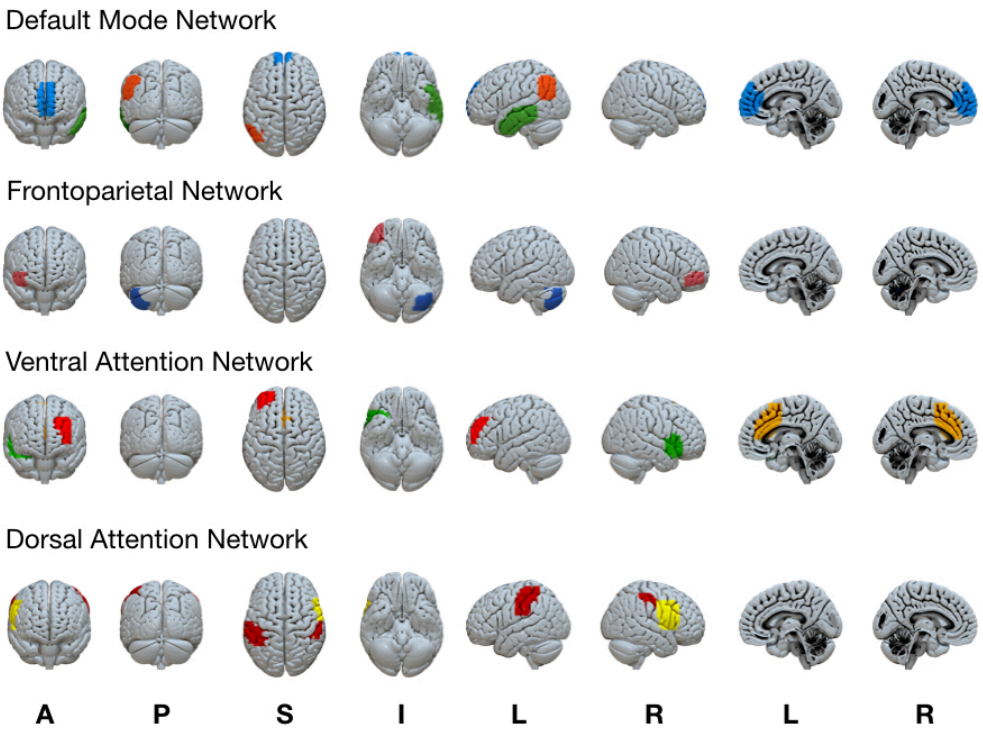

Fig.1 | Group differences in anatomically weighted functional connectivity are displayed for each network. Isolated brain regions were defined using the FATCAT command *3dROIMaker*. Each colour represents a different ROI for each network; Default Mode Network, blue ROI= middle prefrontal cortex, green ROI = left middle temporal gyrus, orange ROI= left angular gyrus; Frontoparietal Network, brown ROI = right orbitofrontal gyrus, blue ROI = left cerebellum; Ventral Attention Network, red ROI= left middle frontal gyrus, green ROI = right insular cortex, orange ROI = anterior cingulate gyrus/paracingulate gyrus; Dorsal Attention Network, red ROI = right and left postcentral gyrus, yellow ROI = right precentral gyrus. ROI =

region of interest, Anatomical positions, A = anterior view, P = posterior view, S = superior view, I = inferior view, L = left view, R= right view.

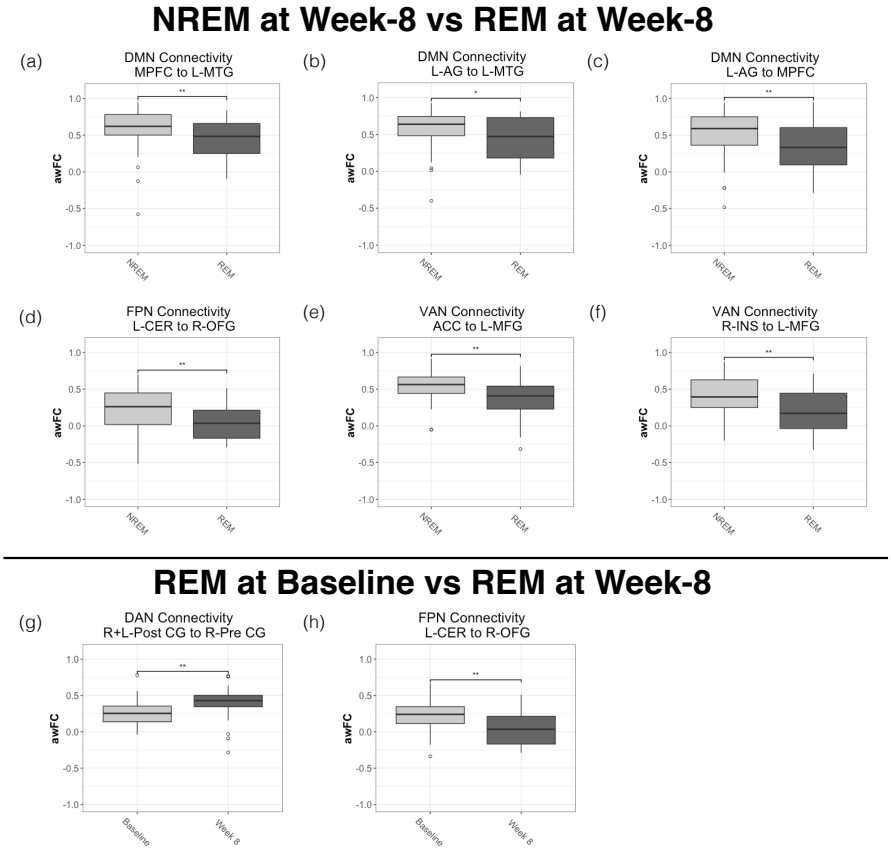

Fig.2 | Boxplots of the anatomically weighted functional connectivity comparing: (a-f) – remitters at week-8 (dark gray boxes) versus non-remitters at week-8 (light gray boxes) and (g-h) remitters at baseline (light gray box) versus remitters at week-8 (dark gray box). Only ROI pairs that demonstrated significant anatomically weighted functional connectivity differences are displayed. Circles represent outliers. Note: DMN = default mode network, FPN = frontoparietal network, VAN = ventral attention network, DAN = dorsal attention network, M-PFC = middle prefrontal cortex, L-Middle Temp = left middle temporal gyrus, L-AG = left angular gyrus, L-CER = left cerebellum, R-OFG = right orbitofrontal gyrus,

R-AG = right angular gyrus, R-INS = right insular cortex, L-middle frontal = left middle frontal gyrus, L-middle frontal = left middle frontal gyrus, ACC = anterior cingulate cortex, R+L-Post CG= right and left post central gyrus, R-Pre CG = right precentral gyrus.

3.6 References

Abo Aoun, M., P Meek, B., & Modirrousta, M. (2019a). Cognitive profiles in major depressive disorder: Comparing remitters and non-remitters to rTMS treatment. *Psychiatry Research*, *279*, 55–61. https://doi.org/10.1016/j.psychres.2019.07.007

Abo Aoun, M., P Meek, B., & Modirrousta, M. (2019b). Cognitive profiles in major depressive disorder: Comparing remitters and non-remitters to rTMS treatment. *Psychiatry Research*, *279*, 55–61. https://doi.org/10.1016/j.psychres.2019.07.007

Aizenstein, H. J., Khalaf, A., Walker, S. E., & Andreescu, C. (2014). Magnetic Resonance Imaging Predictors of Treatment Response in Late-Life Depression. *Journal of Geriatric Psychiatry and Neurology*, *27*(1), 24–32. https://doi.org/10.1177/0891988713516541

Albert, K. M., Potter, G. G., Boyd, B. D., Kang, H., & Taylor, W. D. (2019). Brain network functional connectivity and cognitive performance in major depressive disorder. *Journal of Psychiatric Research*, *110*, 51–56. https://doi.org/10.1016/j.jpsychires.2018.11.020

Ashburner, J., & Ridgway, G. R. (2013). Symmetric Diffeomorphic Modeling of Longitudinal Structural MRI. *Frontiers in Neuroscience*, *6*. https://doi.org/10.3389/fnins.2012.00197

Ayyash, S., Davis, A. D., Alders, G. L., MacQueen, G., Strother, S. C., Hassel, S., Zamyadi, M., Arnott, S. R., Harris, J. K., Lam, R. W., Milev, R., Müller, D. J., Kennedy, S. H.,

Rotzinger, S., Frey, B. N., Minuzzi, L., Hall, G. B., & CAN-BIND Investigator Team. (2021). Exploring brain connectivity changes in major depressive disorder using functional-structural data fusion: A CAN-BIND-1 study. *Human Brain Mapping*. https://doi.org/10.1002/hbm.25590

Ballenger, J. C. (1999). Clinical guidelines for establishing remission in patients with depression and anxiety. *The Journal of Clinical Psychiatry*, *60 Suppl 22*, 29–34.

Bassett, D. S., Brown, J. A., Deshpande, V., Carlson, J. M., & Grafton, S. T. (2011). Conserved and variable architecture of human white matter connectivity. *NeuroImage*, *54*(2), 1262–1279. https://doi.org/10.1016/j.neuroimage.2010.09.006

Bhalla, R. K., Butters, M. A., Mulsant, B. H., Begley, A. E., Zmuda, M. D., Schoderbek, B., Pollock, B. G., Reynolds, C. F., & Becker, J. T. (2006). Persistence of neuropsychologic deficits in the remitted state of late-life depression. *The American Journal of Geriatric Psychiatry: Official Journal of the American Association for Geriatric Psychiatry*, *14*(5), 419–427. https://doi.org/10.1097/01.JGP.0000203130.45421.69

Boulougouris, V., Dalley, J. W., & Robbins, T. W. (2007). Effects of orbitofrontal, infralimbic and prelimbic cortical lesions on serial spatial reversal learning in the rat. *Behavioural Brain Research*, *179*(2), 219–228. https://doi.org/10.1016/j.bbr.2007.02.005

Bower, J. M. (2002). The Organization of Cerebellar Cortical Circuitry Revisited. *Annals of the New York Academy of Sciences*, *978*(1), 135–155. https://doi.org/10.1111/j.1749-6632.2002.tb07562.x

Bowman, F. D., Zhang, L., Derado, G., & Chen, S. (2012). Determining Functional Connectivity using fMRI Data with Diffusion-Based Anatomical Weighting. *NeuroImage*, *62*(3), 1769–1779. https://doi.org/10.1016/j.neuroimage.2012.05.032

Buckner, R. L., Krienen, F. M., Castellanos, A., Diaz, J. C., & Yeo, B. T. T. (2011). The organization of the human cerebellum estimated by intrinsic functional connectivity. *Journal of Neurophysiology*, *106*(5), 2322–2345. https://doi.org/10.1152/jn.00339.2011

Byford, S., Barrett, B., Despiégel, N., & Wade, A. (2011). Impact of Treatment Success on Health Service Use and Cost in Depression. *PharmacoEconomics*, *29*(2), 157–170. https://doi.org/10.2165/11537360-000000000-00000

Churchill, N. W., Spring, R., Afshin-Pour, B., Dong, F., & Strother, S. C. (2015). An Automated, Adaptive Framework for Optimizing Preprocessing Pipelines in Task-Based Functional MRI. *PLOS ONE*, *10*(7), e0131520. https://doi.org/10.1371/journal.pone.0131520

Cipriani, A., Zhou, X., Giovane, C. D., Hetrick, S. E., Qin, B., Whittington, C., Coghill, D., Zhang, Y., Hazell, P., Leucht, S., Cuijpers, P., Pu, J., Cohen, D., Ravindran, A. V., Liu, Y., Michael, K. D., Yang, L., Liu, L., & Xie, P. (2016). Comparative efficacy and tolerability of antidepressants for major depressive disorder in children and adolescents: A network meta-analysis. *The Lancet*, *388*(10047), 881–890. https://doi.org/10.1016/S0140-6736(16)30385-3

Cohen, J. (1998). *Statistical Power Analysis for the Behavioral Sciences* (2nd ed). L. Erlbaum Associates. http://www.utstat.toronto.edu/~brunner/oldclass/378f16/readings/CohenPower.pdf

Conradi, H. J., Ormel, J., & de Jonge, P. (2011). Presence of individual (residual) symptoms during depressive episodes and periods of remission: A 3-year prospective study. *Psychological Medicine*, *41*(6), 1165–1174. https://doi.org/10.1017/S0033291710001911

De Bartolo, P., Mandolesi, L., Federico, F., Foti, F., Cutuli, D., Gelfo, F., & Petrosini, L. (2009). Cerebellar involvement in cognitive flexibility. *Neurobiology of Learning and Memory*, *92*(3), 310–317. https://doi.org/10.1016/j.nlm.2009.03.008

Dennehy, E. B., Robinson, R. L., Stephenson, J. J., Faries, D., Grabner, M., Palli, S. R., Stauffer, V. L., & Marangell, L. B. (2015). Impact of non-remission of depression on costs and resource utilization: From the COmorbidities and symptoms of DEpression (CODE) study. *Current Medical Research and Opinion*, *31*(6), 1165–1177. https://doi.org/10.1185/03007995.2015.1029893

Diagnostic and statistical manual of mental disorders (4th ed.). (2000).

Fava, M., Graves, L. M., Benazzi, F., Scalia, M. J., Iosifescu, D. V., Alpert, J. E., & Papakostas, G. I. (2006). A Cross-Sectional Study of the Prevalence of Cognitive and Physical Symptoms During Long-Term Antidepressant Treatment. *The Journal of Clinical Psychiatry*, *67*(11), 0–0.

Gautam, S., Jain, A., Gautam, M., Vahia, V. N., & Grover, S. (2017). Clinical Practice Guidelines for the management of Depression. *Indian Journal of Psychiatry*, *59*(Suppl 1), S34–S50. https://doi.org/10.4103/0019-5545.196973

Godlewska, B. R., Browning, M., Norbury, R., Cowen, P. J., & Harmer, C. J. (2016). Early changes in emotional processing as a marker of clinical response to SSRI treatment in depression. *Translational Psychiatry*, *6*(11), e957–e957. https://doi.org/10.1038/tp.2016.130

Griffanti, L. (2019, July 9). *MELODIC - FslWiki*. https://fsl.fmrib.ox.ac.uk/fsl/fslwiki/MELODIC

Gualtieri, C. T., & Johnson, L. G. (2006). Reliability and validity of a computerized neurocognitive test battery, CNS Vital Signs. *Archives of Clinical Neuropsychology: The Official Journal of the National Academy of Neuropsychologists*, *21*(7), 623–643. https://doi.org/10.1016/j.acn.2006.05.007

Gudayol-Ferré, E., Guàrdia-Olmos, J., & Peró-Cebollero, M. (2015). Effects of remission speed and improvement of cognitive functions of depressed patients. *Psychiatry Research*, *226*(1), 103–112. https://doi.org/10.1016/j.psychres.2014.11.079

Hair, J., Black, W., Babin, B., & Anderson, R. (2009). *Multivariate Data Analysis* (7th ed.). Pearson. https://www.pearson.ch/HigherEducation/Pearson/EAN/9780138132637/Multivariate-Data-Analysis

Hasselbalch, B. J., Knorr, U., & Kessing, L. V. (2011). Cognitive impairment in the remitted state of unipolar depressive disorder: A systematic review. *Journal of Affective Disorders*, *134*(1–3), 20–31. https://doi.org/10.1016/j.jad.2010.11.011

Honey, C. J., Sporns, O., Cammoun, L., Gigandet, X., Thiran, J. P., Meuli, R., & Hagmann, P. (2009). Predicting human resting-state functional connectivity from structural connectivity. *Proceedings of the National Academy of Sciences of the United States of America*, *106*(6), 2035–2040. https://doi.org/10.1073/pnas.0811168106

Ito, M. (2002). Hopes for cerebellar research in the 21st century. *Cerebellum (London, England)*, *1*(2), 93–94. https://doi.org/10.1080/147342202753671213

Iverson, G. L., Brooks, B. L., & Young, A. H. (2009). Identifying neurocognitive impairment in depression using computerized testing. *Applied Neuropsychology*, *16*(4), 254–261. https://doi.org/10.1080/09084280903297594

Jackson, D. A. (1993). Stopping Rules in Principal Components Analysis: A Comparison of Heuristical and Statistical Approaches. *Ecology*, *74*(8), 2204–2214. https://doi.org/10.2307/1939574

Jaeger, J., Berns, S., Uzelac, S., & Davis-Conway, S. (2006). Neurocognitive deficits and disability in major depressive disorder. *Psychiatry Research*, *145*(1), 39–48. https://doi.org/10.1016/j.psychres.2005.11.011

James, S. L., Abate, D., Abate, K. H., Abay, S. M., Abbafati, C., Abbasi, N., Abbastabar, H., Abd-Allah, F., Abdela, J., Abdelalim, A., Abdollahpour, I., Abdulkader, R. S., Abebe, Z., Abera, S. F., Abil, O. Z., Abraha, H. N., Abu-Raddad, L. J., Abu-Rmeileh, N. M. E., Accrombessi, M. M. K., … Murray, C. J. L. (2018). Global, regional, and national incidence, prevalence, and years lived with disability for 354 diseases and injuries for 195 countries and territories, 1990–2017: A systematic analysis for the Global Burden of Disease Study 2017. *The Lancet*, *392*(10159), 1789–1858. https://doi.org/10.1016/S0140-6736(18)32279-7

Kaiser, R. H., Andrews-Hanna, J. R., Wager, T. D., & Pizzagalli, D. A. (2015a). Large-Scale Network Dysfunction in Major Depressive Disorder: A Meta-analysis of Resting-State Functional Connectivity. *JAMA Psychiatry*, *72*(6), 603–611. https://doi.org/10.1001/jamapsychiatry.2015.0071

Kaiser, R. H., Andrews-Hanna, J. R., Wager, T. D., & Pizzagalli, D. A. (2015b). Large-scale network dysfunction in Major Depressive Disorder: Meta-analysis of resting-state functional connectivity. *JAMA Psychiatry*, *72*(6), 603–611. https://doi.org/10.1001/jamapsychiatry.2015.0071

Kaplan, C., & Zhang, Y. (2012). Assessing the Comparative-Effectiveness of Antidepressants Commonly Prescribed for Depression in the US Medicare Population. *The Journal of Mental Health Policy and Economics*, *15*(4), 171–178.

Karim, H. T., Andreescu, C., Tudorascu, D., Smagula, S. F., Butters, M. A., Karp, J. F., Reynolds, C., & Aizenstein, H. J. (2017). Intrinsic functional connectivity in late-life depression: Trajectories over the course of pharmacotherapy in remitters and non-remitters. *Molecular Psychiatry*, *22*(3), 450–457. https://doi.org/10.1038/mp.2016.55

Kassambara, A. (2017). *Practical Guide To Principal Component Methods in R: PCA, M(CA), FAMD, MFA, HCPC, factoextra*. STHDA.

Kennedy, S. H., Lam, R. W., McIntyre, R. S., Tourjman, S. V., Bhat, V., Blier, P., Hasnain, M., Jollant, F., Levitt, A. J., MacQueen, G. M., McInerney, S. J., McIntosh, D., Milev, R. V., Müller, D. J., Parikh, S. V., Pearson, N. L., Ravindran, A. V., & Uher, R. (2016). Canadian Network for Mood and Anxiety Treatments (CANMAT) 2016 Clinical Guidelines for the Management of Adults with Major Depressive Disorder. *Canadian Journal of Psychiatry. Revue Canadienne de Psychiatrie*, *61*(9), 540–560. https://doi.org/10.1177/0706743716659417

Khoo, A. L., Zhou, H. J., Teng, M., Lin, L., Zhao, Y. J., Soh, L. B., Mok, Y. M., Lim, B. P., & Gwee, K. P. (2015). Network Meta-Analysis and Cost-Effectiveness Analysis of New Generation Antidepressants. *CNS Drugs*, *29*(8), 695–712. https://doi.org/10.1007/s40263-015-0267-6

Korgaonkar, M. S., Goldstein-Piekarski, A. N., Fornito, A., & Williams, L. M. (2020). Intrinsic connectomes are a predictive biomarker of remission in major depressive disorder. *Molecular Psychiatry*, *25*(7), 1537–1549. https://doi.org/10.1038/s41380-019-0574-2

Korgaonkar, M. S., Williams, L. M., Song, Y. J., Usherwood, T., & Grieve, S. M. (2014). Diffusion tensor imaging predictors of treatment outcomes in major depressive disorder. *The British Journal of Psychiatry*, *205*(4), 321–328. https://doi.org/10.1192/bjp.bp.113.140376

Kubitz, N., Mehra, M., Potluri, R. C., Garg, N., & Cossrow, N. (2013). Characterization of Treatment Resistant Depression Episodes in a Cohort of Patients from a US Commercial Claims Database. *PLOS ONE*, *8*(10), e76882. https://doi.org/10.1371/journal.pone.0076882

Lam, R., Milev, R., Rotzinger, S., Andreazza, A., Blier, P., Brenner, C., Daskalakis, Z., Dharsee, M., Downar, J., Evans, K., Farzan, F., Foster, J., Frey, B., Geraci, J., Giacobbe, P., Feilotter, H., Hall, G., Harkness, K., Hassel, S., … Kennedy, S. (2016). Discovering biomarkers for antidepressant response: Protocol from the Canadian biomarker integration network in depression (CAN-BIND) and clinical characteristics of the first patient cohort. *BMC Psychiatry*, *16*. https://doi.org/10.1186/s12888-016-0785-x

Lee, R. S. C., Hermens, D. F., Porter, M. A., & Redoblado-Hodge, M. A. (2012). A meta-analysis of cognitive deficits in first-episode Major Depressive Disorder. *Journal of Affective Disorders*, *140*(2), 113–124. https://doi.org/10.1016/j.jad.2011.10.023

Li, L., Su, Y.-A., Wu, Y.-K., Castellanos, F. X., Li, K., Li, J.-T., Si, T.-M., & Yan, C.-G. (2021). Eight-week antidepressant treatment reduces functional connectivity in first-episode drug-naïve patients with major depressive disorder. *Human Brain Mapping*, *42*(8), 2593–2605. https://doi.org/10.1002/hbm.25391

Lisiecka, D., Meisenzahl, E., Scheuerecker, J., Schoepf, V., Whitty, P., Chaney, A., Moeller, H.-J., Wiesmann, M., & Frodl, T. (2011). Neural correlates of treatment outcome in major

depression. *International Journal of Neuropsychopharmacology*, *14*(4), 521–534. https://doi.org/10.1017/S1461145710001513

MacQueen, G. M., Hassel, S., Arnott, S. R., Addington, J., Bowie, C. R., Bray, S. L., Davis, A. D., Downar, J., Foster, J. A., Frey, B. N., Goldstein, B. I., Hall, G. B., Harkness, K. L., Harris, J., Lam, R. W., Lebel, C., Milev, R., Müller, D. J., Parikh, S. V., … Kennedy, S. (2019). The Canadian Biomarker Integration Network in Depression (CAN-BIND): Magnetic resonance imaging protocols. *Journal of Psychiatry & Neuroscience : JPN*, *44*(4), 223–236. https://doi.org/10.1503/jpn.180036

Mauskopf, J. A., Simon, G. E., Kalsekar, A., Nimsch, C., Dunayevich, E., & Cameron, A. (2009). Nonresponse, partial response, and failure to achieve remission: Humanistic and cost burden in major depressive disorder. *Depression and Anxiety*, *26*(1), 83–97. https://doi.org/10.1002/da.20505

McCall, W. V., & Dunn, A. G. (2003). Cognitive deficits are associated with functional impairment in severely depressed patients. *Psychiatry Research*, *121*(2), 179–184. https://doi.org/10.1016/j.psychres.2003.09.003

McIntyre, R. S., Cha, D. S., Soczynska, J. K., Woldeyohannes, H. O., Gallaugher, L. A., Kudlow, P., Alsuwaidan, M., & Baskaran, A. (2013). COGNITIVE DEFICITS AND FUNCTIONAL OUTCOMES IN MAJOR DEPRESSIVE DISORDER: DETERMINANTS, SUBSTRATES, AND TREATMENT INTERVENTIONS: Review: Cognitive Deficits and Functional Outcomes in MDD. *Depression and Anxiety*, *30*(6), 515–527. https://doi.org/10.1002/da.22063

McIntyre, R. S., Fallu, A., & Konarski, J. Z. (2006). Measurable outcomes in psychiatric disorders: Remission as a marker of wellness. *Clinical Therapeutics*, *28*(11), 1882–1891. https://doi.org/10.1016/j.clinthera.2006.11.007

Middleton, H., Shaw, I., Hull, S., & Feder, G. (2005). NICE guidelines for the management of depression. *BMJ : British Medical Journal*, *330*(7486), 267–268.

Montgomery, S. A., & Asberg, M. (1979). A new depression scale designed to be sensitive to change. *The British Journal of Psychiatry: The Journal of Mental Science*, *134*, 382–389. https://doi.org/10.1192/bjp.134.4.382

Naismith, S. L., Longley, W. A., Scott, E. M., & Hickie, I. B. (2007). Disability in major depression related to self-rated and objectively-measured cognitive deficits: A preliminary study. *BMC Psychiatry*, *7*, 32. https://doi.org/10.1186/1471-244X-7-32

Persson, J., Struckmann, W., Gingnell, M., Fällmar, D., & Bodén, R. (2020). Intermittent theta burst stimulation over the dorsomedial prefrontal cortex modulates resting-state connectivity in depressive patients: A sham-controlled study. *Behavioural Brain Research*, *394*, 112834. https://doi.org/10.1016/j.bbr.2020.112834

R Core Team. (2018). *R: A Language and Environment for Statistical Computing*. https://www.r-project.org/

Refaat, M. (2010). *Data Preparation for Data Mining Using SAS*. Elsevier.

Reppermund, S., Ising, M., Lucae, S., & Zihl, J. (2009). Cognitive impairment in unipolar depression is persistent and non-specific: Further evidence for the final common pathway disorder hypothesis. *Psychological Medicine*, *39*(4), 603–614. https://doi.org/10.1017/S003329170800411X

Robbins, T. W., Gillan, C. M., Smith, D. G., de Wit, S., & Ersche, K. D. (2012). Neurocognitive endophenotypes of impulsivity and compulsivity: Towards dimensional psychiatry. *Trends in Cognitive Sciences*, *16*(1), 81–91. https://doi.org/10.1016/j.tics.2011.11.009

Rush, A. J., Trivedi, M. H., Wisniewski, S. R., Nierenberg, A. A., Stewart, J. W., Warden, D., Niederehe, G., Thase, M. E., Lavori, P. W., Lebowitz, B. D., McGrath, P. J., Rosenbaum, J. F., Sackeim, H. A., Kupfer, D. J., Luther, J., & Fava, M. (2006). Acute and Longer-Term Outcomes in Depressed Outpatients Requiring One or Several Treatment Steps: A STAR*D Report. *American Journal of Psychiatry*, *163*(11), 1905–1917. https://doi.org/10.1176/ajp.2006.163.11.1905

Schloerke, B., Cook, D., Larmarange, J., Briatte, F., Marbach, M., Thoen, E., Elberg, A., Toomet, O., Crowley, J., Hofmann, H., & Wickham, H. (2018). *GGally: Extension to "ggplot2."* https:// CrAn.r-project.org/package=GGally

Schmahmann, J. D. (2004). Disorders of the cerebellum: Ataxia, dysmetria of thought, and the cerebellar cognitive affective syndrome. *The Journal of Neuropsychiatry and Clinical Neurosciences*, *16*(3), 367–378. https://doi.org/10.1176/jnp.16.3.367

Sheehan, D. V., Lecrubier, Y., Sheehan, K. H., Amorim, P., Janavs, J., Weiller, E., Hergueta, T., Baker, R., & Dunbar, G. C. (1998). The Mini-International Neuropsychiatric Interview (M.I.N.I.): The development and validation of a structured diagnostic psychiatric interview for DSM-IV and ICD-10. *The Journal of Clinical Psychiatry*, *59 Suppl 20*, 22-33;quiz 34-57.

Snyder, H. R. (2013). Major depressive disorder is associated with broad impairments on neuropsychological measures of executive function: A meta-analysis and review. *Psychological Bulletin*, *139*(1), 81–132. https://doi.org/10.1037/a0028727

Stahl, S. M. (1999). Why Settle for Silver, When You Can Go for Gold? Response vs. Recovery as the Goal of Antidepressant Therapy: (Brainstorms). *The Journal of Clinical Psychiatry*, *60*(4), 213–214. https://doi.org/10.4088/JCP.v60n0401

Strother, S. C. (2006). Evaluating fMRI preprocessing pipelines. *IEEE Engineering in Medicine and Biology Magazine: The Quarterly Magazine of the Engineering in Medicine & Biology Society*, *25*(2), 27–41. https://doi.org/10.1109/memb.2006.1607667

Taylor, P. A., & Saad, Z. S. (2013). FATCAT: (An Efficient) Functional And Tractographic Connectivity Analysis Toolbox. *Brain Connectivity*, *3*(5), 523–535. https://doi.org/10.1089/brain.2013.0154

Teipel, S. J., Bokde, A. L. W., Meindl, T., Amaro, E., Soldner, J., Reiser, M. F., Herpertz, S. C., Möller, H.-J., & Hampel, H. (2010). White matter microstructure underlying default mode network connectivity in the human brain. *NeuroImage*, *49*(3), 2021–2032. https://doi.org/10.1016/j.neuroimage.2009.10.067

Thach, W. T. (2007). On the mechanism of cerebellar contributions to cognition. *The Cerebellum*, *6*(3), 163–167. https://doi.org/10.1080/14734220701373530

Thase, M. E., Haight, B. R., Richard, N., Rockett, C. B., Mitton, M., Modell, J. G., VanMeter, S., Harriett, A. E., & Wang, Y. (2005). Remission Rates Following Antidepressant Therapy With Bupropion or Selective Serotonin Reuptake Inhibitors: A Meta-Analysis of Original Data From 7 Randomized Controlled Trials. *The Journal of Clinical Psychiatry*, *66*(8), 0–0.

Thase, M. E., Nierenberg, A. A., Vrijland, P., van Oers, H. J. J., Schutte, A.-J., & Simmons, J. H. (2010). Remission with mirtazapine and selective serotonin reuptake inhibitors: A meta-analysis of individual patient data from 15 controlled trials of acute phase treatment of

major depression. *International Clinical Psychopharmacology*, *25*(4), 189–198. https://doi.org/10.1097/YIC.0b013e328330adb2

Trivedi, M. H., Rush, A. J., Wisniewski, S. R., Nierenberg, A. A., Warden, D., Ritz, L., Norquist, G., Howland, R. H., Lebowitz, B., McGrath, P. J., Shores-Wilson, K., Biggs, M. M., Balasubramani, G. K., Fava, M., & STAR*D Study Team. (2006). Evaluation of Outcomes With Citalopram for Depression Using Measurement-Based Care in STAR*D: Implications for Clinical Practice. *American Journal of Psychiatry*, *163*(1), 28–40. https://doi.org/10.1176/appi.ajp.163.1.28

Wang, L., Li, K., Zhang, Q., Zeng, Y., Dai, W., Su, Y., Wang, G., Tan, Y., Jin, Z., Yu, X., & Si, T. (2014). Short-term effects of escitalopram on regional brain function in first-episode drug-naive patients with major depressive disorder assessed by resting-state functional magnetic resonance imaging. *Psychological Medicine*, *44*(7), 1417–1426. https://doi.org/10.1017/S0033291713002031

Wang, L., Xia, M., Li, K., Zeng, Y., Su, Y., Dai, W., Zhang, Q., Jin, Z., Mitchell, P. B., Yu, X., He, Y., & Si, T. (2014). The effects of antidepressant treatment on resting-state functional brain networks in patients with major depressive disorder. *Human Brain Mapping*, *36*(2), 768–778. https://doi.org/10.1002/hbm.22663

Webster, M. (2012, August 13). *FMRIB58_FA - FslWiki*. https://fsl.fmrib.ox.ac.uk/fsl/fslwiki/FMRIB58_FA

Xiao, X., Bentzley, B. S., Cole, E. J., Tischler, C., Stimpson, K. H., Duvio, D., Bishop, J. H., DeSouza, D. D., Schatzberg, A., Keller, C., Sudheimer, K. D., & Williams, N. R. (2019). *Functional connectivity changes with rapid remission from moderate-to-severe major depressive disorder* [Preprint]. Clinical Trials. https://doi.org/10.1101/672154

Yeo, B. T. T., Krienen, F. M., Sepulcre, J., Sabuncu, M. R., Lashkari, D., Hollinshead, M., Roffman, J. L., Smoller, J. W., Zöllei, L., Polimeni, J. R., Fischl, B., Liu, H., & Buckner, R. L. (2011). The organization of the human cerebral cortex estimated by intrinsic functional connectivity. *Journal of Neurophysiology*, *106*(3), 1125–1165. https://doi.org/10.1152/jn.00338.2011

Zheng, K., Wang, H., Liu, J., Xi, Y., Li, L., Zhang, X., Li, J., Yin, H., Tan, Q., Lu, H., & Li, B. (2018). Incapacity to control emotion in major depression may arise from disrupted white matter integrity and OFC-amygdala inhibition. *CNS Neuroscience & Therapeutics*, *24*(11), 1053–1062. https://doi.org/10.1111/cns.12800

Zimmerman, M., McGlinchey, J. B., Posternak, M. A., Friedman, M., Attiullah, N., & Boerescu, D. (2006). How Should Remission From Depression Be Defined? The Depressed Patient's Perspective. *American Journal of Psychiatry*, *163*(1), 148–150. https://doi.org/10.1176/appi.ajp.163.1.148

Chapter 4: Anatomically Weighted Functional Connectivity Analysis Using a Data-Fusion Pipeline Reveals Aberrant Connectivity In Children Exposed To Maternal Adversity: Impact On Middle Childhood. A MAVAN Study.

To be published in: Elsevier Neuroscience

Sondos Ayyash[1], Andrew D. Davis[2], Gésine L. Alders[3], Geoffrey B. Hall[2,3,4]*

[1] School of Biomedical Engineering, McMaster University, Hamilton, ON, Canada

[2] Department of Psychiatry and Behavioural Neurosciences, McMaster University, Hamilton, ON, Canada

[3] Neuroscience Graduate Program, McMaster University, Hamilton, ON, Canada

[4] Department of Psychology Neuroscience & Behaviour, McMaster University, Hamilton, ON, Canada *

4.1 Abstract

Middle childhood is an often-understudied age group. The developing brain is particularly vulnerable to adversity (both pre- and postnatally). This study aimed to determine whether a combined functional-structural connectivity analysis approach is able to detect significant group differences between children exposed to pre- and/or postnatal adversity versus healthy control children during middle childhood. We applied a unique pipeline that combines resting state fMRI functional data with DTI tractography data to yield a metric of functional connectivity that is anatomically weighted. The FATCAT-awFC approach was applied to study typical/atypical

brain connectivity in middle childhood. The results revealed that children exposed to pre- and/or postnatal adversity had a lower awFC compared to controls, in all but one resting-state network – the ventral attention network. Additionally, it was evident that the orientation behavior and psychomotor development at age 3 were predictive of atypical brain connectivity in middle childhood. This is the first study that combines structural and functional connectivity in this manner to study middle childhood brain connectivity changes, providing a new way to understand the brain response to neurodevelopmental challenges.

Key Words:

Development, middle childhood, maternal adversity; structural connectivity; functional connectivity; data fusion; resting-state networks; toolbox

4.2 Introduction

Both prenatal and postnatal adversity are considered a 'global public health concern' with serious health implications for both the mother and the developing child (Almond, 2009; Dadi et al., 2020). A childs' quality of life can be largely dictated by their pre- and postnatal environment (Austin, 2018; Strauss, 1997). This may involve a number of factors including: epigenetics (DeSocio, 2018; Monk et al., 2012), prenatal adversity (i.e. poor maternal nutrition, maternal stress, maternal depression, anxiety, alcohol intake, and substance abuse) (Hellemans et al., 2010; Talge et al., 2007) , and postnatal adversity (i.e. parental style, maladaptive mother-child interactions, abuse, and family conflict) (Burke et al., 2011; Felitti et al., 1998; Marie-

Mitchell & O'Connor, 2013). The root of many of these adversities may be related to poor socio-demographic, social, psychiatric and personal life events (Felitti et al., 1998; A. Murphy et al., 2014). Such adversity can not only lead to a number of chronic illnesses, but also to neurobiological deficits and disorders long term (DeSocio, 2018; Felitti et al., 1998; Hellemans et al., 2010).

Neuroimaging is useful in the detection of brain network changes underlying abnormal neuropsychiatric disorders in children (Peterson, 1995). Structural and functional connectivity are powerful tools for understanding the mechanism behind brain network maturation across age (Dubois et al., 2015). Resting-state functional magnetic resonance imaging (rsfMRI), is an imaging technique that is able to map functional brain networks of cortical and subcortical regions (Lee et al., 2013). Functional connectivity (FC) is computed based on the temporal correlation between distant regions in the brain (Biswal et al., 1995). However, functional connectivity alone is unable to capture how these functional regions are structurally interconnected through white matter tracts. Diffusion tensor imaging (DTI) is an MRI technique that can differentiate different white matter pathways non-invasively (Fernandez-Miranda et al., 2012). Structural connectivity (SC) can be calculated from DTI metrics (i.e. tract count) between brain regions to better understand neuropsychiatric disorders (Ma et al., 2015). Functional connectivity (from rsfMRI) and structural connectivity (from DTI) compliment one another, because they are able to capture unique and complementary features of the brain-network connectomes (Honey et al., 2009; Jessica Damoiseaux & Greicius, 2009; Zimmermann et al., 2018). By combining these two parameters, one is able to utilize all the information embedded in MR scans (Straathof et al., 2020). Examining a combined structural-functional

connectivity metric can be an important tool in studying typical brain development in children in the middle childhood age group. Aberrant connectivity can be indicative of abnormalities in development for children exposed to adversity.

While there are many studies that have explored abnormal brain changes in children exposed to adversity (i.e. children of depressed mothers) during the fetal, neonatal, early childhood, and adolescence years, there are a limited number of studies to date that focus on middle childhood (Farah et al., 2020; Qiu et al., 2015; Tirumalaraju et al., 2020; Wang et al., 2019). Middle childhood typically spans 7-10 years of age (DeFries et al., 1994). Middle childhood is considered an important developmental phase, and abnormal neurodevelopmental disorders during this stage often carry forward into adulthood and manifest as cognitive, emotional, behavioral, interpersonal problems, and overall poor mental health (D. Boyd & Bee, 2012; Mah & Ford-Jones, 2012). Yet, middle childhood remains understudied in neuropsychiatric disorders and is sometimes referred to as the 'forgotten years' of childhood (Mah & Ford-Jones, 2012).

In this paper, we combine FC and SC using a novel approach that uses a toolbox (Taylor & Saad, 2013) in combination with a mathematically dense approach (Bowman et al., 2012). *Functional And Tractographic Analysis Toolbox* (*FATCAT*) consists of a set of AFNI commands that process MRI data. *Anatomically Weighted Functional Connectivity* (*awFC*) model, on the other hand, is the mathematically complex approach that is used to fuse FC and SC with a series of computational steps into a single unit known as the *awFC* metric. The unique combination of these two (*FATCAT* and *awFC model*), results in a faster and more intuitive pipeline than using the *awFC model* alone. This FATCAT-awFC pipeline was first introduced in Ayyash et al

(2021). Here, we build on our previous work, as we apply the *FATCAT-awFC* pipeline, to study brain connectivity changes within resting state networks (RSNs), in the middle childhood age group exposed to pre- and postnatal adversity. One objective of this study was to assess whether there were detectable differences in brain connectivity for the middle childhood age group exposed to pre- and/or postnatal adversity compared to children who were not. Previous work in the literature, has demonstrated that children with pre- and/or postnatal adversity had lower SC and FC between regions of interest (ROIs) within brain networks (Dufford & Kim, 2017; Fan et al., 2017; Luking et al., 2011; Sripada et al., 2014). However, these studies did not combine data in a fused manner to study brain connectivity. Here, we hypothesized that children with pre- and postnatal adversity will have reduced awFC between regions in RSNs compared to controls.

Another objective of this study was to also examine whether behavioural and psychomotor development in toddlerhood (age 3) would be predictive of atypical brain connectivity in middle childhood. A number of longitudinal studies have suggested that behavioural characteristics of children at age 3 are predictive of adult personality characteristics (i.e. emotional stability, social potency, social closeness, alienation, and stress reaction,) (Caspi, 2000; Caspi et al., 2003; Caspi & Silva, 1995). These studies suggested that an early intervention might be necessary to reverse this outcome. By the same token, early developmental outcomes in toddlerhood, such as orienting behaviour and motion in three-year olds, may account for atypical brain connectivity outcomes during middle childhood. As such, three years of age may be potentially a very useful time for the early detection of issues.

The Bayley Scale of Infant Development (BSID-II) is a well-recognized tool used to assess the progress of infant development. The psychomotor development index (PDI) and orientation behaviour (OB) of the Bayley Scale are two metrics of interest for this study. We focused on these two developmental categories given previous animal studies that have demonstrated that the offspring of mothers exposed to prenatal stress had lower scores for orientation, motor maturation (Schneider, 1992; Schneider et al., 1999) and motor activity (Schneider et al., 1999) compared to healthy control mothers. In addition, Schnieder et al (1992) studied the impact prenatal maternal stress had on neurobehavioral development. They found that prenatal maternal stress resulted in motor and attention (measured with orientation) impairments in offspring, compared to controls. These findings are also consistent with human studies indicating that both orientation behaviour and psychomotor development (PDI) are affected in children exposed to prenatal or postnatal maternal adversities. In fact, existing literature has revealed that children from low-income families (Black et al., 2000) or those that are born prematurely (Boyd et al., 2013) exhibited both: lower orientation behaviour and PDI scores(Black et al., 2000; L. A. C. Boyd et al., 2013, p. 2). In addition, a study done by Lyons-Ruth et al (1986), found an association between maternal depression and poor motor development scores (measured with Bayley scale) for infants at one-year old (Lyons-Ruth et al., 1986).

We explored whether early motor and orientation scores at age three could be a potential marker for atypical brain connectivity in middle childhood following exposure to prenatal/postnatal maternal adversity. We hypothesized that behavioural and motor scores at the age of three, would be predictive of atypical RSNs in middle childhood.

4.3 Methods

4.3.1 Subjects, Inclusion/Exclusion, Ethics

We used data from the MAVAN – Maternal Adversity, Vulnerability and Neurodevelopment – study. The MAVAN study is a longitudinal birth cohort study based in Canada that tracked children from birth to age six in Hamilton, Ontario, Canada (O'Donnell et al., 2014). The follow-up study evaluated the offspring of mothers at regular time points, starting at 6 months until the age 12 years old through questionnaires, diagnostic tools and behavioural tasks (O'Donnell et al., 2014). The recruited mothers were included if they were above the age of 18, delivering a singleton pregnancy, and were fluent in English or French. Mothers were excluded if there was a history of incompetent cervix, presence of placenta previa, maternal severe chronic illness, impending delivery, or a fetus affected by a major anomaly. The Ethics committee from the St. Joseph's Hospital approved the protocols for the Hamilton cohort, and the Ethics committee from the Douglas Mental Health University Institute approved the protocols for the Montréal cohort. Enrolment for the study required all mothers to submit a written informed consent. Mothers received a compensation of $25 for every visit.

A subsample of this cohort consisted of thirty-three children that had both fMRI and DTI data available in the middle childhood age group, which was used in this study. Of the sample of thirty-three subjects, those whose head motion exceeded a relative mean displacement of 0.55 mm (n=8) were excluded from the pool- as reported in Satterthwaite et al (2012) (Satterthwaite et al., 2012). Motion exclusion criteria are discussed in greater detail later in this section. In

addition, subjects that had missing resting-state fMRI data points (n=2), contained rsfMRI artifacts (signal inhomogeineity) (n=1), or had missing DTI data (n=5) were omitted from the analysis. This left a total of 17 subjects, 9 children with no pre/postnatal adversity (CON) and 8 children with pre/postnatal adversity (ADV) for analysis. The ratio of male/female participants is 11 females: 6 males; in the CON there are 7 F: 2 M, whereas the ADV group had: 4 F: 4 M. Our population has a mean age of 7.63 (standard deviation = 0.66).

4.3.2 Maternal history of Adversity Score

The Research Ethics Board of St.Joseph's Healthcare approved this study and written consent was acquired from each participant. The Maternal Adversity Vulnerability and Neurodevelopment (MAVAN) study is a birth cohort study of pregnant Canadian mothers and their children. These children were observed longitudinally throughout their development. Pregnant women were assessed at the Women's Health Concerns Clinic (WHCC) with depression between 12 to 24 weeks of gestation. Mothers (with pre- and postnatal adversity and controls) with a current or past history of psychotic disorder were excluded, assessed with the Mini International Neuropsychiatric Interview. Women were included if they were 18 years of age or older, pregnant (up to 24 weeks of gestation), and able to communicate in English. Pre- and postnatal maternal adversity was measured based upon the: Montgomery-Asberg Depression Rating Scale (MADRS) ≥9, Edinburgh Postnatal Depression Scale (EPDS) ≥13, Hamilton Anxiety Rating Scale (HAM-A); State-Trait Anxiety Inventory (STAI) ≥40, and the Center for Epidemiologic Studies Depression (CES-D) Scale.

4.3.3 Image Acquisition Parameters

Magnetic resonance images were obtained on a GE Discovery 750 3T MR scanner (General Electric Healthcare, Milwaukee, WI) with a 32-channel head coil at the Imaging Research Centre, St. Joseph's Healthcare (Hamilton, Canada).

Functional images were acquired using a single-shot gradient-echo echo-planar imaging (EPI) and the acquisition parameters were: TE (echo time) = 35 ms, TR (repetition time) = 3000 ms, flip angle = 90°, matrix = 64 x 64 x 45, voxel size = 3.75 x 3.75 x 3 mm, interslice gap = 0, slice thickness = 3 mm, FOV = 24 cm^2, number of slices = 108, ascending interleaved sequence. Diffusion tensor images were acquired with a single-shot spin-echo EPI sequence, with 66 gradient directions at 1000 s/mm^2. Additional DTI parameters included: TE = 87 ms, TR = 8800 ms, matrix = 122 x 122 x 70, voxel size = 2 x 2 x 2 mm^3, FOV = 24.4 cm^2, 70 ascending interleaved slices, slice thickness = 2 mm (no slice spacing). Three non-diffusion weighted b = 0 s/mm^2 images were also collected.

4.3.4 fMRI Pre-processing

Resting-state functional data were preprocessed using FSL version 6.0.1 (Jenkinson et al., 2012). Standard resting state preprocessing protocols were applied similar to previous resting-state data [See: (Krafft et al., 2014) for reference]. Preprocessing included the following steps: (1) The first three volumes of every participant's functional data were discarded to account for magnetic field homogenization (2) Interleaved slice timing correction (3) brain extraction toolbox (BET) (S. M. Smith, 2002) for skull stripping (4) motion correction using *MCFLIRT* (Saccà et al., 2018)

(5) spatial smoothing using a Gaussian kernel with FWHM = 5mm (6) high pass temporal filtering (0.1 Hz). Functional data was normalized and registered to standard MNI152 space (12 DOF) and resampled to a 4-mm cubic voxel for subsequent analysis. One extra step was introduced in the standard preprocessing pipeline (Goto et al., 2016), which involves despiking the functional data using AFNI (version 18.2.15) as described in (Patel et al., 2014). This method is said to be more effective than other motion correction methods such as scrubbing (Goto et al., 2016).

For the child data in our study (children aged 7-9 years), a standard adult functional brain template (MNI 152) was used for registration and normalization. Previous studies by Wilke et al (2002) and Muzik et al (2000) demonstrated that spatial registration of children data aged 5 and above and 6 and above, respectfully, to adult brains, are acceptable with negligible or minor distortions (if any) (Muzik et al., 2000; Wilke et al., 2002). Additionally, children aged 5 and above do not undergo significant increases in brain volume past the age of five (Casey et al., 2000; Giedd et al., 1996). Therefore, a standard functional MNI-152 template was used.

In this study, five RSN's were investigated that are involved in: internally generated thoughts Default Mode Network (DMN), emotional regulation (Limbic Network; LIM), and higher-order functions (i.e. Ventral Attention Network, Dorsal Attention Network and FrontoParietal Network; VAN, DAN, FPN) as previous literature has reported that connectivity in these RSN's has been impacted due to maternal adversity (Bergh et al., 2018)

4.3.5 Motion correction

Head motion is a major source of artifacts in connectivity studies (Power et al., 2012), and thus, it is necessary to exclude subjects with gross motion that may contaminate the signal (Satterthwaite et al., 2012). A study done by Satterthwaite et al. (2012), deemed gross motion in functional data, as having a relative mean displacement greater than 0.55mm. Therefore, subjects were inspected for gross motion. Subjects with an average relative volume-volume displacement greater than 0.55 mm they were excluded from our study. This resulted in the exclusion of eight subjects from our study.

4.3.6 fMRI Analysis – using FATCAT

A group independent component analysis (GICA) was applied to the resting data using MELODIC (FMRIB Analysis Group, Oxford University) (Beckmann et al., 2005; Beckmann & Smith, 2004). The preprocessed functional data in MNI space was input into the MELODIC GUI with the component number set at 20 and the decomposition approach set to multisession temporal concatenation. Independent components were compared and matched to the standard Yeo 7 network template (Yeo et al., 2011) using a spatial cross correlation – from FATCAT's '*3dMatch*' command *(Taylor & Saad, 2013)*. Of the 20 components generated, 5 networks were matched with a mean correlation of r=0.62. The DMN, FPN, LIM, VAN and DAN were identified and extracted from the components. Five of the networks identified were consistent with standard RSNs. The remaining maps were either taken to be artifactual, noise or simply not matching with the components. The independent components (Z-score maps) were then

thresholded into separate labeled group-level regions of interest (ROIs) using FATCATs '3dROIMaker'. Inflated ROIs were also derived from FATCAT's '*3dROIMaker'* command *(Taylor & Saad, 2013)*, in order to be used for the diffusion data. The ROIs are transformed into diffusion-weighted space and inflated in order to reach white matter tracts (for the diffusion data). The Pearson correlation coefficient was calculated between the mean time courses of each ROI pair, using the non-inflated ROIs with FATCAT's '*3dNetCorr'* command *(Taylor & Saad, 2013)*. The functional connectivity (Pearson correlation) was estimated for each subject. Functional connectivity group differences were then investigated using a Wilcox-test between ADVand CON subjects using R code and corrected for multiple comparisons [will be discussed in greater detail later in this section]. Statistically significant ($p_{adj}<0.05$) group differences were identified and reported in this study as 'conventional functional connectivity'.

4.3.7 DTI Pre-processing

DTI pre-processing steps were performed using a source-code repository (A. D. Davis et al., 2019). Pre-processing involved a combination of FSL and AFNI commands and consisted of the following steps: (1) Diffusion-weighted images and b=0 images were converted from DICOM to NIFIT using dcm2nii (2) Eddy current distortions and motion were corrected (registered to b=0 reference volume) with FSL's '*eddy_correct'* command (Jenkinson et al., 2012) and diffusion vectors were rotated (3) DTI images were skull stripped using FSL's 'BET' (S. M. Smith, 2002) (4) FATCAT's '*3dDWItoDT*' *(Taylor & Saad, 2013)* was applied for diffusion tensor fitting, and FA maps were generated (in diffusion-weighted space) (5) FA maps were spatially normalized to a standard FA template (FMRIB58) for group analysis.

4.3.8 DTI Analysis – using FATCAT

Uncertainty maps from FA and principal eigenvector were generated, with the FATCAT command '*3dDWUncert'*(Taylor & Saad, 2013) to include in probabilistic tractography. Probabilistic tracking was then estimated between inflated ROI-pairs using FATCAT's '3dTrackID'(Taylor & Saad, 2013) with the default standard settings: FA = 0.2, turning angle = 60°, Monte Carlo iterations = 1000. The DTI measures, such as the distance and number of tracts between each inflated group-level ROI pair were estimated for each subject. 'Conventional structural connectivity' was calculated by counting the number of tracts between two ROIs (a DTI metric output by FATCAT). Group-level comparison of structural connectivity was performed to study differences between ADV and CON subjects. Between-group comparisons were performed with a Wilcox-test and corrected for multiple comparisons using r [discussed in greater detail later]. Comparisons that were statistically significant ($p_{adj} < 0.05$) are reported in this study and discussed.

4.3.9 Structural And Functional Connectivity Combined – Using the Anatomically Weighted Functional Connectivity Method

Figure 1 shows how the *FATCAT-awFC* pipeline begins with FATCAT and transitions into the awFC method. From the FATCAT, functional connectivity (from the functional data) and 'tract count' (from the structural data) are output. In turn, these two metrics are used as inputs for the awFC method.

Once '*tract count'* is output from the FATCAT approach (Taylor & Saad, 2013), a number of additional steps were performed using the awFC method to calculate *an improved* structural connectivity measure. These steps include: calculating the probabilities of structural connectivity, performing a Poisson-regression (to adjust for distance bias), computing and incorporating indirect (second-order) structural connectivity between ROI pairs (Bowman et al., 2012). Structural connectivity probabilities were estimated by calculating the 90th percentile of voxel-level counts connecting two ROIs, divided by the total streamlines leaving the ROI (Bowman et al., 2012). Next, the structural connectivity distance-bias was adjusted by fitting a zero-inflated Poisson regression model (Bowman et al., 2012). The Poisson regression was applied using: $\log(\mu(S_{ij}|g_{ij}) = \alpha_0 + \alpha_1 g_{ij}$, where $g_{ij}$is the distance between each region pair, $S_{ij}$is the unbiased number of tracts (Bowman et al., 2012). All possible second-order (indirect) connections were calculated using the equation: $\pi_{ij}=\max[\pi_{ij}, \max_m(\pi_{im}\pi_{mj})]$, where π is the probabilities of structural connectivity, i is the starting ROI, j is target ROI, and m is the third connection (Bowman et al., 2012). The greater connectivity value (between the direct and indirect connectivity) was taken to be the pathway between the connected ROIs (Bowman et al., 2012). Once all of the above mentioned steps are performed, a structural connectivity metric is produced.

FC was produced from the *FATCAT* pipeline and SC was produced from the *awFC method*. Two additional steps were required to combine both in a single metric. To combine FC and SC into a single metric, the dissimilarity metrics were first calculated (Bowman et al., 2012). FC and SC measure entirely different aspects of brain connectivity, whereby functional connectivity

measures the temporal correlation (using Pearson correlation) and structural connectivity measures the tract count between brain regions. Therefore, to generate a modality-independent comparison between structural and functional connectivity, the dissimilarity metric is used (Kriegeskorte et al., 2008). The structural dissimilarity (1 minus structural connectivity) and functional dissimilarity (1 minus functional connectivity) are multiplied to obtain the anatomically weighted functional dissimilarity (awFd). Next, the dissimilarity metric (a combined structural-functional measure) is transformed back to a correlation metric. This metric is known as the anatomically weighted functional connectivity, which is obtained by applying the equation: $1 - |awFd|$ (Bowman et al., 2012). It is transformed back to a correlation metric in order to interpret the data with ease.

4.3.10 Wilcox Test Group Comparisons and Multiple Comparisons Adjustment

A Wilcox test was applied to determine whether there were any significant FC, SC and awFC differences between children with pre/postnatal adversity (ADV) compared to children without pre/postnatal adversity (CON). The function *'wilcox.test()'* was employed to assess pair-wise differences in FC, SC and awFC between the CON and ADV for each ROI-pair within each RSN. Multiple comparisons were corrected for, using the False Discovery Rate (FDR) by Benjamini and Hochberg (Waite & Campbell, 2006) using the function *'p.adjust()'* from the stats package in R (R Core Team, 2018). The significance level was set to $p_{adj} < 0.05$. Significant awFC differences between the CON and ADV groups were visualized using boxplots, with the *'ggplot()'* function from the ggplot2 package (v.2.2.1) in R software (v.4.0.2). Finally, the effect size was calculated using Cohen's *d, 'cohen.d'* function from the effsize package (Tocrchiano,

2017) in R (R Core Team, 2018). A Cohen's d between 0.5 > d > 0.2 is considered small, 0.8 > d > 0.5 moderate and d ≥0.8 large.

4.3.11 Bayley Measures

The Bayley Scales of Infant Development is the most widely reported standard developmental assessment for children 1 to 42 months of age (Bayley, 1993). The infant's behaviour was evaluated within a controlled environment, and a standardized scale. A trained examiner evaluates the infants' behaviour and assigns a BSID score according to his/her judgement of the infant's performance. The BSID-II has three main categories: mental scale, motor scale and behaviour rating scale (Bayley, 1993). However, only two metrics, the psychomotor development index (PDI) and orientation/engagement (from the behaviour rating scale) were evaluated for this study. The Motor scale uses a score known as the psychomotor developmental index (PDI) – it measures the child's muscle coordination, fine and gross motor skills, body and postural control, and recognizing and discriminating objects through touch (Bayley, 1993). The PDI Bayley scale, ranges as follows: (1) >115; Accelerated performance (2) 85-114; within normal limits (3) 70-84; mildly delayed performance (4) < 70; Significantly delayed performance (Bayley, 1993). The Behavioural Rating Scale (BRS), on the other hand, evaluates orientation/engagement – this includes orientation to examiner, social engagement, cooperation, attempts to interact socially, trusting the examiner/lack of fearfulness (Bayley, 1993). The range of BRS scores are considered within a normal range (26–99 percentiles), questionable (11–25th percentile) and non-optimal (< 11th percentile) (Bayley, 1993). Scores <25th percentile on the behavioural scale of the BSID-II are considered sub-optimal.

4.3.12 Regression Analysis

Regression analysis was performed to examine the association between PDI and awFC and between orientation behaviour and awFC for both ADV and CON, for each significant ROI-pair within each RSN. The 'lm' function in the 'stats' R package (R Core Team, 2018) was used. The first linear regression model was set up with the awFC as the dependent variable and PDI as the independent variable. The second linear regression model was set up with the awFC as the dependent variable and the orientation behaviour as the independent variable. Regression analysis was only applied to ROI-pairs with significant awFC differences between groups (CON vs ADV).

4.4 Results

4.4.1 Significant ROI-ROI pairs

A complete listing of the ROIs in each RSN, their associated anatomical location, volume, and MNI coordinates is reported in Table 1. A visual representation of the ROIs that revealed significant connectivity differences for ADV groups compared to CON groups are shown in Figure 2.

4.4.2 ROI-ROI Anatomically Weighted Functional Connectivity Group Differences

Children who had experienced early adversity showed lower awFC in a number of ROI-pairs compared to children who did not. Table 2 details regions where lower awFC were found in ADV compared to CON. In summary, lower awFC was noted for the ADV group compared to CON group in (i) the DMN between the PCC and the left angular gyrus (ii) the FPN between the left inferior frontal gyrus to the lingual gyrus/cerebellum, the FPN between the right superior frontal gyrus and the lingual gyrus/cerebellum (iii) the LIM between the right superior temporal gyrus and the left superior temporal gyrus (iv) the DAN between the right posterior orbitofrontal gyrus and the left inferior temporal gyrus. On the other hand, greater awFC was noted in children who faced adversity compared to children who did not in the VAN between the right anterior orbitofrontal gyrus and the left lingual gyrus/cuneus. The statistical comparisons between ADV and CON groups are shown in the boxplots in Figure 3.

4.4.3 ROI-ROI Functional and Structural Connectivity Group Differences

Functional connectivity differences were observed in the ADV compared to the CON in (i) the DMN between the PCC and the left angular gyrus (ii) the FPN between the left inferior frontal gyrus to the lingual gyrus/cerebellum, the FPN between the right superior frontal gyrus and the lingual gyrus/cerebellum (iii) the LIM between the right superior temporal gyrus and the left superior temporal gyrus (iv) the VAN between the right anterior orbitofrontal gyrus to the left lingual gyrus/cuneus (v) the DAN between the right posterior orbitofrontal gyrus and the left inferior temporal gyrus. See Table 2 for a summary of the results.

Structural connectivity differences were observed for the ADV compared to the CON group in (i) the FPN between the left inferior frontal gyrus and the lingual gyrus/cerebellum. However it did not survive multiple comparisons. See Table 2.

4.4.4 Predictors of brain development

Linear regression tests showed a significant interaction between orientation behavior (as measured by the Bayley scales) and awFC in the VAN ($F(1,12) = 5.032$, $p = 0.045$). FDR corrected p-value for orientation behavior resulted in a $p_{adj} = 0.045$. Linear regression models indicated that a lower orientation behavior score at the age of three was predictive of an atypical (greater) awFC within the VAN in middle childhood.

Further, a linear regression test revealed that there was a significant interaction between PDI and awFC in the FPN ($F(1,12)=5.74$, $p=0.0338$). FDR corrected p-value for PDI resulted in a $p_{adj} = 0.045$. A lower PDI score at the age of three revealed an atypical (lower) awFC in middle childhood.

Table 1 | this table presents nineteen ROIs, their associated anatomical names, peak MNI coordinates and cluster sizes. These nineteen ROIs belong to five resting-state networks, including the default mode, frontoparietal, limbic, ventral attention, and dorsal attention network. ROIs were defined using FATCATs *3dROIMaker* command.

ROI no.	Anatomical names	MNI coordinates	Volume

		x	y	z	(# of voxels)
DEFAULT MODE NETWORK					
1	Medial frontal gyrus (MFG)	2	62	8	7
2	Posterior cingulate cortex (PCC)	-2	-62	24	5
3	Right angular gyrus (R-AG)	46	-58	28	6
4	Left angular gyrus (L-AG)	-46	-58	28	5
FRONTOPARIETAL NETWORK					
5	Left inferior frontal gyrus (L-IFG)	-38	38	12	12
6	Lingual gyrus/cerebellum (LG/CER)	-6	-74	-12	12
7	Right Superior frontal gyrus (R-SFG)	10	38	56	10
LIMBIC NETWORK					
8	Right posterior orbitofrontal gyrus (R-pOFG)	18	38	-24	12
9	Left posterior orbitofrontal gyrus (L-pOFG)	-42	30	-20	12
10	Right superior temporal gyrus (R-STG)	46	14	-44	11
11	Left superior temporal gyrus (L-STG)	-42	2	-52	12
12	Dorsolateral prefrontal cortex	-2	46	32	12

.

	(DLPFC)				
	VENTRAL ATTENTION NETWORK				
13	Left lingual gyrus/Cuneus - Lateral occipital cortex (L-LG/CU)	-14	-98	-16	20
14	Right orbitofrontal gyrus (R-aOFG)	14	70	-16	5
15	Right cerebellum (R-CER)	10	-66	44	20
	DORSAL ATTENTION NETWORK				
16	Right anterior orbitofrontal gyrus (R-aOFG)	14	58	-20	9
17	Right posterior orbitofrontal gyrus (R-pOFG)	22	30	-16	14
18	Right middle frontal gyrus (R-MFG)	38	42	-16	14
19	L-Inferior temporal gyrus (L-ITG)	-50	-54	-16	14

Abbreviations: ROI – region of interest, RSN – resting state network

Table 2 | Connectivity analysis was performed for: structural, functional and anatomically weighted functional connectivity. A Wilcox test was performed to reveal significant brain connectivity differences between children exposed to pre/postnatal adversity (ADV) and children not exposed to pre/postnatal adversity (CON). Significant awFC differences between children exposed to pre/postnatal adversity compared to children not exposed to pre/postnatal adversity

are shown, along with their corresponding structural and functional connectivity group differences (some survived multiple comparisons others did not).

Start ROI	End ROI	SC p-value (FDR corrected)	FC p-value (FDR corrected)	awFC p-value (FDR corrected)	Cohen's D
DEFAULT MODE NETWORK					
PCC	L-AG	0.815	**0.0274***	**0.0274***	0.626 (medium)
FRONTOPARIETAL NETWORK					
L-IFG	LG/CER	**0.041**	**0.006***	**0.0053***	1.66 (large)
R-SFG	LG/CER	0.664	**0.0274***	**0.0274***	1.36 (large)
LIMBIC NETWORK					
R-STG	L-STG	0.095	**0.002****	**0.00149****	1.75 (large)
VENTRAL ATTENTION NETWORK					
R-aOFG	L-LG/CU	0.198	**0.032***	**0.032***	-1.27 (large)
DORSAL ATTENTION NETWORK					
R-pOFG	L-ITG	0.06	**0.00551***	**0.00551***	1.79 (large)

Table displays connectivity values (bold indicates significant ($p < 0.05$)) of structural connectivity, functional connectivity and awFC for each ROI-ROI pair. Note: awFC= anatomically weighted functional connectivity, ROI=region of interest, SC=structural connectivity, FC=functional connectivity, PCC = posterior cingulate cortex, L-AG = left angular gyrus, L-IFG = left inferior frontal gyrus, LG/CER = lingual gyrus/ cerebellum, R-

.

SFG = right superior frontal gyrus, R-STG = right superior temporal gyrus, L-STG = left superior temporal gyrus, R-aOFG = right anterior orbitofrontal gyrus, L-LG/CU = left lingual gyrus/cuneus, R-pOFG = right posterior orbitofrontal gyrus, L-ITG = left inferior temporal gyrus.

*** Survives FDR (q < 0.05), ** Survives FDR (q < 0.01).**

4.5 Discussion

The goal of this study was to apply our novel FATCAT-awFC pipeline (combines structural and functional connectivity) to assess whether maternal adversity impacts brain connectivity in RSN during middle childhood. To study changes in brain connectivity, separate analyses were carried out using: traditional SC, traditional FC and awFC between each ROI pair within each RSN. The RSNs included the: DMN, FPN, LIM, VAN, and DAN. In each of the five RSNs, distinguishable connectivity differences were observed between the ADV and CON groups in our sample of children aged 6-9 years old. Another goal of our research was to determine whether psychomotor development and behavioral scores at the age of three were predictive of atypical brain connectivity in middle childhood. Psychomotor development scores at the age of

three were found to be predictive of typical/atypical connectivity in middle childhood in the FPN and VAN, respectively.

4.5.1 Typical Maturation of RSN in Brain Development

Understanding the typical development trajectories of brain connectivity is essential to conceptualizing atypical connectivity as it relates to adversity. While RSNs are observed in middle childhood (age 7-9 years old), they are not fully matured (Fair et al., 2008). During this time, the brain is maturing, adapting, and changing rapidly (Mah & Ford-Jones, 2012). Brain development involves a number of processes including synaptogenesis, pruning and myelination (Barnea-Goraly et al., 2005; Mah & Ford-Jones, 2012; Muftuler et al., 2012). As unimportant brain connections are being pruned, important connections are further strengthened to improve the speed of information transmitted between brain regions (Andersen, 2003; Luna et al., 2021, p. 20). The interplay of a dual process of integration (i.e. network efficiency) and segregation (i.e. clustering) contributes to this maturation (Dosenbach et al., 2010; Grayson & Fair, 2017). Studying connectivity as it relates to the maturation of RSNs may provide unique insights into typical and atypical brain development (Uddin et al., 2010), which may, in part, be impacted by adverse maternal environments (Webb et al., 2001).

Connectivity in these RSNs can be used to distinguish children exposed to maternal adversity from typically developing children. While we hypothesized that the CON group would have lower awFC compared to ADV, we instead observed greater connectivity between brain regions in the CON compared to ADV in all but one RSN. Connectivity between a ROI-pair within the

VAN displayed the opposite trend with reduced connectivity between brain regions in the CON group compared to the ADV group [this will be discussed in greater detail later in this section]. A possible explanation for the greater awFC in the CON compared to ADV for the DMN, FPN, LIM, and DAN, could be due to the ongoing development of the RSNs architecture (i.e. myelination, tract density to strengthen important connections, etc), which strengthens important connections. Past literature has supported our findings by reporting that the ongoing development of RSNs occurs during middle childhood. For instance, a study by Fair et al (2008) performed a comparative analysis, to study the DMN architecture within two groups: middle childhood (7-9 years old) and young adults (21-31 years old) in healthy individuals. They reported that connectivity between brain regions belonging to the DMN, increases in myelination (to support integration of ROIs belonging to the same network) to form more mature and efficient resting state networks (Fair et al., 2008). Another study done by Szaflarski et al (2006) that assessed children aged 5, 6 and 7 years of age found that the BOLD signal increased in language cortex across age (Szaflarski et al., 2006). Increased BOLD signal was found in regions such as the left angular gyrus, right lingual gyrus, right inferior temporal gyrus, the inferior frontal gyrus, and middle frontal gyrus. The authors proposed that the increased BOLD signal was due in part to increased synaptic myelination of important connections in the language network. As shown from previous studies, the strengthening of connections between brain regions may occur through myelination across middle childhood. Aside from myelination, brain maturation may include the reorganization of brain networks rather than just the fine-tuning (i.e. myelination) of already matured synapses within RSNs. Dosenbach et al (2010) demonstrated that middle childhood is a period of time when functional maturation occurs (Dosenbach et al., 2010). Segregation and integration are signature to functional brain maturation (Fair et al., 2007,

2009; Johnson, 2001; Supekar et al., 2009). Brain development (maturation) across age groups (from childhood into adulthood) is characterized by increased connectivity between ROIs belonging to the same RSN (integration) and decreased connectivity between ROIs belonging to separate RSNs (segregation) (Fair et al., 2009; Rosenberg et al., 2020). Studies have demonstrated that functional maturation continues to undergo changes (i.e. segregation/integration) throughout middle childhood. For instance, a study done by Fair et al (2007), found that functional maturation involved further distinction of two separate RSNs: the frontoparietal network and the cinguloopercular network. This occurred by segregating the aPFC and the dACC regions from the frontoparietal network and integrating of the dACC/msFC into the cinguloopercular network (Fair et al., 2007). Therefore, since we evaluated large-scale RSN in this study, it would be reasonable to observe predominately-increased connectivity between brain regions belonging to the same RSN as a sign of brain maturation (i.e. integration of ROIs belonging to the same RSN and/or increased myelination of important connections).

Since strengthening of brain connectivity may imply integration of brain regions belonging to the same RSN, the lower connectivity observed between the orbitofrontal gyrus and the lingual gyrus in the VAN in our study could be the result of the segregation of these brain regions into separate RSN. The ventral stream of attention is known to be associated with orienting. The orienting network primarily drives the attention network in infancy and early childhood, however the executive control network becomes the main attentional network in charge of control as the brain develops (>3 years) (Posner et al., 2014). The increasing importance of the executive control network results in its continual strengthening and refinement across age (Ruff & Rothbart, 2001). On the other hand, the orienting network that once primarily controlled

attention begins to diminish, but never entirely (Ruff & Rothbart, 2001). Menon (2013), reported that across age, significant strengthening of the executive control network (between the ACC and insula) was found. This could be related to the shift in control of attention from the orienting network in infancy to the executive network in middle childhood. This finding suggests that there is a transition from the immature functional system that supports attentional functions in children to more mature systems in adults. The ventral visual (attention) pathway is known to have six distinct projections that originate from the occipital lobe and extend to cortical and subcortical regions, via a projection known as the occipitotemporal-orbitofrontal pathway (Kravitz et al., 2013). Kravitz and colleagues (2013) found that this pathway (originating from the occipital lobe) has weaker projections extending to the central orbitofrontal gyrus compared to other brain regions in adults (Kravitz et al., 2013). Therefore, as previous studies have suggested, since during childhood the executive control network predominantly controls attention while the orienting network plays a less significant role – the connectivity between the lingual gyrus and the orbitofrontal gyrus may be less used and therefore weakened during middle childhood due to a potential role it plays in visual attention. This may explain why we observed reduced connectivity between these brain regions in the VAN in our study, and may also suggest that increased connectivity within these brain regions could be suggestive of atypical connectivity during middle childhood as a result of adversity.

4.5.2 Adversity and adversity outcomes impact connectivity

A number of studies have found that adversity impacts typical brain development (measured by connectivity strength) within RSNs. For instance, a study done by Marshall et al (2018),

investigated changes in resting-state FC of the ventral striatum, for participants who ranged from 6 to 17 years of age. They found that individuals exposed to socio-economic disadvantage in their early years of life had atypical, reduced FC between the ventral striatum and the anterior part of the medial prefrontal cortex (Marshall et al., 2018). They also found this connectivity to be associated with anxiety (Marshall et al., 2018). Other studies have also reported this connectivity to be associated with depression as well, which Marshall et al (2018) suggest could be caused by affective dysfunction from atypical corticostriatal connectivity. Another study evaluated children (aged 9) from low-income households and found that they had reduced within-network DMN connectivity compared to the children of middle-income families (Sripada et al., 2014). These studies support our findings that maternal adversity impacts the typical development of RSNs, as indicated by reduced connectivity within RSN for the ADV compared to CON.

4.5.3 Group differences in the frontoparietal network

In our study, we found lower awFC between the left inferior frontal gyrus and the cerebellum in ADV compared to CON. A previous study by Li et al (2014), used rs-fMRI to assess children aged 6-16 years using seed-based functional connectivity. They found reduced FC within the FPN and within the frontocerebellar network in children with ADHD compared to controls (Li et al., 2014). Studies have shown that prenatal maternal stress is associated with ADHD in their offspring (Grizenko et al., 2008; Ronald et al., 2011). Therefore, this supports our findings that greater maternal adversity may contribute to ~~an~~ atypical connectivity within the brain networks of their offspring.

Reduced awFC for the ADV compared to CON was also found between the right superior frontal gyrus and the lingual gyrus in the FPN. A study done by Davis et al (2020) found an association between prenatal maternal stress and the cortical thinning of the occipital cortex and frontal cortex. Specifically, fetuses exposed to higher levels of prenatal maternal stress had significantly reduced cortical thickness in the superior frontal gyrus and the lingual gyrus, along with other structures (Davis et al., 2020). Previous studies have demonstrated that brain regions that had cortical thinning, also happened to have weakened connectivity between these brain regions (Bullmore, 2019). Thus, maternal adversity caused by stress may be a factor for the reduced connectivity found in offspring between the right superior frontal gyrus and the lingual gyrus (occipital cortex) in the ADV group compared to CON in our study.

4.5.4 Group differences in the limbic network

Within the limbic network, we found significantly greater awFC group differences for the CON group compared to the ADV in the LIM between the right superior temporal gyrus and left superior temporal gyrus. A study done by Muetzel (2016) evaluated the RSN of children aged 6-10 years of age and found that the within this age group the brain continues to undergo developmental changes. They suggested that the interhemispheric connectivity is strengthened with age (Muetzel et al., 2016). In this study we observed greater connectivity between the left and right superior temporal gyrus of the limbic network for the CON group compared to ADV.

Furthermore, the temporal lobes and amygdala of both hemispheres are connected by the anterior commissure (Klingler & Gloor, 1960). The amygdala is known to play an important role in emotional processing (LeDoux, 2000). Altered interhemispheric connectivity within brain networks was found to correlate to emotional deficits (Saxena et al., 2012). More specifically, Saxena et al. (2012) demonstrated that lower structural connectivity (measured as fractional anisotropy) within the anterior commissure was associated aggression in youth (aged 7-17 years old) (Saxena et al., 2012). Children of depressed mothers have been shown to display aggression, which Keenan-Miller et al (2010) suggested is a result of poor mother-child interactions. In our study, we also identified lower connectivity within this region. It may be suggested that lower awFC in the ADV group may contribute to emotional deficits in children of mothers exposed to greater levels of adversity. Future work will be necessary to examine this question directly.

4.5.5 Group differences in the ventral attention network

In this study, we observed that relative to ADV, CON displayed ~~a~~ greater connectivity within all RSN's except the VAN. A study done by Farah et al (2020), used task based-fMRI to assess brain connectivity changes in preschoolers with mothers who experienced adversity either prenatally or postnatally. They found that maternal depression was associated with greater connectivity between the right visual region (located in the occipital lobe) and the right frontal regions (i.e. dorsolateral prefrontal cortex) in children. Farah et al (2020) suggested, that reduced connectivity in these brain regions may be indicative of children processing fewer positive emotions during visualization (imagination) that accompanies story time (Farah et al., 2020). In a

study done by Van der Werff (2013) increased lingual gyrus connectivity was identified in maltreatment-resilient individuals (van der Werff et al., 2013). The prefrontal cortex is another region of the brain found to play a key role in the mechanism of stress/trauma resilience (Arnsten, 2009). In a review study, done by Bolsinger et al (2018), the trauma resistant individuals were characterized by increased activation of the PFC. Their study suggests that resilient individuals have more cognitive control over their emotions, which is reflected in their brain networks in the form of increased activation in this region (Bolsinger et al., 2018). This finding aligns with our work, as we observed greater connectivity in ADV compared CON. Greater connectivity between these regions may imply that these ADV children have formed resilience to the adverse events they had experienced either prenatally or postnatally.

4.5.6 Group differences in the dorsal attention network

We observed reduced connectivity between the orbitofrontal gyrus to the left inferior temporal gyrus within the DAN for ADV compared to CON. The lateral orbitofrontal cortex shares strong connections with the inferior temporal pole (Martin-Elkins & Horel, 1992). The orbitofrontal gyrus receives and processes information from the temporal pole (Öngür & Price, 2000). A study done by J. L. Hanson et al., 2010 performed tensor-based morphometry and found that children exposed to maltreatment (specifically physical abuse) showed anatomical volume changes in the orbitofrontal gyrus and the inferior temporal gyrus in comparison to controls. Another study done by J. Hanson et al., 2013 demonstrated that children (9-14 years of age) exposed to early neglect exhibited reduced structural connectivity (they refer to as directional organization) measured with DTI-derived fractional anisotropy between the prefrontal and temporal lobes

compared to children that did not. These studies reveal the impact of adversity on the structural connectivity between the frontal lobe and temporal lobe in children. Therefore, our findings may provide additional support that connectivity may be impacted upon exposure to early life adversity, specifically within the DAN.

4.5.7 SC and FC decoupling

Connectivity measures between brain regions that displayed significant functional connectivity group differences did not always display structural connectivity group differences as well [See table 2]. Although not uncommon, the age group of the participants may be a major factor. During middle childhood, functional connectivity is said to reach adult–like levels, whereas the structural connectivity is still undergoing constant change (i.e. pruning and myelination) (Supekar et al., 2010). These structural connectivity changes can result in a *plateau phase* (Levitt, 2003).–Since there are many processes that are taking place during development, including synaptogenesis, pruning and myelination, it can be difficult to detect changes in structural connectivity. In particular, from a structural connectivity standpoint, synaptogenesis (increasing number of tracts) and pruning (decreasing number of tracts), can counterbalance each other for children aged 2-7 years of age (Levitt, 2003). This developmental period is also known as the "plateau phase" (Levitt, 2003). Our population has a mean age of 7.63 years (standard deviation = 0.66), which may explain the observed lack of detectable SC differences between CON and ADV groups in this study. Furthermore, white matter maturation can involve different types of maturation, depending on the connection. Structural connectivity maturation may have included myelination, but would not be detected with our SC approach since the measure of SC

used in this study is tract density. As such, changes in structural connectivity may be more difficult to detect during middle childhood while, group differences in functional connectivity are much more easily identified across this developmental period.

There are several other reasons for the dissociated functional and structural connectivity changes. Inter-subject variability of brain development is substantial (Walhovd et al., 2014). Brain development may be occurring at different rates (i.e. pruning and myelination in different brain networks) for different children, thus not easily detected. The exact timing of when these changes occur for each child may also vary (Marsh et al., 2008). In addition, while the functional connectivity reconfigures due to experiential influences (i.e. adversity), the underlying structural reorganization (structural connectivity) changes at a slower rate (Honey et al., 2010). The structural connectivity may evolve at a slower rate compared to the functional connectivity (Honey et al., 2010). Ultimately, this could result in significant structural connectivity changes going undetected.

4.5.8 Linking Infant Behaviour with Atypical Neural Networks in Middle Childhood

4.5.8.1 Psychomotor Development and underlying FPN

One of the important functions of the SFG is motor activity (Martino et al., 2011), although this brain region is also known to be associated with cognitive control (Vincent et al., 2008), working memory (Courtney, 1998) and resting-state regulation. The superior frontal gyrus is connected to the occipital lobe via the inferior fronto-occipital fasciculus (IFOF). The IFOF is also strongly

connected with the premotor and prefrontal areas, which contribute to movement planning and sensorimotor processing (Caverzasi et al., 2014). The IFOF is known to have six different projections (Kravitz et al., 2013). A study done by Astafiev et al., 2004, revealed that limb movements activated not only motor areas (i.e. primary motor cortex, bilateral secondary somatosensory cortex and supplementary motor area), but visual areas such as the lingual gyrus as well (Astafiev et al., 2004). The lateral occipital cortex (i.e. lingual gyrus) is known to have a modulatory role during the recognition of haptic objects (recognizing objects through touch) (Amedi et al., 2001). In our study the Bayley tests for psychomotor development was used. The Bayley test includes picking up and exploring objects as categories for the PDI – this includes fragile objects (haptic perception) (Normand et al., 1995). Given this interesting link, it seems plausible that there is an association between PDI at age three and brain connectivity strength between the superior frontal gyrus and the lingual gyrus in middle childhood. Another potential explanation may be that motor movement is primarily driven by vision (Glickstein, 2000), and therefore the connectivity between the SFG and the LG (a visual area) would be impacted.

4.5.8.2 Association between PDI during toddlerhood and awFC during middle childhood

In this study, PDI score at age three was found to be associated with atypical connectivity between the SFG and the LG (located in the occipital pole) in middle childhood for children exposed to high levels of maternal adversity. Many studies have suggested that the pre- and postnatal maternal environment, such as maternal smoking during pregnancy (Larsson & Montgomery, 2011), alcohol consumption during breastfeeding (Little et al., 1989), antidepressants during pregnancy (Casper et al., 2003; Galbally et al., 2011; Hanley et al., 2013;

Smith et al., 2013), among many other genetic and environmental factors (Golding et al., 2014), may affect children's motor skills. Previous studies have shown that the quality of spontaneous (motor) movements during early infancy (11-16 weeks) was predictive of behavioral issues and intelligence during middle childhood (7-11 years old) (Butcher et al., 2009). A study done by Grunewaldt et al (2014), found that infants at 3 months of age with atypical motor-repertoire exhibited poorer working memory, poor motor skills, and had more attention and behavioral problems in middle childhood (age 10) as well (Grunewaldt et al., 2014, p. 10). These studies suggest that poor gross motor skills may manifest as poor cognitive skills. Cognition is developed through motor skills because during the earliest years of life infants and toddlers rely on their motor activity to explore their environment (Bruggink et al., 2010; Bushnell & Boudreau, 1993; Butcher et al., 2009). Therefore, weakened motor activity during the early years of a child's life may impact their cognitive and perceptual development throughout their childhood (driven by sensorimotor activity) (Bruggink et al., 2010; Bushnell & Boudreau, 1993; Butcher et al., 2009). As such, it is important to assess motor movements during early life to predict the potentially long-lasting impacts on the neural brain development in middle childhood, which may persist into adulthood. In addition, other studies evaluated the effect childhood adversity - as it relates to drug exposure - on typical development. For instance, a study done by Rosen & Johnson (1982) studied the effect in-utero methadone (an opioid) exposure has on infant development. They found that the two groups (methadone exposed and controls) had statistically significant differences in Bayley PDI measures (Rosen & Johnson, 1982). More specifically, methadone-exposed infants scored lower on the PDI than controls, although all the scores were within the normal range (Rosen & Johnson, 1982). They noted that as infants got older, the difference between both groups would become more apparent and increasingly

significant (Rosen & Johnson, 1982). Similarly, in this study although all subjects were within the normal range of PDI score as described in Rosen & Johnson (1982), the children that were exposed to pre- and/or post-natal maternal adversity had a lower PDI scores than controls.

4.5.8.3 Orienting behaviour and underlying VAN connectivity

The orienting behaviour, first introduced by Pavlov (1927) was described to be an 'investigatory reflex" or a "what-is-it?" exploratory response to novel stimuli (change in environment). The orienting reflex (rapid shifting of attentional focus to unpredicted stimuli) is mediated via the ventral attention network (interchangeably referred to as the ventral Frontoparietal network) (Corbetta et al., 2008; Corbetta & Shulman, 2002).

Goodale and Milner (1992) proposed that the processing of visual information is composed of two main streams: the ventral and dorsal streams. The ventral stream has been known as the 'what' pathway, whereas the dorsal stream is known as the 'how' pathway (Goodale & Milner, 1992). The ventral stream processes information about the structure of the object, whereas the dorsal stream processes the spatial information (Goodale & Milner, 1992). The dorsal stream is well defined, whereas the exact anatomy of the ventral stream is still debated in the literature (Dick & Tremblay, 2012). However, it's been suggested that the inferior fronto-occipital fasciculus (IFOF) is one of the pathways that make up the ventral stream (Axer et al., 2013; Dick & Tremblay, 2012; Weiller et al., 2021). The oribitofrontal gyrus is connected to the ventral occipital lobe (i.e. lingual gyrus) via the inferior fronto-occipital fasciculus (Catani & Thiebautdeschotten, 2008). The IFOF is known to play a role in a number of cognitive tasks including pantomime, language, tool use, arithmetic's or spatial attention (Fridriksson et al.,

2018; Hickok & Poeppel, 2007; Umarova et al., 2010; Vry et al., 2015; Willmes et al., 2014) . The IFOF's role is also suspected to be associated with visual processing (Fox et al., 2008; Rudrauf et al., 2008), visual perception of information (Ashtari, 2012), and re-orienting attention (Doricchi et al., 2008)..

4.5.8.4 Association between orientation behaviour during toddlerhood and awFC during middle childhood

The association between orientation behaviour in infants and atypical brain connectivity in middle childhood as an outcome of high or low maternal adversity score was explored. In this study, we found atypical connectivity for the ADV compared to CON in the VAN between the orbitofrontal gyrus and the lingual gyrus in middle childhood, which was significantly associated with orienting behaviour at age three. A study done by Farber et al (1981) found that infants of mothers with anxiety had a lower orientation scores than infants of mothers who were not anxious (Farber et al., 1981). This supports our findings of lower orientation behaviour in children aged 3 and its association with greater awFC (atypical connectivity). Previous studies have also shown that orientation behaviour (i.e. alertness, awareness, orienting to stimuli) in infants may be predictive of IQ and/or mental functioning later in life (Anderson, 1939; DiLalla et al., 1990; Nelson & Richards, 1938). Orienting behaviour is frequently related to child cognitive development (Lemelin et al., 2006; Sajaniemi et al., 2001). In addition, the right lateral orbitofrontal cortex has been found to contribute to the orienting of visuo-spatial attention (E. R. Murphy et al., 2017). Thus, it may be of value to study orientation behaviour in 3-year-old children to understand the long-term implications early attention and cognition may have

during middle childhood on brain connectivity within the VAN. Our results fit well with existing literature suggesting that maternal adversity may have adverse outcomes on behavioural development. We extended this work to explore the impact adversity outcomes have on brain connectivity changes in middle childhood.

4.5.9 Future directions and limitations

Early development of psychomotor and orientation behaviour at the age of 3 was found to be predictive of atypical brain connectivity within RSNs in middle childhood. While we studied PDI and orientation behaviour at the age of three as predictive variables for connectivity in middle childhood, it would also be interesting to investigate PDI and orientation behaviour in middle childhood as well. Does it become more distinguishable between CON and ADV groups? This question remains an important and interesting area for future research. In addition, this paper investigated atypical RSN development throughout middle childhood as a result of exposure to maternal adversity for children alone. However, it would be interesting to perform a comparative study to evaluate RSN connectivity changes in mother and child. By doing so, one would be able to study potential parallels between mother and child brain connectivity abnormalities as a result of adversity.

Comparison of our data with that of the literature must be interpreted with caution because our sample size is small (17 participants). A study with a larger sample size may be useful in determining the impact of maternal adversity on RSN's connectivity. In addition, there has not

yet been other combined FC-SC studies in middle childhood and early exposure to maternal adversity. Moreover, the age range, which defines middle childhood, varies across studies and should be noted when comparing results. Furthermore, our analysis was limited to a few ROIs per network that represented regions of each of the RSN's, however there are several other ROIs that we did not explore. An appropriate threshold for the most optimal set of ROIs that represent key regions of each network still remains uncertain. It is difficult to determine the most optimal threshold that can produce a set of ROIs that represents key regions of each of the RSN's. In addition inputting different parameters into 3dROIMaker such as a white matter skeleton, CSF mask (which trims ROIs), and volume threshold, and ROI threshold, results in different set of ROIs location, size, and shape. For this reason, it may be difficult to replicate the study with the same set of ROIs per network. In addition, in our study we used DTI to acquire white matter tracts. DTI-based tractography, which involves indirectly measured tract tracing via a water diffusion technique, has its limitations. Crossing, converging, and diverging fibers are difficult to resolve in tractography and prone to error and inaccuracies (Jbabdi & Johansen-Berg, 2011). Crossing fibers in a voxel may result in inaccurate tractography tracing. However, a diffusion imaging technique called diffusion spectrum imaging (DSI), is sensitive to detecting fibers and fiber crossings. Therefore, DSI may be a more suitable technique since we use the number of fiber tracts as the measure for structural connectivity, and a worthwhile approach to consider.

4.5.10 Conclusion

Our results add to a growing body of literature that examines the impact of prenatal/postnatal maternal adversity on neurodevelopment. In particular, this research provides strong evidence of

RSN abnormalities amongst children aged 7-9 who were exposed to early life maternal adversity. We used a novel FATCAT/awFC approach that was designed to simplify a complex and computationally intense model (Bowman et al., 2012), by integrating a toolbox (Taylor & Saad, 2013) in the pipeline, which ultimately resulted in a fast and simplified approach that preserved the abundance information. Our findings are similar to the existing literature of individuals exposed to adversity in early years. However, we extended upon these studies by performing a combined structural-functional connectivity approach to reveal (or study) changes in brain connectivity. Examining awFC can be an important tool in tracking normative brain development in children. Aberrant awFC connectivity can be reflective of atypical brain development in children exposed to adversity. In addition, aberrant connectivity within these networks may play a role in the behavioural issues and neuropsychiatric disorders that are hallmarks of early adversity. As our results show, orientation behavior and psychomotor performance at age 3 may be predictive of aberrant connectivity in middle childhood Our research demonstrates that with our novel FATCAT-awFC pipeline, we were capable of detecting underlying changes in the brain networks among children in the middle childhood age group who were exposed to prenatal and postnatal maternal adversity.

4.5.11 Figures

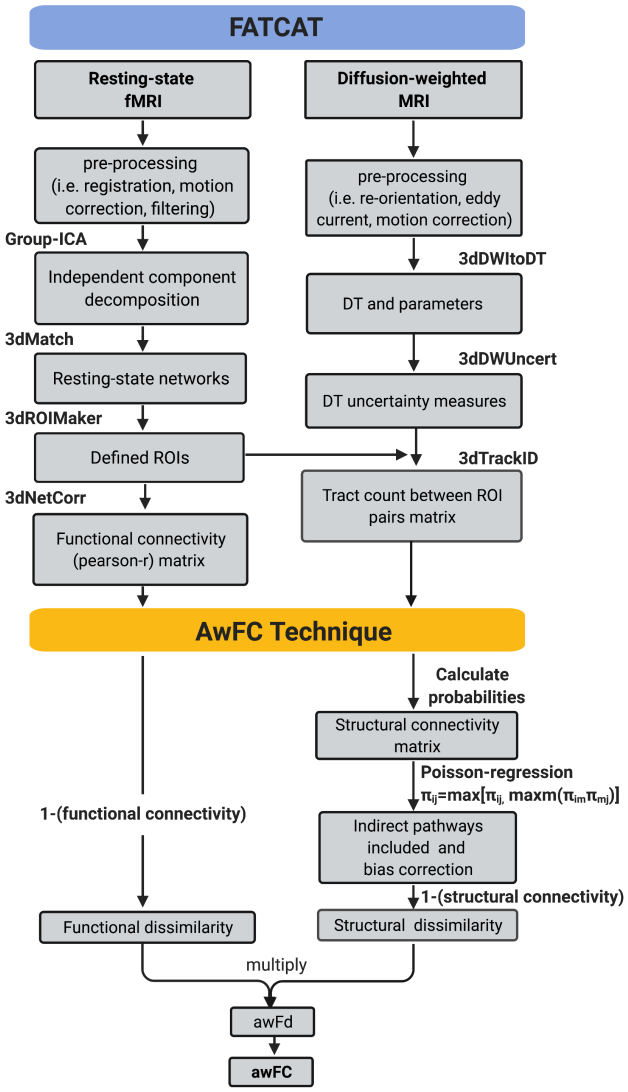

Fig.1 | FATCAT-awFC pipeline. This is a two-stage pipeline, when combined; result in a more straightforward approach for combining fMRI and DTI. The first stage is the 'Functional and Tractographic Connectivity Analysis Toolbox' (FATCAT) pipeline. The outputs include: functional connectivity (derived from fMRI) and the number of tracts (derived from DTI). The second stage of the pipeline is known as the anatomically weighted functional connectivity (awFC), which processes the output of FATCAT to produce the anatomically

.

weighted functional connectivity measure (awFC measure). Note: fMRI = Functional magnetic resonance imaging, DTI = Diffusion tensor imaging, DT = diffusion tensor, ICA = Independent component analysis, ROIs = Regions of interest, SC = Structural connectivity, FC = Functional connectivity, awFd = Anatomically weighted functional dissimilarity, awFC = Anatomically weighted functional connectivity, set of AFNI commands = (3dMatch, 3dROIMaker, 3dNetCorr, 3dDWItoDT, 3dDWUncert, 3dTrackID).

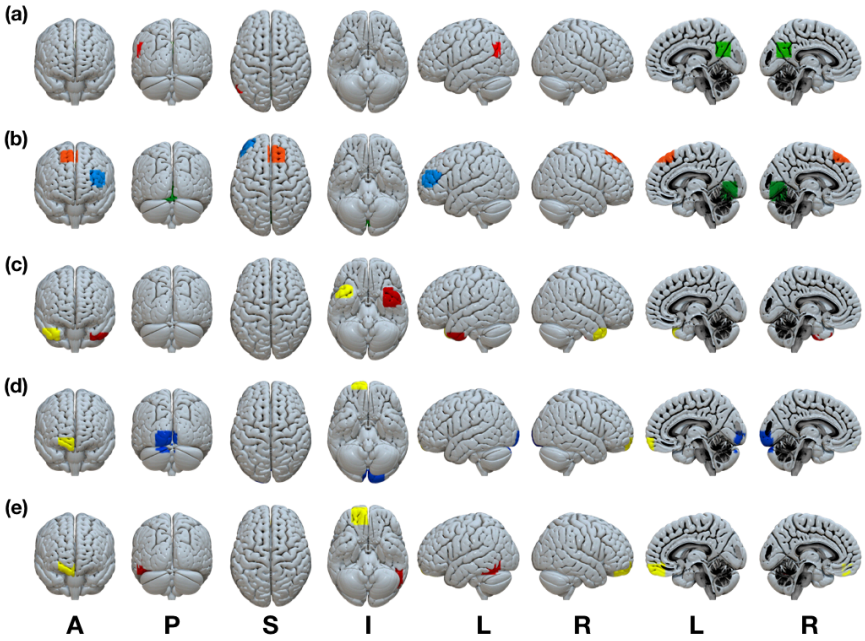

Fig. 2 | Statistically significant anatomically weighted functional connectivity group differences between brain regions are displayed for each network. Isolated brain regions were defined using the FATCAT command *3dROIMaker*. Each colour represents a different ROI for each network a) DMN, green ROI= posterior cingulate cortex, red ROI = left angular gyrus b) FPN, blue ROI = left inferior frontal gyrus, orange ROI = right superior frontal gyrus, green ROI = lingual gyrus/cerebellum c) LIM, yellow ROI= right superior temporal gyrus, red

ROI = left superior temporal gyrus d) VAN, yellow ROI = right anterior orbitofrontal gyrus, blue ROI = left lingual gyrus/cuneus e) DAN, yellow ROI = right posterior orbitofrontal gyrus, red ROI = left inferior temporal gyrus . ROI = region of interest, DMN = default mode network, FPN = frontoparietal network, VAN = ventral attention network, DAN = dorsal attention network. Anatomical positions, A = anterior view, P = posterior view, S = superior view, I = inferior view, L = left view, R= right view.

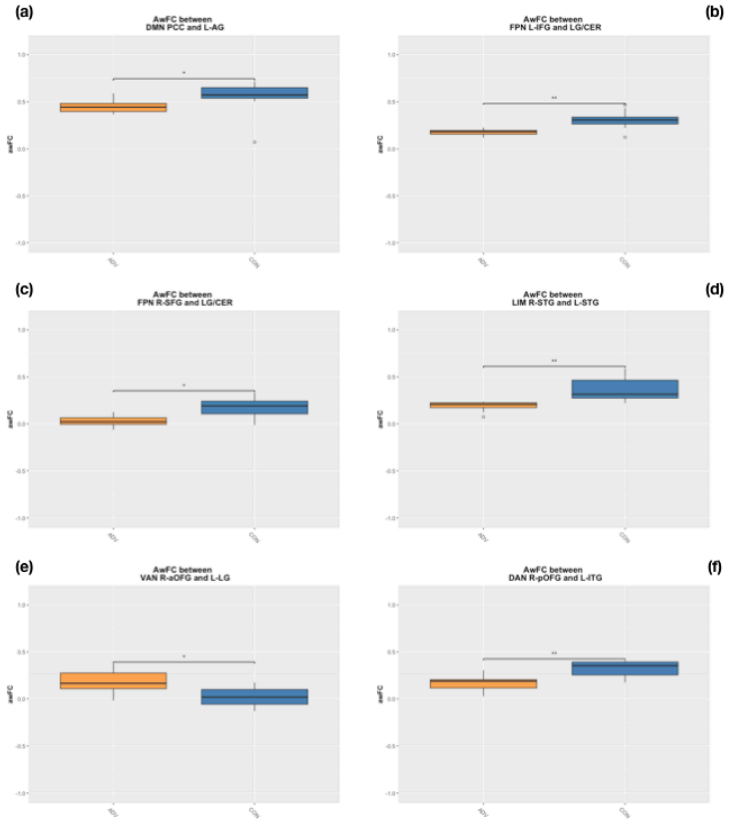

Fig. 3 | Boxplots demonstrate the anatomically weighted functional connectivity strength in children with pre/postnatal adversity (orange boxes) compared to children with no pre/postnatal adversity (blue boxes). Significant differences between ADV and CON are shown within the a) DMN between the PCC and L-AG b) FPN between the L-IFG and the LG/CER c) FPN between the R-SFG and the LG/CER d) LIM between the R-STG and the

L-STG e) VAN between the R-aOFG and L-LG f) DAN between the R-pOFG and L-ITG.

Note: ADV= Children exposed to high pre/postnatal adversity, CON = Control, DMN = Default mode network, FPN = Frontoparietal Network, LIM = Limbic network, VAN = Ventral Attention Network, DAN = Dorsal Attention Network, L- = Left, R- = Right, IFG = Inferior frontal gyrus, LG/CER = Lingual gyrus / Cerebellum, SFG = Superior frontal gyrus, STG = superior temporal gyrus, aOFG = anterior orbitofrontal gyrus, LG = Lingual gyrus, pOFG = posterior orbitofrontal gyrus, ITG = Inferior temporal gyrus.

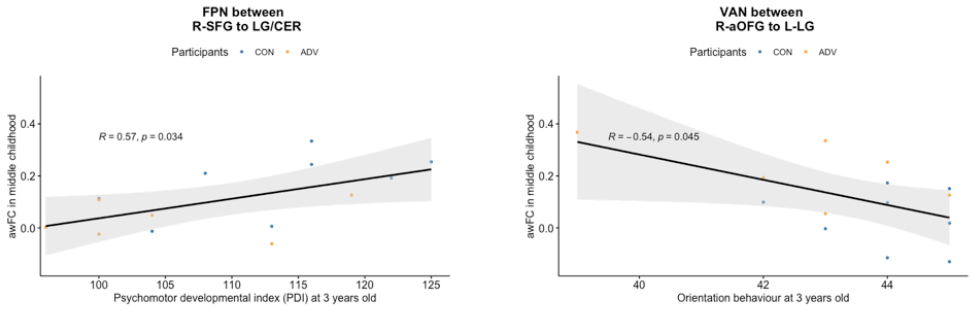

Fig. 4 | Linear regression to demonstrate the relationship between a) psychomotor developmental index (PDI) at age three and awFC within the FPN between the R-SFG and the LG/CER in middle childhood b) orientation behavior at 3 years old and awFC within the VAN between the R-aOFG and L-LG in middle childhood. Significant associations were found between both PDI and orientation behaviour at age 3 and the awFC in middle childhood. Note: FPN = frontoparietal network, VAN = ventral attention network, R-SFG = right superior frontal gyrus, LG/CER = lingual gyrus/cerebellum, R-aOFG = right anterior orbitofrontal gyrus, L-LG = left lingual gyrus, ADV= Children exposed to high pre/postnatal adversity, CON = Controls.

.

4.6 References

Agrati, D., Browne, D., Jonas, W., Meaney, M., Atkinson, L., Steiner, M., Fleming, A. S., & on behalf of the MAVAN research team. (2015). Maternal anxiety from pregnancy to 2 years postpartum: Transactional patterns of maternal early adversity and child temperament. *Archives of Women's Mental Health*, *18*(5), 693–705. https://doi.org/10.1007/s00737-014-0491-y

Almond, P. (2009). Postnatal depression: A global public health perspective. *Perspectives in Public Health*, *129*(5), 221–227. https://doi.org/10.1177/1757913909343882

Amedi, A., Malach, R., Hendler, T., Peled, S., & Zohary, E. (2001). Visuo-haptic object-related activation in the ventral visual pathway. *Nature Neuroscience*, *4*(3), 324–330. https://doi.org/10.1038/85201

Andersen, S. L. (2003). Trajectories of brain development: Point of vulnerability or window of opportunity? *Neuroscience & Biobehavioral Reviews*, *27*(1), 3–18. https://doi.org/10.1016/S0149-7634(03)00005-8

Anderson, L. D. (1939). The Predictive Value of Infancy Tests in Relation to Intelligence at Five Years. *Child Development*, *10*(3), 203. https://doi.org/10.2307/1125763

Arnsten, A. F. T. (2009). Stress signalling pathways that impair prefrontal cortex structure and function. *Nature Reviews. Neuroscience*, *10*(6), 410–422. https://doi.org/10.1038/nrn2648

Ashtari, M. (2012). Anatomy and functional role of the inferior longitudinal fasciculus: A search that has just begun. *Developmental Medicine & Child Neurology*, *54*(1), 6–7. https://doi.org/10.1111/j.1469-8749.2011.04122.x

Astafiev, S. V., Stanley, C. M., Shulman, G. L., & Corbetta, M. (2004). Extrastriate body area in human occipital cortex responds to the performance of motor actions. *Nature Neuroscience*, *7*(5), 542–548. https://doi.org/10.1038/nn1241

Axer, H., Klingner, C. M., & Prescher, A. (2013). Fiber anatomy of dorsal and ventral language streams. *Brain and Language*, *127*(2), 192–204. https://doi.org/10.1016/j.bandl.2012.04.015

Ayyash, S., Davis, A., Alders, Gésine, MacQueen, G., Strother, S., Hassel, Stefanie, Zamyadi, M., Arnott, S., Harris, J., Lam, R., Milev, R., Müller, D., Kennedy, S., Frey, B., Minuzzi, L., Rotzinger, S., & Hall, G. (2021). *Exploring Brain Connectivity Changes in Major Depressive Disorder Using Functional-Structural Data Fusion: A CAN-BIND-1 Study*.

Barnea-Goraly, N., Menon, V., Eckert, M., Tamm, L., Bammer, R., Karchemskiy, A., Dant, C. C., & Reiss, A. L. (2005). White Matter Development During Childhood and Adolescence: A Cross-sectional Diffusion Tensor Imaging Study. *Cerebral Cortex*, *15*(12), 1848–1854. https://doi.org/10.1093/cercor/bhi062

Bayley, N. (1993). *Bayley Scales of Infant Development, Second Edition* (2nd Edition). Psychological Corporation.

Beckmann, C. F., DeLuca, M., Devlin, J. T., & Smith, S. M. (2005). Investigations into resting-state connectivity using independent component analysis. *Philosophical Transactions of the Royal Society of London. Series B, Biological Sciences*, *360*(1457), 1001–1013. https://doi.org/10.1098/rstb.2005.1634

Beckmann, C. F., & Smith, S. M. (2004). Probabilistic independent component analysis for functional magnetic resonance imaging. *IEEE Transactions on Medical Imaging*, *23*(2), 137–152. https://doi.org/10.1109/TMI.2003.822821

Bergh, B. R. H. V. den, Dahnke, R., & Mennes, M. (2018). Prenatal stress and the developing brain: Risks for neurodevelopmental disorders. *Development and Psychopathology*, *30*(3), 743–762. https://doi.org/10.1017/S0954579418000342

Bernstein, D. P., & Fink, L. (1998). *CTQ: Childhood Trauma Questionnaire: A retrospective self-report manual.* San Antonio, TX: Psychological Corp.

Besharov, D. J., & Laumann, L. A. (1997). Don't call it child abuse if It's really poverty. *Journal of Children and Poverty*, *3*(1), 5–36. https://doi.org/10.1080/10796129708412203

Biswal, B., Zerrin Yetkin, F., Haughton, V. M., & Hyde, J. S. (1995). Functional connectivity in the motor cortex of resting human brain using echo-planar mri. *Magnetic Resonance in Medicine*, *34*(4), 537–541. https://doi.org/10.1002/mrm.1910340409

Black, M. M., Hess, C. R., & Berenson-Howard, J. (2000). Toddlers from Low-Income Families Have Below Normal Mental, Motor, and Behavior Scores on the Revised Bayley Scales. *Journal of Applied Developmental Psychology*, *21*(6), 655–666. https://doi.org/10.1016/S0193-3973(00)00059-9

Blanz, B., Schmidt, M. H., & Esser, G. (1991). Familial adversities and child psychiatric disorders. *Journal of Child Psychology and Psychiatry, and Allied Disciplines*, *32*(6), 939–950. https://doi.org/10.1111/j.1469-7610.1991.tb01921.x

Bolsinger, J., Seifritz, E., Kleim, B., & Manoliu, A. (2018). Neuroimaging Correlates of Resilience to Traumatic Events—A Comprehensive Review. *Frontiers in Psychiatry*, *9*. https://doi.org/10.3389/fpsyt.2018.00693

Bowman, F. D., Zhang, L., Derado, G., & Chen, S. (2012). Determining Functional Connectivity using fMRI Data with Diffusion-Based Anatomical Weighting. *NeuroImage*, *62*(3), 1769–1779. https://doi.org/10.1016/j.neuroimage.2012.05.032

Boyd, D., & Bee, H. (2012). *Lifespan Development* (6th ed.). Pearson. https://www.pearson.com/us/higher-education/product/Boyd-Lifespan-Development-6th-Edition/9780205037520.html

Boyd, L. A. C., Msall, M. E., O'Shea, T. M., Allred, E. N., Hounshell, G., & Leviton, A. (2013). Social-emotional delays at 2 years in extremely low gestational age survivors: Correlates of impaired orientation/engagement and emotional regulation. *Early Human Development*, *89*(12), 925–930. https://doi.org/10.1016/j.earlhumdev.2013.09.019

Bruggink, J. L. M., Van Braeckel, K. N., & Bos, A. F. (2010). The Early Motor Repertoire of Children Born Preterm Is Associated With Intelligence at School Age. *PEDIATRICS*, *125*(6), e1356–e1363. https://doi.org/10.1542/peds.2009-2117

Bullmore, E. (2019). Cortical Thickness and Connectivity in Schizophrenia. *American Journal of Psychiatry*, *176*(7), 505–506. https://doi.org/10.1176/appi.ajp.2019.19050509

Burke, N. J., Hellman, J. L., Scott, B. G., Weems, C. F., & Carrion, V. G. (2011). The impact of adverse childhood experiences on an urban pediatric population. *Child Abuse & Neglect*, *35*(6), 408–413. https://doi.org/10.1016/j.chiabu.2011.02.006

Bushnell, E. W., & Boudreau, J. P. (1993). Motor Development and the Mind: The Potential Role of Motor Abilities as a Determinant of Aspects of Perceptual Development. *Child Development*, *64*(4), 1005. https://doi.org/10.2307/1131323

Buss, C., Entringer, S., Moog, N. K., Toepfer, P., Fair, D. A., Simhan, H. N., Heim, C. M., & Wadhwa, P. D. (2017). Intergenerational Transmission of Maternal Childhood Maltreatment Exposure: Implications for Fetal Brain Development. *Journal of the American Academy of Child & Adolescent Psychiatry*, *56*(5), 373–382. https://doi.org/10.1016/j.jaac.2017.03.001

Butcher, P. R., van Braeckel, K., Bouma, A., Einspieler, C., Stremmelaar, E. F., & Bos, A. F. (2009). The quality of preterm infants' spontaneous movements: An early indicator of intelligence and behaviour at school age. *Journal of Child Psychology and Psychiatry*, *50*(8), 920–930. https://doi.org/10.1111/j.1469-7610.2009.02066.x

Casey, B. J., Giedd, J. N., & Thomas, K. M. (2000). Structural and functional brain development and its relation to cognitive development. *Biological Psychology*, *54*(1), 241–257. https://doi.org/10.1016/S0301-0511(00)00058-2

Casper, R. C., Fleisher, B. E., Lee-Ancajas, J. C., Gilles, A., Gaylor, E., DeBattista, A., & Hoyme, H. E. (2003). Follow-up of children of depressed mothers exposed or not exposed to antidepressant drugs during pregnancy. *The Journal of Pediatrics*, *142*(4), 402–408. https://doi.org/10.1067/mpd.2003.139

Caspi, A. (2000). The child is father of the man: Personality continuities from childhood to adulthood. *Journal of Personality and Social Psychology*, *78*(1), 158–172. https://doi.org/10.1037/0022-3514.78.1.158

Caspi, A., Harrington, H., Milne, B., Amell, J. W., Theodore, R. F., & Moffitt, T. E. (2003). Children's behavioral styles at age 3 are linked to their adult personality traits at age 26. *Journal of Personality*, *71*(4), 495–513. https://doi.org/10.1111/1467-6494.7104001

Caspi, A., & Silva, P. A. (1995). Temperamental Qualities at Age Three Predict Personality Traits in Young Adulthood: Longitudinal Evidence from a Birth Cohort. *Child Development*, *66*(2), 486–498. https://doi.org/10.2307/1131592

Catani, M., & Thiebautdeschotten, M. (2008). A diffusion tensor imaging tractography atlas for virtual in vivo dissections. *Cortex*, *44*(8), 1105–1132. https://doi.org/10.1016/j.cortex.2008.05.004

Caverzasi, E., Papinutto, N., Amirbekian, B., Berger, M. S., & Henry, R. G. (2014). Q-Ball of Inferior Fronto-Occipital Fasciculus and Beyond. *PLOS ONE*, *9*(6), e100274. https://doi.org/10.1371/journal.pone.0100274

Collishaw, S., Dunn, J., O'Connor, T. G., Golding, J., & THE AVON LONGITUDINAL STUDY OF PARENTS AND CHILDREN STUDY TEAM. (2007). Maternal childhood abuse and offspring adjustment over time. *Development and Psychopathology*, *19*(02). https://doi.org/10.1017/S0954579407070186

Corbetta, M., Patel, G., & Shulman, G. L. (2008). The Reorienting System of the Human Brain: From Environment to Theory of Mind. *Neuron*, *58*(3), 306–324. https://doi.org/10.1016/j.neuron.2008.04.017

Corbetta, M., & Shulman, G. L. (2002). Control of goal-directed and stimulus-driven attention in the brain. *Nature Reviews Neuroscience*, *3*(3), 201–215. https://doi.org/10.1038/nrn755

Courtney, S. M. (1998). An Area Specialized for Spatial Working Memory in Human Frontal Cortex. *Science*, *279*(5355), 1347–1351. https://doi.org/10.1126/science.279.5355.1347

Dadi, A. F., Miller, E. R., Bisetegn, T. A., & Mwanri, L. (2020). Global burden of antenatal depression and its association with adverse birth outcomes: An umbrella review. *BMC Public Health*, *20*(1), 173. https://doi.org/10.1186/s12889-020-8293-9

Davis, A. D., Hassel, S., Arnott, S. R., Harris, J., Lam, R. W., Milev, R., Rotzinger, S., Zamyadi, M., Frey, B. N., Minuzzi, L., Strother, S. C., MacQueen, G. M., Kennedy, S., & Hall, G. B. (2019). White Matter Indices of Medication Response in Major Depression: A Diffusion Tensor Imaging Study. *Biological Psychiatry: Cognitive Neuroscience and Neuroimaging*, *4*(10), 913–924. https://doi.org/10.1016/j.bpsc.2019.05.016

Davis, E. P., Hankin, B. L., Glynn, L. M., Head, K., Kim, D. J., & Sandman, C. A. (2020). Prenatal Maternal Stress, Child Cortical Thickness, and Adolescent Depressive Symptoms. *Child Development*, *91*(2), e432–e450. https://doi.org/10.1111/cdev.13252

Davis, E. P., Head, K., Buss, C., & Sandman, C. A. (2017). Prenatal maternal cortisol concentrations predict neurodevelopment in middle childhood. *Psychoneuroendocrinology*, *75*, 56–63. https://doi.org/10.1016/j.psyneuen.2016.10.005

Davis, E. P., & Narayan, A. J. (2020). Pregnancy as a period of risk, adaptation, and resilience for mothers and infants. *Development and Psychopathology*, *32*(5), 1625–1639. https://doi.org/10.1017/S0954579420001121

Dean, D. C., Planalp, E. M., Wooten, W., Kecskemeti, S. R., Adluru, N., Schmidt, C. K., Frye, C., Birn, R. M., Burghy, C. A., Schmidt, N. L., Styner, M. A., Short, S. J., Kalin, N. H., Goldsmith, H. H., Alexander, A. L., & Davidson, R. J. (2018). Association of Prenatal Maternal Depression and Anxiety Symptoms With Infant White Matter Microstructure. *JAMA Pediatrics*, *172*(10), 973. https://doi.org/10.1001/jamapediatrics.2018.2132

Deater-Deckard, K., Dodge, K. A., Bates, J. E., & Pettit, G. S. (1998). Multiple risk factors in the development of externalizing behavior problems: Group and individual differences. *Development and Psychopathology*, *10*(3), 469–493. https://doi.org/10.1017/s0954579498001709

DeFries, J. C., Plomin, R., & Fulker, D. W. (1994). *Nature and nurture during middle childhood*. Cambridge, MA: Blackwell Publishing.

Dégeilh, F., Bernier, A., Leblanc, É., Daneault, V., & Beauchamp, M. H. (2018). Quality of maternal behaviour during infancy predicts functional connectivity between default mode

network and salience network 9 years later. *Developmental Cognitive Neuroscience*, *34*, 53–62. https://doi.org/10.1016/j.dcn.2018.06.003

DeSocio, J. E. (2018). Epigenetics, maternal prenatal psychosocial stress, and infant mental health. *Archives of Psychiatric Nursing*, *32*(6), 901–906. https://doi.org/10.1016/j.apnu.2018.09.001

Dick, A. S., & Tremblay, P. (2012). Beyond the arcuate fasciculus: Consensus and controversy in the connectional anatomy of language. *Brain*, *135*(12), 3529–3550. https://doi.org/10.1093/brain/aws222

DiLalla, L. F., Thompson, L. A., Plomin, R., Phillips, K., Fagan, J. F., Haith, M. M., Cyphers, L. H., & Fulker, D. W. (1990). Infant predictors of preschool and adult IQ: A study of infant twins and their parents. *Developmental Psychology*, *26*(5), 759–769. https://doi.org/10.1037/0012-1649.26.5.759

Doricchi, F., Thiebautdeschotten, M., Tomaiuolo, F., & Bartolomeo, P. (2008). White matter (dis)connections and gray matter (dys)functions in visual neglect: Gaining insights into the brain networks of spatial awareness. *Cortex*, *44*(8), 983–995. https://doi.org/10.1016/j.cortex.2008.03.006

Dosenbach, N. U. F., Nardos, B., Cohen, A. L., Fair, D. A., Power, J. D., Church, J. A., Nelson, S. M., Wig, G. S., Vogel, A. C., Lessov-Schlaggar, C. N., Barnes, K. A., Dubis, J. W., Feczko, E., Coalson, R. S., Pruett, J. R., Barch, D. M., Petersen, S. E., & Schlaggar, B. L. (2010). Prediction of Individual Brain Maturity Using fMRI. *Science*, *329*(5997), 1358–1361. https://doi.org/10.1126/science.1194144

Dubois, J., Kostovic, I., & Judas, M. (2015). Development of structural and functional connectivity. In *Brain Mapping: An Encyclopedic Reference* (Vol. 2, pp. 423–437). https://hal.archives-ouvertes.fr/hal-02436274

Ebbesson, S. O. E. (1984). Evolution and ontogeny of neural circuits. *Behavioral and Brain Sciences*, *7*(3), 321–331. https://doi.org/10.1017/S0140525X00018379

Elgar, F. J., Curtis, L. J., McGrath, P. J., Waschbusch, D. A., & Stewart, S. H. (2003). Antecedent-Consequence Conditions in Maternal Mood and Child Adjustment: A Four-Year Cross-Lagged Study. *Journal of Clinical Child & Adolescent Psychology*, *32*(3), 362–374. https://doi.org/10.1207/S15374424JCCP3203_05

Fair, D. A., Cohen, A. L., Dosenbach, N. U. F., Church, J. A., Miezin, F. M., Barch, D. M., Raichle, M. E., Petersen, S. E., & Schlaggar, B. L. (2008). The maturing architecture of the brain's default network. *Proceedings of the National Academy of Sciences of the United States of America*, *105*(10), 4028–4032. https://doi.org/10.1073/pnas.0800376105

Fair, D. A., Cohen, A. L., Power, J. D., Dosenbach, N. U. F., Church, J. A., Miezin, F. M., Schlaggar, B. L., & Petersen, S. E. (2009). Functional Brain Networks Develop from a "Local to Distributed" Organization. *PLOS Computational Biology*, *5*(5), e1000381. https://doi.org/10.1371/journal.pcbi.1000381

Fair, D. A., Dosenbach, N. U. F., Church, J. A., Cohen, A. L., Brahmbhatt, S., Miezin, F. M., Barch, D. M., Raichle, M. E., Petersen, S. E., & Schlaggar, B. L. (2007). Development of distinct control networks through segregation and integration. *Proceedings of the National Academy of Sciences of the United States of America*, *104*(33), 13507–13512. https://doi.org/10.1073/pnas.0705843104

Farah, R., Greenwood, P., Dudley, J., Hutton, J., Ammerman, R. T., Phelan, K., Holland, S., & Horowitz-Kraus, T. (2020). Maternal depression is associated with altered functional connectivity between neural circuits related to visual, auditory, and cognitive processing during stories listening in preschoolers. *Behavioral and Brain Functions : BBF*, *16*. https://doi.org/10.1186/s12993-020-00167-5

Farber, E. A., Vaughn, B., & Egeland, B. (1981). The relationship of prenatal maternal anxiety to infant behavior and mother-infant interaction during the first six months of life. *Early Human Development*, *5*(3), 267–277. https://doi.org/10.1016/0378-3782(81)90034-7

Felitti, V. J., Anda, R. F., Nordenberg, D., Williamson, D. F., Spitz, A. M., Edwards, V., Koss, M. P., & Marks, J. S. (1998). Relationship of childhood abuse and household dysfunction to many of the leading causes of death in adults. The Adverse Childhood Experiences (ACE) Study. *American Journal of Preventive Medicine*, *14*(4), 245–258. https://doi.org/10.1016/s0749-3797(98)00017-8

Fernandez-Miranda, J. C., Pathak, S., Engh, J., Jarbo, K., Verstynen, T., Yeh, F.-C., Wang, Y., Mintz, A., Boada, F., Schneider, W., & Friedlander, R. (2012). High-definition fiber tractography of the human brain: Neuroanatomical validation and neurosurgical applications. *Neurosurgery*, *71*(2), 430–453. https://doi.org/10.1227/NEU.0b013e3182592faa

Folger, A. T., Eismann, E. A., Stephenson, N. B., Shapiro, R. A., Macaluso, M., Brownrigg, M. E., & Gillespie, R. J. (2018). Parental Adverse Childhood Experiences and Offspring Development at 2 Years of Age. *Pediatrics*, *141*(4). https://doi.org/10.1542/peds.2017-2826

Fox, C., Iaria, G., & Barton, J. (2008). Disconnection in prosopagnosia and face processing. *Cortex*, *44*(8), 996–1009. https://doi.org/10.1016/j.cortex.2008.04.003

Fridriksson, J., den Ouden, D.-B., Hillis, A. E., Hickok, G., Rorden, C., Basilakos, A., Yourganov, G., & Bonilha, L. (2018). Anatomy of aphasia revisited. *Brain*, *141*(3), 848–862. https://doi.org/10.1093/brain/awx363

Galbally, M., Lewis, A. J., & Buist, A. (2011). Developmental outcomes of children exposed to antidepressants in pregnancy. *The Australian and New Zealand Journal of Psychiatry*, *45*(5), 393–399. https://doi.org/10.3109/00048674.2010.549995

Garon-Bissonnette, J., Duguay, G., Lemieux, R., Dubois-Comtois, K., & Berthelot, N. (2021). Maternal childhood abuse and neglect predicts offspring development in early childhood: The roles of reflective functioning and child sex. *Child Abuse & Neglect*, 105030. https://doi.org/10.1016/j.chiabu.2021.105030

Giedd, J. N., Snell, J. W., Lange, N., Rajapakse, J. C., Casey, B. J., Kozuch, P. L., Vaituzis, A. C., Vauss, Y. C., Hamburger, S. D., Kaysen, D., & Rapoport, J. L. (1996). Quantitative Magnetic Resonance Imaging of Human Brain Development: Ages 4–18. *Cerebral Cortex*, *6*(4), 551–559. https://doi.org/10.1093/cercor/6.4.551

Glickstein, M. (2000). How are visual areas of the brain connected to motor areas for the sensory guidance of movement? *Trends in Neurosciences*, *23*(12), 613–617. https://doi.org/10.1016/S0166-2236(00)01681-7

Golding, J., Emmett, P., Iles-Caven, Y., Steer, C., & Lingam, R. (2014). A review of environmental contributions to childhood motor skills. *Journal of Child Neurology*, *29*(11), 1531–1547. https://doi.org/10.1177/0883073813507483

Goodale, M. A., & Milner, A. D. (1992). Separate visual pathways for perception and action. *Trends in Neurosciences*, *15*(1), 20–25. https://doi.org/10.1016/0166-2236(92)90344-8

Goto, M., Abe, O., Miyati, T., Yamasue, H., Gomi, T., & Takeda, T. (2016). Head Motion and Correction Methods in Resting-state Functional MRI. *Magnetic Resonance in Medical Sciences: MRMS: An Official Journal of Japan Society of Magnetic Resonance in Medicine*, *15*(2), 178–186. https://doi.org/10.2463/mrms.rev.2015-0060

Gottfried, A. W. (2013). *Home Environment and Early Cognitive Development: Longitudinal Research*. Academic Press.

Grayson, D. S., & Fair, D. A. (2017). Development of large-scale functional networks from birth to adulthood: A guide to the neuroimaging literature. *NeuroImage*, *160*, 15–31. https://doi.org/10.1016/j.neuroimage.2017.01.079

Grizenko, N., Shayan, Y. R., Polotskaia, A., Ter-Stepanian, M., & Joober, R. (2008). Relation of maternal stress during pregnancy to symptom severity and response to treatment in children with ADHD. *Journal of Psychiatry & Neuroscience : JPN*, *33*(1), 10–16.

Grunewaldt, K. H., Fjørtoft, T., Bjuland, K. J., Brubakk, A.-M., Eikenes, L., Håberg, A. K., Løhaugen, G. C. C., & Skranes, J. (2014). Follow-up at age 10years in ELBW children—Functional outcome, brain morphology and results from motor assessments in infancy. *Early Human Development*, *90*(10), 571–578. https://doi.org/10.1016/j.earlhumdev.2014.07.005

Hanley, G. E., Brain, U., & Oberlander, T. F. (2013). Infant developmental outcomes following prenatal exposure to antidepressants, and maternal depressed mood and positive affect. *Early Human Development*, *89*(8), 519–524. https://doi.org/10.1016/j.earlhumdev.2012.12.012

Hanson, J., Adluru, N., Chung, M., Alexander, A., Davidson, R., & Pollak, S. (2013). Early neglect is associated with alterations in white matter integrity and cognitive functioning. *Child Development*, *84*(5). https://doi.org/10.1111/cdev.12069

Hanson, J. L., Chung, M. K., Avants, B. B., Shirtcliff, E. A., Gee, J. C., Davidson, R. J., & Pollak, S. D. (2010). Early Stress Is Associated with Alterations in the Orbitofrontal Cortex: A Tensor-Based Morphometry Investigation of Brain Structure and Behavioral Risk. *The Journal of Neuroscience*, *30*(22), 7466–7472. https://doi.org/10.1523/JNEUROSCI.0859-10.2010

Hart, B., & Risley, T. R. (1992). American parenting of language-learning children: Persisting differences in family-child interactions observed in natural home environments. *Developmental Psychology*, *28*(6), 1096–1105. https://doi.org/10.1037/0012-1649.28.6.1096

Hay, R. E., Reynolds, J. E., Grohs, M. N., Paniukov, D., Giesbrecht, G. F., Letourneau, N., Dewey, D., & Lebel, C. (2020). Amygdala-Prefrontal Structural Connectivity Mediates the Relationship between Prenatal Depression and Behavior in Preschool Boys. *The Journal of Neuroscience*, *40*(36), 6969–6977. https://doi.org/10.1523/JNEUROSCI.0481-20.2020

Hellemans, K. G. C., Sliwowska, J. H., Verma, P., & Weinberg, J. (2010). Prenatal alcohol exposure: Fetal programming and later life vulnerability to stress, depression and anxiety disorders. *Neuroscience & Biobehavioral Reviews*, *34*(6), 791–807. https://doi.org/10.1016/j.neubiorev.2009.06.004

Hendrix, C. L., Dilks, D. D., McKenna, B. G., Dunlop, A. L., Corwin, E. J., & Brennan, P. A. (2021). Maternal Childhood Adversity Associates With Frontoamygdala Connectivity in

Neonates. *Biological Psychiatry: Cognitive Neuroscience and Neuroimaging*, *6*(4), 470–478. https://doi.org/10.1016/j.bpsc.2020.11.003

Hickok, G., & Poeppel, D. (2007). The cortical organization of speech processing. *Nature Reviews Neuroscience*, *8*(5), 393–402. https://doi.org/10.1038/nrn2113

Honey, C. J., Sporns, O., Cammoun, L., Gigandet, X., Thiran, J. P., Meuli, R., & Hagmann, P. (2009). Predicting human resting-state functional connectivity from structural connectivity. *Proceedings of the National Academy of Sciences*, *106*(6), 2035–2040. https://doi.org/10.1073/pnas.0811168106

Honey, C. J., Thivierge, J.-P., & Sporns, O. (2010). Can structure predict function in the human brain? *NeuroImage*, *52*(3), 766–776. https://doi.org/10.1016/j.neuroimage.2010.01.071

Jbabdi, S., & Johansen-Berg, H. (2011). Tractography: Where do we go from here? *Brain Connectivity*, *1*(3), 169–183. https://doi.org/10.1089/brain.2011.0033

Jenkinson, M., Beckmann, C. F., Behrens, T. E. J., Woolrich, M. W., & Smith, S. M. (2012). FSL. *NeuroImage*, *62*(2), 782–790. https://doi.org/10.1016/j.neuroimage.2011.09.015

Jessica Damoiseaux, & Greicius, M. (2009). Greater than the sum of its parts: A review of studies combining structural connectivity and resting-state functional connectivity. *Brain Structure & Function*, *213*(6), 525–533. https://doi.org/10.1007/s00429-009-0208-6

Johnson, M. H. (2001). Functional brain development in humans. *Nature Reviews Neuroscience*, *2*(7), 475–483. https://doi.org/10.1038/35081509

Jolles, D. D., van Buchem, M. A., Crone, E. A., & Rombouts, S. A. R. B. (2011). A Comprehensive Study of Whole-Brain Functional Connectivity in Children and Young Adults. *Cerebral Cortex*, *21*(2), 385–391. https://doi.org/10.1093/cercor/bhq104

Keenan-Miller, D., Hammen, C., & Brennan, P. A. (2010). Mediators of Aggression Among Young Adult Offspring of Depressed Mothers. *Journal of Abnormal Psychology*, *119*(4), 836–849. https://doi.org/10.1037/a0021079

Klingler, J., & Gloor, P. (1960). The connections of the amygdala and of the anterior temporal cortex in the human brain. *Journal of Comparative Neurology*, *115*(3), 333–369. https://doi.org/10.1002/cne.901150305

Konrad, K., Neufang, S., Thiel, C. M., Specht, K., Hanisch, C., Fan, J., Herpertz-Dahlmann, B., & Fink, G. R. (2005). Development of attentional networks: An fMRI study with children and adults. *NeuroImage*, *28*(2), 429–439. https://doi.org/10.1016/j.neuroimage.2005.06.065

Krafft, C. E., Pierce, J. E., Schwarz, N. F., Chi, L., Weinberger, A. L., Schaeffer, D. J., Rodrigue, A. L., Camchong, J., Allison, J. D., Yanasak, N. E., Liu, T., Davis, C. L., & McDowell, J. E. (2014). An eight month randomized controlled exercise intervention alters resting state synchrony in overweight children. *Neuroscience*, *256*, 445–455. https://doi.org/10.1016/j.neuroscience.2013.09.052

Kravitz, D. J., Saleem, K. S., Baker, C. I., Ungerleider, L. G., & Mishkin, M. (2013). The ventral visual pathway: An expanded neural framework for the processing of object quality. *Trends in Cognitive Sciences*, *17*(1), 26–49. https://doi.org/10.1016/j.tics.2012.10.011

Kriegeskorte, N., Mur, M., & Bandettini, P. (2008). Representational Similarity Analysis – Connecting the Branches of Systems Neuroscience. *Frontiers in Systems Neuroscience*, *2*. https://doi.org/10.3389/neuro.06.004.2008

Langrock, A. M., Compas, B. E., Keller, G., Merchant, M. J., & Copeland, M. E. (2002). Coping With the Stress of Parental Depression: Parents' Reports of Children's Coping,

Emotional, and Behavioral Problems. *Journal of Clinical Child & Adolescent Psychology*, *31*(3), 312–324. https://doi.org/10.1207/S15374424JCCP3103_03

Larsson, M., & Montgomery, S. M. (2011). Maternal smoking during pregnancy and physical control and coordination among offspring. *Journal of Epidemiology and Community Health*, *65*(12), 1151–1158. https://doi.org/10.1136/jech.2008.085241

LeDoux, J. E. (2000). Emotion Circuits in the Brain. *Annual Review of Neuroscience*, *23*(1), 155–184. https://doi.org/10.1146/annurev.neuro.23.1.155

Lee, M. H., Smyser, C. D., & Shimony, J. S. (2013). Resting-state fMRI: A review of methods and clinical applications. *AJNR. American Journal of Neuroradiology*, *34*(10), 1866–1872. https://doi.org/10.3174/ajnr.A3263

Lemelin, J.-P., Tarabulsy, G. M., & Provost, M. A. (2006). Predicting Preschool Cognitive Development from Infant Temperament, Maternal Sensitivity, and Psychosocial Risk. *Merrill-Palmer Quarterly*, *52*(4), 779–806.

Letourneau, N., Dewey, D., Kaplan, B. J., Ntanda, H., Novick, J., Thomas, J. C., Deane, A. J., Leung, B., Pon, K., Giesbrecht, G. F., & the APrON Study Team. (2019). Intergenerational transmission of adverse childhood experiences via maternal depression and anxiety and moderation by child sex. *Journal of Developmental Origins of Health and Disease*, *10*(1), 88–99. https://doi.org/10.1017/S2040174418000648

Levitt, P. (2003). Structural and functional maturation of the developing primate brain. *The Journal of Pediatrics*, *143*(4, Supplement), 35–45. https://doi.org/10.1067/S0022-3476(03)00400-1

Li, F., He, N., Li, Y., Chen, L., Huang, X., Lui, S., Guo, L., Kemp, G. J., & Gong, Q. (2014). Intrinsic Brain Abnormalities in Attention Deficit Hyperactivity Disorder: A Resting-

State Functional MR Imaging Study. *Radiology*, *272*(2), 514–523. https://doi.org/10.1148/radiol.14131622

Little, R. E., Anderson, K. W., Ervin, C. H., Worthington-Roberts, B., & Clarren, S. K. (1989). Maternal alcohol use during breast-feeding and infant mental and motor development at one year. *The New England Journal of Medicine*, *321*(7), 425–430. https://doi.org/10.1056/NEJM198908173210703

Luna, B., Tervo-Clemmens, B., & Calabro, F. J. (2021). Considerations When Characterizing Adolescent Neurocognitive Development. *Biological Psychiatry*, *89*(2), 96–98. https://doi.org/10.1016/j.biopsych.2020.04.026

Lupien, S. J., McEwen, B. S., Gunnar, M. R., & Heim, C. (2009). Effects of stress throughout the lifespan on the brain, behaviour and cognition. *Nature Reviews Neuroscience*, *10*(6), 434–445. https://doi.org/10.1038/nrn2639

Lyons-Ruth, K., Zoll, D., Connell, D., & Grunebaum, H. U. (1986). The depressed mother and her one-year-old infant: Environment, interaction, attachment, and infant development. *New Directions for Child and Adolescent Development*, *1986*(34), 61–82. https://doi.org/10.1002/cd.23219863407

Madigan, S., Wade, M., Plamondon, A., Maguire, J. L., & Jenkins, J. M. (2017). Maternal Adverse Childhood Experience and Infant Health: Biomedical and Psychosocial Risks as Intermediary Mechanisms. *The Journal of Pediatrics*, *187*, 282-289.e1. https://doi.org/10.1016/j.jpeds.2017.04.052

Mah, V. K., & Ford-Jones, E. L. (2012). Spotlight on middle childhood: Rejuvenating the 'forgotten years.' *Paediatrics & Child Health*, *17*(2), 81–83.

Marie-Mitchell, A., & O'Connor, T. G. (2013). Adverse childhood experiences: Translating knowledge into identification of children at risk for poor outcomes. *Academic Pediatrics*, *13*(1), 14–19. https://doi.org/10.1016/j.acap.2012.10.006

Marsh, R., Gerber, A. J., & Peterson, B. S. (2008). Neuroimaging Studies of Normal Brain Development and Their Relevance for Understanding Childhood Neuropsychiatric Disorders. *Journal of the American Academy of Child and Adolescent Psychiatry*, *47*(11), 1233–1251. https://doi.org/10.1097/CHI.0b013e318185e703

Marshall, N. A., Marusak, H. A., Sala-Hamrick, K. J., Crespo, L. M., Rabinak, C. A., & Thomason, M. E. (2018). Socioeconomic disadvantage and altered corticostriatal circuitry in urban youth. *Human Brain Mapping*, *39*(5), 1982–1994. https://doi.org/10.1002/hbm.23978

Martin-Elkins, C. L., & Horel, J. A. (1992). Cortical afferents to behaviorally defined regions of the inferior temporal and parahippocampal gyri as demonstrated by WGA-HRP. *The Journal of Comparative Neurology*, *321*(2), 177–192. https://doi.org/10.1002/cne.903210202

Martino, J., Gabarrós, A., Deus, J., Juncadella, M., Acebes, J. J., Torres, A., & Pujol, J. (2011). Intrasurgical mapping of complex motor function in the superior frontal gyrus. *Neuroscience*, *179*, 131–142. https://doi.org/10.1016/j.neuroscience.2011.01.047

McDonald, S. W., Madigan, S., Racine, N., Benzies, K., Tomfohr, L., & Tough, S. (2019). Maternal adverse childhood experiences, mental health, and child behaviour at age 3: The all our families community cohort study. *Preventive Medicine*, *118*, 286–294. https://doi.org/10.1016/j.ypmed.2018.11.013

McDonnell, C. G., & Valentino, K. (2016). Intergenerational Effects of Childhood Trauma: Evaluating Pathways Among Maternal ACEs, Perinatal Depressive Symptoms, and Infant Outcomes. *Child Maltreatment*, *21*(4), 317–326. https://doi.org/10.1177/1077559516659556

Menon, V. (2013). Developmental pathways to functional brain networks: Emerging principles. *Trends in Cognitive Sciences*, *17*(12), 627–640. https://doi.org/10.1016/j.tics.2013.09.015

Miranda, J. K., de la Osa, N., Granero, R., & Ezpeleta, L. (2013). Maternal Childhood Abuse, Intimate Partner Violence, and Child Psychopathology: The Mediator Role of Mothers' Mental Health. *Violence Against Women*, *19*(1), 50–68. https://doi.org/10.1177/1077801212475337

Monk, C., Spicer, J., & Champagne, F. A. (2012). Linking prenatal maternal adversity to developmental outcomes in infants: The role of epigenetic pathways. *Development and Psychopathology*, *24*(4), 1361–1376. https://doi.org/10.1017/S0954579412000764

Muetzel, R. L., Blanken, L. M. E., Thijssen, S., van der Lugt, A., Jaddoe, V. W. V., Verhulst, F. C., Tiemeier, H., & White, T. (2016). Resting-state networks in 6-to-10 year old children. *Human Brain Mapping*, *37*(12), 4286–4300. https://doi.org/10.1002/hbm.23309

Muftuler, L. T., Davis, E. P., Buss, C., Solodkin, A., Su, M. Y., Head, K. M., Hasso, A. N., & Sandman, C. A. (2012). Development of white matter pathways in typically developing preadolescent children. *Brain Research*, *1466*, 33–43. https://doi.org/10.1016/j.brainres.2012.05.035

Murmu, M. S., Salomon, S., Biala, Y., Weinstock, M., Braun, K., & Bock, J. (2006). Changes of spine density and dendritic complexity in the prefrontal cortex in offspring of mothers

exposed to stress during pregnancy. *European Journal of Neuroscience*, *24*(5), 1477–1487. https://doi.org/10.1111/j.1460-9568.2006.05024.x

Murphy, A., Steele, M., Dube, S. R., Bate, J., Bonuck, K., Meissner, P., Goldman, H., & Steele, H. (2014). Adverse Childhood Experiences (ACEs) questionnaire and Adult Attachment Interview (AAI): Implications for parent child relationships. *Child Abuse & Neglect*, *38*(2), 224–233. https://doi.org/10.1016/j.chiabu.2013.09.004

Murphy, E. R., Norr, M., Strang, J. F., Kenworthy, L., Gaillard, W. D., & Vaidya, C. J. (2017). Neural Basis of Visual Attentional Orienting in Childhood Autism Spectrum Disorders. *Journal of Autism and Developmental Disorders*, *47*(1), 58–67. https://doi.org/10.1007/s10803-016-2928-9

Muzik, O., Chugani, D. C., Juhász, C., Shen, C., & Chugani, H. T. (2000). Statistical parametric mapping: Assessment of application in children. *NeuroImage*, *12*(5), 538–549. https://doi.org/10.1006/nimg.2000.0651

Nelson, V. L., & Richards, T. W. (1938). Studies in Mental Development: I. Performance on Gesell Items at Six Months and its Predictive Value for Performance on Mental Tests at two and Three Years. *The Pedagogical Seminary and Journal of Genetic Psychology*, *52*(2), 303–325. https://doi.org/10.1080/08856559.1938.10534318

Normand, M. T. L., Vaivre-Douret, L., & Delfosse, M. J. (1995). Language and motor development in pre-term children: Some questions. *Child: Care, Health and Development*, *21*(2), 119–133. https://doi.org/10.1111/j.1365-2214.1995.tb00414.x

O'Donnell, K. A., Gaudreau, H., Colalillo, S., Steiner, M., Atkinson, L., Moss, E., Goldberg, S., Karama, S., Matthews, S. G., Lydon, J. E., Silveira, P. P., Wazana, A. D., Levitan, R. D., Sokolowski, M. B., Kennedy, J. L., Fleming, A., & Meaney, M. J. (2014). The Maternal

Adversity, Vulnerability and Neurodevelopment Project: Theory and Methodology. *The Canadian Journal of Psychiatry*, *59*(9), 497–508. https://doi.org/10.1177/070674371405900906

O'Donnell, K., O'Connor, T. G., & Glover, V. (2009). Prenatal stress and neurodevelopment of the child: Focus on the HPA axis and role of the placenta. *Developmental Neuroscience*, *31*(4), 285–292. https://doi.org/10.1159/000216539

Öngür, D., & Price, J. L. (2000). The Organization of Networks within the Orbital and Medial Prefrontal Cortex of Rats, Monkeys and Humans. *Cerebral Cortex*, *10*(3), 206–219. https://doi.org/10.1093/cercor/10.3.206

Park, H.-J., & Friston, K. (2013). Structural and Functional Brain Networks: From Connections to Cognition. *Science*, *342*(6158), 1238411. https://doi.org/10.1126/science.1238411

Patel, A. X., Kundu, P., Rubinov, M., Jones, P. S., Vértes, P. E., Ersche, K. D., Suckling, J., & Bullmore, E. T. (2014). A wavelet method for modeling and despiking motion artifacts from resting-state fMRI time series. *NeuroImage*, *95*, 287–304. https://doi.org/10.1016/j.neuroimage.2014.03.012

Peterson, B. S. (1995). Neuroimaging in Child and Adolescent Neuropsychiatric Disorders. *Journal of the American Academy of Child & Adolescent Psychiatry*, *34*(12), 1560–1576. https://doi.org/10.1097/00004583-199512000-00006

Posner, J., Cha, J., Roy, A. K., Peterson, B. S., Bansal, R., Gustafsson, H. C., Raffanello, E., Gingrich, J., & Monk, C. (2016). Alterations in amygdala–prefrontal circuits in infants exposed to prenatal maternal depression. *Translational Psychiatry*, *6*(11), e935–e935. https://doi.org/10.1038/tp.2016.146

Posner, M. I., Rothbart, M. K., Sheese, B. E., & Voelker, P. (2012). Control networks and neuromodulators of early development. *Developmental Psychology*, *48*(3), 827–835. https://doi.org/10.1037/a0025530

Posner, M. I., Rothbart, M. K., Sheese, B. E., & Voelker, P. (2014). Developing Attention: Behavioral and Brain Mechanisms. *Advances in Neuroscience*, *2014*, e405094. https://doi.org/10.1155/2014/405094

Power, J. D., Barnes, K. A., Snyder, A. Z., Schlaggar, B. L., & Petersen, S. E. (2012). Spurious but systematic correlations in functional connectivity MRI networks arise from subject motion. *NeuroImage*, *59*(3), 2142–2154. https://doi.org/10.1016/j.neuroimage.2011.10.018

Pozzi, E., Vijayakumar, N., Byrne, M. L., Bray, K. O., Seal, M., Richmond, S., Zalesky, A., & Whittle, S. L. (2021). Maternal parenting behavior and functional connectivity development in children: A longitudinal fMRI study. *Developmental Cognitive Neuroscience*, *48*, 100946. https://doi.org/10.1016/j.dcn.2021.100946

R Core Team. (2018). *R: A Language and Environment for Statistical Computing*. https://www.r-project.org/

Rifkin-Graboi, A., Meaney, M. J., Chen, H., Bai, J., Hameed, W. B., Tint, M. T., Broekman, B. F. P., Chong, Y.-S., Gluckman, P. D., Fortier, M. V., & Qiu, A. (2015). Antenatal Maternal Anxiety Predicts Variations in Neural Structures Implicated in Anxiety Disorders in Newborns. *Journal of the American Academy of Child & Adolescent Psychiatry*, *54*(4), 313-321.e2. https://doi.org/10.1016/j.jaac.2015.01.013

Ronald, A., Pennell, C. E., & Whitehouse, A. J. O. (2011). Prenatal Maternal Stress Associated with ADHD and Autistic Traits in early Childhood. *Frontiers in Psychology*, *1*. https://doi.org/10.3389/fpsyg.2010.00223

Rosen, T. S., & Johnson, H. L. (1982). Children of methadone-maintained mothers: Follow-up to 18 months of age. *The Journal of Pediatrics*, *101*(2), 192–196. https://doi.org/10.1016/S0022-3476(82)80115-7

Rosenberg, B. M., Mennigen, E., Monti, M. M., & Kaiser, R. H. (2020). Functional Segregation of Human Brain Networks Across the Lifespan: An Exploratory Analysis of Static and Dynamic Resting-State Functional Connectivity. *Frontiers in Neuroscience*, *14*. https://doi.org/10.3389/fnins.2020.561594

Rothbart, M. K., Sheese, B. E., Rueda, M. R., & Posner, M. I. (2011). Developing Mechanisms of Self-Regulation in Early Life. *Emotion Review*, *3*(2), 207–213. https://doi.org/10.1177/1754073910387943

Rudrauf, D., Mehta, S., & Grabowski, T. (2008). Disconnection's renaissance takes shape: Formal incorporation in group-level lesion studies. *Cortex*, *44*(8), 1084–1096. https://doi.org/10.1016/j.cortex.2008.05.005

Ruff, H. A., & Rothbart, M. K. (2001). *Attention in Early Development: Themes and Variations*. Oxford University Press.

Saccà, V., Sarica, A., Novellino, F., Barone, S., Tallarico, T., Filippelli, E., Granata, A., Valentino, P., & Quattrone, A. (2018). *Evaluation of the MCFLIRT Correction Algorithm in Head Motion from Resting State fMRI Data*. https://doi.org/10.1999/1307-6892/10008625

Sajaniemi, N., Hakamies-Blomqvist, L., Katainen, S., & von Wendt, L. (2001). Early cognitive and behavioral predictors of later performance: A follow-up study of ELBW children from ages 2 to 4. *Early Childhood Research Quarterly*, *16*(3), 343–361. https://doi.org/10.1016/S0885-2006(01)00107-7

Sandman, C. A., Glynn, L. M., & Davis, E. P. (2016). Neurobehavioral Consequences of Fetal Exposure to Gestational Stress. In N. Reissland & B. S. Kisilevsky (Eds.), *Fetal Development* (pp. 229–265). Springer International Publishing. https://doi.org/10.1007/978-3-319-22023-9_13

Satterthwaite, T. D., Wolf, D. H., Loughead, J., Ruparel, K., Elliott, M. A., Hakon, H., Gur, R. C., & Gur, R. E. (2012). Impact of In-Scanner Head Motion on Multiple Measures of Functional Connectivity: Relevance for Studies of Neurodevelopment in Youth. *NeuroImage*, *60*(1), 623–632. https://doi.org/10.1016/j.neuroimage.2011.12.063

Saxena, K., Tamm, L., Walley, A., Simmons, A., Rollins, N., Chia, J., Soares, J. C., Emslie, G. J., Fan, X., & Huang, H. (2012). A Preliminary Investigation of Corpus Callosum and Anterior Commissure Aberrations in Aggressive Youth with Bipolar Disorders. *Journal of Child and Adolescent Psychopharmacology*, *22*(2), 112–119. https://doi.org/10.1089/cap.2011.0063

Schneider, M. L. (1992). The effect of mild stress during pregnancy on birthweight and neuromotor maturation in rhesus monkey infants (Macaca mulatta). *Infant Behavior and Development*, *15*(4), 389–403. https://doi.org/10.1016/0163-6383(92)80009-J

Schneider, M. L., Roughton, E. C., Koehler, A. J., & Lubach, G. R. (1999). Growth and Development Following Prenatal Stress Exposure in Primates: An Examination of

Ontogenetic Vulnerability. *Child Development*, *70*(2), 263–274. https://doi.org/10.1111/1467-8624.00020

Seeley, W. W., Menon, V., Schatzberg, A. F., Keller, J., Glover, G. H., Kenna, H., Reiss, A. L., & Greicius, M. D. (2007). Dissociable Intrinsic Connectivity Networks for Salience Processing and Executive Control. *Journal of Neuroscience*, *27*(9), 2349–2356. https://doi.org/10.1523/JNEUROSCI.5587-06.2007

Shonkoff, J. P., Garner, A. S., The Committee on Psychosocial Aspects of Child and Family Health, C. on E. C., Siegel, B. S., Dobbins, M. I., Earls, M. F., Garner, A. S., McGuinn, L., Pascoe, J., & Wood, D. L. (2012). The Lifelong Effects of Early Childhood Adversity and Toxic Stress. *Pediatrics*, *129*(1), e232–e246. https://doi.org/10.1542/peds.2011-2663

Smith, M. V., Sung, A., Shah, B., Mayes, L., Klein, D. S., & Yonkers, K. A. (2013). Neurobehavioral assessment of infants born at term and in utero exposure to serotonin reuptake inhibitors. *Early Human Development*, *89*(2), 81–86. https://doi.org/10.1016/j.earlhumdev.2012.08.001

Smith, S. M. (2002). Fast robust automated brain extraction. *Human Brain Mapping*, *17*(3), 143–155. https://doi.org/10.1002/hbm.10062

Sripada, R. K., Swain, J. E., Evans, G. W., Welsh, R. C., & Liberzon, I. (2014). Childhood Poverty and Stress Reactivity Are Associated with Aberrant Functional Connectivity in Default Mode Network. *Neuropsychopharmacology*, *39*(9), 2244–2251. https://doi.org/10.1038/npp.2014.75

Straathof, M., Sinke, M. R. T., Roelofs, T. J. M., Blezer, E. L. A., Sarabdjitsingh, R. A., van der Toorn, A., Schmitt, O., Otte, W. M., & Dijkhuizen, R. M. (2020). Distinct structure-

function relationships across cortical regions and connectivity scales in the rat brain. *Scientific Reports*, *10*(1), 56. https://doi.org/10.1038/s41598-019-56834-9

Supekar, K., Musen, M., & Menon, V. (2009). Development of Large-Scale Functional Brain Networks in Children. *PLOS Biology*, *7*(7), e1000157. https://doi.org/10.1371/journal.pbio.1000157

Supekar, K., Uddin, L. Q., Prater, K., Amin, H., Greicius, M. D., & Menon, V. (2010). Development of functional and structural connectivity within the default mode network in young children. *NeuroImage*, *52*(1), 290–301. https://doi.org/10.1016/j.neuroimage.2010.04.009

Szaflarski, J. P., Schmithorst, V. J., Altaye, M., Byars, A. W., Ret, J., Plante, E., & Holland, S. K. (2006). A longitudinal functional magnetic resonance imaging study of language development in children 5 to 11 years old. *Annals of Neurology*, *59*(5), 796–807. https://doi.org/10.1002/ana.20817

Talge, N. M., Neal, C., Glover, V., & the Early Stress, Translational Research and Prevention Science Network: Fetal and Neonatal Experience on Child and Adolescent Mental Health. (2007). Antenatal maternal stress and long-term effects on child neurodevelopment: How and why? *Journal of Child Psychology and Psychiatry*, *48*(3–4), 245–261. https://doi.org/10.1111/j.1469-7610.2006.01714.x

Taylor, P. A., & Saad, Z. S. (2013). FATCAT: (An Efficient) Functional And Tractographic Connectivity Analysis Toolbox. *Brain Connectivity*, *3*(5), 523–535. https://doi.org/10.1089/brain.2013.0154

Tocrchiano, M. (2017). *effsize: Efficient effect size computation*. R package version 0.7.

Uddin, L. Q., Supekar, K., & Menon, V. (2010). Typical and atypical development of functional human brain networks: Insights from resting-state fMRI. *Frontiers in Systems Neuroscience*, *4*. https://doi.org/10.3389/fnsys.2010.00021

Umarova, R. M., Saur, D., Schnell, S., Kaller, C. P., Vry, M.-S., Glauche, V., Rijntjes, M., Hennig, J., Kiselev, V., & Weiller, C. (2010). Structural Connectivity for Visuospatial Attention: Significance of Ventral Pathways. *Cerebral Cortex*, *20*(1), 121–129. https://doi.org/10.1093/cercor/bhp086

Van den Bergh, B. R. H., van den Heuvel, M. I., Lahti, M., Braeken, M., de Rooij, S. R., Entringer, S., Hoyer, D., Roseboom, T., Räikkönen, K., King, S., & Schwab, M. (2020). Prenatal developmental origins of behavior and mental health: The influence of maternal stress in pregnancy. *Neuroscience & Biobehavioral Reviews*, *117*, 26–64. https://doi.org/10.1016/j.neubiorev.2017.07.003

van der Werff, S. J. A., Pannekoek, J. N., Veer, I. M., van Tol, M.-J., Aleman, A., Veltman, D. J., Zitman, F. G., Rombouts, S. A. R. B., Elzinga, B. M., & van der Wee, N. J. A. (2013). Resilience to childhood maltreatment is associated with increased resting-state functional connectivity of the salience network with the lingual gyrus. *Child Abuse & Neglect*, *37*(11), 1021–1029. https://doi.org/10.1016/j.chiabu.2013.07.008

Vincent, J. L., Kahn, I., Snyder, A. Z., Raichle, M. E., & Buckner, R. L. (2008). Evidence for a Frontoparietal Control System Revealed by Intrinsic Functional Connectivity. *Journal of Neurophysiology*, *100*(6), 3328–3342. https://doi.org/10.1152/jn.90355.2008

Vry, M.-S., Tritschler, L. C., Hamzei, F., Rijntjes, M., Kaller, C. P., Hoeren, M., Umarova, R., Glauche, V., Hermsdoerfer, J., Goldenberg, G., Hennig, J., & Weiller, C. (2015). The

ventral fiber pathway for pantomime of object use. *NeuroImage*, *106*, 252–263. https://doi.org/10.1016/j.neuroimage.2014.11.002

Waite, T. A., & Campbell, L. G. (2006). Controlling the false discovery rate and increasing statistical power in ecological studies. *Ecoscience*, *13*(4), 439–442. https://doi.org/10.2980/1195-6860(2006)13[439:CTFDRA]2.0.CO;2

Walhovd, K. B., Tamnes, C. K., & Fjell, A. M. (2014). Brain structural maturation and the foundations of cognitive behavioral development. *Current Opinion in Neurology*, *27*(2), 176–184. https://doi.org/10.1097/WCO.0000000000000074

Webb, S. J., Monk, C. S., & Nelson, C. A. (2001). Mechanisms of postnatal neurobiological development: Implications for human development. *Developmental Neuropsychology*, *19*(2), 147–171. https://doi.org/10.1207/S15326942DN1902_2

Weiller, C., Reisert, M., Peto, I., Hennig, J., Makris, N., Petrides, M., Rijntjes, M., & Egger, K. (2021). The ventral pathway of the human brain: A continuous association tract system. *NeuroImage*, *234*, 117977. https://doi.org/10.1016/j.neuroimage.2021.117977

Werhahn, J. E., Mohl, S., Willinger, D., Smigielski, L., Roth, A., Hofstetter, C., Stämpfli, P., Naaijen, J., Mulder, L. M., Glennon, J. C., Hoekstra, P. J., Dietrich, A., Kleine Deters, R., Aggensteiner, P. M., Holz, N. E., Baumeister, S., Banaschewski, T., Saam, M. C., Schulze, U. M. E., … Brandeis, D. (2020). Aggression subtypes relate to distinct resting state functional connectivity in children and adolescents with disruptive behavior. *European Child & Adolescent Psychiatry*. https://doi.org/10.1007/s00787-020-01601-9

Wilke, M., Schmithorst, V. J., & Holland, S. K. (2002). Assessment of spatial normalization of whole-brain magnetic resonance images in children. *Human Brain Mapping*, *17*(1), 48–60. https://doi.org/10.1002/hbm.10053

Willmes, K., Moeller, K., & Klein, E. (2014). Where numbers meet words: A common ventral network for semantic classification. *Scandinavian Journal of Psychology*, *55*(3), 202–211. https://doi.org/10.1111/sjop.12098

Wozniak, J. R., Mueller, B. A., Muetzel, R. L., Bell, C. J., Hoecker, H. L., Nelson, M. L., Chang, P.-N., & Lim, K. O. (2011). Inter-Hemispheric Functional Connectivity Disruption in Children With Prenatal Alcohol Exposure. *Alcoholism: Clinical and Experimental Research*, *35*(5), 849–861. https://doi.org/10.1111/j.1530-0277.2010.01415.x

Wu, Y., Lu, Y.-C., Jacobs, M., Pradhan, S., Kapse, K., Zhao, L., Niforatos-Andescavage, N., Vezina, G., du Plessis, A. J., & Limperopoulos, C. (2020). Association of Prenatal Maternal Psychological Distress With Fetal Brain Growth, Metabolism, and Cortical Maturation. *JAMA Network Open*, *3*(1), e1919940–e1919940. https://doi.org/10.1001/jamanetworkopen.2019.19940

Yeo, B. T. T., Krienen, F. M., Sepulcre, J., Sabuncu, M. R., Lashkari, D., Hollinshead, M., Roffman, J. L., Smoller, J. W., Zöllei, L., Polimeni, J. R., Fischl, B., Liu, H., & Buckner, R. L. (2011). The organization of the human cerebral cortex estimated by intrinsic functional connectivity. *Journal of Neurophysiology*, *106*(3), 1125–1165. https://doi.org/10.1152/jn.00338.2011

Yin, Y., Li, L., Jin, C., Hu, X., Duan, L., Eyler, L. T., Gong, Q., Song, M., Jiang, T., Liao, M., Zhang, Y., & Li, W. (2011). Abnormal baseline brain activity in posttraumatic stress disorder: A resting-state functional magnetic resonance imaging study. *Neuroscience Letters*, *498*(3), 185–189. https://doi.org/10.1016/j.neulet.2011.02.069

Zimmermann, J., Griffiths, J. D., & McIntosh, A. R. (2018). Unique Mapping of Structural and Functional Connectivity on Cognition. *Journal of Neuroscience*, *38*(45), 9658–9667. https://doi.org/10.1523/JNEUROSCI.0900-18.2018

Chapter 5: General Discussion

5.1 Designing a faster and simpler pipeline for the combined structural and functional connectivity analysis of brain networks

The main goal of my thesis was to develop a pipeline for the analysis of a combined structural and functional connectivity metric that could easily be applied across different scientific projects. Our priority was to produce a pipeline that was easy to understand, had reduced processing time compared to other methods, was flexible and compatible with different computers (didn't need special equipment/hardware/software), and utilized open-source software packages with freely available tools. We accomplished this by combining a well-established AFNI toolbox (a software package for the analysis of fMRI and DTI data), known as FATCAT (Taylor & Saad, 2013) with a mathematically dense data fusion approach known as the awFC technique (Bowman et al., 2012). Taylor and Saad (2013), demonstrated that the FATCAT AFNI commands had a much faster execution speed for processing probabilistic tractography compared to FSL (a software for the analysis of fMRI and DTI). The original awFC technique relied on FSL to process probabilistic tractography. By including AFNI FATCAT in our pipeline, it improved the speed of the analysis and the execution speed of the awFC technique. The added advantage of incorporating fMRI/DTI analysis packages (AFNI commands from FATCAT) as a part of our pipeline was the application of mathematical formulas and algorithms that can be initiated with ease using a single command at a time. In addition, the utility of FATCAT, which consists of set of AFNI commands, was designed to be intuitive because FATCAT follows a suggested pipeline with the set of functions that are run in an order in which they are typically applied. In addition,

FATCAT is also capable of processing a large quantity of data conveniently with batch processing (beneficial for large datasets). Aside from that, each AFNI command provides users with different options (i.e. arguments) for more flexibility and specialization so that users may add new capabilities to it (as they see fit for their project). Therefore, allowing users the flexibility to choose the parameters they wish to modify and not being completely automated is an added advantage (i.e. choose the parameters for DTI tractography, such as turning angle). Although we designed the pipeline with fMRI/DTI in mind, the toolbox is compatible with other data types such as task-based fMRI. The awFC approach (Bowman et al., 2012), on the other hand, offers the sophistication of combining two connectivity metrics together in a fused approach to produce a single measure containing a wealth of information. It also corrects the data for distance bias, and includes indirect structural connectivity to better correspond with functional connectivity (Bowman et al., 2012). This hybrid pipeline combined the advantages of a convenient neuroimaging toolbox and a sophisticated data fusion approach, to produce the FATCAT-awFC approach (Ayyash et al., 2021).

Designing a pipeline for combining functional and structural connectivity was done solely for this thesis. The vision for the pipeline was that other researchers could use it in the future, perhaps even modified slightly for different applications to study different neuropsychiatric disorders. Although the focus in this thesis is resting-state functional data, there are other data types that can be incorporated as well, such as task-based fMRI.

5.2 Functional ROIs and Tractography

An important component of the FATCAT-awFC pipeline is ROI-refinement. In the literature, there is no clear convention on the best method for ROI size/selection (Sohn et al., 2015). Some papers choose to use predefined ROIs (Rosazza et al., 2012) others use a data-driven approach (Koush et al., 2019). In addition, ROI sizes also range greatly in the literature from large ROIs encompassing multiple brain regions at a time (Chu et al., 2018) to smaller brain regions encompassing a voxel or two (Sohn et al., 2015). There is no set standard practice for selecting a set of functional ROIs (i.e. thresholding arbitrarily) (Sohn et al., 2015). The FATCAT approach used in our pipeline for selecting ROIs involved the selection of a threshold that seemed fairly representative of a particular network. It was observed that larger ROIs tend to average out the signal, due to neighboring activations and deactivations canceling each other out, and result in the loss of potentially interesting information/findings (Mueller et al., 2013; Poldrack, 2007). We deduced that since larger ROIs average out the signal across the entire region, we could increase the threshold of the map and obtain the smaller more targeted activated voxels while eliminating unactivated (or less activated) voxels that contribute noise to the signal (Cohen & DuBois, 1999). However, increasing the threshold is not necessarily a solution due to the following tradeoff. While smaller ROIs seem to detect more specific brain regions, they have greater variability in matching the exact location of the ROI across the brains of subjects (Cohen & DuBois, 1999) . They are difficult to accurately map on different subjects' brains due to the variability of brain size and shape (Cole et al., 2010). Larger ROIs may leave more room for covering similar brain regions (Sohn et al., 2015) and have less variability between subjects and more reproducibility of results (Song et al., 2016). In the first paper, the depression paper (Chapter 2), the ROIs were large and encompassed many brain regions at a time with an average ROI size of 594 voxels. The second paper, the remitters paper (Chapter 3), the average ROI size was 54 voxels. Finally,

the third paper (Chapter 4), the adversity paper, included ROIs with an average size of 11 voxels. This illustrates the challenges that arose when attempting to define the optimal threshold setting for ROI selection.

Another added complication to ROI threshold selection, is that the location and size of the ROI can greatly impact the calculation of the white matter tracts connecting two brain regions (Sohn et al., 2015). This in turn, may greatly influence the structural and functional connectivity profiles (Li et al., 2012). Regardless of the utmost importance of ROI selection, it remains a great challenge in the neuroimaging community for various reasons including (Liu, 2011): a) the boundaries being unclear between cortical regions (Van Essen & Dierker, 2007) b) The great variability across individuals' brain anatomy, function and connectivity (Brett et al., 2002) c) properties of ROIs are highly non-linear within and around the ROI (Li et al., 2012).

5.3 Limitations to the Method

In this section, I am going to discuss some of the processing steps that were explored, but due to various reasons, were not included in our pipeline for the analysis. This information may be of value methodologically for future research in this area. Initially when designing a pipeline that combined structural and functional connectivity in a data fusion approach, we applied the processing steps incrementally from 3 subjects, to 10 subjects, to 40 subjects and so on, while refining the process.

We were interested in assessing subject specific RSNs. While resting-state networks are consistent across subjects, there is not always an exact correspondence among the nodes identified within each particular network across individual subjects (Cole et al., 2010). Previous research has demonstrated that subject-specific ROI selection is more reliable and sensitive in a multi-subject analysis (Nieto-Castañón & Fedorenko, 2012). To generate subject-level RSNs, we incorporated a technique known as dual regression (Beckmann et al., 2009; Erhardt et al., 2011) into the pipeline, following the Group ICA step. This applied the regression of the group-ICA spatial maps against the functional dataset of each individual subject (Nickerson et al., 2017). The group-ICA components were used as a set of spatial regressors in a multiple regression analysis (Nickerson et al., 2017). This generated subject-level spatial maps and subject specific time series for each component (i.e. resting-state networks) for each subject (Nickerson et al., 2017). However, there were clear limitations when performing dual regression to obtain subject-specific RSNs. Subject-specific RSNs lacked the consistency of functional ROIs across subjects. Some ROIs were undetected because functional brain ROIs may be missing in in particular subjects (Gordon et al., 2017). Furthermore, ROIs were substantially different in size, location and shape, making it more difficult to compare across subjects. This naturally occurs due to the inter-subject variability of RSN (Mueller et al., 2013). Thus, it was very difficult to draw inferences about different spatial maps across multiple subjects (Calhoun et al., 2001). There are different levels of motion, artifacts and noise for data collected from each subject (Cohen & DuBois, 1999), as such, producing similar spatial ROIs across subjects would be difficult to achieve (Cohen & DuBois, 1999). This meant that when setting a threshold across subjects-level functional data, in the *3dROIMaker step* (Taylor & Saad, 2013), the result was an inconsistent number of ROIs produced within each RSN.

We also attempted to manually (through trial and error) find the threshold suitable for each subjects' functional data, that produced a similar number of ROIs. However, even through visual inspection, it was impossible to achieve a common spatial map across all subjects. For instance, the first subject's (subject1) RSN for the DMN was separated into 5 ROIs, whereas another subject (subject2) the DMN was separated into 6 ROIs. We attempted to set a higher threshold for subject2 to achieve the same 5 ROIs. Instead, this only resulted in the breaking apart of an ROI into two separate ROIs , resulting in 7 ROIs that were distributed differently than those observed in subject1. This validated our previous observation that, even manually setting the threshold for each individual subject, would not achieve a consistent number of ROIs and common brain regions for ROIs across subjects. The FATCAT toolbox lacks the ability to produce localized/subject specific ROIs that have a consistent number of ROIs across participants. The FATCAT is only able to apply the traditional ROI group analysis approach to study connectivity across subjects. Therefore, we decided to apply group level ICA only, and transform the group-level ROIs back into each subjects' functional data space.

An argument can be made against group-level analysis, in that the variability in ROI location, size and shape is part of the distribution of individual networks (Van Essen & Dierker, 2007). There is the concern of generalizing these functional ROIs for subjects that don't even have these functional activations (Michael et al., 2014). However, there is merit to group-level ROI analysis because a common set of spatial maps are needed when comparing across subjects, (Calhoun et al., 2001). Common spatial maps are not achievable with individual-level ICA making it difficult to draw inferences about the data (Salman et al., 2019). Group ICA allows

users to have common spatial maps to draw inferences about the dataset (Calhoun et al., 2001). The benefit of performing group ICA, is its robust ability to detect resting-state networks compared to individual-level ICA that has difficulty robustly detecting RSNs (Rytty et al., 2013).

This thesis presents a pipeline for the faster and more intuitive analysis of a combined functional-structural connectivity that can be used for studying the functional and structural connectivity of the human brain. Our technical contributions offer new solutions to difficult neuroimaging data fusion approaches. We propose that applying the fused structural-functional connectivity for identifying atypical connectivity in different groups will help elevate research beyond that ascertained from traditional structural or functional connectivity alone. Researchers are increasingly beginning to understand the power and depth of information provided by using a multimodal approach to assess complex psychological issues (Calhoun & Sui, 2016). This has made multimodal analysis appealing over the years, however, it is underutilized due to its complex nature (Calhoun & Sui, 2016). Thus, our FATCAT-awFC was applied to evaluate different populations.

5.4 Neural circuitry abnormalities underlying MDD

In Chapter 2, we assembled the FATCAT-awFC pipeline and applied it to MDD data. When we combined the functional and structural connectivity data via the FATCAT-awFC pipeline, we were able to observe significant awFC differences between groups (MDD vs HC) in two RSNs. First, decreased connectivity (MDD<HC) in the DMN was found between the occipital lobe (covering parts of the cerebellum) and the PCC. Second, decreased connectivity (MDD<HC) was

observed in the VAN between the left temporal lobe and the right DLPFC. Third, decreased connectivity was observed in the VAN between the right temporal lobe and the right DLPFC. Decreased awFC following MDD may represent a weakening of important connections that are typically more strongly connected to one another in healthy adults. This information may be of value for assessing underlying connectivity that may differentiate healthy from MDD patients and may help us better understand the underlying changes that brain connectivity may undergo in MDD.

5.5 Neural circuitry abnormalities underlying REM and NREM in MDD

The results of the first study (MDD vs HC) prompted us to investigate connectivity changes in a different population. In chapter 3, we wanted to investigate brain connectivity changes using our FATCAT-awFC pipeline in MDD patients administered escitalopram antidepressant. We were also interested in studying the connectivity differences characteristic of patients that reach remission (REM) compared to MDD participants that did not reach remission (NREM). We were also interested in assessing connectivity changes for REM at baseline compared to REM at week-8. In relation to NREM at week8, REM at week8 had significantly different connectivity between brain regions in four RSNs. To examine the question of what changes distinguish REM from NREM at week-8, we found decreased connectivity ($REM_{week8} < NR_{week8}$) in the DMN were found between three region pairs: between the left angular gyrus and the middle prefrontal cortex, between the middle prefrontal cortex and the left middle temporal gyrus, and finally between the left angular gyrus and the left middle temporal gyrus. In addition, decreased

connectivity (REM_{week8} <NR_{week8}) in the FPN was observed between the left cerebellum to the right orbitofrontal gyrus. Third, decreased connectivity (REM_{week8} <NR_{week8}) in the VAN between the: right insula and left middle frontal gyrus and between the ACC and the left middle frontal gyrus.

To examine the question of what changes occur with a favorable response to medication, we compared remitters at baseline to remitters post-treatment at week-8. We observed increased connectivity (REM_{week8} > $REM_{baseline}$) in the DAN between the right and left postcentral gyrus and the right precentral gyrus, we also observed decreased connectivity (REM_{week8} < $REM_{baseline}$) in the FPN between the left cerebellum and the right orbitofrontal gyrus. Our findings demonstrate that there are connectivity differences that exist between MDD remitters and non-remitters. This work helps to shed light on the circuitry within RSNs that predicts a favorable response to treatment. .

5.6 Neural circuitry abnormalities within middle childhood caused by pre- and/or postnatal adversity

In Chapter 4, we investigated atypical brain development for children with pre- and/or postnatal adversity compared to children without pre- and/or postnatal adversity using our FATCAT-awFC pipeline. Statistically significant awFC group differences were discovered in five RSNs. Firstly, decreased connectivity (ADV<CON) in the DMN was found between the PCC and the left angular gyrus. Secondly, decreased connectivity (ADV < CON) in the FPN was observed between the: left inferior frontal gyrus and the lingual gyrus/cerebellum, and between the right superior frontal gyrus and the lingual gyrus/cerebellum. Thirdly, decreased connectivity (ADV <

CON) was found in the LIM between the right superior temporal gyrus and the left superior temporal gyrus. Fourthly, increased connectivity (ADV > CON) was found in the VAN between the right anterior orbitofrontal gyrus and the left lingual gyrus. Finally, decreased connectivity (ADV < CON) was observed in the DAN between the posterior orbitofrontal gyrus and the left inferior temporal gyrus. This study helps us better understand the complex circuitry during middle childhood and the RSNs that are impacted as a result of pre- and/or postnatal adversity on this age group.

5.7 Connectivity across studies

Although functional brain ROIs across our studies are not directly comparable, due to the variability that is associated with selecting functionally-derived ROIs, conclusions may still be made about our findings.

Common to both Chapter 2 and Chapter 3, it was evident that with the use of our FATCAT-awFC pipeline, we were able to demonstrate that two RSNs, the DMN and the VAN were impacted in MDD: 1) in MDD versus controls in our first study, 2) between REM and NREM at week-8, post antidepressant therapy, in our second study. Only the DMN and VAN differentiated MDD from controls in the first study. The second study (remitters paper) differentiated connectivity for REM and NREM at week-8 in three RSNs: DMN VAN and FPN. NREM demonstrated atypical connectivity compared to REM, as either decreases or increases compared to REM. Atypical connectivity may appear as either greater or weaker connectivity strength (Mattiaccio et al., 2016). On the other hand, post-therapy connectivity changes for the MDD

population may indicate, “normalizing” that happens in remission post-antidepressant treatment, whereby atypical connectivity is adjusted/corrected (Aizenstein et al., 2014; Xiao et al., 2019).

Another analysis in Chapter 3, involved comparing remitters at baseline to remitters at week-8. Interestingly, for this analysis, there was greater connectivity in the DAN for remitters at week-8 compared to remitters at baseline. The opposite trend was observed for FPN from baseline to week-8. We suspect that this may reflect the normalization of connectivity post pharmacotherapy.

In Chapter 4, it was pre- and/or postnatal adversity that reflected as atypical connectivity in the developing brain of children in the middle childhood age-group within five RSNs: DMN, FPN, LIM, VAN, DAN, compared to children without pre- or postnatal adversity. This showed up as predominantly as reduced connectivity, although there was one instance where the opposite trend was observed. Atypical connectivity can appear as either decreased/increased connectivity (Mattiaccio et al., 2016). The FATCAT-awFC pipeline was capable of identifying atypical neurocircuitry in the developing child as a result of adversity.

5.8 Future work

The purpose of our study was to combine functional and structural connectivity to achieve a better representation of underlying brain connectivity with the help of a convenient pipeline that included the use of a well substantiated, publically available, and recognized, toolbox. However, there is much to be done to further improve this pipeline. The method that used for identifying

structural connectivity in this research was DTI tractography. However, DTI fiber tractography has inherent limitations. DTI tractography generates the trajectory of water molecules based on the principal eigenvector (the main direction of diffusion), which is beneficial when there is a single tract passing in a voxel (Descoteaux, 1999). However, the brain typically has many crossing fibers (Tuch et al., 2002). This can pose a serious issue when attempting to delineate fibers in a single voxel composed of multiple fibers (Descoteaux, 1999). A known limitation to DTI tractography is its inability to resolve crossing fibers (Descoteaux, 1999). In the case of complex fibers, where major fiber tracts cross (i.e. semiovale), it is difficult to accurately represent complex fiber orientations with standard DTI tractography methods. Tensors are used in diffusion imaging, but tensors may misrepresent the axon direction if there are multiple fibers crossing (Asken et al., 2018). The tensor measures diffusivity in only 6 gradient directions in q-space (Descoteaux, 1999). Diffusion in other directions is unreliable and may be inaccurate. DTI relies on the Gaussian assumption that the diffusion shape is smooth between sparsely measured points (Descoteaux, 1999). High Angular Resolution Diffusion Imaging (HARDI), on the other hand, provides a more thorough view of diffusion (Descoteaux, 1999). HARDI (Caverzasi et al., 2014) can improve tractography, and resolve regions of crossing fibers, since it serves multiple fiber orientations at each voxel (Descoteaux, 1999). Therefore, a solution to the tensor used in DTI would be to use HARDI instead, which would be a worthwhile substitution for DTI as it has been reported to improve accuracy and sensibility (Bucci et al., 2013). The FATCAT toolbox already is designed to accept either DTI or HARDI data in the pipeline. Substituting HARDI for DTI can easily be done in the FATCAT (Taylor & Saad, 2013) pipeline and may offer more accurate structural connectivity measures to the pipeline. This may in turn provide richer information that is more correctly depictive of the white matter tracts.

Aside from the DTI side of the FATCAT-awFC pipeline, it would be of interest to improve the functional side as well. As previously discussed, when identifying the functional ROIs, the FATCAT approach is capable of only handling group ROIs. However, a clever workaround would be to perform functional localization for obtaining subject-specific ROIs in standard space. This would allow us to preserve the common spatial maps and the consistency in the number of ROIs across subjects, while maintaining variability that naturally happens across subjects. Nieto-Castañón & Fedorenko (2012) proposed a subject-specific ROI approach that involved functional localization that allowed the *selective* aggregation of voxels with a supra-threshold response. This may be applied after generating the group-level ROIs in order to achieve common ROIs and a consistent number of ROIs. However, within each subject's spatial map, functional localization would allow for a more accurate measure (higher correlation and less variance) of network connectivity (Sohn et al., 2015). This in turn, will produce a more precise representation of the connectivity, both functional and structural of each subject while eliminating noise from the signal. While (Nieto-Castañón & Fedorenko, 2012) proposed an SPM toolbox for selecting localized fMRI ROIs, we worried that incorporating too many different analyses software may increase the complexity of the model. However, this may be something to consider in the future. Thus, the addition of a toolbox (i.e. SPM toolbox for functional localization of ROIs) [See: https://www.nitrc.org/project/list_screenshots.php?group_id=415&screenshot_id=291] for optimally functionally localizing the ROIs, from the group-level ROIs, could potentially be an open suggestion for incorporating it into the FATCAT-awFC pipeline. This could be a step after the Group ICA that is performed across subjects. However, incorporating additional software

may decrease the simple design and intuitiveness of the FATCAT-awFC pipeline and increase learning time of the software. While this may increase processing speed to an extent, it will greatly refine the ROI selection per subject and increase accuracy of network connectivity (Sohn et al., 2015). These two adjustments: the tractography of choice and the functional ROI selection may further advance the FATCAT-awFC pipeline to increase accuracy of the model.

5.9 General Conclusion

In summary, for my Ph.D. thesis I first developed a new pipeline for analyzing brain connectivity with a data fusion approach in a more intuitive and faster approach, and ensured to choose freely available software and flexible tools that can be applied to a number of applications for current and future scientists. Secondly, I contributed to the field of neuroscience research by investigating the brain connectivity that is impacted in MDD and researched the differences in brain connectivity for REM and NREM at week-8, and REM at baseline compared to REM at week-8. I also assessed how this neuropsychiatric disorder may be associated with cognition in NREM. Finally I evaluated how pre- and/or postnatal adversity may impact child development for the middle childhood age group compared to their healthy counterparts. We also studied the association brain connectivity in middle childhood has with behavioral responses and psychomotor developmental index at age three, to observe whether there may be a predictive indication of atypical connectivity in children early on. I hope that my research serves an example of how to incorporate the ease of a toolbox with the sophistication of a data fusion

approach to produce a pipeline that offers a simpler and more intuitive approach that makes use of powerful emerging data fusion approaches to improve research.

5.10 References

Aizenstein, H. J., Khalaf, A., Walker, S. E., & Andreescu, C. (2014). Magnetic Resonance Imaging Predictors of Treatment Response in Late-Life Depression. *Journal of Geriatric Psychiatry and Neurology*, *27*(1), 24–32. https://doi.org/10.1177/0891988713516541

Asken, B. M., DeKosky, S. T., Clugston, J. R., Jaffee, M. S., & Bauer, R. M. (2018). Diffusion tensor imaging (DTI) findings in adult civilian, military, and sport-related mild traumatic brain injury (mTBI): A systematic critical review. *Brain Imaging and Behavior*, *12*(2), 585–612. https://doi.org/10.1007/s11682-017-9708-9

Ayyash, S., Davis, A. D., Alders, G. L., MacQueen, G., Strother, S. C., Hassel, S., Zamyadi, M., Arnott, S. R., Harris, J. K., Lam, R. W., Milev, R., Müller, D. J., Kennedy, S. H., Rotzinger, S., Frey, B. N., Minuzzi, L., Hall, G. B., & CAN-BIND Investigator Team. (2021). Exploring brain connectivity changes in major depressive disorder using functional-structural data fusion: A CAN-BIND-1 study. *Human Brain Mapping*. https://doi.org/10.1002/hbm.25590

Beckmann, C., Mackay, C., Filippini, N., & Smith, S. (2009). Group comparison of resting-state FMRI data using multi-subject ICA and dual regression. *NeuroImage*, *47*, S148. https://doi.org/10.1016/S1053-8119(09)71511-3

Bowman, F. D., Zhang, L., Derado, G., & Chen, S. (2012). Determining Functional Connectivity using fMRI Data with Diffusion-Based Anatomical Weighting. *NeuroImage*, *62*(3), 1769–1779. https://doi.org/10.1016/j.neuroimage.2012.05.032

Brett, M., Johnsrude, I. S., & Owen, A. M. (2002). The problem of functional localization in the human brain. *Nature Reviews Neuroscience*, *3*(3), 243–249. https://doi.org/10.1038/nrn756

Bucci, M., Mandelli, M. L., Berman, J. I., Amirbekian, B., Nguyen, C., Berger, M. S., & Henry, R. G. (2013). Quantifying diffusion MRI tractography of the corticospinal tract in brain tumors with deterministic and probabilistic methods. *NeuroImage : Clinical*, *3*, 361–368. https://doi.org/10.1016/j.nicl.2013.08.008

Calhoun, V., Adali, T., Pearlson, G., & Pekar, J. (2001). *Group Ica Of Functional Mri Data: Separability, Stationarity, And Inference*. 6.

Calhoun, V. D., Adali, T., Pearlson, G. D., & Pekar, J. J. (2001). A method for making group inferences from functional MRI data using independent component analysis. *Human Brain Mapping*, 140–151.

Calhoun, V. D., & Sui, J. (2016). Multimodal fusion of brain imaging data: A key to finding the missing link(s) in complex mental illness. *Biological Psychiatry : Cognitive Neuroscience and Neuroimaging*, *1*(3), 230–244. https://doi.org/10.1016/j.bpsc.2015.12.005

Caverzasi, E., Papinutto, N., Amirbekian, B., Berger, M. S., & Henry, R. G. (2014). Q-Ball of Inferior Fronto-Occipital Fasciculus and Beyond. *PLOS ONE*, *9*(6), e100274. https://doi.org/10.1371/journal.pone.0100274

Chu, C., Fan, L., & Jiang, T. (2018). *Characterization of functional diversity of the human brain based on intrinsic connectivity networks* (p. 475855). https://doi.org/10.1101/475855

Cohen, M. S., & DuBois, R. M. (1999). Stability, repeatability, and the expression of signal magnitude in functional magnetic resonance imaging. *Journal of Magnetic Resonance*

Imaging, *10*(1), 33–40. https://doi.org/10.1002/(SICI)1522-2586(199907)10:1<33::AID-JMRI5>3.0.CO;2-N

Cole, D. M., Smith, S. M., & Beckmann, C. F. (2010). Advances and Pitfalls in the Analysis and Interpretation of Resting-State FMRI Data. *Frontiers in Systems Neuroscience*, *4*, 8. https://doi.org/10.3389/fnsys.2010.00008

Descoteaux, M. (1999). High Angular Resolution Diffusion Imaging (HARDI). In J. G. Webster, *Wiley Encyclopedia of Electrical and Electronics Engineering* (pp. 1–25). John Wiley & Sons, Inc. https://doi.org/10.1002/047134608X.W8258

Erhardt, E. B., Rachakonda, S., Bedrick, E., Allen, E., Adali, T., & Calhoun, V. D. (2011). Comparison of multi-subject ICA methods for analysis of fMRI data. *Human Brain Mapping*, *32*(12), 2075–2095. https://doi.org/10.1002/hbm.21170

Gordon, E. M., Laumann, T. O., Adeyemo, B., Gilmore, A. W., Nelson, S. M., Dosenbach, N. U. F., & Petersen, S. E. (2017). Individual-specific features of brain systems identified with resting state functional correlations. *NeuroImage*, *146*, 918–939. https://doi.org/10.1016/j.neuroimage.2016.08.032

Koush, Y., Masala, N., Scharnowski, F., & Van De Ville, D. (2019). Data-driven tensor independent component analysis for model-based connectivity neurofeedback. *NeuroImage*, *184*, 214–226. https://doi.org/10.1016/j.neuroimage.2018.08.067

Li, K., Guo, L., Zhu, D., Hu, X., Han, J., & Liu, T. (2012). Individual Functional ROI Optimization Via Maximization of Group-Wise Consistency of Structural and Functional Profiles. *Neuroinformatics*, *10*(3), 225–242. https://doi.org/10.1007/s12021-012-9142-5

Liu, T. (2011). A few thoughts on brain ROIs. *Brain Imaging and Behavior*, *5*(3), 189–202. https://doi.org/10.1007/s11682-011-9123-6

Mattiaccio, L. M., Coman, I. L., Schreiner, M. J., Antshel, K. M., Fremont, W. P., Bearden, C. E., & Kates, W. R. (2016). Atypical functional connectivity in resting-state networks of individuals with 22q11.2 deletion syndrome: Associations with neurocognitive and psychiatric functioning. *Journal of Neurodevelopmental Disorders*, *8*(1), 2. https://doi.org/10.1186/s11689-016-9135-z

Michael, A. M., Anderson, M., Miller, R. L., Adalı, T., & Calhoun, V. D. (2014). Preserving subject variability in group fMRI analysis: Performance evaluation of GICA vs. IVA. *Frontiers in Systems Neuroscience*, *8*. https://doi.org/10.3389/fnsys.2014.00106

Mueller, S., Wang, D., Fox, M. D., Yeo, B. T. T., Sepulcre, J., Sabuncu, M. R., Shafee, R., Lu, J., & Liu, H. (2013). Individual Variability in Functional Connectivity Architecture of the Human Brain. *Neuron*, *77*(3), 586–595. https://doi.org/10.1016/j.neuron.2012.12.028

Nickerson, L. D., Smith, S. M., Öngür, D., & Beckmann, C. F. (2017). Using Dual Regression to Investigate Network Shape and Amplitude in Functional Connectivity Analyses. *Frontiers in Neuroscience*, *11*. https://doi.org/10.3389/fnins.2017.00115

Nieto-Castañón, A., & Fedorenko, E. (2012). Subject-specific functional localizers increase sensitivity and functional resolution of multi-subject analyses. *NeuroImage*, *63*(3), 1646–1669. https://doi.org/10.1016/j.neuroimage.2012.06.065

Poldrack, R. A. (2007). Region of interest analysis for fMRI. *Social Cognitive and Affective Neuroscience*, *2*(1), 67–70. https://doi.org/10.1093/scan/nsm006

Rosazza, C., Minati, L., Ghielmetti, F., Mandelli, M. L., & Bruzzone, M. G. (2012). Functional Connectivity during Resting-State Functional MR Imaging: Study of the Correspondence between Independent Component Analysis and Region-of-Interest−Based Methods.

American Journal of Neuroradiology, *33*(1), 180–187. https://doi.org/10.3174/ajnr.A2733

Rytty, R., Nikkinen, J., Paavola, L., Abou Elseoud, A., Moilanen, V., Visuri, A., Tervonen, O., Renton, A., Traynor, B., Kiviniemi, V., & Remes, A. (2013). GroupICA dual regression analysis of resting state networks in a behavioral variant of frontotemporal dementia. *Frontiers in Human Neuroscience*, *7*, 461. https://doi.org/10.3389/fnhum.2013.00461

Salman, M. S., Du, Y., Lin, D., Fu, Z., Fedorov, A., Damaraju, E., Sui, J., Chen, J., Mayer, A. R., Posse, S., Mathalon, D. H., Ford, J. M., Van Erp, T., & Calhoun, V. D. (2019). Group ICA for identifying biomarkers in schizophrenia: 'Adaptive' networks via spatially constrained ICA show more sensitivity to group differences than spatio-temporal regression. *NeuroImage: Clinical*, *22*, 101747. https://doi.org/10.1016/j.nicl.2019.101747

Sohn, W. S., Yoo, K., Lee, Y.-B., Seo, S. W., Na, D. L., & Jeong, Y. (2015). Influence of ROI selection on resting state functional connectivity: An individualized approach for resting state fMRI analysis. *Frontiers in Neuroscience*, *9*. https://doi.org/10.3389/fnins.2015.00280

Song, X., Panych, L. P., & Chen, N.-K. (2016). Data-Driven and Predefined ROI-Based Quantification of Long-Term Resting-State fMRI Reproducibility. *Brain Connectivity*, *6*(2), 136–151. https://doi.org/10.1089/brain.2015.0349

Taylor, P. A., & Saad, Z. S. (2013). FATCAT: (An Efficient) Functional And Tractographic Connectivity Analysis Toolbox. *Brain Connectivity*, *3*(5), 523–535. https://doi.org/10.1089/brain.2013.0154

Tuch, D. S., Reese, T. G., Wiegell, M. R., Makris, N., Belliveau, J. W., & Wedeen, V. J. (2002). High angular resolution diffusion imaging reveals intravoxel white matter fiber

heterogeneity. *Magnetic Resonance in Medicine*, *48*(4), 577–582. https://doi.org/10.1002/mrm.10268

Van Essen, D. C., & Dierker, D. L. (2007). Surface-Based and Probabilistic Atlases of Primate Cerebral Cortex. *Neuron*, *56*(2), 209–225. https://doi.org/10.1016/j.neuron.2007.10.015

Xiao, X., Bentzley, B. S., Cole, E. J., Tischler, C., Stimpson, K. H., Duvio, D., Bishop, J. H., DeSouza, D. D., Schatzberg, A., Keller, C., Sudheimer, K. D., & Williams, N. R. (2019). *Functional connectivity changes with rapid remission from moderate-to-severe major depressive disorder* [Preprint]. Clinical Trials. https://doi.org/10.1101/672154

Appendices

Chapter 2 Supplementary Information

.1 Generating structural connectivity matrix

In the awFC approach (Bowman et al., 2012), probabilities of structural connectivity are calculated by dividing the number of tracts running from ROI-to-ROI, by the total number of streamlines leaving the starting ROI. This is not a typical step performed for the probabilistic tractography. According to Zhang ,2010) incorporating this step (calculation of structural connectivity probabilities) results in higher overlap of structural and functional connectivity. However, calculating structural probabilities alone does not capture the full nature of structural connectivity. Structural connectivity exhibits distance-dependent correlation bias, meaning that long-range connection (ROI pairs further apart) have weaker structural connectivity, while short-range connections (pairs of ROIs closer together) display stronger structural connectivity (Geerligs et al., 2016). Bias correction is a necessary step for adjusting structural connectivity values.

.2 Functional and structural connectivity combined into one unit (awFC)

When measuring connectivity values using two different imaging modalities, we expect an overlap in the sampled data. However, each modality measures connectivity values in different ways (i.e. functional connectivity measures temporally correlated regions, structural connectivity measures number of tracts) (Kriegeskorte et al., 2008). A modality-independent comparison of connectivity values is achieved through dissimilarity. The dissimilarity matrix is sensitive to

both activation difference and the correlation (Kriegeskorte et al., 2008). Liu et al (2018) and Kriegeskorte et al (2018), have suggested that multiplicatively combining multimodal sources better captures cross-modal signal correlations by reducing the cost associated with the weaker modality and encouraging the discovery of truly important patterns from each modality. Therefore, combining information from different modalities, in theory, is capable of providing more robust inference on connectivity (Liu et al., 2018).

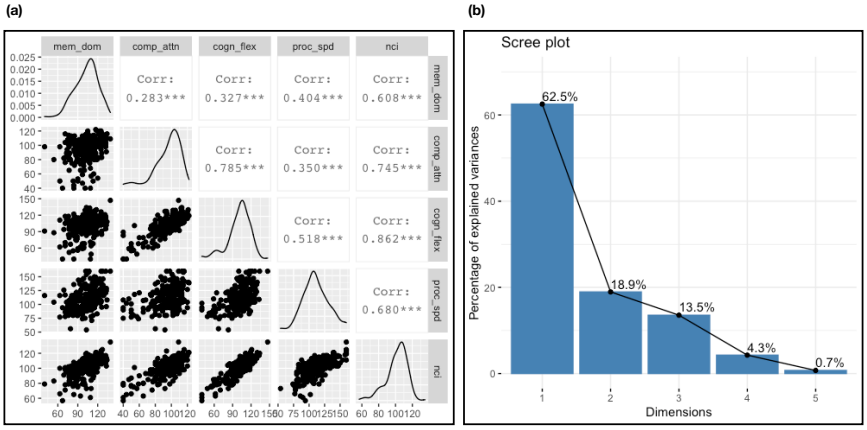

Supplementary Fig 1. (a) A pair plot with all the variables (memory domain, complex attention, cognitive flexibility, processing speed and neurocognitive index) showing the Pearson's correlation coefficients demonstrates multicollinearity exists among variables. (b) Scree Plot shows the eigenvalues/variance for each of the principal components. The number of principal components that were retained in our study was determined at the first 'elbow' of the plot. Note: Mem_dom- memory domain, comp_attn – complex attention, cogn_flex – cognitive flexibility, proc_spd –processing speed, nci – neurocognitive index, Corr – correlation.

.3 Chapter 3 Supplementary Information

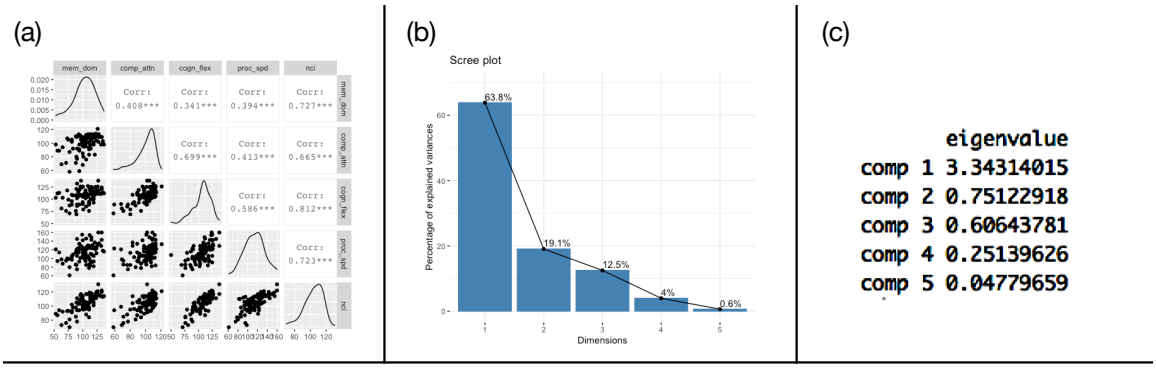

Supplementary Fig.1 | Principal component analysis was performed to overcome multicollinearity among the variables (a) Pair-wise plots of the cognitive variables were compared using Pearson correlation to assess multicollinearity. An asterisk indicated a statistically significant correlation between variables. This was performed with *ggpairs* function from the "GGally" package **(b) Scree plot, whereby the x-axis represents each of the principal components (output from PCA). The y-axis is the percentage of explained variance. The first principal component explains 63.8% of total variance in the data. The first 'elbow' of the plot indicates that only the first PC should be retained (c) Eigenvalues for each principal component, whereby Eigenvalues > 1.0 are retained – only the first PC meets this criteria. These plots were all derived in R. Note: Mem_dom- memory domain, comp_attn – complex attention, cogn_flex – cognitive flexibility, proc_spd –processing speed, nci – neurocognitive index, Corr – correlation, PC – Principal component.**